University of Rhode Island
DigitalCommons@URI

Open Access Dissertations

2008

Design and Evaluation of Nucleoside Derivatives for Targeted Drug Delivery and Therapeutic Applications

Hitesh Kumar Agarwal
University of Rhode Island

Follow this and additional works at: https://digitalcommons.uri.edu/oa_diss

Recommended Citation

Agarwal, Hitesh Kumar, "Design and Evaluation of Nucleoside Derivatives for Targeted Drug Delivery and Therapeutic Applications" (2008). *Open Access Dissertations.* Paper 507.
https://digitalcommons.uri.edu/oa_diss/507

This Dissertation is brought to you for free and open access by DigitalCommons@URI. It has been accepted for inclusion in Open Access Dissertations by an authorized administrator of DigitalCommons@URI. For more information, please contact digitalcommons@etal.uri.edu.

www.manaraa.com

DESIGN AND EVALUATION OF NUCLEOSIDE DERIVATIVES FOR TARGETED DRUG DELIVERY AND THERAPEUTIC APPLICATIONS

BY

HITESH KUMAR AGARWAL

A DISSERTATION SUBMITTED IN PARTIAL FULFILLMENT OF THE REQUIREMENTS OF THE DEGREE OF

DOCTOR OF PHILOSOPHY

IN

MEDICINAL CHEMISTRY

UNIVERSITY OF RHODE ISLAND

2008

DOCTOR OF PHILOSOPHY DISSERTATION

OF

HITESH KUMAR AGARWAL

APPROVED:

Thesis Committee

Major Professor:

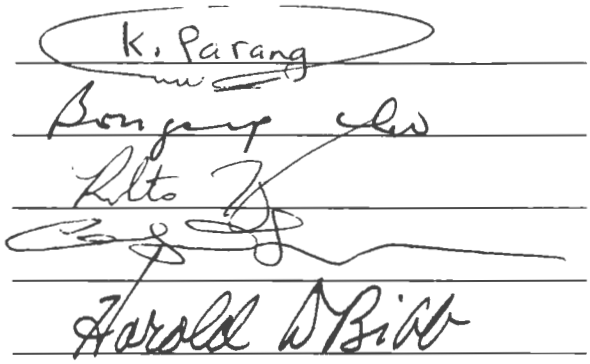

DEAN OF THE GRADUATE SCHOOL

UNIVERSITY OF RHODE ISLAND

2008

www.mana

Abstract

2′,3′-Dideoxynucleoside analogs are commonly used as anti-HIV, anti-HBV, and anti-cancer drugs. Despite of their potent activities, there are some major limitations in using 2′,3′-dideoxynucleosides as therapeutic agents. The nucleosides have usually poor cellular uptake because of their hydrophilic nature. Some of the nucleoside analogs, such as anti-HIV agents, become ineffective after multiple administrations because of the development of the drug resistance, and therefore they must be administered in combination therapy. It is hard to deliver the nucleoside analogs to a particular tissue for site specific targeting. Furthermore, nucleoside analogs undergo three intracellular phosphorylation steps to become active. The first phosphorylation step is slow and a rate-limiting process for several compounds.

Herein, we report the synthesis and evaluation of 2′,3′-dideoxynucleoside conjugates with fatty acids, peptides, other nucleosides, fatty acyl phosphotriesters, or polymer derivatives. The primary hypothesis of this project was that conjugation of nucleosides with other compounds offers a novel strategy in designing compounds with enhanced anti-HIV activity. This combination may result in development of anti-HIV agents having enhanced lipophilicity, longer duration of action by sustained intracellular release of active substrates at adequate concentrations, higher uptake into infected cells, and/or site specificity. The development of viral resistance to the nucleosides would occur at a slower rate than to either compound alone. Furthermore, some of the compounds may be used to bypass first rate-limiting phosphorylation step.

المنارة للاستشارات

www.m

In the first two chapters, synthesis and anti-HIV activities of fatty acyl derivatives of Zidovudine (AZT), Allovudine (FLT), Emtricitabine (FTC), Lamivudine (3TC), and Stavudine (d4T) are discussed. Among all the compounds, 5′-*O*-myristoyl derivative of FTC (**2.31**, EC_{50} = 70 nM against cell-free virus) exhibited the best anti-HIV profile when compared with other fatty acyl derivatives of other nucleosides and the physical mixture of FTC and myristic acid. 5′-*O*-Fatty acyl derivatives of FLT, 5′-*O*-(12-azidododecanoyl) derivative of FLT (KP-1), and 5′-*O*-(12-thioethyldodecanoyl)thymidine (KP-17), also displayed good activity against cell-free (EC_{50} values of <0.2 to 0.4 μM, respectively) and cell-associated (EC_{50} values of 0.9 to 1.0 μM, respectively) virus and minimal cellular toxicity. Cellular uptake studies for 5′-*O*-fatty acyl derivatives of FLT and 3TC were conducted on CCRF-CEM cell line using a 5(6)-carboxyfluorescein derivative attached through 12-aminododecanoic acid as a linker to the nucleosides. The fluorescence-based studies indicated that the fatty acyl derivatives of FLT and 3TC have a higher cellular uptake versus that of the corresponding parent nucleoside substituted with a short alkyl group, such as β-alanine. The cellular uptake was concentration- and time-dependent.

In the third chapter, the synthesis and anti-HIV activities of succinate, suberate, and peptide derivatives of AZT, FLT, and 3TC are discussed. The compounds were designed in such a way to have 1 to 3 nucleosides. The hypothesis underlying this project is that the conjugates are able to deliver 1 to 3 nucleoside analogs to the HIV-infected cells. Some of the nucleoside-peptide conjugates were also substituted with the fatty acids. Peptides conjugated with fatty acids and nucleosides exhibited higher anti-

المنارة للاستشارات
www.ma

HIV activities when compared with those substituted only with nucleosides. Increasing the number of anti-HIV nucleosides to 2 or 3 on the peptide chain enhanced the anti-HIV potency. A glutamic acid ester derivative, FLT-Succinate-AZT(glutamyl)-3TC, containing three different nucleosides was the most active compound among all the derivatives with an EC_{50} value of 0.9 μM.

Chapter 4 describes the synthesis of FLT from thymidine using a solid-phase method to circumvent some of the problems associated with the solution-phase methods, such as multiple protecting and deprotecting steps.

Fifth chapter discusses the synthesis and anti-HIV activities of phosphotriesters of AZT and FLT. The conjugates were expected to get hydrolyzed inside the cell, to release nucleoside monophosphates, and to bypass first rate limiting phosphorylation step. The synthesized phosphotriester derivatives showed only modest anti-HIV activity, significantly lower than that of their parent nucleosides

In chapter 6, synthesis and characterization of dextran prodrug (3TCSD) of the antiviral drug 3TC is discussed. Dextran-3TC conjugate was synthesized to localize 3TC selectively in the liver and provide sustained release of the drug by the action of liver lysosomes. Liver accumulation of conjugated 3TC was enhanced by 50 fold when compared to that of parent drug.

المنارة للاستشارات
www.mar

In chapter 7 the synthesis and biological evaluation of double-barreled conjugates of sodium cellulose sulfate (CS) with 2′,3′-dideoxynucleosides analogs (AZT, FLT and 3TC) using different linkers are described. Cellulose sulfate is a polyanionic polymer which blocks HIV entry into the cells by interacting with the positive charge of viral gp120 protein. Nucleosides analogs act as reverse transcriptase inhibitors (RTIs). Conjugates were expected to undergo enzymatic hydrolysis and thereby releasing nucleosides and cellulose sulfate targeting two different strains of virus. Cellulose sulfate conjugates of nucleosides containing an acetate linker showed good activity against both R5 and X4 strains of HIV. For example a CS-AZT conjugate (acetate linker; 1.73% loading) was more effective than CS, especially against the R5 HIV-1 lab-adapted strain BaL. Similarly, sodium cellulose sulfate-acetate-FLT and showed better anti-HIV profile than sodium cellulose sulfate and the mixture of sodium cellulose sulfate and FLT.

Overall, the research described in this dissertation demonstrated that conjugation of anti-HIV nucleoside analogs with appropriate compounds (e.g., fatty acids, polymers, peptides groups, or other nucleosides) is an alternative strategy for designing more effective anti-HIV agents that can be further developed as therapeutic or preventative agents.

المنارة للاستشارات
www.mar

ACKNOWLEDGEMENTS

I would like to dedicate this work to my parents for the unparalleled love and support they bestowed upon me lifelong. I am grateful to my family for their matchless dedication towards my studies. I am grateful to my sister Dr. Jayashri Sarkar, for her useful suggestions as a colleague and constant support as a family member.

I am extremely grateful to my major advisor Dr. Keykavous Parang for his extensive and invaluable guidance and support, both inquisitively and financially, throughout my graduate study at the University of Rhode Island. I am fortunate to have his highly enterprising and accommodative guidance. I thank him for his patience and support at every point of my research. It has been a great pleasure working with and learning under him.

I express my gratitude to Dr. Gustavo Doncel, CONRAD, at Eastern Virginia Medical School, for his valuable support in carrying out the anti-HIV activities for the synthesized compounds. I thank him for his help in analyzing the biological data and his suggestions at each step in all the research project developments.

I am grateful to Dr. Anil Kumar for training me in the field of chemistry. He has been a good mentor during my course of Ph.D. I thank him for guiding me throughout all the challenges and the difficult moments of the work. I am grateful to Dr. Roberta King, Dr. Gongqin Sun and Dr. Bongsup Cho for their encouragement, discussions and helpful

المنارة للاستشارات
www.man

suggestions that made my research comfortable. I am grateful to Dr. Aftab Ahmed for his extended help and support for operating the ESI-Mass spectrometer, SELDI-Mass spectrometer and HPLC.

I would also like to thank Dr. Reza Mehvar (Department of Pharmaceutical Sciences, Texas Tech University Health Sciences Center, TX) for his support in my research work. My sincere thanks to Krishna C. Chimalakonda from Department of Pharmaceutical Sciences, Texas Tech University Health Sciences Center, TX for contributions in my research work.

I thank all the faculty, staff and friends at the University of Rhode Island for a great fun-filled time. I thank Dr. Guofeng Ye, Megrose Quiterio, Amelia Lyman, Michael Hanley, Dr. Sitaram Bhavaraju, Kelly Loethan and Dr. Yousef Ahmadibeni for their help with the experimentation. I thank Dr. Rakesh Tiwari and Dr. Xianfeng Gu for their valuable suggestions as group members during research work. I thank Aaron Socha for his help while working with NMR spectroscopy.

I would like to acknowledge USAID-CONRAD (HRN-A-00-98-00020-00) for providing me funding during first two years of Ph.D.

Preface

This thesis is written in the manuscript format. This work is dedicated to my beloved parents whose constant support and unmatched love guided me throughout the period of this study.

Chapter 1 and Chapter 2 discuss the synthesis and biological evaluations of fatty acyl derivatives of various ddNs including FLT, AZT, 3TC, FTC, and d4T. Nucleosides and myristic acid analogs act as RT inhibitors (RTIs) and viral NMT inhibitors, respectively. It was expected that the conjugation of compounds to enhance the lipophilicity and thus the cellular uptake and to reduce the toxicity associated with nucleosides. Furthermore, development of viral resistance to two active drugs would occur at a slower rate than to either compound alone.

In Chapter 3, various peptide, succinate and suberate derivatives of nucleosides were synthesized and evaluated for anti-HIV activities. Derivatives were synthesized in such a way to allow the incorporation of several anti-HIV nucleosides in one compound for combinational therapy. Peptide derivatives were myristoylated at *N*-terminal to improve the cellular uptake. The derivatives were expected to release different nucleosides intracellularly, to provide synergic effect, and to reduce the viral drug resistance.

Chapter 4 deals with reported solution-phase methods for the synthesis of 3′-fluoro-3′-deoxythymidine (FLT) are cumbersome, require purification of intermediates,

and include several protecting/deprotecting steps. To circumvent these problems, a solid-phase strategy was designed for the synthesis of FLT.

In Chapter 5 nucleosides are converted into their monophosphate, diphosphate and finally to triphosphate by enzymatic phosphorylation. Conversion to nucleoside monophosphate is the rate-limiting step. Several phosphate triester derivatives of FLT and AZT with myristic acid analogues were synthesized using glycol as a linker in order to improve their cellular uptake and bypass rate-limiting monophosphorylation.

In Chapter 6, 3TC is used to treat hepatitis B viral infection. Treatment of HBV infection is significantly dependent on its distribution and accumulation in the liver. Therefore, 3TC was conjugated with dextran (25 kD) by using succinate linker to synthesize 3TC-succinate-dextran conjugates. Since dextran (25 kD) has the capacity to accumulate in the liver, the conjugate was expected to get hydrolyzed inside the liver releasing free 3TC. Using this approach allowed a higher amount of 3TC to target the liver.

Capter 7 deals with cellulose sulfate that belongs to the category of sulfonate and sulfate polyanionic microbicides which inhibitors HIV entry and sperm-function. Bifunctional conjugates containing AZT or FLT as RTIs and cellulose sulfate as HIV entry blockers were synthesized. The conjugates were expected to provide additional bisubstrate compounds having synergistic and broad-spectrum activity against susceptible and AZT-resistant strains and sperm and STD-pathogen inhibiting properties.

TABLE OF CONTENTS

List of Tables

Chapter 1

Chapter 2

Chapter 3

Chapter 5

Chapter 6

Chapter 7

List of Figures

Introduction

Chapter 1

Chapter 6

List of Schemes

Chapter 4

Chapter 5

Chapter 6

Chapter 7

List of Abbreviations

3TC	: Lamivudine, 2',3'-dideoxy-3'-thiacytidine
3TCS	: 3TC Succinate
3TCSD	: 3TC-Succinate-Dextran
5FU	: Floxuridine, 5-fluoro-2'-deoxyuridine
AcOH	: Acetic Acid
AI	: Antiviral Index
AIDS	: Acquired Immunodeficiency Syndrome
AUC	: Area Under Curve
AZT	: Zidovudine, 3'-azido-3' deoxythymidine
t-BuOOH	: *tert*-butyl hydroperoxide
CCR5	: Chemokine (C-C motif) Receptor 5
CD4	: Cluster of Differentiation 4
CS	: Cellulose Sulfate
CSA	: Cellulose Sulfate Acetate
CTC	: Cell- to- Cell Transmission Assay
CTS	: Cytotoxicity Assay
CXCR4	: Chemokine (CXC motif) Receptor 4
d4T	: Stavudine, 2',3'-didehydro-2',3'-dideoxythymidine
DAST	: Diethylaminosulfur trifluoride
ddN	: 2′,3′-Dideoxynucleoside
DCM	: Dichloromethane

DIAD : Diisopropylazodicarboxylate

DIC : N,N'-diisopropylcarbodiimide

DIPEA : Diisopropylethylamine

DMAP : Dimethylaminopyridine

DMF : Dimethylformamide

DMSO : Dimethylsulfoxide

DMTr-Cl : 4,4′-Dimethoxytrityl Chloride

EC_{50} : 50% Effective Concentration

FAM : 5(6)-carboxyfluorescein

FLT : Alovudine, 3'-fluoro-3' deoxythymidine

FTC : Emtricitabine, 2',3'-dideoxy-5-fluoro-3'-thiacytidine

gp41 : Glycoprotein 41

gp120 : Glycoprotein 120

HAART : Highly Active Anti-Reteroviral Therapy

HBTU : 2-(1H-benzotriazole-1-yl)-1,1,3,3-tetramethyluronium hexafluorophosphate

HBV : Hepatitis B Virus

HeLa : Human cervical carcinoma

HIV : Human immunodeficiency virus

HPLC : High Performance Liquid Chromatography

IC_{50} : 50% Inhibitory Concentration

IL-1α : Interleukin (1α) Proinflammatory Cytokine

MDR : Multidrug Resistant

N9	: Nonoxynol 9
NMM	: *N*-methylmorpholine
NMR	: Nuclear Magnetic Resonance
NMT	: *N*-myristoyl Transferase
ppm	: Parts Per Millions
RPC	: Reversed-phase Chromatography
RT	: Reverse Transcriptase
RTI	: Reverse Transcriptase Inhibitor
SEC	: Size Exclusion Chromatography
TBAF	: Tetrabutylammonium Fluoride
TBDMS	: *tert*-butyldimethylsilyl
TFA	: Trifluoroacetic acid
TFV	: Tenofovir, (R)-9-(2-phosphonomethoxypropyl)adenine
THF	: Tetrahydrofuran
TPP	: Triphenylphosphine
STD	: Sexually Transmitted Diseases
VBI(IIIB)	: Viral Entry Inhibition Assay (Lymphocytotropic Strain)
VBI(BaL)	: Viral Entry Inhibition Assay (Monocytotropic Strain)

Introduction

1. Human Immunodeficiency Virus (HIV)

Human immunodeficiency virus (HIV) is a reterovirus, which mainly targets the immune cells, such as T-lymphocytes, monocytes, B lymphocytes, and macrophages that have CD4, a member of the immunoglobulin superfamily (Costin, 2007). The infection induces progressive loss of immune system, which ultimately results in the opportunistic infections and malignancies associated with acquired immunodeficiency syndrome (AIDS). According to the UNAIDS reports almost 33.2 million people were living with HIV at the end of 2007, a year in which 2.5 million people were newly infected with HIV infection and 2.1 million died of AIDS. Current antiretroviral drugs do not eliminate HIV and restore the immune system completely. However, all combination therapy can reduce the viral replication to the minimum level to prevent the advance of the infection. Another problem is the continued development of drug-resistant virus to current antiretroviral drugs. Thus, there is an urgent need to discover new, safe, and potent anti-HIV agents and preventive strategies as existing therapies succumb to newly developed resistant virus.

HIV shares features common to all retroviruses and is able to route genetic information from RNA to DNA. This is accomplished by a unique enzyme, Reverse transcriptase (RT), which is encoded by a gene within the retroviral genome. HIV contains three different types of structural proteins named the external glycoprotein (Env), the capsid protein (Gag), and the viral enzymes necessary for replication (Pol)

proteins. Env proteins (gp 120 and gp41) are responsible for viral binding with the host cell membrane and for the infectivity of the viral particle by means of attachment to specific cellular receptors. Gag proteins are responsible for forming the reteroviral core (capsid). Pol proteins include pr integrases, RT, and protease which are responsible for viral replication (Cohen et al., 2008).

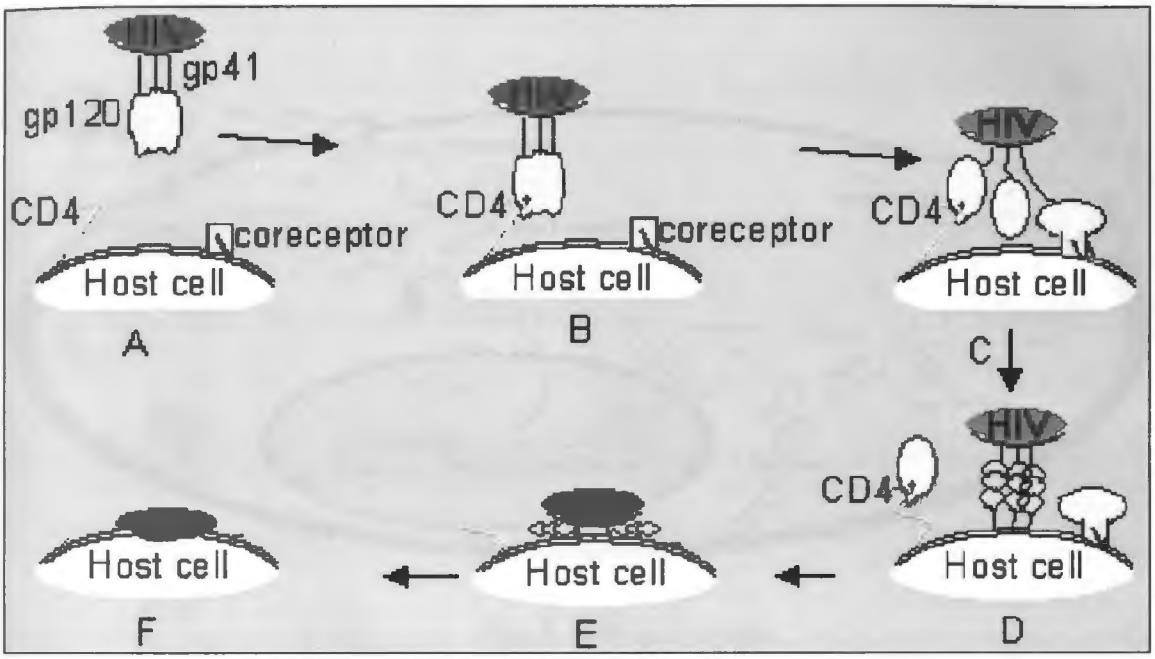

Fig 1:(A) HIV and host cell; (B) Binding of gp120 at CD4 inducing changes in gp120; (C) Attachment of gp120 with coreceptor; (D) Dissociation of gp41 from gp120; (E) Confirmation changes in gp41 leading to hairpin formation bringing the two membranes closer; (F) fusion of viral envelope and release of viral content in cell

HIV life cycle starts with the attachment of HIV gp120 Env proteins to the host cell membrane receptors. First, HIV Env gp120 glycoprotein binds to CD4 receptor of the host cell (Dimitrov et al., 2005 and Weissenhorn et al., 1997). This binding induces conformational changes in gp120 molecule and exposes its other binding sites becoming suitable for attachment with coreceptors. Coreceptor binding

leads to another conformational change in the viral envelope leading to gp120 dissociation from gp41. Exposure of hydrophobic gp41 domains results in gp41-cell membrane interaction. Finally, HR1 and HR2 regions of gp41 form a six-helix hairpin like structure bringing the two membranes closer to each other initiating fusion process and release of viral contents in the host cell (Fig. 1).

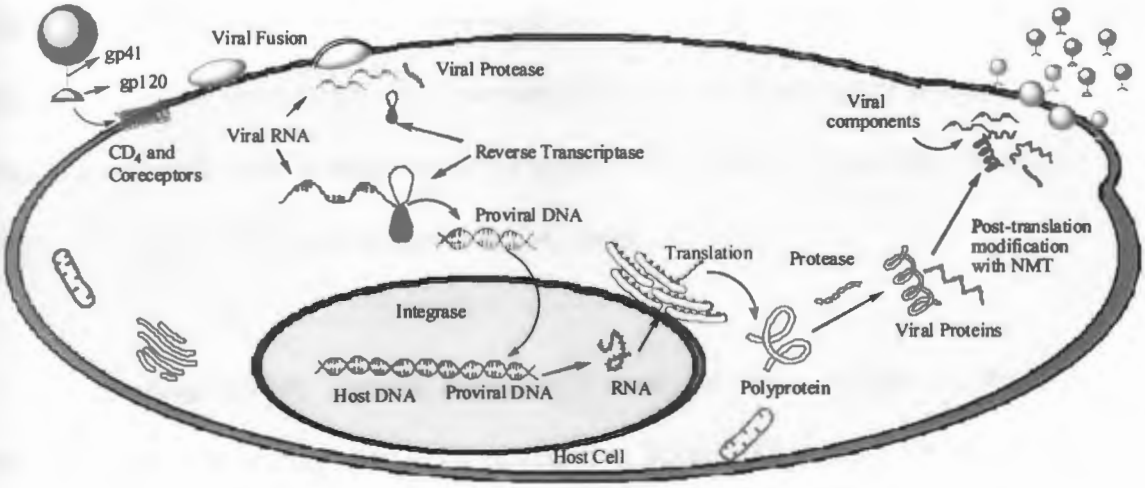

Fig. 2. HIV Life cycle

Once inside the host cell, the single stranded RNA gets converted into the double stranded DNA by the action of RT (Fig. 2). Proviral DNA is then incorporated into the host cell DNA by the action of integrase enzyme. Proviral DNA produces viral RNA, which after translation forms polyproteins. Polyproteins undergo post-translation by the action of protease enzyme to form functional proteins. These proteins are further myristoylated at *N*-terminal glycine residue in the presence of *N*-myristoyl transferase (NMT) enzyme to make them lipophilic. Lipophilic proteins

along with the genetic material move towards the cell membrane resulting in the formations of virus particles (Farazi et al., 2001; Wu et al., 2004).

2. R5 and X4 Strains of HIV-1

Positively charged V3 loop of the viral protein gp120 interacts with the negatively charged CD4 receptor, CCR5, and CXCR4 coreceptors (Kajumo et al., 2000, Cheng-Mayer et al., 1997). Transmembrane chemokine receptors belong to two different classes of receptors C-X-C (α-receptor) and C-C (β-receptor) (Deng et al., 1996). The classification is on the basis of separation of first two cysteines by single amino acid in C-X-C class and adjacent in C-C class.

Depending on the type of coreceptors used for viral binding to the cell membrane, HIV can be classified in two categories; R5 and X4 strains of virus. These two strains show completely different interactions with the host cells and produce different pathogenic effects (Pollaskis et al., 2004, Fais et al., 1999). R5 strain of virus interacts with CCR5 chemokine coreceptors for cell-binding (monocytotropic strain, M-tropic) (Cheng-Mayer et al., 1997, Knox et al., 2004, Alkhatib et al., 1996). X4 strains of virus uses CXCR4 coreceptors to enter in the cells (lymphocytotropic strain, T-tropic) (Yi et al., 1999, Kajumo et al., 2000). X4-strains of HIV contain higher strength of positive charges at V3 loop than R5 virus (Shattock et al., 2002, Meylan et al., 1994). Therefore, X4 virus interacts much better with the cell-membrane than R5, but at the same time are more vulnerable to polyanionic entry blockers.

3. 2′,3′-Dideoxynucleoside Analogs as Reverse Transcriptase Inhibitors

2′,3′-Dideoxynucleoside (ddN) analogs are used as the commercial drugs for the treatment of HIV infection, AIDS, hepatitis B virus (HBV), and cancer. Several ddNs, such as 2',3'-dideoxy-3'-thiacytidine (lamivudine, 3TC), 2',3'-didehydro-2',3'-dideoxythymidine (stavudine, d4T), 2',3'-dideoxy-5-fluoro-3'-thiacytidine (emtricitabine, FTC), 2',3'-dideoxycytidine (zalcitabine, ddC), 3'-azido-3' deoxythymidine (zidovudine, AZT), (R)-9-(2-phosphonomethoxypropyl)adenine (tenofovir, TFV), and 5-fluoro-2'-deoxyuridine (Floxuridine, 5FU) are commercially used as in combination therapy with other drugs.

In order to produce their pharmacological effects, on entering the cells the majority of ddNs are phosphorylated intracellularly to monophosphates, diphosphates, and triphosphates in the presence of host cellular kinases. RT is a key enzyme in the replicative cycle of HIV and HBV. In case of anti-retroviral therapy, ddNs are called RT inhibitors. For example, anti-HIV ddNs are prodrugs that must enter the infected cell and then be phosphorylated to the active triphosphates by host cell kinases. As triphosphates, the ddNs act through inhibition of RT by means of substrate competition with natural deoxynucleosides and through chain termination of the nascent DNA being transcribed by the viral RT by means of incorporation of the ddN triphosphates that lacks the 3′-hydroxyl group (Lee et al., 2001, Nikolenko et al., 2005). Fig. 3 shows the activation of AZT as a representative example.

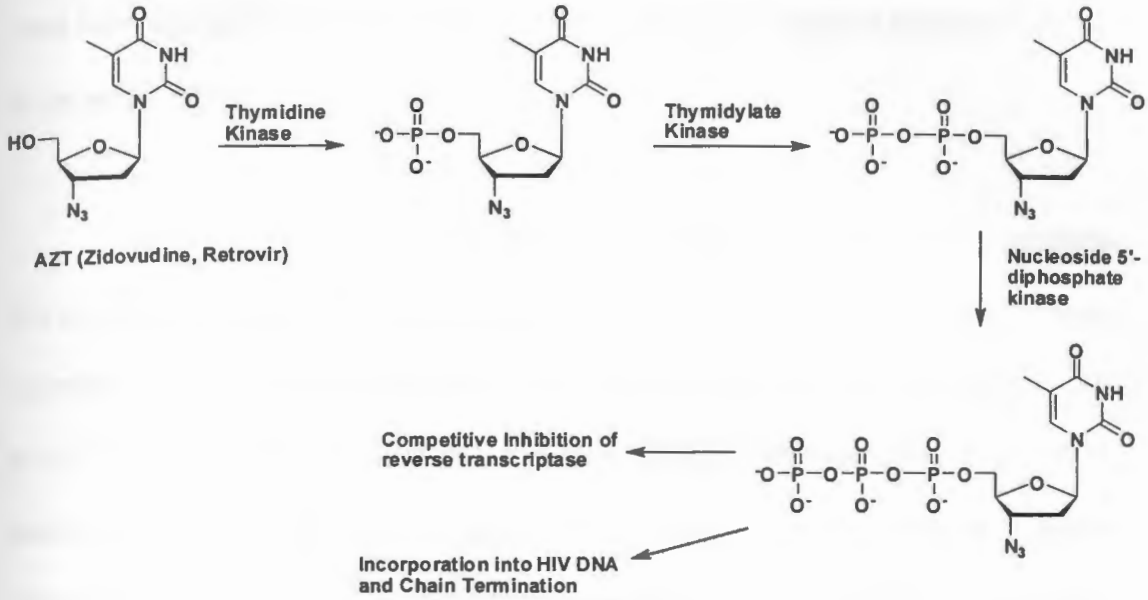

Fig. 3: Mechanism of anti-HIV activity of AZT.

The major problems with ddNs are their high level of clinical toxicities such as bone marrow suppression and neuropathy For example, AZT triphosphate also inhibits mitochondrial DNA polymerase (Lewis et al., 2006, Lund et al., 2007). Thus, treatment with ddNs faces several challenges, such as a low therapeutic index caused in part by inhibition of cellular polymerases, absolute dependence on host cell kinase-mediated activation (Fig. 1), limited brain uptake, short half-life in blood, low potential for metabolic activation, and the rapid development of resistance to drugs by HIV-1. Some important limitations are discussed briefly.

The hydrophilic nature of ddNs leads to limited cellular uptake and bioavailability. Extensive efforts have been carried out to synthesize lipophilic prodrugs of anti-HIV nucleosides (Parang et al., 1998, 1997). The lipophilic prodrugs

must have acceptable stability prior to cellular uptake and selective biotransformation to the active species.

The individuals being treated with the ddNs stops responding to the treatment due to drug resistance. The continual use of ddNs often results in emergence of drug-resistant virus. For example, single point mutation at Met184 with Val and Ile results in 3TC and FTC resistant HIV strains (Mulder et al., 2008, Sarafianos et al., 1999, Diallo et al., 2003). HIV also produces resistance against d4T by K65R mutation (Garcia-Lerma et al., 2007). Similarly, mutation at Met 552 with Val and Ile results in 3TC and FTC resistant HBV strains (Das et al., 2001). Viruses with resistance mutations accumulate, sometimes with complete replacement of wild-type virus by drug resistant mutants.

Combination therapy for controlling HIV-1 infections involving different classes of anti-HIV drugs provides several potential advantages to reduce the drug resistance (Zdanowicz, 2006). Two or more drugs may have additive or synergistic interactions that produce better efficacy than either drug alone. In highly active anti-reteroviral therapy (HAART) HIV is targeted by different classes of reverse transcriptase inhibitors along with protease inhibitors.

Furthermore, the first phosphorylation step of conversion of several ddNs to their monophosphates is a slow and rate-limiting process (Van et al., 1990). In attempts to bypass the first rate-limiting phosphorylation step in the metabolic conversion of nucleoside analogs, numerous prodrugs of 5′-monophosphate types, such as neutral species of phosphotriester derivatives of nucleosides have been

proposed (Parang et al., 2000) which are readily taken by the infected cells. After the action of hydrolytic enzymes, phosphotriesters results are converted to active nucleoside monophosphate intracellularly.

4. Objectives of research

Various ddN conjugates with fatty acids, peptides, other nucleosides, and polymer derivatives were synthesized with an intention to develop multifunctional anti-HIV-1 agents. The hypothesis underlying this project was that safe, potent, and broad-spectrum multifunctional anti-HIV agents can be designed to deliver and release different active species intracellularly at the same time. Furthermore, development of viral resistance to several active drugs would occur at a much slower rate than to either compound alone. Subtype and mutant coverage will also be enhanced. Specific objectives for each class of compounds are discussed here briefly.

Chapter 1 and Chapter 2

First two chapters discuss the synthesis and biological evaluations of fatty acyl derivatives of various ddNs including 3′-fluoro-3′-deoxythymidine (FLT), AZT, 3TC, FTC, and d4T. Nucleosides and myristic acid analogs act as RT inhibitors (RTIs) and viral NMT inhibitors, respectively. It was expected that the conjugation of compounds to enhance the lipophilicity and thus the cellular uptake and to reduce the toxicity associated with nucleosides. Furthermore, development of viral resistance to two active drugs would occur at a slower rate than to either compound alone.

Chapter 3

Various peptide, succinate and suberate derivatives of nucleosides were synthesized and evaluated for anti-HIV activities. Derivatives were synthesized in such a way to allow the incorporation of several anti-HIV nucleosides in one compound for combinational therapy. Peptide derivatives were myristoylated at *N*-terminal to improve the cellular uptake. The derivatives were expected to release different nucleosides intracellularly, to provide synergic effect, and to reduce the viral drug resistance.

Chapter 4

Reported solution-phase methods for the synthesis of FLT are cumbersome, require purification of intermediates, and include several protecting/deprotecting steps. To circumvent these problems, a solid-phase strategy was designed for the synthesis of FLT (Agarwal et al., 2007)

Chapter 5

Nucleosides are converted into their monophosphate, diphosphate and finally to triphosphate by enzymatic phosphorylation. Conversion to nucleoside monophosphate is the rate-limiting step. Several phosphate triester derivatives of FLT and AZT with myristic acid analogues were synthesized using glycol as a linker in order to improve their cellular uptake and bypass rate-limiting monophosphorylation (Agarwal et al., 2008).

Chapter 6

3TC is used to treat hepatitis B viral infection. Treatment of HBV infection is significantly dependent on its distribution and accumulation in the liver. Therefore, 3TC was conjugated with dextran (25 kD) by using succinate linker to synthesize 3TC-succinate-dextran conjugates (Chimalakonda et al., 2007). Since dextran (25 kD) has the capacity to accumulate in the liver, the conjugate was expected to get hydrolyzed inside the liver releasing free 3TC. Using this approach allowed a higher amount of 3TC to target the liver.

Chapter 7

Cellulose sulfate belongs to the category of sulfonate and sulfate polyanionic microbicides which inhibitors HIV entry (Ketas et al., 2003; Chan and Kim, 1998) and sperm-function (Anderson et al., 2000). Bifunctional conjugates containing AZT or FLT as RTIs and cellulose sulfate as HIV entry blockers were synthesized. The conjugates were expected to provide additional bisubstrate compounds having synergistic and broad-spectrum activity against susceptible and AZT-resistant strains and sperm and STD-pathogen inhibiting properties.

5. References

Agarwal, H. K., Doncel, G. F., Parang, K. Synthesis and anti-HIV activities of phosphate triester derivatives of 3'-fluoro-2',3'-dideoxythymidine and 3'-azido-2',3'-dideoxythymidine. *Tet. Lett.*, **2008**, 49, 4905-4907.

Agarwal, H. K., Parang, K. Application of solid phase chemistry for the synthesis of 3'-fluoro-3'-deoxythymidine. *Nucleoside, Nucleotide Nucleic acid.*, **2007**, 26, 317-322.

Alkhatib, G., Combadiere, C., Broder, C. C., Feng, Y., Kennedy, P. E., Murphy, P. M., Berger, E. A. CC-CKR5: A RANTES, MIP-1α and MIP-1β receptor as a fusion cofactor for macrophage-tropic HIV-1. *Science*, **1996**, 272, 1955-1958.

Anderson, R. A., Chany, C., Feathergill, K., Diao, X., Cooper, M., Kirkpatrick, R., Spear, P., Waller, D. P., Doncel, G. F., Zaneveld L. J. D. Evaluation of the potential of poly(styrene-4-sulfonate) as an effective preventative agent against conception and sexually transmitted diseases. *J. Androl.*, **2000**, *21*, 862-875.

Chan, D. C. and Kim, P. S. HIV entry and its inhibition. *Cell*, **1998**, 93, 681-684.

Cheng-Mayer, C., Liu, R., Landau, N. R., Stamatatos, L. Macrophage Tropism of human immunodeficiency virus type 1 and utilization of the CC-CKR5 coreceptor. *J. Virol.*, **1997**, 71, 1657-1661.

Chimalakonda, K. C., Agarwal, H. K., Kumar, A., Parang, K., Mehvar, R. Synthesis, analysis, in vitro characterization and in vivo disposition of a lamivudine-dextran conjugate for selective antiviral delivery to the liver. *Bioconjug. Chem.*, **2007**, 18, 2097-2108.

Cohen, M. S., Hellmann, N., Levy, J. A., DeCock, K. and Lange J. The spread, treatment, and prevention of HIV-1: evolution of a global pandemic. *J. Clin. Invest.*, **2008**, 118, 1244-1254.

Costin, J. M. Cytopathic Mechanisms of HIV-1. *Virol. J.*, **2007**, 4, 100-122.

Das, K., Xiong, X., Yang, H., Westland, C. E., Gibbs, C. S., Sarafianos, S. G., Arnold, E. Molecular modeling and biochemical characterization reveal the mechanism of hepatitis b virus polymerase resistance to lamivudine (3TC) and emtricitabine (FTC). *J. Virol.*, **2001**, 75, 4771-4779.

Deng, H., Liu, R., Ellmeier, W., Choe, S., Unutmaz, D., Burkhart, M., Marzio, P. D., Marmon, S., Sutton, R. E., Hill, C. M., Davis, C. B., Peiper, S. C., Schall, T. J., Littman, D. R., Landau, N. R. Identification of a major co-receptor for primary isolates of HIV-1. *Nature*, **1996**, 381, 661-666.

Diallo, K., Götte, M., Wainberg1, M. A. Molecular Impact of the M184V Mutation in Human Immunodeficiency Virus Type 1 Reverse Transcriptase. *Antimicrob. Agents Chemother.*, **2003**, 47, 3377-3383.

Dimitrov, A. S., Louis, J. M., Bewley, C. A., Clore, M. G., Blumenthal, R. Conformational changes in HIV-1 gp41 in the course of HIV-1 envelope glycoprotein-mediated fusion and inactivation. *Biochemistry*, **2005**, 44, 12471-12479.

Fais, S., Lapenta, C., Santini, S. M., Spada, M., Parlato, S., Logozzi, M., Rizza, P., Belardelli, R. Human immunodeficiency virus type 1 strains R5 and X4 induce different pathogenic effects in hu-PBL-SCID mice, depending on the state of activation/differentiation of human target cells at the time of primary infection. *J. Virol.*, **1999**, 73, 6453-6459.

Farazi, T. A., Waksman, and G., Gordon, J. I. The Biology and Enzymology of Protein *N*-Myristoylation. *J. Biol. Chem.*, **2001**, 276, 39501–39504.

García-Lerma, J. G., MacInnes, H., Bennett, D., Reid, P., Nidtha, S., Weinstock, H., Kaplan, J. E., Heneine, W. A novel genetic pathway of human immunodeficiency virus type 1 resistance to stavudine mediated by the K65R mutation. *J. Virol.*, **2003**, 77, 5685–5693.

Kajumo, F., Thompson, D. A. D., Guo, Y. and Dragic, T. Entry of R5X4 and X4 HIV-1 strains is mediated by negatively charged and tyrosine residues in the amino-terminal domain and the second extracellular loop of CXCR4. *Virology*, **2000**, 271, 240-247.

Ketas, T. J., Frank, I., Klasse, P. J., Sullivan, B. M., Gardner, J. P., Spenlehauer, C., Nesin, M., Olson, W. C., Moore, J. P., Pope, M. Human immunodeficiency virus type 1 attachment, coreceptor, and fusion inhibitors are active against both direct and trans infection of primary cells. *J. Virol.*, **2003**, 77, 2762-2767.

Knox, K. S., Day, R. B., Wood, K. L., Kohli, L. L., Hage, C. A., Foresman, B. H., Schnizlein-Bick, C. T., Twigg, H. L. Macrophages exposed to lymphotropic and monocytotropic HIV induce similar CTL responses despite differences in productive infection. *Cell. Immunol.*, **2004**, 229, 130-138.

Lee, K., Chu, C. K. Molecular modeling approach to understanding the mode of action of L-nucleosides as antiviral agents. *Antimicrob. Agents Chemother.*, **2001**, 45, 138–144.

Lewisa, W., Kohlera, J. J., Hosseinia, S. H., Haasea, C. P., Copelandb, W. C., Bienstockb, R. J., Ludawaya, T., McNaughta, J., Russa, R., Stuarta, T., Santoiannia, R. Antiretroviral nucleosides, deoxynucleotide carrier and mitochondrial DNA: evidence supporting the DNA pol γ hypothesis. *AIDS*, **2006**, 20, 675–684.

Lund, K. C., Peterson, L. L., and Wallace, K. B. Absence of a Universal Mechanism of Mitochondrial Toxicity by Nucleoside Analogs. *Antimicrob. Agents Chemother.*, **2007**, 51, 2531–2539.

Meylan, P. R. A., Kornbluth, R. S., Zbinden, I., Dichman, D. D. Influence of host cell type and V3 loop of the surface glycoprotein on susceptibility of human immunodeficiency virus type 1 to polyanion compounds. *Antimicrob. Agents Chemother.*, **1994**, 38, 2910-2916.

Mulder, L. C. F., Harari, A., Simon, V. Cytidine deamination induced HIV-1 drug resistance. *Proc. Natl. Acad. Sci. U. S. A.* **2008**, 105, 5501–5506.

Nikolenko, G. N., Palmer, S., Maldarelli, M., Mellors, j. W., Coffin, J. M., Pathak, V. K. Mechanism for nucleoside analog-mediated abrogation of HIV-1 replication: Balance between RNase H activity and nucleotide excision. *Proc. Natl. Acad. Sci. U. S. A.* **2005**, 102, 2093–2098.

Parang, K., Wiebe, L. I., Knaus, E. E. Syntheses and biological evaluation of 5'-*O*-myristoyl derivatives of thymidine against human immunodeficiency virus (HIV-1). *Antiviral. Chem. Chemother.*, **1997**, 8, 417-427.

Parang, K., Knaus, E. E., Wiebe, L. I. Synthesis, *in vitro* anti-HIV structure-activity relationships and stability of 5'-*O*-myristoyl analogue derivatives of 3'-azido-2',3'-dideoxythymidine as potential prodrugs of 3'-azido-2',3'-dideoxythymidine (AZT). *Antiviral. Chem. Chemother.*, **1998**, 9, 311-323.

Parang, K., Wiebe, L. I., Knaus, E. E. *In vivo* pharmacokinetic parameters, liver and brain uptake of (±)-3'-azido-2',3'-dideoxy-5'-*O*-(2-bromomyristoyl)thymidine as potential prodrug of 3'-azido-3'-deoxythymidine. *J. Pharm. Pharmacol.* **1998**, 50, 989-996.

Parang, K., Knaus, E. E., Wiebe, L. I. Synthesis, *in vitro* anti-HIV activity, and biological stability of 5'-*O*-myristoyl analogue derivatives of 3'-fluoro-2',3'-dideoxythymidine (FLT) as potential prodrugs of FLT. *Nucleosides & Nucleotides*, **1998**, 17, 987-1008.

Parang, K., Wiebe, L. I., Knaus, E. E. Novel approaches in designing prodrugs of AZT. *Curr. Med. Chem.*, **2000**, 7, 995-1039.

Pollakis, G., Abebe, A., Kliphuis, A., Chalaby, M. I. M., Bakker, M., Mengistu, Y., Brouwer, M., Goudsmit, J., Schuitemaker, H.. Paxton W. A. Phenotypic and genotypic comparisons of CCR5- and CXCR4-tropic human immunodeficiency virus type 1 biological clones isolated from subtype C-infected individuals. *J. Virol.*, **2004**, 78, 2841-2852.

Sarafianos, S. G., Das, K., Clark, Jr., A. D., Ding, J., Boyer, P. L., Hughes, S. H., Arnold, E. Lamivudine (3TC) resistance in HIV-1 reverse transcriptase involves steric hindrance with b-branched amino acids. *Proc. Natl. Acad. Sci. U. S. A.*, **1999**, 96, 10027-10032.

Shattock, R. J. and Doms, R. W. AIDS models: Microbicides could learn from vaccines. *Nat. Med.*, **2002**, 8, 425.

Van Roey, J. P., Taylor, E. W., Chu, C. K., Shinazi, R. F. Correlation of molecular conformation and activity of reverse transcriptase inhibitors. *Ann. N. Y. Acad. Sci.*, **1990**, 616, 29–40.

Weissenhorn, W., Dessen, A., Harrison, S. C., Skehel, J. J., Wiley, D. C. Atomic structure of the ectodomain from HIV-1 gp41. *Nature*, **1997**, 387, 426-430.

Wu, Z., Alexandratos, J., Ericksen, B., Lubkowshi, J., Gallo, R. C., Lu, W. Total chemical synthesis of N-myristoylated HIV-1 matrix protein p17: Structural and mechanistic implications of p17 myristoylation. *Proc. Natl. Acad. Sci. U. S. A.*, **2004**, 101, 11587-11592.

Yi, Y., Isaacs, S. N., Williams, D. A., Frank, I., Schols, D., Clerco, E. D., Kolson, D. L., Collman, R. G. Role of CXCR4 in cell-cell fusion and infection of monocyte-derived macrophages by primary human immunodeficiency virus type 1 (HIV-1) strains: Two distinct mechanisms of HIV-1 dual tropism. *J. Virol.*, **1999**, 73, 7117-7125.

Zdanowicz, M. M. The pharmacology of HIV drug resistance. *Am. J. Pharm. Educ.*, **2006**, 70, 100-122.

Chapter 1

Synthesis and Biological Evaluation of 5′-*O*-Fatty Acyl Ester Derivatives of 3′-Fluoro-2′,3′-dideoxythymidine

Hitesh K. Agarwal,[a] Guofeng Ye,[a] Megrose Quiterio,[a] Anil Kumar,[a] Amelia Lyman,[a] Gustavo F. Doncel,[b] Keykavous Parang[a]

[a]Department of Biomedical and Pharmaceutical Sciences, University of Rhode Island, Kingston, RI, USA, 02881;

[b]CONRAD, Department of Obstetrics and Gynecology, Eastern Virginia Medical School, Norfolk, VA, USA 23507

1.1. Abstract

A number of 5′-*O*-fatty acyl derivatives of 3′-fluoro-2′,3′-dideoxythymidine (FLT) were synthesized and their anti-HIV activities were evaluated and compared with the corresponding 5′-*O*-fatty acyl derivatives of 3′-azido-2′,3′-dideoxythymidine (AZT). Various assays such as anti-HIV activity against cell-free and cell-associated virus, multidrug resistant virus, vaginal cell viability studies, and sperm viability studies were performed for the selected compounds. Among the compounds, 5′-*O*-(12-azidododecanoyl) (KP-1), 5′-*O*-myristoyl (KP-16), and 5′-*O*-(12-thioethyldodecanoyl) (KP-17) derivatives of FLT with EC_{50} values of 0.4 μM, 1.1 μM, and < 0.2 μM, respectively, against cell-free virus were found the most potent compounds with minimal cellular toxicity, and were selected for further studies. The tetradecanol ether analogs of FLT (**1.7**, EC_{50} = 176 μM) and AZT (**1.8**, EC_{50} = 27.6 μM) were found to be inactive under similar conditions because of the lack of hydrolysis to the parent compounds, nucleosides and myristic acid. The data suggest that the ester hydrolysis to FLT or AZT and fatty acids was critical for producing the anti-HIV activity. A number of FLT derivatives were further studied to determine their physicochemical properties (e.g., solubility, Log P, pKa) and cellular uptake. Cellular uptake studies were conducted on CCRF-CEM cell line using 5(6)-carboxyfluorescein derivatives of FLT attached through β-alanine (**1.5**) or 12-aminododecanoic acid (**1.6**) as linkers. Fluorescein-substituted analog of FLT with long chain length (**1.6**) showed > 12 times better cellular uptake profile than analog with short chain length (**1.5**). Cellular uptake studies revealed that the attachment of fatty acid improves the cellular uptake of the

nucleoside conjugate. KP-1 and KP-17 are currently under evaluation in the preclinical studies.

1.2. Introduction

Alovudine (FLT, 3′-fluoro-2′,3′-dideoxythymidine) is a thymidine nucleoside analogue and a potent human immunodeficiency virus (HIV) reverse transcriptase (RT) inhibitor. FLT showed 10 times more potency against HIV 1 when compared with Zidovudine (AZT) and was even active against AZT resistant virus (Kong et al., 1992). FLT displayed similar pharmacokinetic parameters as AZT and Stavudine (d4T) in monkey and rats (Schinazi et al., 1990 and Boudinot et al., 1991).

Once enters the cell, FLT gets converted into FLT triphosphate by the action of host cellular kinases (Kong et al., 1992). FLT triphosphate is then incorporated into the DNA of HIV leading to chain termination at 3'-position. FLT is also a potent inhibitor of RT enzyme, which coverts viral RNA into proviral DNA (Mansuri et al., 1990) (Figure 1.1).

FLT was under clinical evaluation from 1990–1992. The studies were stopped after FLT failed phase II clinical trials because of the observed hematological toxicities including neutropenia, leucopenia, and anemia (Rusconi, 2003). The toxicity of FLT was suggested to be the result of DNA damage and apoptosis (Sundseth et al., 1996). In 2001, Medivir (Sweden) again started the phase II clinical trials of FLT (Rusconi, 2003). The trials were conducted on fifteen HIV infected patients with 7.5

mg/day alovudine and all the patients showed significant reduction in HIV load with no serious side effects. In the latest study, alovudine was used in doses of 0.5, 1.0 and 2.0 mg/day for four weeks to test the viral inhibition (Ghosn et al., 2007). The results indicated that FLT produced modest viral load reduction but could not produce the desired clinical anti-viral activity.

N-Myristoyl transferase (NMT) enzyme is involved in catalyzing the myristoylation of several proteins in HIV life cycle (e.g., capsid protein p17, $Pr160^{gag\text{-}pol}$, $Pr55^{gag}$, $p27^{nef}$). At *N*-terminal glycine, viral proteins (gag and nef) are covalently attached to myristic acid in the presence of NMT. Myristic acid attachment makes the proteins more hydrophobic, which improves protein-protein and protein-membrane interactions (Farazi et al., 2001). For example, after the *N*-myristoylation, p17 protein localizes itself towards the cell membrane, where new virus is produced (Wu et al., 2004) (Figure 1.1).

The replication of HIV-1 can be inhibited by heteroatom-containing analogs of myristic acid without accompanying cellular toxicity (Bryant et al., 1993, Takamune et al., 2002). It has been previously reported that several fatty acids, such as 2-methoxydodecanoic acid, 4-oxatetradecanoic acid, and 12-thioethyldodecanoic acid, reduce HIV-1 replication in acutely infected T-lymphocytes. For example, 12-thioethyldodecanoic acid was moderately active (EC_{50} = 9.4 μM) against HIV-infected T4 lymphocytes (Parang et al., 1997).

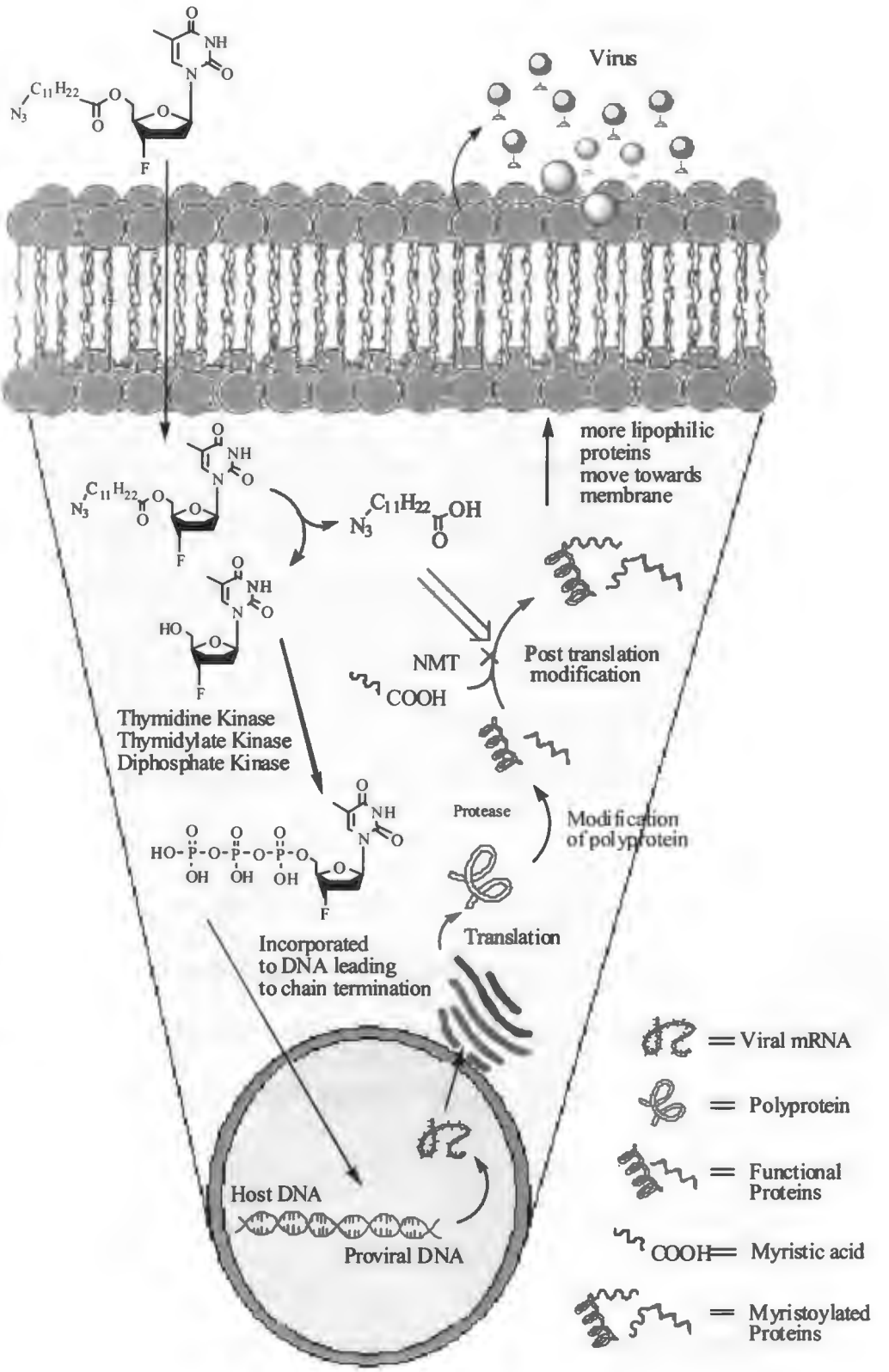

Figure 1.1. Proposed mechanism of action of 5′-*O*-fatty acyl derivatives of nucleosides.

It is hypothesized that the attachment of nucleoside analogs to the long chain myristic acid analogs enhances their lipophilicity and thus their cellular uptake. Once the ester conjugate enters the cells, it gets hydrolyzed by esterases and generates two active molecules, nucleoside analog and fatty acid, targeting reverse transcriptase (RT) and *N*-myristoyl transferase (NMT) enzymes, respectively (Figure 1.1).

A number of 5′-*O*-fatty acyl derivatives of FLT were previously reported to have better and wider activity profile than FLT (Parang et al., 1996, 1997). These compounds were designed to act as bifunctional anti-HIV agents targeting two important enzymes for viral reproduction. Herein, we report the synthesis of additional compounds, a more extensive evaluation of biological activities of 5′-*O*-fatty acyl derivatives of FLT in comparison with 5′-*O*-fatty acyl derivatives of AZT and parent nucleosides, cellular uptake, mechanistic studies, and their applications as anti-HIV agents and microbicides.

Microbicides are the compounds that can be applied inside the vagina or rectum topically to protect against sexually transmitted diseases including HIV. There is an urgent need to develop a safe over-the-counter intravaginal/intrarectal anti-HIV microbicide for prevention of HIV transmission.

1.3. Materials and Methods

1.3.1. Materials

FLT was synthesized in 5 g scale according to the previously reported method (Herdewijn et al., 1987). FLT and AZT were purchased from Euro Asia Tran

Continental (Bombay, India) for large-scale synthesis of ester conjugates. 12-Bromododecanoic acid was purchased from Sigma Aldrich Chemical Co. 5(6)-Carboxyfluorescein (FAM) was purchased from Novabiochem. All the other reagents including solvents were purchased from Fisher scientific.

The products were purified on a Phenomenex®Gemini 10 μm ODS reversed-phase column (2.1 × 25 cm) with Hitachi HPLC system using a gradient system at constant flow rate of 17 ml/min (Table 1.1).

Table 1.1. HPLC method used for purification of the compounds.

Time (min)	Water Concentration A (%)	Acetonitrile Concentration B (%)	Flow rate (mL/min)
0.00	100.0	0.0	1.0
1.0	100.0	0.0	17.0
45.0	0.0	100.0	17.0
55.0	0.0	100.0	17.0
59.0	100.0	0.0	17.0
60.0	100.0	0.0	1.0

The purity of the compounds was confirmed by using analytical Hitachi analytical HPLC system on a C18 column (Grace Allsphere ODS 2-3 μ, 150 X 4.6 mm) using a gradient system (water:acetonitrile 30:70 v/v) at constant flow rate of 1 ml/min with a UV detection at 265 nm. The chemical structures of final products were characterized by nuclear magnetic resonance spectrometry (^{1}H NMR and ^{13}C NMR) determined on a Bruker NMR spectrometer (400 MHz) and confirmed by a high-resolution PE Biosystems Mariner API time-of-flight electrospray mass spectrometer..

Chemical shifts are reported in parts per millions (ppm) and confirmed by a high-resolution PE Biosystems Mariner API time-of-flight electrospray mass spectrometer. For cellular uptake studies, cells were analyzed by flow cytometry (FACSCalibur: Becton Dickinson) using FITC channel and CellQuest software. Cell-viability studies were conducted using Cellometer Auto T.4 (Nexcelom Biosciences). The real time microscopy in live CCRF-CEM cell line with or with compounds were imaged using ZEISS Axioplan 2 light microscope equipped with transmitted light microscopy with a differential-interference contrast method and an Achroplan 40X objective.

1.3.2. Chemistry

1.3.2.1. 5′-*O*-(Fatty Acyl) Ester Derivatives of FLT and AZT

First, Several 5′-*O*-(fatty acyl) ester derivatives of FLT and AZT were synthesized at scale of 100 mg according to the previously reported procedure (Parang et al., 1998) by the reaction of FLT and fatty acyl chloride derivatives in the presence of 4-dimethylaminopyridine (DMAP). In the next step, three FLT esters [5′-*O*-(myristoyl)-3′-fluoro-2′,3′-dideoxythymidine (KP-16), 3′-fluoro-2′,3′-dideoxy-5′-*O*-(12-azidododecanoyl)thymidine (KP-1), and 3′-fluoro-2′,3′-dideoxy-5′-*O*-(12-thioethyldodecanoyl)thymidine (KP-17)] were synthesized at larger scale of 5 g, and 25 g. Fatty acyl chloride derivatives were synthesized by the reaction of fatty acids with oxalyl chloride.

In general, a reaction mixture consisting of the appropriate fatty acid (1.3 mmol), oxalyl chloride (0.25 g, 1.95 mmol), and anhydrous benzene (18 mL) was stirred at room temperature (25 °C) for 1 h. the yellow solution thus obtained was

evaporated to dryness under reduced pressure. The residual oil was dissolved in benzene (18 mL) and the solution was added dropwise to an ice-cold, stirred solution consisting of the AZT (0.34 g, 1.3 mmol) or the FLT (0.32 g, 1.3 mmol), DMAP (0.23 g, 1.9 mmol) and anhydrous benzene (18 mL) under anhydrous conditions. The solution was stirred in an ice bath for 1 h and then refluxed in an oil bath for about 3 h. the mixture was cooled and diluted with benzene (72 mL). The organic solution was washed with saturated aqueous sodium carbonate (2 × 11 mL) and then with water (2 × 11 mL). The organic layer was dried over anhydrous sodium sulfate and was evaporated to dryness. The residue consisting of one major product was purified by silica gel chromatography using chloroform as eluent to yield the product. The procedure was used for the synthesis of most of ester analogs, unless noted otherwise.

(±)-3′-Azido-2′,3′-dideoxy-5′-*O*-(pentadecanoyl)thymidine (KP-6). Oil; yield (100 mg, 90%); ^{1}H NMR (400 MHz, $CDCl_3$, δ ppm): 8.00-8.10 (br s, 1H, N-*H*), 7.24 (s, 1H, H-6), 6.10-6.18 (m, 1H, H-1′), 4.39 (dd, J = 12.2 and 4.3 Hz, 1H, H-5′), 4.31 (dd, J = 12.2 and 4.3 Hz, 1H, H-5″), 4.15-4.23 (m, 1H, H-3′), 4.09 (dd, = 4.3 and 8.7 Hz, 1H, H-4′), 2.28-2.52 (m, 3H, C*H*$_2$COO, H-2″, H-2′), 1.95 (s, 3H, 5-C*H*$_3$), 1.60-1.72 (m, 2H, C*H*$_2$CH$_2$COO), 1.22-1.31 (br s, 22H, methylene protons), 0.89 (t, J = 6.4 Hz, 3H, CH_3).

(±)-3′-Azido-2′,3′-dideoxy-5′-*O*-(2-methoxyteradecanoyl)thymidine (KP-8). Oil; yield (100 mg, 90%); ^{1}H NMR (400 MHz, $CDCl_3$, δ ppm): 9.00 (s, 1H, N-*H*), 7.28 (s, 1H, H-6), 6.17 (t, J = 6.2 Hz, 1H, H-1′), 4.50 (dd, J = 12.2 and 3.7 Hz, 1H, H-5′), 4.35

(dd, J = 12.2 and 3.7 Hz, 1H, H-5″), 4.20 (ddd, J = 7.6, 6.2, and 5.0 Hz, 1H, H-3′), 4.10 (ddd, = 5.0, 3.7, and 3.0 Hz, 1H, H-4′), 3.38 (t, J = 7.6 Hz, 1H, C*H*CO), 3.39 (s, 3H, OCH_3), 2.50 (ddd, J = 13.9, 6.2, and 6.2 Hz, 1H, H-2″), 2.37 (ddd, J = 13.9, 7.6 and 6.2 Hz, H-2″), 1.95 (s, 3H, 5-CH_3), 1.70-1.80 (m, 2H, CH_2CH(OCH$_3$)), 1.32-1.42 (m, 2H, CH_2CH$_2$CH(OCH$_3$)), 1.22-1.31 (br m, 18H, methylene protons), 0.89 (t, J = 7.6 Hz, 3H, CH$_3$); HR-MS (ESI-TOF) (m/z): $C_{25}H_{41}N_5O_6$, calcd, 507.3057; found, 530.6788 $[M + Na]^+$.

(±)-3′-Fluoro-2′,3′-dideoxy-5′-*O*-(2-methoxyteradecanoyl)thymidine (KP-15). Oil; yield (100 mg, 90%); ^{1}H NMR (400 MHz, $CDCl_3$, δ ppm): 8.50 (s, 1H, N*H*), 7.31 (s, 1H, H-6), 6.40 (dd, J = 9.0 and 5.6 Hz, 1H, H-1′), 5.08-5.26 (dd, J = 52.5 and 5.5 Hz, 1H, H-3′), 4.46 (dt, J = 25.6 and 4.0 Hz, 1H, H-4′), 4.55 (dd, J = 12.5 and 4.1 Hz, 1H, H-5′), 4.25 (dd, J = 12.5 and 4.1 Hz, 1H, H-5″), 3.38 (t, J = 7.6 Hz, 1H, C*H*CO), 1.95 (s, 3H, 5-CH$_3$), 2.55-2.72 (m, 1H, H-2″), 2.15-2.25 (m, 1H, H-2′), 1.70-1.80 (m, 2H, CH_2CH(OCH$_3$)), 1.32-1.42 (m, 2H, CH_2CH$_2$CH(OCH$_3$)), 1.20-1.30 (br m, 18H, methylene protons), 0.87 (t, J = 7.6 Hz 3H, CH$_3$). HR-MS (ESI-TOF) (m/z): $C_{25}H_{41}FN_2O_6$, calcd, 484.2949; found, $[M + Na]^+$.

1.3.2.2. 5(6)-Carboxyfluorescein Derivatives of FLT

General Procedure for the Synthesis of 3′-Fluoro-2′,3′-dideoxy-5′-*O*-(3-aminopropanoyl)thymidine (1.3) and 3′-Fluoro-2′,3′-dideoxy-5′-*O*-(12-aminododecanoyl)thymidine (1.4). FLT (0.60 mmol, 150 mg), the appropriate Fmoc-amino acid (1.2 mmol), and 2-(1H-benzotriazole-1-yl)-1,1,3,3-

tetramethyluronium hexafluorophosphate (HBTU, 500 mg, 1.3 mmol) were dissolved in dry DMF (10 mL) and dry *N*-methylmorpholine (2 mL). The solution was stirred overnight at room temperature. Reaction mixture was concentrated and dried under reduced pressure to afford crude 5′-*O*-Fmoc-amino acid derivatives of FLT, **1.1** and **1.2**. The crude products compounds were dissolved in THF (10 mL). To the reaction mixture was added piperidine (6 μL, 0.06 mmol), 1-octanethiol (10 mM solution in THF, 6 mmol, 0.6 mL). The reaction mixture was allowed to stir for 1 h at room temperature. The reaction solution was concentrated at reduced pressure. The residue was purified with reversed phase HPLC using C_{18} column and using a gradient system water/acetonitile as solvents as described above.

3′-Fluoro-2′,3′-dideoxy-5′-*O*-(3-aminopropanoyl)thymidine (1.3). White Powder; yield (100 mg, 55%). HR-MS (ESI-TOF) (m/z): $C_{13}H_{18}FN_3O_5$: calcd. 315.1230; found 316.3369 $[M + H]^+$, 631.4397 $[2M + H]^+$.

3′-Fluoro-2′,3′-dideoxy-5′-*O*-(12-aminododecanoyl)thymidine (1.4). White Powder; yield (150 mg, 57%). ^{1}H NMR (400 MHz, CD_3OD, δ ppm): 11.38 (s, 1H, N*H*), 7.81-7.98 (br s, 2H, NH_2), 7.45 (s, 1H, H-6), 6.18 (t, J = 7.9 Hz, H-1′), 5.30 (dd, J = 53.2 and 4.2 Hz, 1H, H-3′), 4.15-4.36 (m, 3H, H-5′, H-5″, H-4′), 3.15 (t, J = 8.2 Hz, 2H, CH_2NH), 2.68-2.82 (m, 2H, CH_2CO), 2.21-2.52 (m, 4H, CH_2CH_2NH, H-2′, H-2″), 1.76 (s, 3H, 5-CH_3), 1.05-1.24 (br m, 16H, methylene envelope); ^{13}C NMR (DMSO-d_6, 100 MHz, δ ppm): 173.08 (COO), 164.07 (C-4 *C*=O), 150.87 (C-2 *C*=O), 136.08 (C-6), 110.03 (C-5), 94.38 (d, J = 175.5 Hz, C-3′), 84.66 (C-1′), 82.03 (d, J =

25.8 Hz, C-4′), 63.49 (d, J = 10.6 Hz, C-5′), 55.32, 51.54 (CH_2NH), 36.33 (d, J = 20.6 Hz, C-2′), 33.73 (CH_2COO), 29.30, 29.25, 29.12, 28.96, 28.91, 28.84, 27.41, 26.23, 24.79, 23.51 (methylene carbons), 13.86 (5-CH_3). HR-MS (ESI-TOF) (m/z): $C_{22}H_{36}FN_3O_5$: calcd. 441.5367; found 442.1974 $[M + H]^+$, 883.5248 $[2M + H]^+$.

General Procedure for the Synthesis of 5′-*O*-(5(6)-Carboxyfluorescein) Derivatives of FLT (1.5 and 1.6)

FLT was attached to 5(6)-carboxyfluorescein through β-alanine and 12-aminododecanoic acid as linkers. A mixture of 5(6)-carboxyfluroscein (430 mg, 1.15 mmol), the corresponding FLT-amino acid (**1.3** and **1.4**, 0.29 mmoL), and HBTU (440 mg, 1.15 mmol) were dissolved in dry DMF (10 mL) and diisopropylethylamine (DIPEA, 2 mL, 15 mmol) and stirred overnight at room temperature. Reaction mixture was concentrated and dried under vacuum. Final compounds were purified with reversed phase HPLC using C_{18} column and water/acetonitile as solvents as described above.

3′-Fluoro-2′,3′-dideoxy-5′-*O*-(3-(N(5(6)-carboxyfluorescein)aminopropanoyl)thymidine (1.5). Yield (25 mg, 15 %). ^1H NMR (400 MHz, CD_3OD, δ ppm): 8.48 (s, 0.5H, FAM-Ar-H, 5 or 6 isomer), 8.19 (d, J = 8.2 Hz, 0.5H, FAM-Ar-H, 5 or 6 isomer), 8.04, 8.13 (two dd, J = 1.6 and 8.0 Hz, 1H, FAM-Ar-H), 7.58 (s, 0.5H, FAM-Ar-H, 5 or 6 isomer), 7.20-7.42 (m, 1H, H-6, and 0.5 H FAM-Ar-H, 5 or 6 isomer), 6.96-7.05 (m, 4H, FAM-Ar-H), 6.84 (d, J = 8.9 Hz, 2H, FAM-Ar-H), 6.11 and 6.17 (two dd, J = 5.6 and 8.9, 1H, H-1′), 5.16 and 5.23

(two dd, J = 53.3 and 5.0 Hz, 1H, H-3′), 4.20-4.40 (m, 3H, H-5′ and H-5″, H-4′), 3.53 and 3.64 (two t, J = 6.5 Hz, 2H, CH_2NH), 2.10-2.74 (m, 4H, H-2′, H-2″, CH_2CO), 1.72 and 1.78 (two s, 3H, 5-CH_3); ^{13}C NMR (CD_3CN, 100 MHz, δ ppm): 172.63 (COO), 172.47 (NHCO), 168.06, 165.63, 156.25 (FAM-Ar-*C*), 160.49 (C-4 *C*=O), 151.20, 151.14 (C-2 *C*=O), 139.64, 133.27, 131.43, 129.24, 129.60, 127.37, 127.82, 126.07 (FAM-Ar-*C*), 136.46, 136.52 (C-6), 116.84 (FAM-Ar-*C*), 113.47, 113.58 (C-5), 102.83 (FAM-Ar-*C*), 94.31, 94.19 (two d, J = 176.5 Hz, C-3′), 85.53, 85.57 (C-1′), 82.57, 82.48 (two d, J = 26.8 Hz, C-4′), 64.13, 64.00 (two d, J = 11.2 Hz, C-5′), 55.11, 49.09 (*C*H_2NH), 36.07, 35.97 (C-2′), 33.76, 33.89 (*C*H_2COO), 11.95, 12.01 (5-*C*H_3). HR-MS (ESI-TOF) (m/z): $C_{34}H_{28}FN_3O_{11}$: calcd. 673.1708; found 674.5083 [M + H]$^+$, 1348.6951 [2M + H]$^+$.

3′-Fluoro-2′,3′-dideoxy-5′-*O*-(12-(N(5(6)-carboxyfluorescein)aminododecanoyl)thymidine (1.6). Yield (30 mg, 13%); ^{1}H NMR (400 MHz, CD_3OD, δ ppm): 8.45 (s, 0.5H, FAM-Ar-H, 5 or 6 isomer), 8.17 (dd, J = 1.5 and 8.0 Hz, 0.5H, FAM-Ar-H, 5 or 6 isomer), 8.10 (s, 1H, FAM-Ar-H), 7.64 (s, 0.5H, FAM-Ar-H, 5 or 6 isomer), 7.43 (s, 1H, H-6), 7.30 (d, J = 5.1 Hz, 0.5H, FAM-Ar-H, 5 or 6 isomer), 6.76 (s, 1H, FAM-Ar-H), 6.70 (dd, J = 3.2 and 8.7 Hz, 3H, FAM-Ar-H), 6.61 (dd, J = 2.0 and 8.7 Hz, 2H, FAM-Ar-H), 6.16-6.26 (m, 1H, H-1′), 5.20 (dd, J = 53.4 and 4.9 Hz, 1H, H-3′), 4.30-4.45 (m, 2H, H-5′ and H-5″), 4.19 (d, J = 5.5 and 13.6 Hz, 1H, H-4′), 3.38 (t, J = 7.0 Hz, 2H, CH_2NH), 2.44-2.63 (m, 1H, H-2′), 2.15-2.38 (m, 3H, CH_2CO, H-2″), 1.83 (s, 3H, 5-CH_3), 1.47-1.66 (m, 4H, CH_2CH_2COO, CH_2CH_2-NH), 1.05-1.24 (br m, 16H, methylene envelope); ^{13}C NMR

(CD_3OD, 100 MHz, δ ppm): 174.85 (COO), 170.11 (NHCO), 168.34, 166.35, 155.35 (FAM-Ar-*C*), 163.45 (C-4 *C*=O), 152.29 (C-2 *C*=O), 142.15, 138.28, 137.40, 131.01, 129.46, 126.86, 126.08, (FAM-Ar-*C*), 135.12 (C-6), 115.14 (FAM-Ar-*C*), 112.02 (C-5), 103.72 (FAM-Ar-*C*), 95.32 (d, J = 177.6 Hz, C-3′), 86.92 (C-1′), 84.15 (d, J = 26.3 Hz, C-4′), 64.66 (d, J = 11.7 Hz, C-5′), 54.98, 41.40 (CH_2NH), 38.83 (d, J = 21.0 Hz, C-2′), 35.02 (CH_2COO), 30.77, 30.74, 30.68, 30.59, 30.54, 30.45, 30.41, 30.34, 30.26, 30.21, 28.18, 26.10 (methylene carbons), 12.81 (5-CH_3). HR-MS (ESI-TOF) (m/z): $C_{43}H_{46}FN_3O_{11}$: calcd. 799.3116; found 800.4325 $[M + H]^+$.

1.3.2.3. General Procedure for the Synthesis of 3′-Fluoro-2′,3′-dideoxy-5′-*O*-(tetradecanyl)thymidine (1.7) and 3′-Azido-2′,3′-dideoxy-5′-*O*-(tetradecanyl)thymidine (1.8). Ether derivatives of AZT and FLT were synthesized by using Mitsunobu reaction. AZT or FLT (100 mg, 0.4 mmol), tetradecanol (0.8 mmol), and triphenylphosphine (TPP, 210 mg, 0.8 mmol) were dissolved in DMF (10 mL). To the reaction mixture was added diisopropylazodicarboxylate (DIAD, 100 mg, 0.5 mmol)). The mixture was stirred for 5 h at room temperature. The solvent was removed *in vacuo*. The residue was purified by reversed phase HPLC using C_{18} column and water/acetonitile as solvents as described above.

3′-Fluoro-2′,3′-dideoxy-5′-*O*-(tetradecanyl)thymidine (1.7). White Powder; yield (80 mg, 50%); ^1H NMR (400 MHz, $CDCl_3$, δ ppm): 7.52 (s, 1H, H-6), 6.19 (dd, J = 9.0 and 5.6 Hz, 1H, H-1′), 5.18 (dd, J = 54.0 and 4.6 Hz, 1H, H-3′), 4.18 (d, J = 27.5 Hz, 1H, H-4′), 3.65-3.86 (m, 4H, CH_2O, H-5′ and H-5″), 2.34-2.52 (m, 1H, H-2′),

2.10-2.34 (m, 1H, H-2″), 1.77 (s, 3H, 5-CH_3), 1.37-1.55 (m, 2H, CH_2CH_2O), 1.05-1.24 (br s, 20 H, methylene envelope), 0.74 (s, 3H, CH_3); ^{13}C NMR ($CDCl_3$, 100 MHz, δ ppm): 163.35 (C-4 *C*=O), 150.65 (C-2 *C*=O), 134.57 (C-6), 109.98 (C-5), 94.37 (d, J = 176.8 Hz, C-3′), 86.75 (C-1′), 85.20 (d, J = 24.2 Hz, C-4′), 61.95 (d, J = 11.0 Hz, C-5′), 41.28 (*C*H_2-O), 38.15 (d, J = 20.9 Hz, C-2′), 32.45, 31.65, 29.38, 29.28, 29.22, 29.08, 27.31, 26.72, 25.54, 22.41 (methylene carbons), 13.81 (*C*H_3), 12.94 (5-*C*H_3). HR-MS (ESI-TOF) (m/z): $C_{24}H_{41}FN_2O_4$: calcd. 440.305; found 441.1052 $[M + H]^+$.

3′-Azido-2′,3′-dideoxy-5′-*O*-(tetradecanyl)thymidine (1.8). White Powder; yield (90 mg, 50%. ^{1}H NMR (400 MHz, $CDCl_3$, δ ppm): 7.35 (s, 1H, H-6), 6.02 (t, J = 6.6 Hz, 1H, H-1′), 4.35 (dd, J = 5.1, 11.5 Hz, 1H, H-3′), 3.88-3.96 (m, 2H, H-5′ and H-5″), 3.85 (t, J = 7.3 Hz, 1H, *C*H_2O), 3.76 (d, J = 10.6 Hz, 1H, H-4′), 2.40-2.54 (m, 1H, H-2′), 2.28-2.40 (m, 1H, H-2″), 1.86 (s, 3H, 5-CH_3), 1.53 (t, J = 6.3 Hz, 2H, CH_2CH_2O), 1.12-1.30 (br s, 20H,methylene envelope), 0.82 (t, J = 6.6 Hz, 3H, CH_3); ^{13}C NMR ($CDCl_3$, 100 MHz, δ ppm): 163.28 (C-4 *C*=O), 150.72 (C-2 *C*=O), 134.58 (C-6), 110.29 (C-5), 87.23 (C-1′), 84.47 (C-4′), 61.89 (C-5′), 59.90 (C-3′), 41.46 (*C*H_2O), 37.35 (C-2′), 31.85, 29.58, 29.53, 29.48, 29.28, 29.24, 27.51, 26.93, 22.62, (methylene carbons), 14.05 (*C*H_3), 13.22 (5-*C*H_3). HR-MS (ESI-TOF) (m/z): $C_{24}H_{41}N_5O_4$: calcd. 463.3159; found 464.1528 $[M + H]^+$.

1.3.3. Physicochemical Properties (pKa, Log P, Log D., Solubility).

Physicochemical properties including pKa, LogD, and solubility were determined for KP-1 as a model compound.

1.3.3.1. pKa

The pK_a of KP-1 was determined using the D-PAS (spectroscopic) technique. The sample was initially titrated in a fast titration between pH 1.8 and pH 12.1 at concentrations of 33–49 μM under aqueous conditions. Precipitation of the sample from solution was observed below approximately pH 11. The sample was subsequently titrated under methanol-water cosolvent conditions in two triple titrations from pH 12.2 to pH 3.7 at concentrations of 31–49 μM. The methanol ratio varied from to 25.5–50.8%. No precipitation of the sample from solution was observed under this condition. The pK_a was determined from the spectroscopic data by Yasuda-Shedlovsky extrapolation of the individual obtained results. KP-1 was found to have an aqueous pKa value of 9.67 ± 0.02 determined by spectroscopic method under methanol-water cosolvent conditions.

1.3.3.2. Log P and Log D

It was not possible to measure the partition coefficient of the fatty acyl derivatives of FLT and AZT in standard *n*-octanol/water mixture, because of the insolubility of the compounds in water. The Log P of KP-1 was initially investigated by the pH-metric (potentiometric) method. The sample was titrated in three triple titrations from pH 2.5 to pH 11.9 at concentrations of 0.7–1.1mM in various ratios of octanol/water. The results indicated high sample lipophilicity although the Log P could not be determined potentiometrically due to the apparent pK_a in octanol shifting out of the measurable range.

Log D Determination by LDA- Liquid Liquid Distribution Chromatography

The Log D at pH 7.4 was measured as 5.04 using liquid chromatography. The ProfilerLDA is an isocratic chromatography system, which uses an octanol-coated column with octanol saturated mobile phases adjusted to pH 7.4.

A set of standard compounds with well known Log D octanol values are run through the column before the samples, the generated retention times are used as a calibration curve to relate retention times generated for sample compounds to Log D (Table 1.2., Figure 1.2).

Table 1.2. Log D values and retention time for standard compounds

Standard Name	**LDA Calibration 3**	
Compounds	**LogD**	**Retention Time**
Benzophenone	3.1800	109.00
Diphenylamine	3.5000	197.70
Diphenylether	4.0000	420.79
Dibutylphtalate	4.6000	1067.35

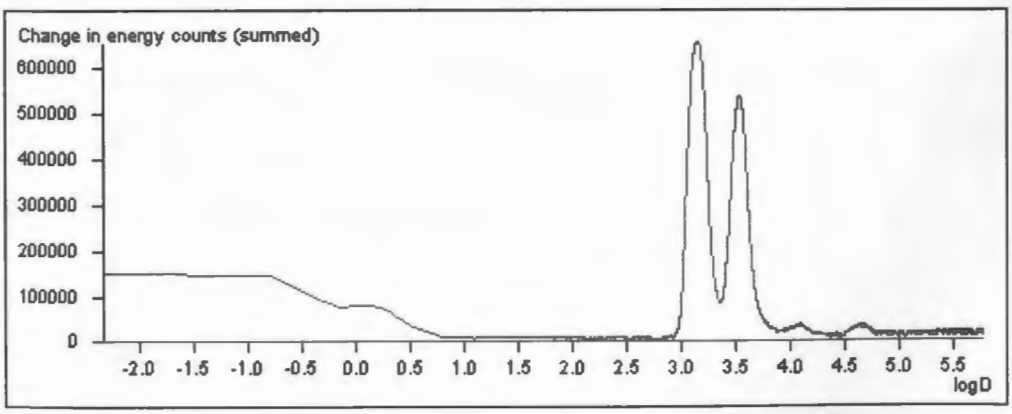

Figure 1.2. Standard curve (LDA Calibration 3) for Standard compounds.

Detection was carried out by using an UV diode array. A multi-wavelength peak location system is used to home on the largest peak present in the chromatogram. This reduces interference from impurity peaks to a minimum (assuming that impurities are much smaller in size than the sample peak). It is assumed that the largest peak in the chromatogram is the compound of interest as there is no positive identification in this system (e.g. MS detection). A value of 5.04 was obtained, which should correspond to the neutral Log P, in consideration of the sample pKa (Figure 1.3, Table 1.3).

Table 1.3. LogD values and retention time for KP-1

Test Name	KP-1	
Compounds	**LogD**	**Retention Time**
KP-1	5.04	2205.69

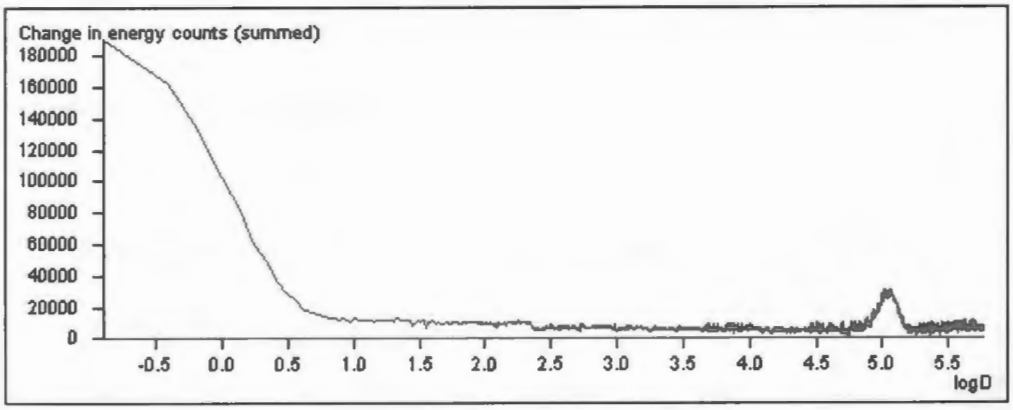

Figure 1.3. LDA calibration 3 curve for KP-1

1.3.3.3. Solubility

Difficulties were also encountered in our solubility analysis of KP-1 due to the low sample solubility in ionized form and suspected sample decomposition at high pH.

We were able to determine an upper limit for the sample solubility of 510 nM by shake-flask methodology, however.

The sample solubility was initially analyzed using the Sirius CheqSol method. The sample was titrated under aqueous conditions from pH 12.1 to low pH at an initial concentration of 3.1 mM. As full sample dissolution was not evident at the start of the CheqSol study, the experiment was paused and the sample was sonicated in an ultrasonic bath containing hot water, for several minutes. When the experiment was resumed, sample precipitate was only observed below approximately pH 7, where a second sample ionization stage was apparent. We consider the sample to have decomposed to produce another species with a significantly lower acidic pK_a during the "hot"-sonification at high pH. To avoid further complication due to sample decomposition, the sample solubility was subsequently investigated by shake-flask methodology with UV-spectroscopic sample detection.

To produce a saturated solution of KP-1, approximately 1 mg of solid material was added to 10 mL of aqueous solution, adjusted to pH 2.3 with 0.5 M HCl. The sample was then sonicated in an ultrasonic bath for several hours (at room temperature) before being left to equilibrate for a period of approximately three days. The supernatant was then filtered under vacuum through a 0.2 μm PVDF filter plate, and the UV absorption spectrum of the sample was measured (after adjusting the pH of the solution to 11.8 with 0.5M KOH). Molar absorption coefficients of KP-1 were obtained at pH 11.8 for 25 μM, 50 μM and 100 μM solutions of KP-1, in order to

quantify the concentration of sample in the saturated supernatant. The UV-absorption signal (0.0039) of the supernatant at the absorption maximum of KP-1 (264 nm, σ = 7650 $dm^3cm^{-1}Mol^{-1}$) (Figure 1.4) was close to the detection limit of the apparatus and it is considered appropriate to quote the solubility value determined as an upper limit. The intrinsic aqueous solubility of KP-1 is therefore determined to be <510 nM. KP-1 was completely soluble in ethanol (>30 mg/mL) and the mixture of water/methanol (60:40). KP-1 was less soluble in DMSO (~4.1 mg/mL).

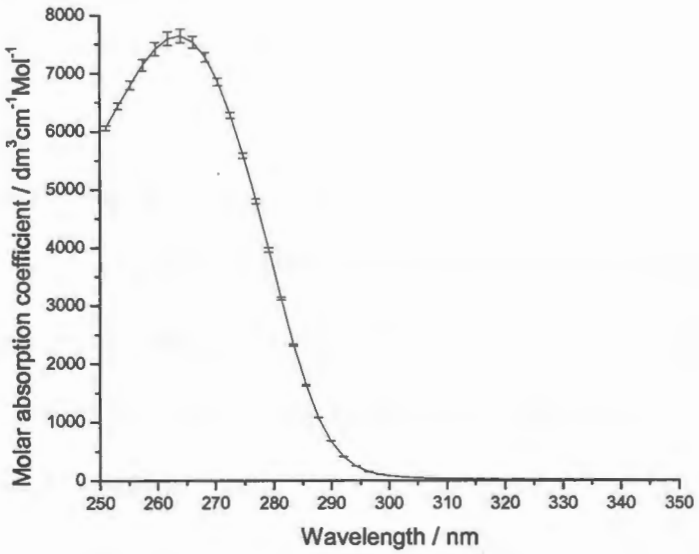

Figure 1.4. Average KP-1 molar extinction coefficients between 250–350 nm at pH 11.8. The curve is the average of spectra collected at sample concentrations of 25μM, 50μM and 100μM.

1.3.4. Anti-HIV Assays

Anti-HIV activities of the compounds were evaluated according to the previously reported procedure (Krebs et al., 1999). In summary, HeLa (Human cervical carcinoma: ATCC CCL-2.1) cell line was used to measure inactivation of both cell-free virus preparations and virus-infected cell preparations. Cells were plated

in culture plates 24 hrs prior to each experiment. Cell-free viral preparations of HIV-1 strains IIIB (lymphocytotropic strain) and BaL (monocytotropic strain) were used for cell-free assay. For cell-associated assay, SulT1 cells were infected with IIIB virus 5 days prior to the experiment. Cell-free virus and virus-infected cells were mixed with different compounds and diluted to make different concentrations. The mixture was further diluted with the buffer and added to the HeLa cells. The cells were incubated at 37 °C for 48 h, stained for β-galctosidease expression and compared with β-galctosidease expression from the β-gal-positive cells in absence of any microbicidal compound to get IC_{50} values.

1.3.5. Cellular Uptake Study

All of the stock solutions for compounds FAM, **1.5**, and **1.6** were prepared in DMSO. The human T lymphoblastoid cells CCRF-CEM (ATCC No. CCL-119) were grown on 25 cm^2 cell culture flasks with RMPI-1640 medium containing 10% fetal bovine serum. Upon reaching about 70% confluency, the cells were treated as described below and incubated for 1 h or longer at 37 °C.

1.3.5.1. Cellular Uptake of FAM, 1.5 and 1.6 at Different Time Points

When the cells reached about 70% confluency, FAM, **1.5**, or **1.6** (1 mL, 20 μM) in RMPI-1640 medium were added to 1 mL of cells to make the final concentration as 10 μM. The cells were incubated for 0.5, 1, 2, 4 and 8 h at 37 °C. Then the flow cytometry assays were performed as described below.

1.3.5.2. Cellular Uptake of 1.6 at Different Concentrations

When the cells reached about 70% confluency, 1 mL of graded concentrations (0, 10, 20, 40, 80, and 200 μM in RMPI-1640) of **1.6** was added to 1 mL of cells to make the final concentration as 0, 5, 10, 20, 40 and 100 μM. The cells were incubated for 1 h at 37 °C. Then the flow cytometry assays were performed as described below.

1.3.5.3. Cellular Uptake of FAM, 1.5 and 1.6 with Trypsin Treatment

The assays were performed as previously described in section 1.3.5.1 at 1 h time point with the exception that the cells used were incubated with 0.25% trypsin/0.53 mM EDTA for 5 min before washing with PBS (pH 7.4) for flow cytometry studies.

1.3.5.4. Flow Cytometry

The cells were washed twice with PBS (pH 7.4) at 2000 rpm for 5 min. Then the cells were analyzed by flow cytometry (FACSCalibur: Becton Dickinson) using FITC channel and CellQuest software. The data presented are based on the mean fluorescence signal for 10000 cells collected. All the assays were carried out in triplicate.

1.3.6. Cell Viability Assay

When the cells reached about 70% confluency, the cells were incubated with a solution of CCRF-CEM cell alone or 10 μM FAM, **1.5**, or **1.6** for 24 h at 37 °C. Then 20 μL of the cells from each flask were treated with 2 μL of trypan blue (0.1%) for 1

min. The cells were then transferred to a Cellometer® counting slide and analyzed using Cellometer® Auto T.4 (Nexcelom Bioscience). All the assays were performed in triplicate.

1.3.7. Real Time Fluorescence Microscopy in Live CCRF-CEM Cell Line

The cellular uptake studies and intracellular localization of CCRF-CEM cell alone, or incubated with **1.5** and **1.6** were imaged using a ZEISS Axioplan 2 light microscope equipped with transmitted light microscopy with a differential-interference contrast method and an Achroplan 40X objective. The human T lymphoblastoid cells CCRF-CEM (ATCC No. CCL-119) were grown on 60 mm Petri Dishes with RPMI-1640 medium containing 10% fetal bovine serum. Upon reaching about 70% confluency, the cells were incubated with a solution of 10 μM **1.5** or **1.6** for 1 h at 37 °C. The cells were then observed under the fluorescent microscope under bright field and FITC channels (480/520 nm).

1.4. Results and Discussion

1.4.1. Chemistry

1.4.1.1. 5′-*O*-(Fatty acyl) Ester Derivatives of FLT and AZT

FLT was synthesized using thymidine as the starting material according to previously reported procedure (Herdewijn et al., 1987). 5′-*O*-(Fatty acyl) ester derivatives of FLT and AZT (Table 1.4) were synthesized from the reaction of FLT or AZT with the corresponding fatty acyl chloride in the presence of oxalyl chloride and DMAP as described previously (Parang et al; 1998) at the scale of 100 mg . KP-1, KP-

16, and KP-17 showed higher potency and minimal cellular toxicity when compared to the other compounds (Table 1.2). KP-1 and KP-17 were then synthesized in larger scale (25 g) for further biological evaluation, preclinical and formulation studies. Compounds were purified first by using silica gel column chromatography and then HPLC to achieve >99% purity.

Table 1.4. Chemical structures of 5'-*O*-fatty acyl derivatives of AZT and FLT.

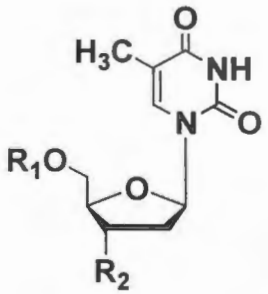

Compd.	R_1	R_2	Compd.	R_1	R_2
AZT	H	N_3	**KP-10**	$CH_3(CH_2)_4O(CH_2)_7CO$	N_3
FLT	H	F	**KP-12**	$Br(CH_2)_{11}CO$	F
KP-1	$N_3(CH_2)_{11}CO$	F	**KP-13**	$CH_3(CH_2)_4S(CH_2)_7CO$	F
KP-2	$CH_3(CH_2)_4S(CH_2)_7CO$	N_3	**KP-15**	$CH_3(CH_2)_{11}CH(OMe)CO$	F
KP-3	$CH_3CH_2S(CH_2)_{10}CO$	N_3	**KP-16**	$CH_3(CH_2)_{12}CO$	F
KP-4	$Br(CH_2)_{11}CO$	N_3	**KP-17**	$CH_3CH_2S(CH_2)_{11}CO$	F
KP-5	$CH_3(CH_2)_{12}CO$	N_3	**1.4**	$NH_2(CH_2)_{11}CO$	F
KP-6	$CH_3(CH_2)_{13}CO$	N_3	**1.7**	$CH_3(CH_2)_{13}O$	F
KP-8	$CH_3(CH_2)_{11}CH(OMe)CO$	N_3	**1.8**	$CH_3(CH_2)_{13}O$	N_3
KP-9	$CH_3(CH_2)_9O(CH_2)_2CO$	N_3			

1.4.1.2 5(6)-Carboxyfluorescein derivatives of FLT

FLT was attached to 5(6)-carboxyfluorescein using β-alanine and 12-aminododecanoic acid as linkers. First, FLT was reacted with the corresponding Fmoc-amino acid in presence of HBTU and DIPEA. Second, *N*-Fmoc deprotection to

free amino group was achieved in the presence of piperidine. Finally, FAM was attached to free amino group in the presence of HBTU and DIPEA to afford 5(6)-carboxyfluorescein derivatives of FLT, **1.5** and **1.6** (Scheme 1.1). These compounds were used for cellular uptake studies to determine cellular uptake profile of fatty acyl ester derivatives of FLT. FLT attached to FAM through β-alanine (**1.5**) was used as a control FLT analog. FLT attached to FAM through 12-aminododecanoyl (**1.6**) was used as an analog of 5'-*O*-(12-azidododecanoyl)-3'-fluoro-2',3'-dideoxy-thymidine (KP-1) and other fatty acid ester analogs of FLT.

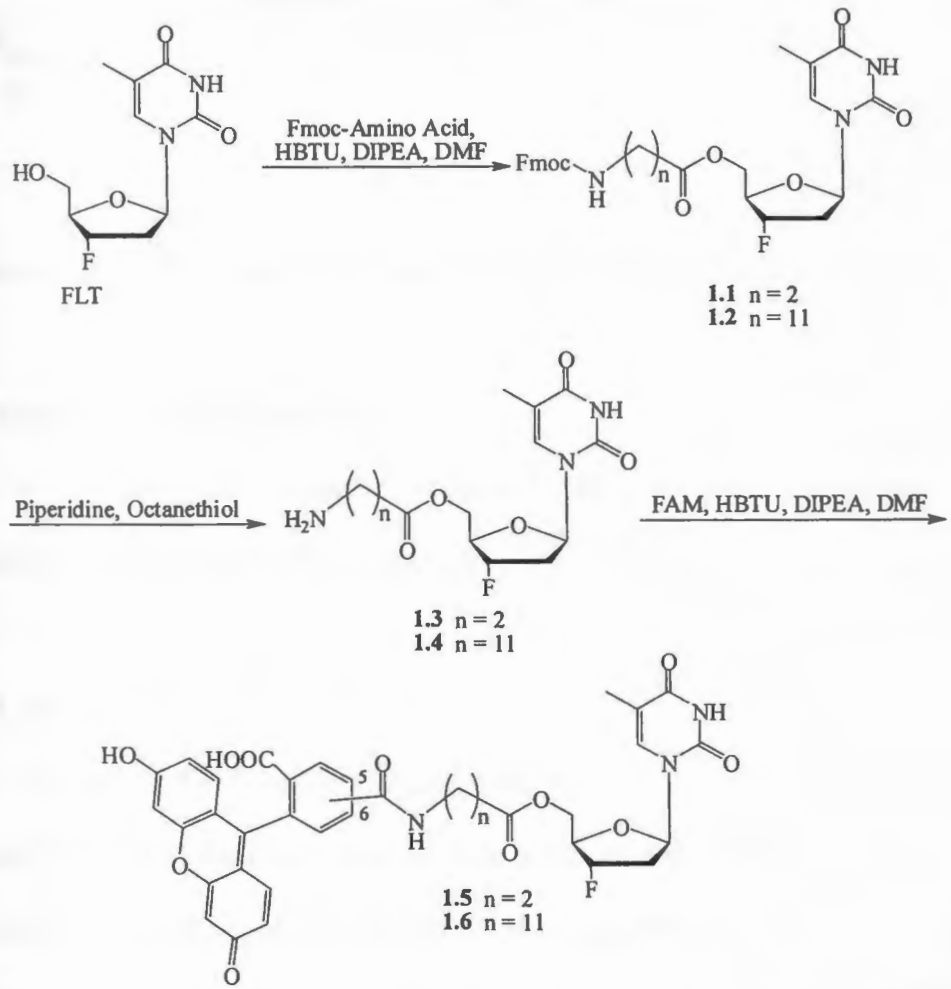

Scheme 1.1. Synthesis of 5'-carboxyfluorescein derivatives of FLT (**1.5** and **1.6**) through different linkers.

1.4.1.3. 5′-*O*-(Tetradecanol) ether derivatives of AZT and FLT

AZT and FLT were reacted with tetradecanol in the presence of TPP and DIAD using Mitsunobu conditions to afford 5′-*O*-(tetradecanol) ether derivatives of AZT and FLT (**1.7** and **1.8**) (Scheme 1.2).

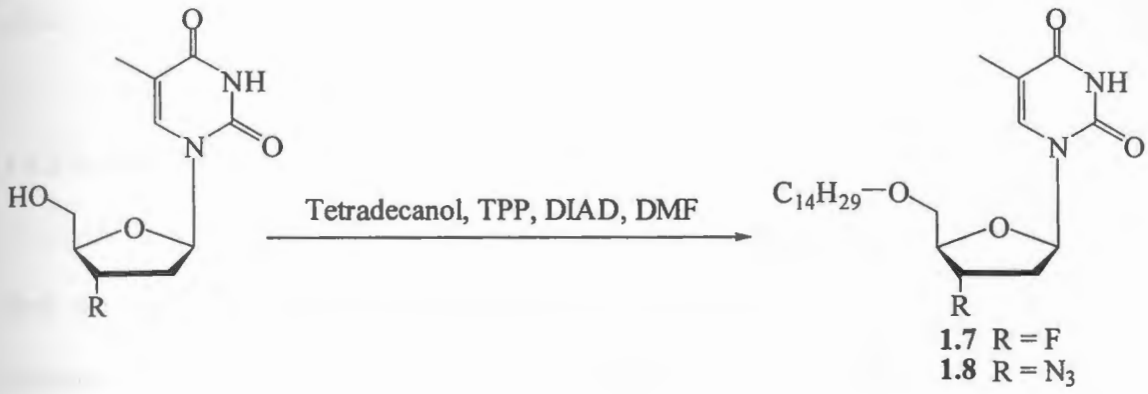

Scheme 1.2. Synthesis of 5′-*O*-(tetradecanol) ether derivatives of FLT and AZT.

1.4.2. Physicochemical Properties

Physicochemical properties including pKa, LogD, and solubility were determined for KP-1 as a model compound

1.4.2.1. pKa

The pK_a of KP-1 was determined using the D-PAS (spectroscopic) technique. The sample was subsequently titrated under methanol-water cosolvent conditions in two triple titrations from pH 12.2 to pH 3.7 at concentrations of 31–49 μM. The pK_a was determined from the spectroscopic data with an aqueous value of 9.67± 0.02, obtained by Yasuda-Shedlovsky extrapolation of the individual results obtained.

1.4.2.2. Log P and Log D

The Log D was measured at pH 7.4 by liquid chromatography. The ProfilerLDA is an isocratic chromatography system, which uses an octanol-coated column with octanol saturated mobile phases adjusted to pH 7.4. A value of 5.04 was obtained, which should correspond to the neutral Log P, in consideration of the sample pKa.

1.4.2.3. Solubility

An upper limit for the sample solubility of 510 nM was determined by shake-flask methodology with UV-spectroscopic sample detection. To produce a saturated solution of KP-1, approximately 1 mg of solid material was added to 10 mL of aqueous solution, adjusted to pH 2.3 with 0.5 M HCl. The sample was then sonicated in an ultrasonic bath for several hours at room temperature and then equilibrated for a period of approximately three days. The supernatant was then filtered, and the UV absorption spectrum of the sample was measured. The UV-absorption signal (0.0039) of the supernatant at the absorption maximum of KP-1 (264 nm, $\sigma = 7650$ $dm^3cm^{-1}Mol^{-1}$) was close to the detection limit of the apparatus and it is considered appropriate to quote the solubility value determined as an upper limit. The intrinsic aqueous solubility of KP-1 is therefore determined to be <510 nM. KP-1 was completely soluble in ethanol (>30 mg/mL) and the mixture of water/methanol (60:40). KP-1 was less soluble in DMSO (~4.1 mg/mL).

1.4.3. Biological Activities

Tables 1.5-1.8 illustrate anti-HIV-1 activities against cell-free and cell-associated virus, anti-sperm activity, vaginal cell cytotoxicity, and sperm inhibiting properties of the compounds. In summary, structure-function analysis revealed that the anti-HIV activity of 5′-substituted derivatives of FLT and AZT was clearly dependent on the nature of the 3′-substituent. 5′-*O*-Fatty acyl derivatives of FLT exhibited higher anti-HIV activities against HIV when compared to 5′-*O*-fatty acyl derivatives of AZT derivatives. For example, FLT derivatives (KP-1, KP-16, and KP-17) were more potent inhibitors of HIV replication than AZT derivatives (KP-2, KP-3, and KP-4) and AZT under the similar assay conditions. The FLT ester conjugate KP-16 was approximately 15-fold more potent than AZT in viral entry inhibition assay (lymphocytotropic strain) (Table 1.5). These results suggest that the increased inhibition by fatty acyl ester derivatives of FLT, KP-1, KP-15, KP-16, and KP-17, may be due to the intracellular release of FLT that is more potent than AZT released by fatty acyl ester derivatives of AZT. The inability of fatty acyl derivatives of AZT, KP-2, KP-4, and KP-6, to enhance antiviral activity compared to AZT may be due to incomplete intracellular hydrolysis of the conjugates under the *in vitro* assay conditions.

5′-*O*-Ether substituted FLT and AZT, **1.7** and **1.8**, had tetradecanyl (myristyl) group instead of tetradecanoyl (myristoyl) ester group. The ether bond is not susceptible to the cleavage action of esterases, thus the hydrolysis of the tetradecanyl group from the conjugate in **1.7** and **1.8** is not possible. Ether derivatives of FLT and

AZT substituted with 5′-tetradecanol (**1.7** and **1.8**, Scheme 1.2) were significantly were less potent than the corresponding 5′-*O*-(tetradecanoyl) ester derivatives (KP-16 and KP-5). The data demonstrate that the ester bonds are important in enabling anti-HIV activity of fatty acyl ester derivatives of FLT and AZT. The ester moiety in the conjugates needs to be hydrolyzed rendering parent nucleosides and fatty acids. The data demonstrate the importance of ester group in 5′-fatty acyl derivatives of AZT and FLT, such as KP-6 and KP-16. The same conclusion can be extrapolated to KP-1 and KP-17. The ester group in KP-1 and KP-17 needs to be hydrolyzed to produce active moieties with anti-HIV activity. In other words, the anti-HIV activity is not due to the incorporation of the compounds in the HIV membrane and/or detergent effect, since lipophilic ether derivatives, **1.7** and **1.8**, were not potent anti-HIV agents.

Furthermore, the anti-HIV activity of 5′-substituted derivatives of FLT and AZT was dependent on the nature of the 5′-substituent. Among FLT derivatives, KP-1, KP-15, KP-16, and KP-17 derivatives had significant anti-HIV activity at concentrations that were not cytotoxic. As shown in Table 1.5, compounds KP-1, KP-16, and KP-17 displayed EC_{50} values against cell-free X4 and R5 viruses below 1 μM. KP-1, KP-16, and KP-17 were at least 7-fold more potent against X4 HIV-1 when compared with AZT. KP-1, KP-16, and KP-17 were also active against cell-associated HIV with EC_{50} values between 2.3 and 12.6 μM. On the other hand, FLT and AZT were not active against cell-associated virus, at least under the conditions tested. The difference in the activity of fatty acyl derivatives of FLT compared to each other and FLT may be due to their difference in their rate of uptake and intracellular hydrolysis

yielding two antiviral agents, FLT and fatty acid analog, targeting different enzymes in HIV life cycle.

Table 1.5. Anti-HIV activities of fatty acyl ester derivatives of AZT and FLT

Compound Code	CTS[a] EC(50)[b] (μM)	VBI(IIIB)[c] EC(50) (μM)	VBI(BaL)[d] EC(50) (μM)	CTC[e] EC(50) (μM)
KP-1	1598	0.9	0.4	12.6
KP-2	>202	9.3	12.9	>202
KP-3	>101	7.7	5.2	90.7
KP-4	>190	14.8	4.6	>190
KP-5	629	3.1	5	629
KP-6	611	17.9	4.5	611
KP-8	197	9.7	6.7	197
KP-9	>209	6.7	2.1	>209
KP-10	>209	4.8	6.1	>209
KP-12	>198	1.8	<0.2	>198
KP-13	64	11.4	4.4	64
KP-15	>206	1	0.2	>206
KP-16	606	0.7	1.1	6.4
KP-17	>2000	1	<0.2	2.3
1.4	>226	1.5	-	-
1.6	>125	5.4	-	-
1.7	179	180	176	>227
1.8	205	125	27.6	>216
AZT	375	10.9	14.2	>375
FLT	1598	0.8	0.4	>410
C-1[f]	64.0	71.7	46.7	48.6
C-2[g]	>1000	1.6	85.9	5.1
DMSO	>1000	>1000	>1000	>1000

[a]Cytotoxicity assay; [b]50% Effective concentration; [c]Viral entry inhibition assay (lymphocytotropic strain); [d]Viral entry inhibition assay (monocytotropic strain); [e]Cell- to- cell transmission assay (IIIB); [f]Virucidal control; [g]Viral-entry inhibition control.

Table 1.6 displays the anti-HIV activity (in μg/mL) of FLT and AZT, their equimolar mixtures with fatty acids, and their corresponding ester conjugates. It was observed that the 5'-*O*-myristoyl ester conjugate of FLT (KP-16) was more consistent

in displaying antiviral activity against cell-associated virus compared to FLT, AZT, and physical mixtures of FLT or AZT with fatty acids (50:50 in equimolar ratio; **1.9-1.11**). All three physical mixtures, **1.9** (myristic acid and AZT (50:50)), **1.10** (myristic acid and FLT (50:50)), and **1.11** (12-bromododecanoic acid and AZT (50:50)), showed lower inhibitory potency against cell-associated HIV compared to KP-1 and KP-17. Compound **1.10** exhibited higher potency than that of FLT in cell-associated virus, but not as much as KP-1 and KP-17, suggesting the conjugation is required for efficient inhibition of cell-associated virus. Compound **1.11** was about 2-fold weaker inhibitor than the corresponding conjugate KP-4 (5'-*O*-(12-bromododeconyol)AZT) against IIIB and Bal strains. The comparative studies of physical mixtures with the corresponding ester conjugate indicated that the esterification is important for the inhibitor activity, especially against cell-associated virus.

In general, these data indicate that the nature of a substituent(s) on the fatty acid chain and the presence of fluorine or azide at 3′-position are determinants of anti-HIV activity. The decreased activities observed for certain analogs may be due to slower regeneration of the parent nucleoside or slower uptake of the fatty acyl derivative. The ability of fatty acyl derivatives of FLT, such as KP-1 and KP-17, to control cell to cell transmission of virus whereas FLT is not active at all, could be due to their higher cellular uptake compared to FLT in infected cells and enhanced delivery of FLT in infected cells. Additionally, KP-1 and KP-17 are also releasing myristic acid analogs intracelularly that can inhibit the post-translation modification of

viral proteins, such as protein myristoylation, and eventually blocking the release of new virus for infecting other cells.

Table 1.6. Comparison of anti-HIV activities of fatty acyl derivatives of AZT and FLT with physical mixtures of AZT or FLT + fatty acids

Compound Code	Chemical Name	CTS[a] EC(50)[b] (μg/mL)	VBI(IIIB)[c] EC(50) (μg/mL)	VBI(BaL)[d] EC(50) (μg/mL)	CTC[e] EC(50) (μg/mL)
AZT	AZT	>100	2.9	3.8	>100
FLT	FLT	>100	0.2	0.1	>100
KP-1	5′-*O*-(12-azidododecanoyl)FLT	746.7	0.4	0.2	5.9
KP-17	5′-*O*-(12-thioethyldodecanoyl)FLT	>1000	0.5	<0.1	1.1
KP-5	5′-*O*-(Myristoyl)AZT	>100	1.5	2.4	>100
1.9	Myristic acid + AZT (50:50)	>100	0.7	22.9	>100
KP-16	5′-*O*-(Myristoyl)FLT	>100	0.3	0.5	2.9
1.10	Myristic acid + FLT (50:50)	>100	< 0.1	0.4	15.6
KP-4	5′-*O*-(12-Bromododecanoyl_AZT	>100	7.8	2.4	>100
1.11	12-bromododecanoic acid + AZT (50:50)	>100	19	4.8	>100

[a]Cytotoxicity assay; [b]50% Effective concentration; [c]Viral entry inhibition assay (lymphocytotropic strain); [d]Viral entry inhibition assay (monocytotropic strain); [e]Cell- to- cell transmission assay (IIIB).

1.4.4. Anti-HIV Activities Against MDR Isolates

KP-1, KP-2, KP-16, and KP-17 were further tested against R5 and multidrug resistant (MDR) clinical isolates. Results indicated that several FLT derivatives

exhibited antiviral activity against HIV-1, lab-adapted, clinical isolates, and resistant virus. For example, FLT derivatives (KP-1, KP-16, and KP-17) were more potent inhibitors of HIV replication than AZT and AZT derivatives under the conditions employed in the assays. While AZT and KP-2 showed a drop in activity against MDR virus (>10 fold), FLT, KP-1, KP-16 and KP-17 showed similar potencies against R5 and MDR isolates (Table 1.7). KP-1 was at least 100-fold more potent against MDR virus when compared to that of AZT. KP-1, KP-16 and KP-17 were found to be safe compounds for cell viability studies as their toxic concentration limits were >40. AZT and FLT on the other hand displayed toxicity even at half the concentration. KP-2 not only showed less activity but also demonstrated high toxicity towards the cells at very low concentration. The impact of the compounds was further studied by looking at their antiviral index which is the ratio of TC_{50}/IC_{50}. KP-1, KP-16 and KP-17 had >4 times better AI_{50} values than FLT and >30 times effective values than AZT.

1.4.5. Cytotoxicity and Proinflammatory Effects

Compounds cytotoxicity was evaluated using human vaginal cells (VK-2). Contrary to N-9 (used as positive control), at 1 mg/mL, highest concentration tested, KP-1, KP-16, and KP-17 did not show significant cytotoxic effects during a 6 h incubation at multiple concentrations (Figure 1.5). Furthermore, although FLT is considerably more cytotoxic than AZT toward uninfected lymphocytes, 5'-fatty acyl derivatives of FLT did not exhibit higher toxicity in epithelial cell and vaginal cell cytotoxicity assays (Figure 1.5). All analogs of FLT demonstrated lower toxicity than FLT probably due to a sustained release of FLT upon the hydrolysis of the conjugates.

Table 1.7. Anti-HIV evaluation of FLT Derivatives, KP-1, KP-2, KP-16, and KP-17, in PBMC assay

Compound code	Solvent	Type of Virus	Endpoint	IC_{50} (μg/ml)[a]	TC_{50}[b]	AI_{50}[c]
KP-1	DMSO	R5	RT	0.0064	>42.8	>6700
		MDR	RT	0.0064	>42.8	>7451
KP-2	medium	R5	RT	0.0605	>10.1	>163
		MDR	RT	1.8576	>10.1	>5.46
KP-16	DMSO	R5	RT	0.0066	>44.0	>7044
		MDR	RT	0.0044	>44.0	>8669
KP-17	DMSO	R5	RT	0.0041	>41.1	>8649
		MDR	RT	0.00411	>41.1	>8370
AZT	dH_20	R5	RT	0.0749	>18.7	>207
		MDR	RT	1.2359	>18.7	>15.2
FLT	DMSO	R5	RT	0.0040	>20.5	>485
		MDR	RT	0.0123	>20.5	>1,457

[a]IC_{50} = The minimum drug concentration that inhibits HIV-induced cytopathic effect by 50%, calculated by using a regression analysis program for semilog curve fitting; [b]TC_{50} = The minimum drug concentration that reduces cell viability by 50%; [c]AI = Abbreviation for Antiviral Index. A measurement of the potential activity of drug, calculated by dividing the TC_{50} by the IC_{50}; R5 = 92TH014; MDR = Multidrug resistant virus 7324-1.

Furthermore, unlike N-9, KP-1, KP-16, and, KP-17 did not induce the release of IL-1α, a powerful proinflammatory cytokine (Figures 1.6 and 1.7).

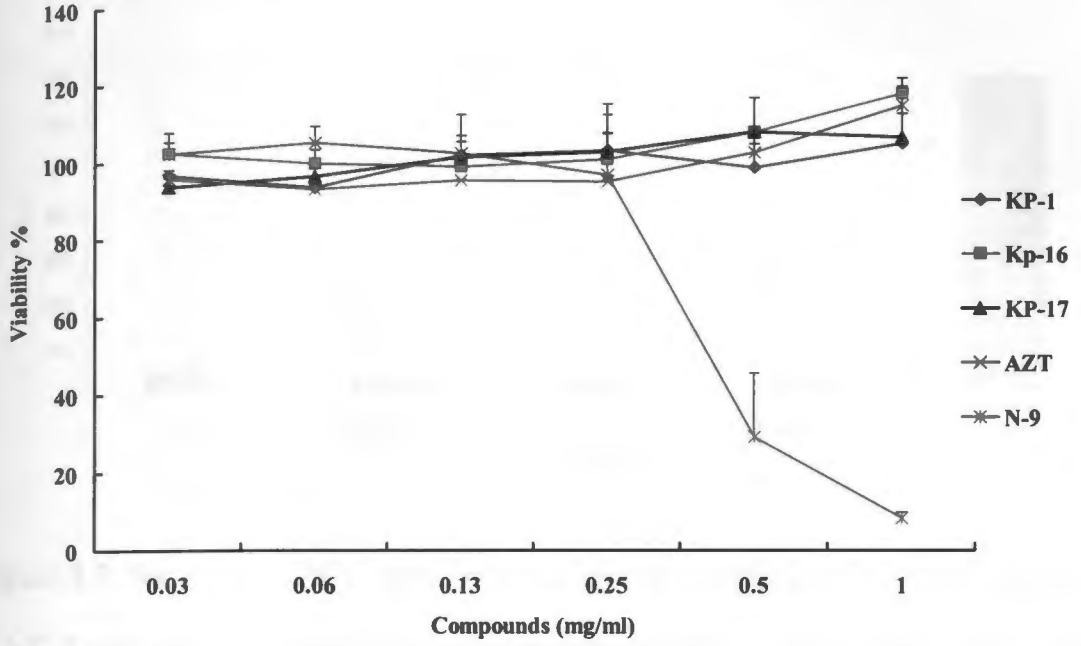

Figure 1.5. Dose-response curves of vaginal cytotoxicity in VK-2 cells (MTS assay) for KP-1, KP-16, KP-17, AZT, and N-9 after 6 h incubation

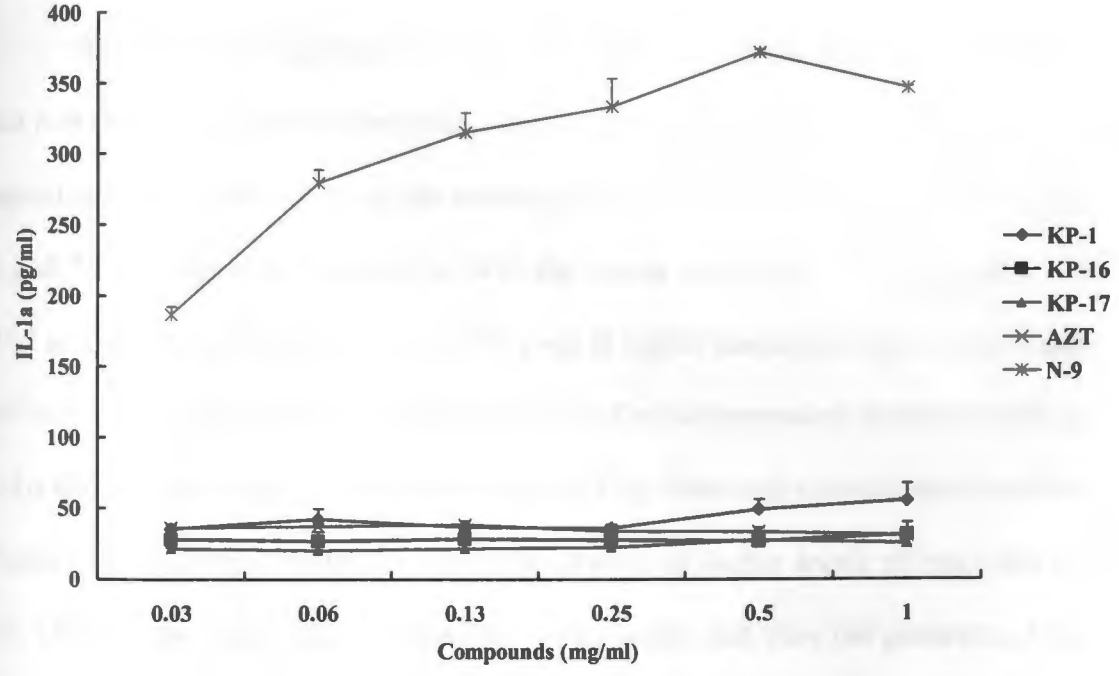

Figure 1.6. Proinflammatory cytokine (IL-1a) production in VK-2 Cells (ELISA) after a 6 h incubation in the presence of KP-1, KP-16, KP-17, AZT, and N-9.

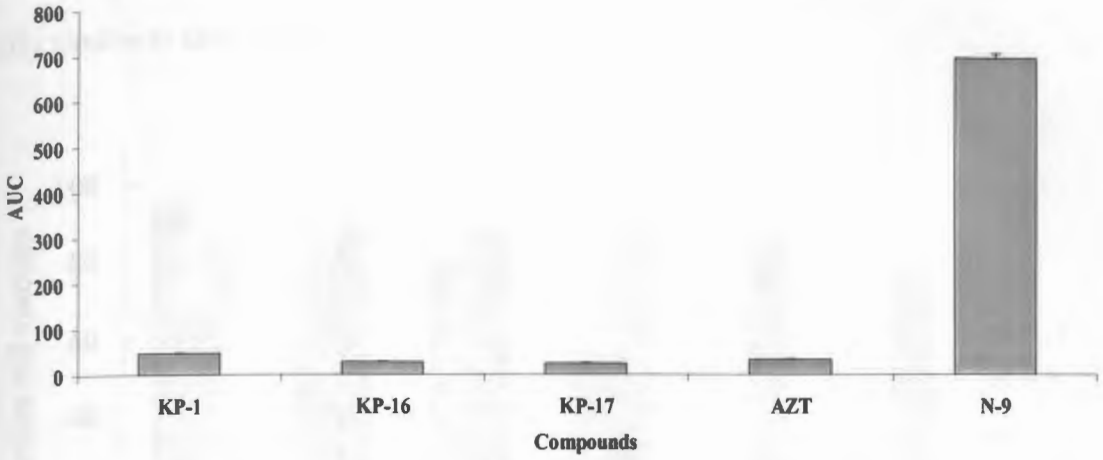

Figure 1.7. Summary of AUC Data for proinflammatory cytokine (IL-1α) production in VK-2 cells after a 6 h incubation in the presence of KP-1, KP-16, KP-17, AZT, and N-9.

KP-2 showed significantly less cytotoxicity and proinflammatory potential than N-9 (Figure 1.8), while displaying potent anti-HIV activity. The percentage of the vaginal cell that could survive at the concentration of 50 and 100 μg/mL of KP-2 was 86 and 73% respectively, whereas for N-9, the values were below 4% suggesting that KP-2 is much safer in comparison to N-9 even at higher concentrations. It was found that N-9 was producing very high concentration of proinflammatory cytokines such as IL-1α and IL-6 in comparison to KP-2 (Figure 1.9). Observed cytotoxicity from N-9 (Figure 1.8) could be correlated with the generation of higher levels of cytokines by N-9. On the other hand, KP-2 did not show cytotoxicity and were not generating high amount of cytokines. Similar assays were performed with other compounds in two

different sets and the cytokines generation for all the compounds except KP-12 was nearly similar to that of KP-2 (Figure 1.10).

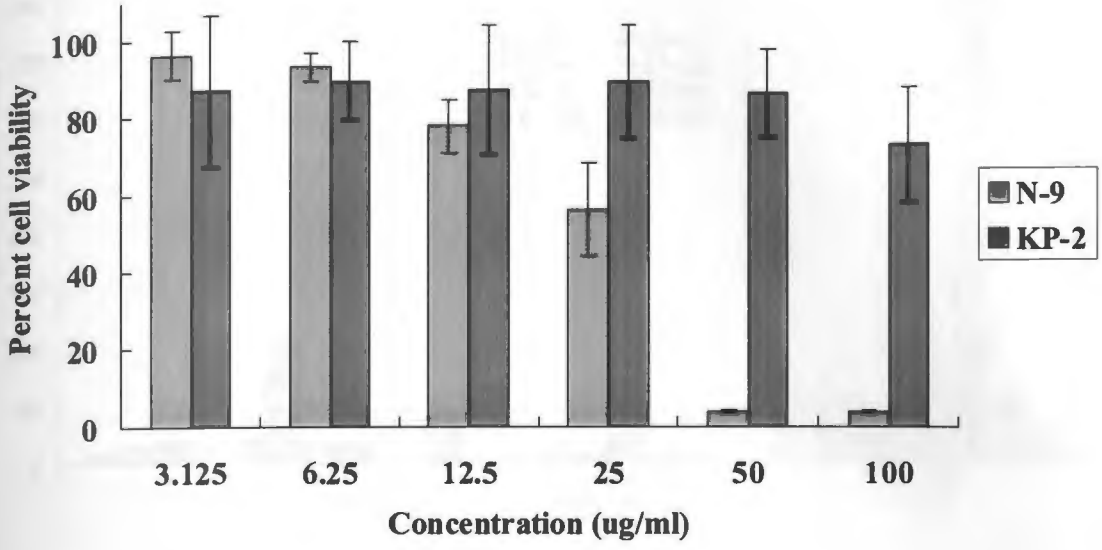

Figure 1.8. *In vitro* assay for vaginal cytotoxicity

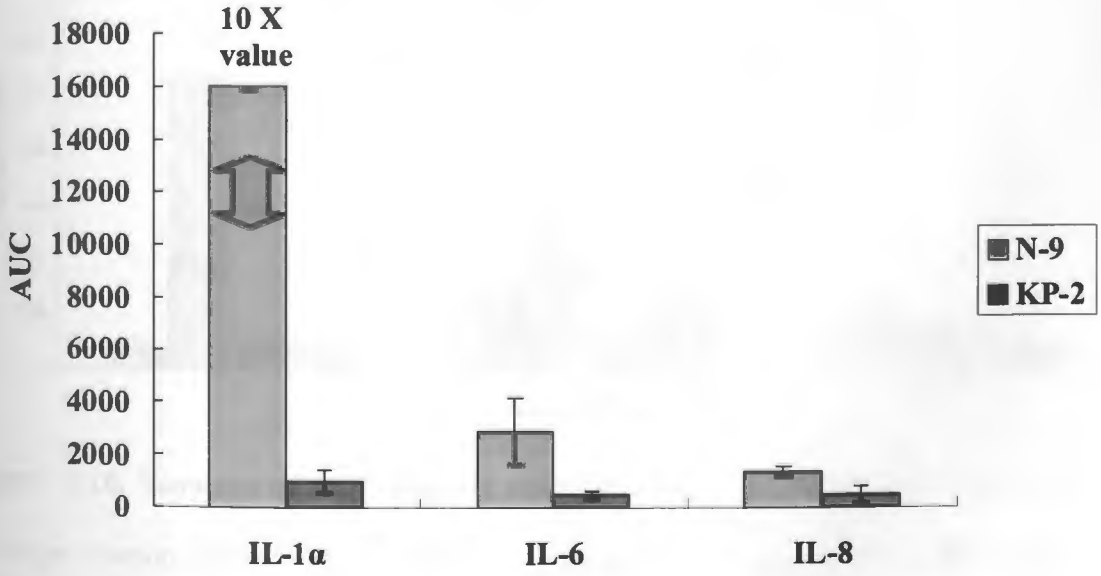

Figure 1.9. *In vitro* assays for proinflammatory cytokine production.

Note: Value of IL-1α for N-9 is 10 times the actual values

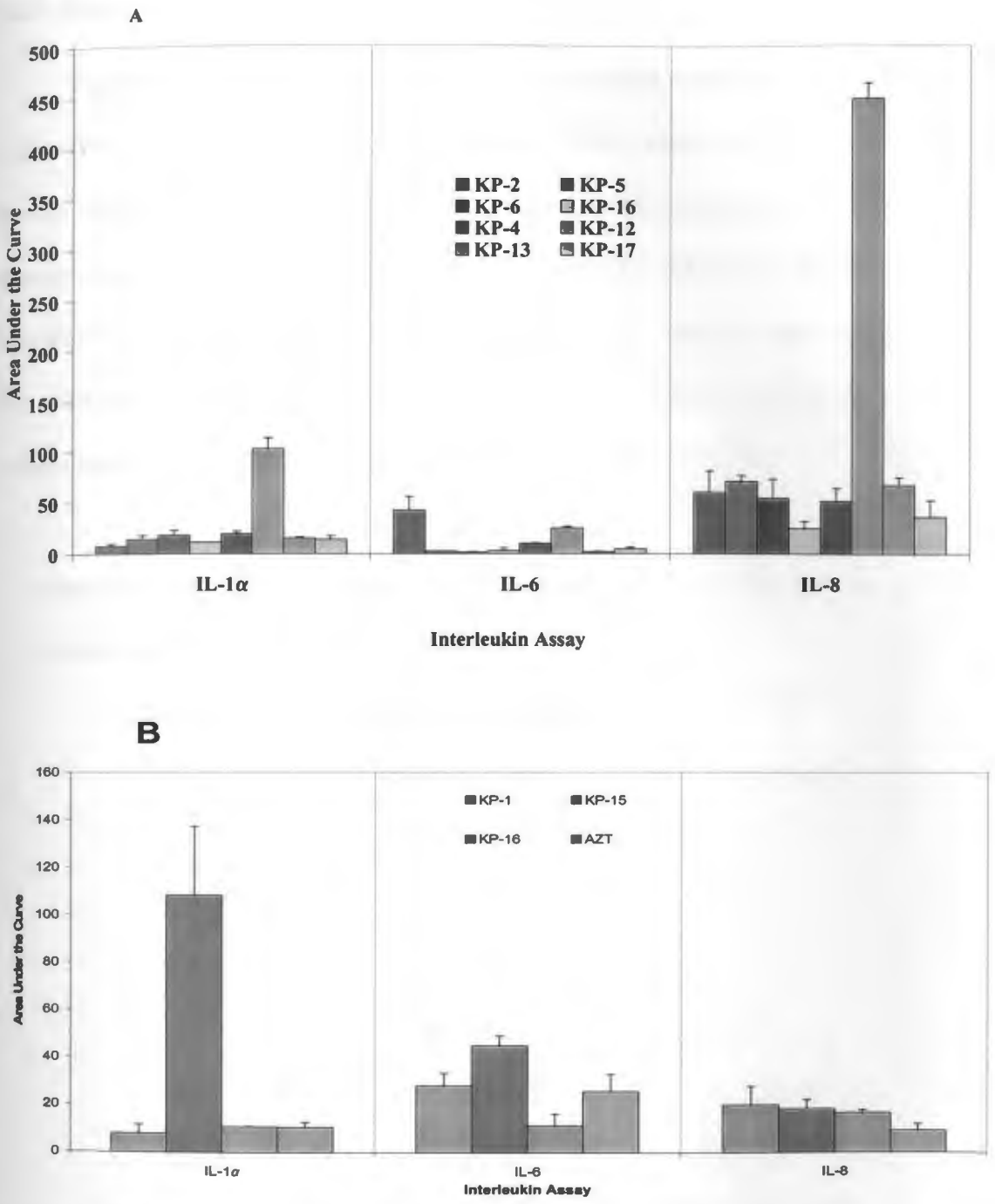

Figure 1.10. Summary of AUC Data for proinflammatory cytokine (IL-1α, IL-6 and IL-8) production after 6 h incubation. (A) Compounds KP-2, KP-4, KP-5, KP-6, KP-12, KP-13, KP-16, KP-17. (B) Compounds KP-1, KP-15, KP-16, and AZT.

1.4.6. Spermicidal Activity.

The spermicidal activities of several fatty acids have been previously reported (Brown-Woodman et al., 1985; Jianzhong et al., 1987). None of these derivatives showed significant spermicidal activity (Figure 1.11). In a dose-response study to evaluate spermicidal activity, compounds KP-1, KP-16, and KP-17 did not show significant sperm immobilizing or spermicidal activity, even at their maximum concentrations (1 mg/mL). KP-7, one of the FLT analogs, displayed sperm-immobilizing activity, although it was comparatively weak (Table 1.8).

Table 1.8. Spermicidal activity of submitted analogs using modified Sander-Cramer assay.

Compound Code	Highest Spermicidal Dilution (1/X)[a]	M.E.C. (mg/ml)[b]
KP-1	3.2 ± 0.4	3.5±0.5
KP-3	2.4 ± 0.4	4.5±0.4
KP-7	12.8 ± 4.3	1.1±0.2
KP-14	8.8 ± 1.8	1.4±0.3
N-9	227.2 ± 104.2	0.227±0.101
DMSO	3.6 ± 0.4	N.A.[c]

[a]Solvent = DMSO, initial concentration = 10 mg/mL. Values are expressed as means ± SE; [b]Minimum Effective Concentration; [c]Not assayed.

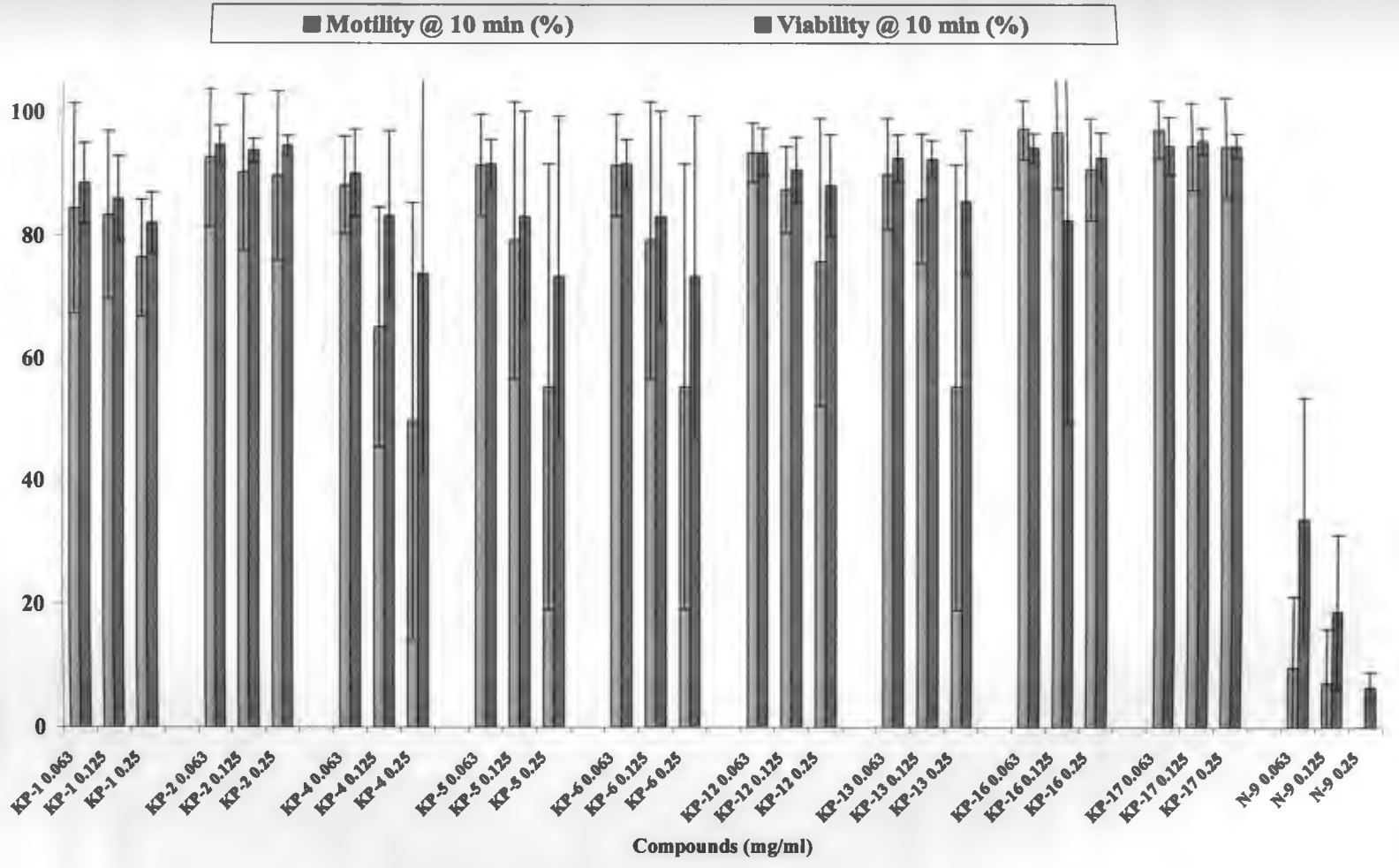

Figure 1.11. *In vitro* assays for spermicidal activity of fatty acyl derivatives of FLT and AZT.

1.4.7. Cellular Uptake Study

Cellular uptake profile of 5'-*O*-fatty acyl derivatives were investigated in comparison with FLT. FLT attached to FAM through β-alanine (**1.5**) was used as a control FLT analog. FLT attached to FAM through 12-aminododecanoic acid (**1.6**) was used as an analog of 3'-fluoro-2',3'-dideoxy-5'-O-(12-azidododecanoyl)thymidine (KP-1) and other fatty acid ester analogues of FLT. 3'-Fluoro-2',3'-dideoxy-5'-*O*-(12-[redacted]odododecanoyl)thymidine (**1.4**) showed anti-HIV activities comparable to other fatty acyl derivatives of FLT. Fluorescein-labeled fatty acyl ester derivative of FLT (**1.6**) showed slightly lower anti-HIV activity when compared with unsubstituted 12-[redacted]minododecanoyl derivative (**1.4**).

The human T lymphoblastoid cells (CCRF-CEM, ATCC No. CCL-119) were used for the study and were grown to the 70% confluency in the culture media. The cells were incubated with the fluorescein-substituted conjugates (**1.5** and **1.6**) in different time periods, concentrations, and in the presence or absence of trypsin (Figures 1.12-1.14). DMSO and FAM were used as control for the study. The cells were analyzed by flow cytometry (FACSCalibur: Becton Dickinson) using FITC channel and CellQuest software. The data presented are based on the mean fluorescence signal for 10000 cells collected. All the assays were carried out in triplicate.

First, cells were incubated with 10 μM of the compounds in different time periods (0.5 h, 1 h, 2 h, 4 h and 8 h, Figure 1.12). Compound **1.6** exhibited 10-15 fold higher cellular uptake than that of **1.5** and FAM alone. The results clearly indicate that presence

of long chain enhances the cellular uptake of FLT, by increasing lipophilicity. The continuous incubation of cells with compounds up to 8 h did not show significant difference in the cellular uptake, suggesting that most of the fatty acyl ester derivative is absorbed into cells within first 30 minutes incubation and the cellular uptake was not time dependent.

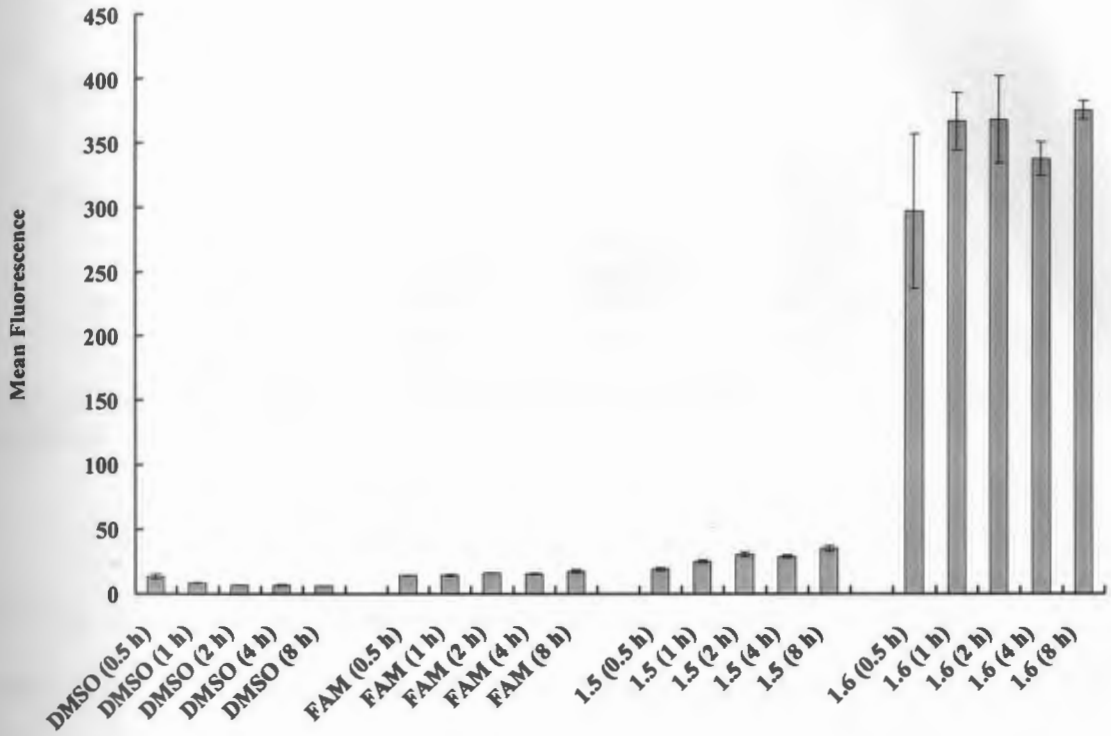

Figure 1.12. Cellular uptake studies for 5(6)-carboxyfluorescein derivatives of FLT (**1.5** and **1.6**) along with FAM and DMSO as controls at different time intervals.

Cells were then incubated with different concentrations (5, 10, 20, 40 and 100 μM) of carboxyfluorescein derivative of FLT, **1.6** for 1 h (Figure 1.13). The data suggested that the cellular uptake was concentration dependent.

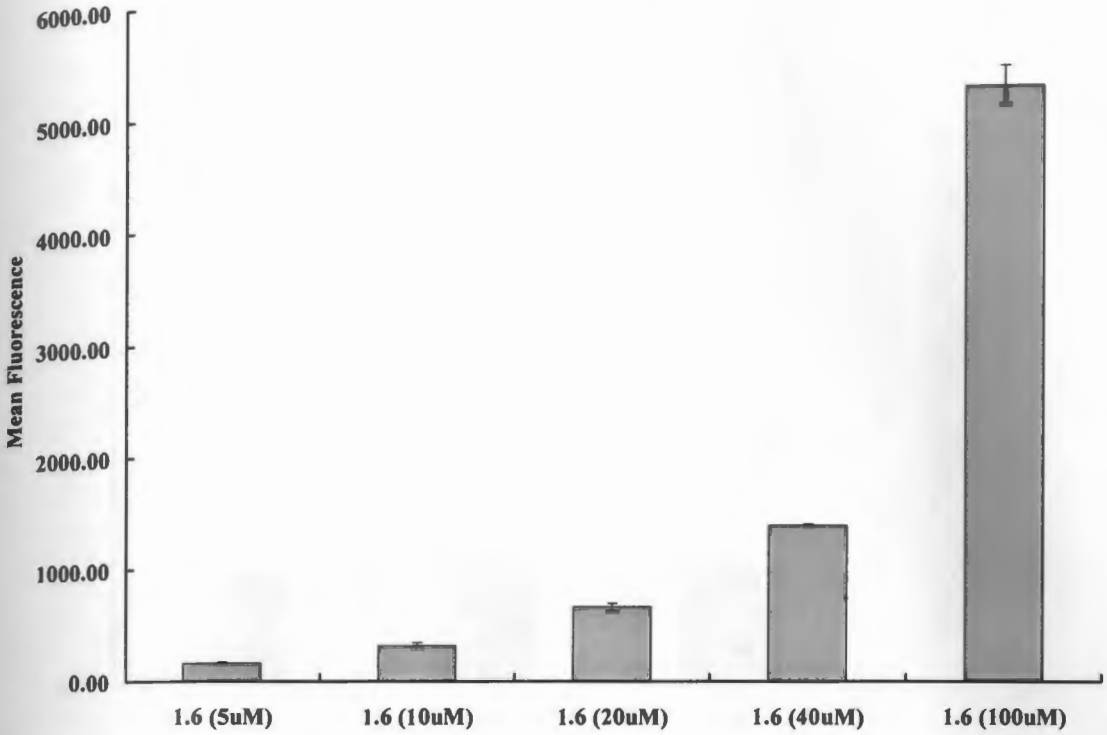

Figure 1.13. Cellular uptake studies for 5(6)-carboxyfluorescein derivative of FLT (**1.6**) at different concentrations.

To confirm that the enhanced uptake of 5(6)-carboxyfluorescein derivative of FLT, **1.6**, is not due to the absorption on the cell membrane surface, cells were incubated with 10 μM of DMSO, FAM, **1.5**, and **1.6** for 1 h and then treated with trypsin for 5 min to wash the adsorbed molecules (if any) from the cell membrane. The cellular uptake studies after trypsin treatment showed that the cellular uptake of **1.6** was still much higher than those of control compounds, FAM and **1.5** (Figure 1.14), suggesting that the higher cellular uptake of **1.6** is not due to artificial absorption to the cell membrane.

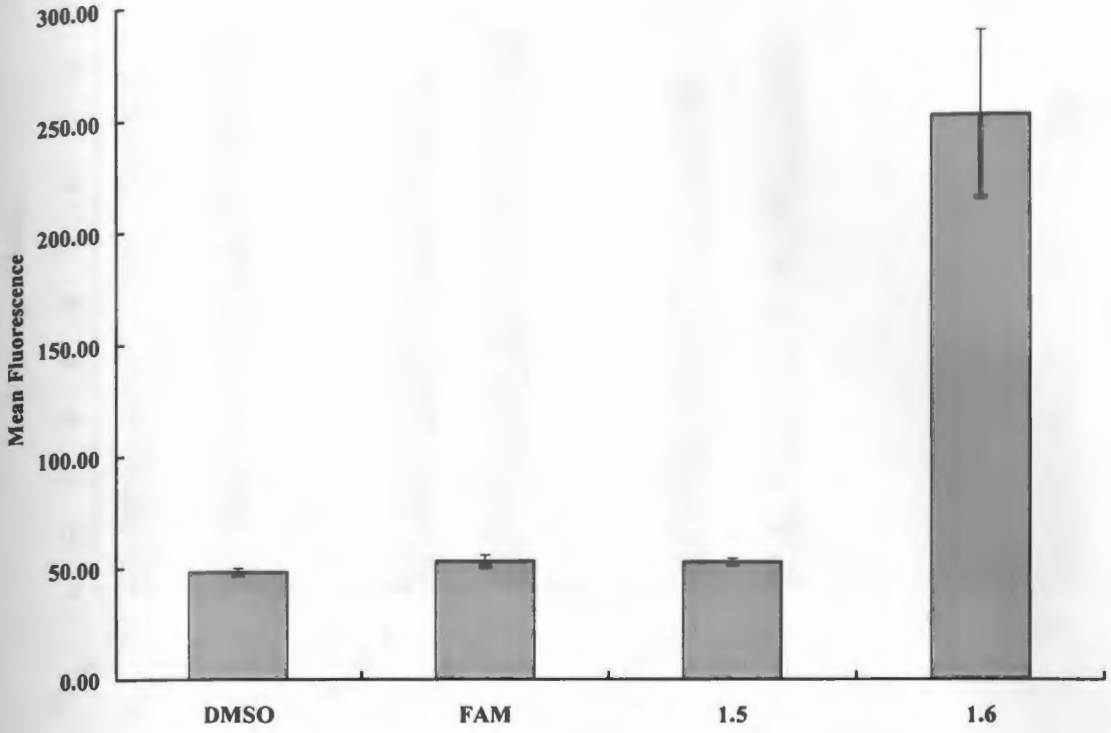

Figure 1.14. Cellular uptake studies for 5(6)-carboxyfluorescein derivatives of FLT (**1.5** and **1.6**) along with FAM and DMSO as controls after treatment with trypsin.

1.4.8. Cell Viability Study

Cell viability study was performed to analyze the effect of FAM, **1.5**, and **1.6** on the live cells. CCRF-CEM cells were incubated with 10 μM of the compounds and mixed with trypan blue (0.1%) to color the dead cells. The percentage of viability was calculated by using Cellometer Auto T.4 (Nexcelom Bioscience). It was observed that at least 80% of the cells were viable in presence of the compounds in 24 h incubation period (Figure 1.15).

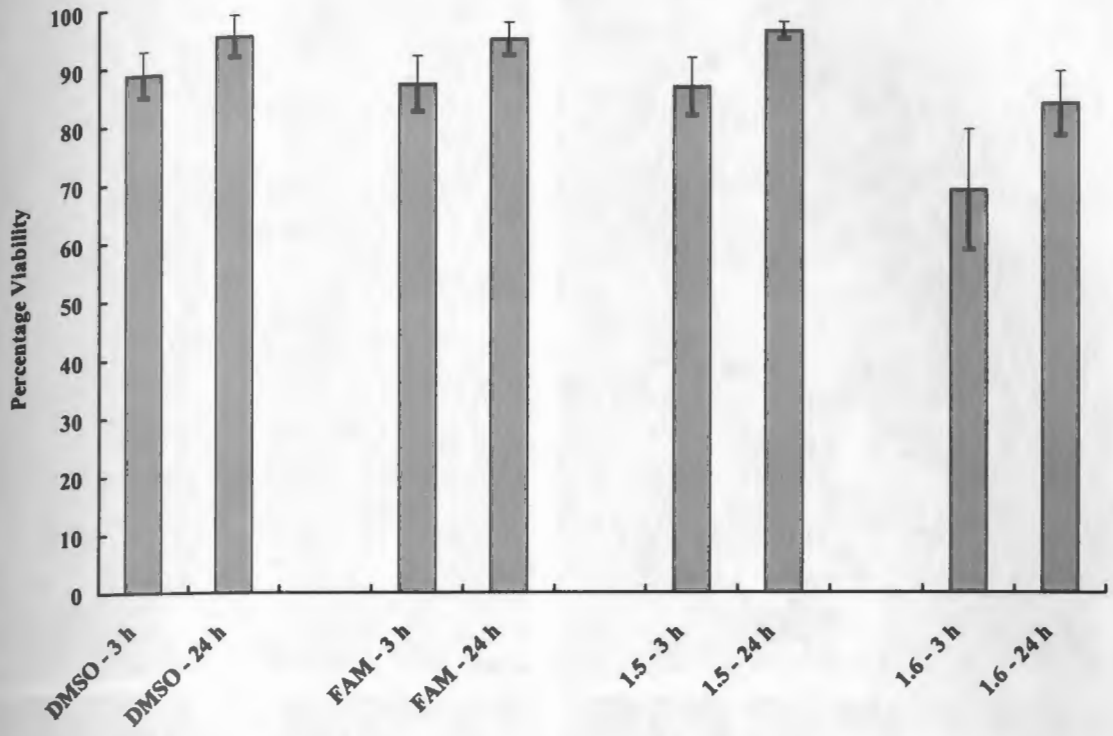

Figure 1.15. Cell viability assay after 3h and 24 h incubation of **1.5** and **1.6** with CCRF-CEM cells. DMSO and FAM were used as positive controls.

1.4.9. Real Time Fluorescence Microscopy in Live CCRF-CEM Cells

CCRF-CEM cells were incubated with 10 μM of DMSO, FAM, **1.5** and **1.6** for 1 h and were imaged using light microscope (ZEISS Axioplan 2) equipped with transmitted light microscopy with a differential-interference contrast method and an Achroplan 40X objective. Cells showed no significant fluorescence when incubated with DMSO, FAM, and 1.5 (Figure 1.16). On the other hand, cells incubated with **1.6** showed fluorescence. The results further confirm the higher cellular uptake of **1.6**, a fatty acyl derivative of FLT, in comparison to **1.5** and FAM alone. In general, these data indicate that the fatty acyl derivatives of nucleosides have better cellular uptake than their parent nucleosides.

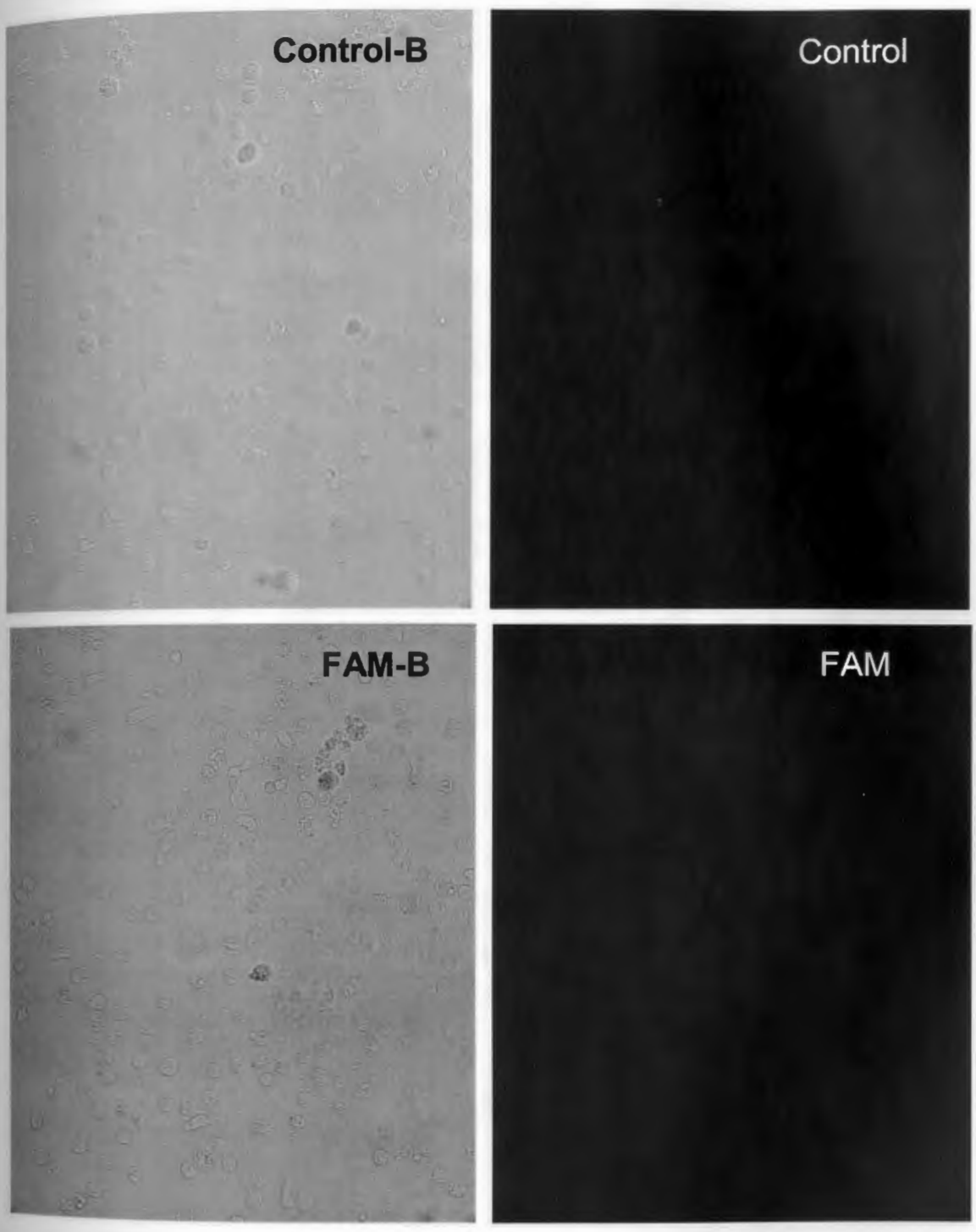
Control-B
Control
FAM-B
FAM

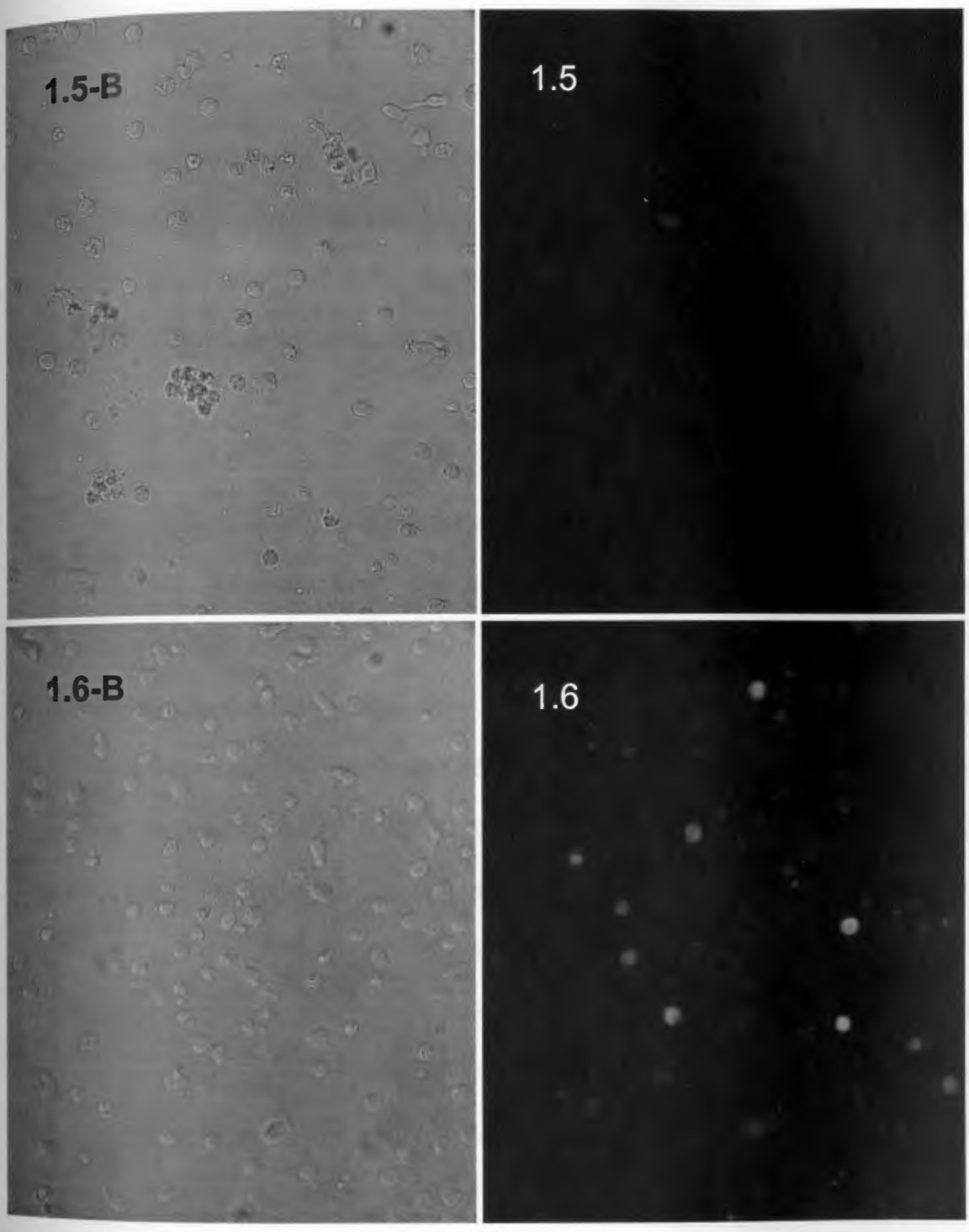

Figure 1.16. Real time fluorescence microscopy in live CCRF-CEM cell line. Control = DMSO, FAM = 5(6)-carboxyfluorescein.

1.5. Conclusions.

Several bifunctional 5′-*O*-fatty acyl derivatives of FLT were designed and synthesized as prodrugs of FLT, a nucleoside reverse transcriptase inhibitor, and their biological activities were evaluated as anti-HIV agents and microbicides. It was expected that after intracellular hydrolysis, the compounds would release two active parent analogs, FLT and fatty acid, targeting RT and NMT, respectively, involved in HIV life cycle.

Among all the compounds, KP-1, KP-16, and KP-17 were found to have better anti-HIV activity profile when compared with FLT, AZT, and 5′-*O*-fatty acyl derivatives of AZT. KP-1, KP-16, and KP-17 were active against cell-free virus (lymphocytotropic and monocytotropic strains). Furthermore, KP-1, KP-16, and KP-17 showed significantly higher activity against cell-associated virus when compared with AZT and FLT. These compounds were equally active against R5 and MDR, while AZT was not active against multidrug resistant virus. KP-1, KP-16 and KP-17 exhibited >4 and >30 times better antiviral index, respectively, than FLT and AZT. The compounds did not show any significant cytotoxicity in vaginal cells when compared with N-9 (a commercial microbicidal drug) suggesting that the compounds may be safer than N-9 for microbicidal applications. The 5′-*O*-ether derivatives of FLT and AZT (**1.7** and **1.8**) showed significantly less anti-HIV activity than the corresponding 5′-*O*-fatty acyl ester derivatives (KP-16 and KP-5), confirming the hypothesis that the hydrolysis of the prodrug to the parent analogs was critical for generation of anti-HIV activity.

The presence of long chain fatty acid at 5′-position enhanced the lipophilicity of FLT and the cellular uptake as was shown by cellular uptake studies of 5′-

carboxyfluroscein derivatives of FLT containing short chain (**1.5**) and long chain (**1.6**) alkyl ester groups. FACS experiments showed that **1.6** had at least 8-fold higher cellular uptake in CCRF-CEM cells than **1.5**. Fluorescence microscopy of the cells incubated with these compounds further confirmed the FACS results as cells incubated with **1.6** showed significantly higher fluorescence when compared with cells incubated with FAM and **1.5**. These results suggest that the increased inhibition by KP-1, KP-16, and KP-17 may be due to a higher intracellular level of active nucleoside achieved by the conjugate. The high activity of these compounds was possibly due to their increased rate of uptake and intracellular hydrolysis yielding two antiviral agents with different targets, FLT and fatty acid analog.

KP-1 and KP-17 are currently undergoing further preclinical studies, such as ADMET, animal toxicity, lactobacillus inhibition, and preformulation studies. These compounds may be used as topical microbicidal applications (such as vaginal insert or jellies) to prevent HIV infection during the sexual activity. These data provided insights for more rational design of additional potent and safe anti-HIV microbicides using the FLT as the parent nucleoside. When taken together, the results will have significant implications for the design of more potent and innovative anti-HIV agents.

1.6. Acknowledgments

Support for this subproject (MSA-03-367) was provided by CONRAD, Eastern Virginia Medical School under a Cooperative Agreement (HRN-A-00-98-00020-00) with the United States Agency for International Development (USAID). The views expressed by the authors do not necessarily reflect the views of USAID or CONRAD.

1.7. References

Boudinot, F. D., Smith, S. G., Funderburg, E. D., and Schinazi R. F. Pharmacokinetics of 3'-fluoro-3'-deoxythymidine and 3'-deoxy-2',3'-didehydrothymidine in rats. *Antimicrob. Agents Chemther.*, **1991**, 35, 747-749.

Bryant, M. L., McWherter, C. A., Kishore, N. S., Gokel, G. W., and Gordon, J. I. MyristoylCoA: Protein *N*-myristoyltransferase as a therapeutic target for inhibiting replication of human immunodeficiency virus-1. *Perspect. Drug Dis. Des.*, **1993**, *1*, 193-209.

Farazi, T. A., Waksman, and G., Gordon, J. I. The biology and enzymology of protein *N*-Myristoylation. *J. Biol. Chem.*, **2001**, 276, 39501–39504.

Furuishi, K., Matsuoko, H., Takama, M., Takahashi, I., Misumi, S., and Shoji, S. Blockage of N-myristoylation of HIV-1 Gag induces the production of impotent progeny virus. *Biochem. Biophys. Res. Commun.*, **1997**, 237, 504-511.

Ghosn, J., Quinson, A-M., Sabo, N. D., Cotte, L., Piketty, C., Dorléacq, N., Bravo, M-L., Mayers, D., Harmenberg, J., Mårdh, G., Valdez, H., and Katlama, C. Antiviral activity of low-dose alovudine in antiretroviral experienced patients: results from a 4-week randomized, double-blind, placebo-controlled dose-ranging trial. *HIV Med.*, **2007**, 8, 142-147

Herdewijn, P., Balzarini, J., De Clercq E., Pauwels, R., Baba, M., Broder, and S., Vanderhaeghe, H. 3'-Substituted 2',3'-dideoxynucleoide analogues as potential anti-HIV (HTLV-III/LAV) agents. *J. Med. Chem.* **1987**, 30, 1270-1278.

Kong, X. B., Zhu, Q. Y., Vidal, P. M., Watanabe, K. A., Polsky, B., Armstrong, D., Ostrander, M., Stanley A. Lang, S. A., Muchmore, E. And Chou T. C. Comparisons of anti-human immunodeficiency virus activities, cellular transport, and plasma and intracellular pharmacokinetics of 3'-fluoro-3'-deoxythymidine and 3'-azido-3'-deoxythymidine. *Antimicrob. Agents Chemother.*, **1992**, 36, 808-818.

Krebs, F. C., Miller, S. R., Malamud, D., Howett, M. K., Wigdahl, B. Inactivation of human immunodeficiency virus type 1 by nonoxynol-9, C21G, or an alkyl sulfate, sodium dodecyl sulfate. *Antiviral Res.* **1999**, 43, 147-163.

Mansuri, M. M., Hitchcock, M. J. M., Buroker, R. A., Bregman, C. L., Ghazzouli, I., Desiderio, J. V., Starrett, J. E., Sterzycki, R. Z. and Martin, J. C. Comparison of in vitro biological properties and mouse toxicities of three thymidine analogs active against human immunodeficiency virus. *Antimicrob. Agents Chemother.*, **1990**, 34, 637-641.

Parang, K., Knaus, E. E., Wiebe, L. I., Sardari, S., Daneshtalab, M., Csizmadia, F. Synthesis and antifungal activities of myristic acid analogs. *Arch. Pharm.-Pharm. Med. Chem.* **1996**, 329, 475-482.

Parang, K., Wiebe, L. I., Knaus, E. E., Huang, J.-S., Tyrrell, D. L., Csizmadia, F. *In vitro* antiviral activities of myristic acid analogs against human immunodeficiency and hepatitis B viruses. *Antiviral Res.* **1997**, 34, 75-90.

Rusconi, S., Moonis, M., Merrill, D. P., Pallai, P. V., Neidhardt, E. A., Singh, S. K., Willis, K. J., Osburne, M. S., Profy, A. T., Jenson, J. C., Hirsch, M. S. Naphthalene sulfonate polymers with CD4-blocking and anti-human immunodeficiency virus type 1 activities. *Antimicrob. Agents Chemother.*, **1996**, 40, 234-236.

Schinazi, R. F., Boudinot, F. D., Doshi, K. J., Mcclure, H. M. Pharmacokinetics of 3'-fluoro-3'-deoxythymidine and 3'-deoxy-2',3'-didehydrothymidine in rhesus monkeys. *Antimicrob. Agents Chemother.*, **1990**, 34, 1214-1219.

Sundseth, R., Joyner, S. S., Moore, J. T. Dornsife, R. E., Dev, I. K. The anti-human immunodeficiency virus agent 3'-fluorothymidine induces DNA damage and apoptosis in human lymphoblastoid cells. *Antimicrob. Agents Chemother.*, **1996**, 40, 331–335.

Takamune, N., Hamada, H. Misumi, S. And Shoji, S. Novel strategy for anti-HIV-1 action: selective cytotoxic effect of *N*-myristoyltransferase inhibitor on HIV-1 infected cells. *FEBS letters*, **2002**, 527, 138-142.

Wu, Z., Alexandratos, J., Ericksen, B., Lubkowshi, J., Gallo, R. C., Lu, W. Total chemical synthesis of N-myristoylated HIV-1 matrix protein p17: Structural and mechanistic implications of p17 myristoylation. *Proc. Natl. Acad. Sci. U. S. A.*, **2004**, 101, 11587-11592.

Chapter 2

Synthesis and Biological Evaluation of Fatty Acyl Ester Derivatives of 2',3'-Didehydro-2',3'-dideoxythymidine, 2',3'-Dideoxy-3'-thiacytidine, and 5-Fluoro-2',3'-dideoxy-3'-thiacytidine

Hitesh K. Agarwal,[a] Michael Hanley,[a] Guofeng Ye,[a] Sitaram Bhavaraju,[a] Megrose Quiterio,[a] Kelly Loethan,[a] Gustavo F. Doncel,[b] Keykavous Parang[a]

[a]Department of Biomedical and Pharmaceutical Sciences, University of Rhode Island, Kingston, RI, USA, 02881;[b]CONRAD, Department of Obstetrics and Gynecology, Eastern Virginia Medical School, Norfolk, VA, USA 23507

2.1. Abstract

A number of fatty acyl derivatives of 2',3'-didehydro-2',3'-dideoxythymidine (Stavudine, d4T), (-)-5-fluoro-2',3'-dideoxy-3'-thiacytidine (Emtricitabine, FTC), and (-)-2',3'-dideoxy-3'-thiacytidine (Lamivudine, 3TC) were synthesized. Anti-HIV activities of the compounds were evaluated and compared against cell-free and cell-associated virus. Fatty acyl derivatives of FTC (EC_{50} = 0.04–0.2 μM) were the most potent compounds when compared with the corresponding fatty acyl derivatives of AZT, FLT, d4T, and 3TC derivatives (EC_{50} = 0.2–12.9 μM). Among the compounds, 5'-*O*-myristoyl derivative of FTC (**2.31**) was found to be the most potent compound with minimal cellular toxicity. Compound **2.31** exhibited 10-fold higher anti-HIV activity against cell-free virus (EC_{50} = 0.07 μM) versus to FTC (EC_{50} = 0.7 μM). The anti-HIV activity of **2.31** against cell-associated virus (EC_{50} = 3.7 μM) was 24 times higher when compared with FTC (EC_{50} = 88.6 μM). Furthermore, 5'-*O*-12-azidododecanoyl derivative of FTC (**2.32**, EC_{50} = 0.2 μM) showed 4 and 10 times higher anti-HIV activities than FTC against cell-free and cell-associated virus, respectively. Among 3TC derivative, 5'-*O*-myristoyl (**2.16**, EC_{50} >0.2 μM) and 5'-*O*-12-azidododecanoyl (**2.17**, EC_{50} = 0.7 μM) derivatives of 3TC exhibited at least 57- and 16-fold higher anti-HIV activities than 3TC (**2.1**, EC_{50} = 11.3 μM) against cell-free virus, respectively. Cellular uptake studies were conducted on CCRF-CEM cell line using 5(6)-carboxyfluorescein derivatives of 3TC attached through β-alanine (**2.38**) or 12-aminododecanoic acid (**2.39**) as linkers. Fluorescein-substituted analog of 3TC with long chain length (**2.39**) showed3-6 fold higher cellular uptake profile than analog with short chain length (**2.39**) and 5(6)-carboxyfluorescein. The data

revealed that the attachment of fatty acid enhances the cellular uptake of the nucleoside conjugate.

2.2. Introduction

3TC, FTC, and d4T are the nucleoside reverse transcriptase (RT) inhibitors that inhibit human immunodeficiency virus-1 (HIV-1) replication. These drugs are commercially used in combination with two or more other anti-HIV drugs in Highly Active Antiretroviral Therapy (HAART) program. For example, 3TC and FTC are used in combination with Abacavir and Tenofovir, respectively, in the treatment of HIV infection (Masho et al., 2007). These drugs are known to have higher therapeutic index than AZT and FLT and show also anti-HIV activity against AZT resistant virus (Mansuri et al., 1990).

Lamivudine is a (-)-2',3'-dideoxy-3'-thiacytidine analog that is used in the treatment of both HIV-1 and hepatitis disease. Two isomers [(-) and (+)] of 2',3'-dideoxy-3'-thiacytidine show different biological profiles against HIV. (-)-Isomer is six-fold higher activity against HIV when compared with that of (+)-isomer and is nearly two times less cytotoxic, therefore it is used in clinic (Skalski et al., 1993). Although Lamivudine has good activity against wild type HIV, a single point mutation at 184 residue results in 3TC-resistant mutant virus (M184V/I) (Mulder et al., 2008, Sarafianos et al., 1999, Diallo et al., 2003). Several studies have provided different reasons for resistance development, such as cytidine deamination and the generation of steric

hindrance at 184 amino acid residues. Similar to the HIV, mutation at Met552 with Val and Ile (M552V/I) results in 3TC and FTC resistant HBV strains (Das et al., 2001).

Stavudine is a thymidine nucleoside analog and was approved in 1994 for treatment against HIV-1. d4T is well absorbed orally and is metabolized intracellularly to d4T 5'-triphosphate. d4T shows synergic effect with the other anti-HIV drugs and is generally used in triple therapy. Application of d4T as anti-HIV agent faces major challenges in the form of drug resistance. Different point mutations in RT, such as V75T and K65R, reduces d4T sensitivity against virus (Gracia-Lerma et al., 2003; Hurst and Noble, 1999).

FTC, a 5-fluoro derivative of 3TC, is 10-17 times more potent than 3TC. FTC and 3TC share common mechanism of action and drug resistance patterns (Masho et al., 2007). It is suggested that use of FTC with Tenofovir results in a higher barrier to drug resistance (Gallant et al., 2006; Pozniak et al., 2006).

N-Myristoyl transferase (NMT) enzyme is involved in catalyzing the myristoylation of several proteins in HIV life cycle (e.g., capsid protein p17, $Pr160^{gag\text{-}pol}$, $Pr55^{gag}$, $p27^{nef}$). At *N*-terminal glycine, viral proteins (gag and nef) are covalently attached to myristic acid in the presence of NMT. Myristic acid attachment makes the proteins more hydrophobic, which improves protein-protein and protein-membrane interactions (Farazi et al., 2001). For example, after the *N*-myristoylation, p17 protein localizes itself towards the cell membrane, where new virus is produced (Wu et al., 2004)

The replication of HIV-1 can be inhibited by heteroatom-containing analogs of myristic acid without accompanying cellular toxicity (Bryant et al., 1993, Takamune et al., 2002). It has been previously reported that several fatty acids, such as 2-methoxydodecanoic acid, 4-oxatetradecanoic acid, and 12-thioethyldodecanoic acid, reduce HIV-1 replication in acutely infected T-lymphocytes. For example, 12-thioethyldodecanoic acid was moderately active (EC_{50} = 9.4 μM) against HIV-infected T4 lymphocytes (Parang et al., 1997).

It is hypothesized that the attachment of nucleoside analogs to the long chain myristic acid analogs enhances their lipophilicity and thus their cellular uptake. Once the ester conjugate enters the cells; it gets hydrolyzed by esterases; and generates two active molecules, nucleoside analog and fatty acid targeting RT and NMT enzymes, respectively.

We previously reported the synthesis and evaluation of fatty acyl derivatives of AZT and FLT (chapter 1). Herein, we report the synthesis of fatty acyl derivatives of 3TC, FTC, and d4T, their anti-HIV activities, spermicidal activity, and cellular uptake profiles. Three fatty acids, myristic acid, 12-azidododecanoic acid, and 12-thioethyldodecanoic acid, were conjugated with the nucleosides. The selection of the fatty acids was based on the anti-HIV activities of the corresponding fatty acyl derivatives of FLT (chapter I). The conjugation of fatty acids to the selected nucleosides may result in development of anti-HIV agents having enhanced lipophilicity, longer

duration of action by sustained intracellular release of active substrates at adequate concentrations, and higher uptake into infected cells.

2.3. Materials and Methods

2.3.1. Materials.

Lamivudine (3TC) and Emtricitabin (FTC) were purchased from Euro Asia Tran Continental (Bombay, India). Stavudine (d4T) was purchased from Kemprotec (Middlesbrough, U.K.). 12-Bromododecanoic acid was purchased from Sigma Aldrich Chemical Co. 5(6)-Carboxyfluorescein (FAM) was purchased from Novabiochem. All the other reagents including solvents were purchased from Fisher scientific.

The products were purified on a Phenomenex®Gemini 10 μm ODS reversed-phase column (2.1 × 25 cm) with Hitachi HPLC system using a gradient system at constant flow rate of 17 ml/min (Table 2.1).

Table 2.1. HPLC method used for purification of the final compounds.

Time (min)	Water Concentration A (%)	Acetonitrile Concentration B (%)	Flow rate (mL/min)
0.00	100.0	0.0	1.0
1.0	100.0	0.0	17.0
45.0	0.0	100.0	17.0
55.0	0.0	100.0	17.0
59.0	100.0	0.0	17.0
60.0	100.0	0.0	1.0

The purity of the compounds was confirmed by using analytical Hitachi analytical HPLC system on a C18 column (Grace Allsphere ODS 2-3 μ, 150 X 4.6 mm) using a gradient system (water:acetonitrile 30:70 v/v) at constant flow rate of 1 ml/min with a UV detection at 265 nm. The chemical structures of final products were characterized by nuclear magnetic resonance spectrometry (^{1}H NMR and ^{13}C NMR) determined on a Bruker NMR spectrometer (400 MHz) and confirmed by a high-resolution PE Biosystems Mariner API time-of-flight electrospray mass spectrometer. Chemical shifts are reported in parts per millions (ppm). For cellular uptake studies, cells were analyzed by flow cytometry (FACSCalibur: Becton Dickinson) using FITC channel and CellQuest software. Cell-viability studies were conducted using Cellometer Auto T.4 (Nexcelom Biosciences). The real time microscopy in live CCRF-CEM cell line with or with compounds were imaged using ZEISS Axioplan 2 light microscope equipped with transmitted light microscopy with a differential-interference contrast method and an Achroplan 40X objective.

2.3.2. Chemistry

(-)-N_4,5'-(Ditetradecanoyl)-2',3'-dideoxy-3'-thiacytidine (2.2) and (-)-N_4,5'-di(12-azidododecanoyl)-2',3'-dideoxy-3'-thiacytidine (2.3)

In general, a reaction mixture consisting of the appropriate fatty acid (1.0 mmol), oxalyl chloride (100 μL, 1.2 mmol), and anhydrous benzene (18 mL) was stirred at room temperature (25 °C) for 1 h. The yellow solution thus obtained was evaporated to dryness under reduced pressure to prepare acid chloride. Lamivudine (**2.1**, 100 mg, 0.44 mmol) and 4-dimethylaminopyridine (DMAP, 160 mg, 1.3 mmol) were dissolved in dry benzene

(20 mL). The freshly prepared acid chloride (1.1 mmol) from the reaction of fatty acid with oxalyl chloride was added to the mixture. The reaction mixture was refluxed at 100 °C for 4 h. After the completion of reaction, the reaction mixture was cooled down to room temperature and neutralized with 5% sodium bicarbonate solution. Benzene layer was separated and aqueous layer was extracted with dichloromethane (3 × 100 mL). The Organic layer was separated and mixed with the benzene layer and concentrated at reduced pressure. The residue was purified with silica gel column chromatography using dichloromethane and methanol (0-1%) as eluents.

(-)-N_4,5'-(Ditetradecanoyl)-2',3'-dideoxy-3'-thiacytidine (2.2). Yield (155 mg, 53%); ^{1}H NMR (400 MHz, $CDCl_3$, δ ppm): 8.90-9.40 (br s, 1H, N*H*), 8.16 (d, *J* = 7.5 Hz, 1H, H-6), 7.48 (d, *J* = 7.5 Hz, 1H, H-5), 6.34 (dd, *J* = 3.2 and 5.1 Hz 1H, H-1'), 5.41 (t, *J* = 3.8 Hz, 1H, H-4'), 4.65 (dd, *J* = 12.5 and 4.8 Hz, 1H, H-5''), 4.45 (dd, *J* = 12.5, 3.0 Hz, 1H, H-5'), 3.64 (dd, *J* = 5.1, 12.6 Hz, 1H, H-2''), 3.29 (dd, *J* = 3.2, 12.6 Hz, 1H, H-2'), 2.47 (t, *J* = 7.6 Hz, 2H, C*H*$_2$CO), 2.40 (t, *J* = 7.6 Hz, 2H, C*H*$_2$CO), 1.60-1.75 (m, 4H, C*H*$_2$CH$_2$CO), 1.20-1.40 (br m, 40H, methylene protons), 0.89 (t, *J* = 6.7 Hz, 6H, C*H*$_3$); ^{13}C NMR (DMSO-d_6, 100 MHz, δ ppm): 175.06 (*C*ONH), 173.39 (*C*OO), 163.21 (C-4), 154.89 (C-2 C=O), 145.87 (C-6), 95.59 (C-5), 88.70 (C-1'), 87.75 (C-4'), 62.49 (C-5'), 38.31 (C-2'), 37.00 (*C*H$_2$CONH), 34.27, 32.00, 29.73, 29.63, 29.47, 29.43, 29.26, 29.16, 25.14, 22.77 (methylene carbons), 14.48 (*C*H$_3$). HR-MS (ESI-TOF) (m/z): $C_{36}H_{63}N_3O_5S$, calcd, 649.9675; found, 650.1885 $[M + H]^+$.

(-)-N_4,5'-Di(12-azidododecanoyl)-2',3'-dideoxy-3'-thiacytidine (2.3). Yield (170 mg, 55%); ^{1}H NMR (400 MHz, $CDCl_3$, δ ppm): 8.90-9.12 (br s, 1H, *NH*), 8.18 (d, *J* = 7.2 Hz, 1H, H-6), 7.49 (d, *J* = 7.2 Hz, 1H, H-5), 6.36 (m, 1H, H-1'), 5.43 (dd, *J* = 4.9, 3.0 Hz, 1H, H-4'), 4.67 (dd, *J* = 12.5 and 4.9 Hz, 1H, H-5''), 4.47 (dd, *J* = 12.5 and 3.0 Hz, 1H, H-5'), 3.64 (dd, *J* = 12.6 and 5.4 Hz, 1H, H-2''), 3.20-3.34 (m, 5H, H-2', C*H*$_2$N$_3$), 2.49 (t, *J* = 7.2 Hz, 2H, C*H*$_2$CO), 2.42 (t, *J* = 7.2 Hz, 2H, C*H*$_2$CO), 1.55-1.79 (m, 8H, -C*H*$_2$CH$_2$CO, C*H*$_2$CH$_2$N$_3$), 1.20-1.45 (br m, 28H, methylene protons); ^{13}C NMR ($CDCl_3$, 100 MHz, δ ppm): 179.51 (*C*ONH), 174.52 (*C*OO), 163.20 (C-4), 146.10 (C-6), 96.50 (C-5), 88.60 (C-1'), 83.84 (C-4'), 64.82 (C-5'), 63.06, 51.87 (*C*H$_2$N$_3$), 39.43 (C-2'), 37.96 (*C*H$_2$CONH), 34.80 (*C*H$_2$COO), 34.47, 29.84, 29.78, 29.63, 29.53, 29.47, 29.23, 29.20, 27.10, 25.14 (methylene carbons). HR-MS (ESI-TOF) (m/z): $C_{32}H_{53}N_9O_5S$, calcd, 675.8855; found, 676.6085 $[M + H]^+$.

(-)-5'-*O*-(*t*-Butyldimethylsilyl)-2',3'-dideoxy-3'-thiacytidine (2.4). Lamivudine (**2.1**, 1.09 mmol, 250 mg), *tert*-butyldimethylsilyl chloride (500 mg, 3.27 mmol), and imidazole (230 mg, 3.27 mmol) were dissolved in dry DMF (10 mL) and the reaction mixture was stirred for 18 h at room temperature. The solvent was concentrated at reduced pressure and the residue was purified with silica gel column chromatography using dichloromethane and methanol (0-5%) as eluents to yield **2.4** (350 mg, 95%); ^{1}H NMR (400 MHz, $CDCl_3$, δ ppm): 8.21 (d, *J* = 7.6 Hz, 1H, H-6), 6.32 (dd, *J* = 5.2 and 2.8 Hz, 1H, H-1'), 6.02 (d, *J* = 7.6 Hz, 1H, H-5), 5.26 (t, *J* = 3.0 Hz, 1H, H-4'), 4.18 (dd, *J* = 11.8 and 3.0 Hz, 1H, H-5''), 3.96 (dd, *J* = 11.8 and 3.0 Hz, 1H, H-5'), 3.54 (dd, *J* = 12.5 and 5.2 Hz, 1H, H-2''), 3.19 (dd, *J* = 12.5 and 2.8 Hz, 1H, H-2'), 0.95 (s, 9H, (C*H*$_3$)$_3$C),

0.15 (s, 6H, CH_3Si); HR-MS (ESI-TOF) (m/z): $C_{14}H_{25}N_3O_3SSi$, calcd, 343.1386; found, 344.3933 $[M + H]^+$, 686.4590 $[2M + H]^+$.

(-)-5'-*O*-(*t*-Butyldimethylsilyl)-N_4(tetradecanoyl)-2',3'-dideoxy-3'-thiacytidine (2.5), (-)-5'-*O*-(*t*-Butyldimethylsilyl)-N_4(12-azidododecanoyl)-2',3'-dideoxy-3'-thiacytidine (2.6), and (-)-5'-*O*-(*t*-Butyldimethylsilyl)-N_4(12-thioethyldodecanoyl)-2',3'-dideoxy-3'-thiacytidine (2.7). Compound **2.4** (140 mg, 0.4 mmol) and DMAP (70 mg, 0.6 mmol) were dissolved in dry benzene (10 mL). The corresponding acid chloride (0.48 mmol) (prepared as described above) was added dropwise and the reaction mixture was refluxed for 4 h at 100 °C. The reaction mixture was cooled down to room temperature and neutralized with saturated sodium bicarbonate solution (100 mL). The benzene layer was separated and aqueous layer was extracted with dichloromethane (3 × 100 mL). The organic layer was separated and mixed with benzene layer and concentrated at reduced pressure. The residue was purified with silica gel column chromatography using dichloromethane and methanol (0-1%) as eluents to afford **2.5-2.7**.

2.5. Yield (110 mg, 50%); ^{1}H NMR (400 MHz, CD_3OD, δ ppm): 8.12 (d, J = 7.5 Hz, 1H, H-6), 6.24 (dd, J = 5.3, 3.5 Hz, 1H, H-1'), 5.81 (d, J = 7.5 Hz, 1H, H-5), 5.26 (t, J = 3.3 Hz, 1H, H-4'), 4.09 (dd, J = 11.7 and 3.3 Hz, 1H, H-5''), 3.96 (dd, J = 11.7 and 3.3 Hz, 1H, H-5'), 3.49 (dd, J = 12.2 and 5.3 Hz, 1H, H-2''), 3.11 (dd, J = 12.2 and 3.5 Hz, 1H, H-2'), 2.24 (t, J = 7.4 Hz, 2H, CH_2CO), 1.56 (t, J = 7.1 Hz, 2H, CH_2CH$_2$CO), 1.20-1.35 (br m, 20H, methylene protons), 0.91 (s, 9H, (CH_3)$_3$C), 0.86 (t, J = 6.8 Hz, 3H, CH_3),

0.11 (s, 6H, C*H*$_3$Si); HR-MS (ESI-TOF) (m/z): $C_{28}H_{51}N_3O_4SSi$, calcd, 553.8727; found, 554.1020 $[M + H]^+$.

2.6. Yield (110 mg, 50%). ^{1}H NMR (400 MHz, $CDCl_3$, δ ppm): 8.40-8.69 (br s, 2H, N*H* and *H*-6), 7.44 (d, *J* = 7.3 Hz, 1H, H-5), 6.37-6.41 (m, 1H, H-1'), 5.33 (t, *J* = 2.5 Hz, 1H, H-4'), 4.27 (dd, *J* = 11.9 and 2.5 Hz, 1H, H-5"), 4.01 (dd, *J* = 11.9 and 2.5 Hz, 1H, H-5'), 3.64 (dd, *J* = 12.7 and 5.2 Hz, 1H, H-2"), 3.27-3.30 (m, 3H, H-2', C*H*$_2$N$_3$), 2.47 (s, 2H, C*H*$_2$CO), 1.60-1.82 (m, 4H, C*H*$_2$CH$_2$CO, C*H*$_2$CH$_2$N$_3$), 1.28-1.45 (br m, 14H, methylene protons), 0.99 (s, 9H, (C*H*$_3$)$_3$C), 0.18 (s, 6H, C*H*$_3$Si); HR-MS (ESI-TOF) (m/z): $C_{26}H_{46}N_6O_4SSi$, calcd, 556.8317; found, 567.0023 $[M + H]^+$.

2.7. Yield (110 mg, 50 %); ^{1}H NMR (400 MHz, $CDCl_3$, δ ppm) 9.29-9.41 (br s, 1H, N*H*), 8.60 (d, *J* = 7.5, 1H, H-6), 7.46 (d, *J* = 7.5, 1H, H-5), 6.37 (dd, *J* = 5.2 and 2.3 Hz, 1H, H-1'), 5.32 (t, *J* = 2.2, 1H, H-4'), 4.68 (dd, *J* = 11.9 and 2.2 Hz, 1H, H-5"), 4.00 (dd, *J* = 11.9 and 2.2 Hz, 1H, H-5'), 3.63 (dd, *J* = 12.7, 5.2, 1H, H-2"), 3.29 (d, *J* = 12.7, 1H, H-2'), 2.53-2.62 (m, 4H, C*H*$_2$SC*H*$_2$), 2.39 (t, *J* = 7.5, 2H, C*H*$_2$COO), 1.52-1.83 (m, 4H, C*H*$_2$CH$_2$COO and SCH$_2$C*H*$_2$), 1.21-1.50 (br m, 17H, methylene protons, C*H*$_3$CH$_2$S), 0.99 (s, 9H, (C*H*$_3$)$_3$C), 0.18 (s, 6H, C*H*$_3$Si); HR-MS (ESI-TOF) (m/z): $C_{28}H_{51}N_3O_4S_2Si$, calcd, 585.3077; found, 585.8926 $[M + H]^+$, 607.8040 $[M + Na]^+$.

(-)-N$_4$(Tetradecanoyl)-2',3'-dideoxy-3'-thiacytidine (2.8), (-)-N$_4$(12-azidododecanoyl)-2',3'-dideoxy-3'-thiacytidine (2.9), and (-)-N$_4$(12-bromoethyldodecanoyl)-2',3'-dideoxy-3'-thiacytidine (2.10). Tetrabutylammonium

fluoride (1.5 mL, 1M) was added to **2.5-2.7** (150 mg) and the reaction mixture was stirred at room temperature for 3 h. Solvent was concentrated at reduced pressure and the residue was purified with silica gel column chromatography using dichloromethane and methanol (0-1%) as eluents to afford **2.8-2.10**.

2.8. Yield (55 mg, 65%); ^{1}H NMR (400 MHz, DMSO-d_6, δ ppm): 10.85 (s, 1H, *N*H), 8.38 (d, *J* = 7.5 Hz, 1H, H-6), 7.23 (d, *J* = 7.5 Hz, 1H, H-5), 6.21 (dd, *J* = 5.2 and 3.2 Hz, 1H, H-1'), 5.26 (t, *J* = 4.1 Hz, 1H, H-4'), 3.82-3.85 (br s, 2H, H-5" and H-5'), 3.56 (dd, *J* = 12.3 and 5.2 Hz, 1H, H-2"), 3.20 (dd, *J* = 12.3 and 3.2 Hz, 1H, H-2'), 2.38 (t, *J* = 7.3 Hz, 2H, C*H*$_2$CO), 1.53 (t, *J* = 6.5 Hz, 2H, C*H*$_2$CH$_2$CO), 1.15-1.35 (s, 20H, methylene protons), 0.89 (t, *J* = 6.7 Hz, 3H, C*H*$_3$); ^{13}C NMR (DMSO-d_6, 100 MHz, δ ppm): 174.80 (*C*OO), 163.41 (C-4), 155.11 (C-2 C=O), 146.17 (C-6), 95.8 (C-5), 88.90 (C-1'), 87.94 (C-4'), 62.70 (C-5'), 38.51 (C-2'), 37.16 (*C*H$_2$CONH), 32.16, 29.92, 29.88, 29.73, 29.57, 29.30, 25.28, 22.96 (methylene carbons), 14.77 (C*H*$_3$); HR-MS (ESI-TOF) (m/z): $C_{22}H_{37}N_3O_4S$, calcd, 439.6119; found, 440.3352 $[M + H]^+$, 462.2543 $[M + Na]^+$, 878.1789 $[2M + H]^+$, 900.0877 $[2M + Na]^+$.

2.9. Yield (50 mg, 60%); ^{1}H NMR (400 MHz, $CDCl_3$, δ ppm): 8.45-8.47 (br s, 2H, N*H*, H-6), 7.49 (d, *J* = 7.5 Hz, 1H, H-5), 6.38 (dd, *J* = 5.3 and 3.4 Hz, 1H, H-1'), 5.41 (t, *J* = 3.2 Hz, 1H, H-4'), 4.21 (dd, *J* = 12.7 and 3.2 Hz, 1H, H-5"), 4.01 (dd, *J* = 12.7 and 3.2 Hz, 1H, H-5'), 3.68 (dd, *J* = 12.5 and 5.3 Hz, 1H, H-2"), 3.27-3.31 (m, 3H, H-2', C*H*$_2$N$_3$), 2.48 (t, *J* = 6.8 Hz, 2H, C*H*$_2$CO), 1.58-1.68 (m, 4H, C*H*$_2$CH$_2$CO, C*H*$_2$CH$_2$N$_3$), 1.25-1.45 (br m, 14H, methylene protons); ^{13}C NMR ($CDCl_3$, 100 MHz, δ ppm): 173.65 (*C*OO),

162.40 (C-4), 155.04 (C-2 C=O), 145.47 (C-6), 96.28 (C-5), 88.32 (C-1'), 88.23 (C-4'), 62.99 (C-5'), 51.67 (CH_2N_3), 39.18 (C-2'), 38.05 (CH_2CONH), 29.61, 29.54, 29.45, 29.31, 29.19, 29.02, 26.89, 25.03 (methylene carbons); HR-MS (ESI-TOF) (m/z): $C_{20}H_{32}N_6O_4S$, calcd, 452.5709; found, 453.2421 $[M + H]^+$, 903.9628 $[2M + H]^+$.

2.10. Yield (50 mg, 50%); ^1H NMR (400 MHz, $CDCl_3$, δ ppm): 8.58 (s, 1H, N*H*), 8.02-8.07 (br s, 1H, H-6), 6.26-6.30 (br s, 1H, H-5), 6.13-6.17 (m, 1H, H-1'), 5.35 (d, J = 2.8 Hz, 1H, H-4'), 4.59-4.72 (m, 1H, H-5''), 4.35-4.45 (m, 1H, H-5'), 3.53-3.65 (m, 1H, H-2''), 3.20-3.32 (m, 1H, H-2'), 2.45-2.75 (m, 4H, CH_2SCH_2), 2.33-2.43 (m, 2H, CH_2COO), 1.53-1.70 (m, 4H, SCH_2CH_2, CH_2CH_2CO), 1.20-1.40 (br m, 17H, methylene protons, CH_3CH_2S); ^{13}C NMR ($CDCl_3$, 100 MHz, δ ppm): 174.08 (*C*OO), 163.02 (C-4), 155.44 (C-2 *C*=O), 145.85 (C-6), 96.73 (C-5), 88.61 (C-1'), 88.48 (C-4'), 63.14 (C-5'), 39.38 (C-2'), 38.10 (CH_2CONH), 34.83, 32.06, 26.31-30.10, 25.32 (methylene carbons), 15.23 (CH_3); HR-MS (ESI-TOF) (m/z): $C_{22}H_{37}N_3O_4S_2$, calcd, 471.6769; found, 472.1656 $[M + H]^+$, 941.7961 $[2M + H]^+$.

(-)-5'-*O*-(*t*-Butyldimethylsilyl)-N_4-(4,4'-dimethoxytrityl)-2',3'-dideoxy-3'-thiacytidine (2.11). Compound 2.4 (600 mg, 1.75 mmol) was dissolved in dry pyridine (10 mL). A solution of 4,4'-dimethoxytrityl chloride (DMTr-Cl, 1.4 mg, 4.4 mmol) in 10 mL pyridine was added to the reaction mixture dropwise at 0 °C. The reaction mixture was stirred for 30 min. The temperature was raised to room temperature and stirring was continued overnight. The reaction mixture was neutralized with saturated sodium bicarbonate solution (500 mL) and was extracted with dichloromethane (3 × 200 mL). The organic

layer was separated and concentrated *in vacuo*. The residue was purified with silica gel column chromatography using dichloromethane and methanol (0-1 %) as eluents to yield **2.11** (1.05 g, 90%).

^{1}H NMR (400 MHz, $CDCl_3$, δ ppm): 7.81 (d, J = 7.7 Hz, 1H, H-6), 7.74 (dd, J = 5.7 and 3.3 Hz, 1H, DMTr proton), 7.55 (dd, J = 5.7 and 3.2 Hz, 1H, DMTr proton), 7.12-7.33 (m, 7H, DMTr protons), 6.82-6.88 (m, 4H, DMTr protons), 6.33 (dd, J = 5.2 and 3.0 Hz, 1H, H-1'), 5.17-5.22 (m, 1H, H-4'), 5.03 (d, J = 7.7 Hz, 1H, H-5), 4.38 (dd, J = 14.3 and 7.1 Hz, 1H, H-5"), 4.06 (dd, J = 11.8 and 3.1 Hz, 1H, H-5'), 3.81 (s, 6H, DMTr-OCH_3), 3.52 (dd, J = 12.2 and 5.2 Hz, 1H, H-2"), 3.17 (dd, J = 12.2 and 3.0 Hz, 1H, H-2'), 0.80 (s, 9H, (CH_3)$_3$C), 0.06 (s, 6H, CH_3Si); HR-MS (ESI-TOF) (m/z): $C_{35}H_{43}N_3O_5SSi$, calcd, 645.8835; found, 686.4624 $(M+K)^+$, 1289.3671 $(2M+H)^+$.

(-)-N_4-(4,4'-Dimethoxytrityl)-2',3'-dideoxy-3'-thiacytidine (2.12). Compound **2.11** (1 g, 1.55 mmol) was dissolved in tetrabutylammonium fluoride (4.65 ml, 1 M, 4.65 mmol,) and stirred for 3 h. The reaction mixture was concentrated at reduced pressure and the residue was purified with silica gel column chromatography using dichloromethane (2% triethylamine) and methanol (0-1%) as eluents to yield **2.12** (820 mg, 90%).

^{1}H NMR (400 MHz, CD_3OD, δ ppm): 8.53 (d, J = 7.8 Hz, 1H, H-6), 7.32-7.34 (m, 2H, DMTr protons), 7.17-7.23 (m, 6H, DMTr protons), 7.11-7.13 (m, 1H, DMTr protons), 6.75-7.78 (m, 4H, DMTr protons), 6.22 (dd, J = 5.3 and 2.5 Hz, 1H, H-1'), 6.01 (d, J = 7.8 Hz, 1H, H-5), 5.25 (t, J = 3.2, 1H, H-4'), 3.99 (dd, J = 12.8 and 3.2 Hz, 1H, H-5"), 3.84 (dd, J = 12.8 and 3.2 Hz, 1H, H-5'), 3.69 (s, 6H, DMTr-OCH_3), 3.51 (dd, J = 12.6 and 5.3 Hz, 1H, H-2"), 3.27 (dd, J = 12.6 and 2.5 Hz, 1H, H-2'); HR-MS (ESI-TOF)

(m/z): $C_{29}H_{29}N_3O_5S$, calcd, 531.1828; found, 531.92 $[M + H]^+$, 632.6916 $[M + TEA)]^+$, 1061.1780 $[2M + 1]^+$.

(-)-N_4-(4,4′-Dimethoxytrityl)-5'-*O*-(tetradecanoyl)-2',3'-dideoxy-3'-thiacytidine (2.13), (-)-5'-*O*-(12-azidododecanoyl)-N_4-(4,4′-dimethoxytrityl)-2',3'-dideoxy-3'-thiacytidine (2.14), and (-)-N_4-(4,4′-dimethoxytrityl)-5'-*O*-(12-thioethyldodecanoyl)-2',3'-dideoxy-3'-thiacytidine (2.15). Compound **2.12** (150 mg, 0.30 mmol), the corresponding fatty acid (0.60 mmol), and 2-(1H-benzotriazole-1-yl)-1,1,3,3-tetramethyluronium hexafluorophosphate (HBTU, 250 mg, 0.65 mmol) were dissolved in dry DMF (10 mL). Diisopropylethylamine (DIPEA, 2 mL, 15 mmol) was added to the reaction mixture and stirring was continued overnight at room temperature. The reaction mixture was concentrated at reduced pressure and the residue was purified with silica gel column chromatography using dichloromethane (2% triethylamine) as eluents to afford **2.13-2.15**.

2.13. Yield (100 mg, 50%); ^{1}H NMR (400 MHz, CD_3OD, δ ppm) 8.62 (d, J = 7.8 Hz, 1H, H-6), 7.40-7.43 (m, 2H, DMTr protons), 7.26-7.30 (m, 6H, DMTr protons), 7.18-7.22 (m, 1H, DMTr proton), 6.85 (d, J = 8.9 Hz, 4H, DMTr protons), 6.28-6.32 (m, 1H, H-1'), 6.08 (d, J = 7.8 Hz, 1H, H-5), 5.34 (t, J = 3.1 Hz, 1H, H-4'), 4.07 (dd, J = 12.8 and 3.1 Hz, 1H, H-5''), 3.92 (dd, J = 12.9 and 3.1 Hz, 1H, H-5'), 3.78 (s, 6H, DMTr-OCH_3), 3.60 (dd, J = 5.3 and 12.3 Hz, 1H, H-2''), 3.36 (d, J = 12.3 Hz, 1H, H-2'), 2.29 (t, J = 7.3 Hz, 2H, CH_2CO), 1.60 (t, J = 6.8 Hz, 2H, CH_2CH$_2$CO), 1.20-1.42 (br m, 20H, methylene

protons), 0.91 (s, J = 6.6 Hz, 3H, CH_3). HR-MS (ESI-TOF) (m/z): $C_{43}H_{55}N_3O_6S$, calcd, 741.3812; found, 742.35 $[M + H]^+$, 843.4629 $[M + TEA]^+$, 1483.7079 $[2M + H]^+$.

(-)-5'-*O*-(Tetradecanoyl)-2',3'-dideoxy-3'-thiacytidine (2.16), (-)-5'-*O*-(12-azidododecanoyl)-2',3'-dideoxy-3'-thiacytidine (2.17) and (-)-5'-*O*-(12-thioethyldodecanoyl)-2',3'-dideoxy-3'-thiacytidine (2.18): Acetic acid (AcOH, 80%, 10 mL) was added to compounds **2.13-2.15** (0.25 mmol). The reaction mixture was heated at 80 °C for 30 min. The reaction mixture was concentrated at reduced pressure and the residue was purified with silica gel column chromatography using dichloromethane as the eluent to afford **2.16-2.18**.

2.16. Yield (50 mg, 65%); ^{1}H NMR (400 MHz, $CDCl_3$, δ ppm): 7.72 (d, J = 7.5 Hz, 1H, H-6), 6.30 (t, J = 4.7 Hz, 1H, H-1'), 5.97 (d, J = 7.5 Hz, 1H, H-5), 5.32 (dd, J = 3.5 and 5.5 Hz, 1H, H-4'), 4.51 (dd, J = 12.1 and 5.5 Hz, 1H, H-5"), 4.35 (dd, J = 12.1 and 3.5 Hz, 1H, H-5'), 3.52 (dd, J = 12.0 and 5.4 Hz, 1H, H-2"), 3.09 (dd, J = 12.0 and 4.7 Hz, 1H, H-2'), 2.34 (t, J = 7.6 Hz, 2H, CH_2CO), 1.49-1.72 (m, 2H, CH_2CH$_2$CO), 1.18-1.42 (br m, 20H, methylene protons), 0.87 (s, J = 6.7 Hz, 3H, CH_3); ^{13}C NMR ($CDCl_3$, 100 MHz, δ ppm): 173.39 (*C*OO), 165.98 (C-4), 155.64 (C-2 C=O), 140.73 (C-6), 94.96 (C-5), 87.79 (C-1'), 83.21 (C-4'), 64.48 (C-5'), 38.22 (C-2'), 34.24 (*C*H$_2$COO), 32.10, 29.87, 29.84, 29.79, 29.65, 29.54, 29.45, 29.31, 25.03, 22.88 (methylene carbons), 14.33 (*C*H$_3$); HR-MS (ESI-TOF) (m/z): $C_{22}H_{37}N_3O_4S$, calcd, 439.2505; found, 440.2835 $[M + H]^+$.

2.17. Yield (50 mg, 65%); ^{1}H NMR (400 MHz, CD_3OD, δ ppm): 7.71 (d, J = 7.5 Hz, 1H, H-6), 6.29 (dd, J = 5.2 and 3.8 Hz, 1H, H-1'), 6.01 (d, J = 7.5 Hz, 1H, H-5), 5.33 (dd, J = 3.2 and 5.4 Hz, 1H, H-4'), 4.51 (dd, J = 12.2 and 5.4 Hz, 1H, H-5''), 4.35 (dd, J = 12.2 and 3.2 Hz, 1H, H-5'), 3.52 (dd, J = 12.0 and 5.2Hz, 1H, H-2''), 3.21-3.28 (m, 2H, CH_2N_3), 3.08 (dd, J = 12.0 and 3.8 Hz, 1H, H-2'), 2.34 (t, J = 7.5 Hz, 2H, CH_2CO), 1.54-1.64 (m, 4H, CH_2CH_2CO, $CH_2CH_2N_3$), 1.22-1.38 (br m, 14H, methylene protons); ^{13}C NMR (CD_3OD, 100 MHz, δ ppm): 173.40 (*C*OO), 164.96 (C-4), 154.96 (C-2 C=O), 140.98 (C-6), 95.31 (C-5), 87.64 (C-1'), 83.51 (C-4'), 64.32 (C-5'), 51.64 (CH_2N_3), 38.20 (C-2'), 34.19 (CH_2CO), 29.88, 29.71, 29.60, 29.54, 29.39, 29.29, 29.24, 28.98, 26.86, 24.98, (methylene carbons); HR-MS (ESI-TOF) (m/z): $C_{20}H_{32}N_6O_4S$, calcd, 452.2206; found, 453.1729 $[M + H]^+$.

2.18. Yield (50 mg, 65%); ^{1}H NMR (400 MHz, CD_3OD, δ ppm): 7.64 (d, J = 7.4 Hz, 1H, H-6), 6.29-6.35 (m, 1H, H-1'), 5.91 (d, J = 7.4 Hz, 1H, H-5), 5.30-5.34 (m, 1H, H-4'), 4.49 (dd, J = 12.0 and 5.7 Hz, 1H, H-5''), 4.35 (dd, J = 12.0 and 3.2 Hz, 1H, H-5'), 3.50 (dd, J = 12.0 and 5.3 Hz, 1H, H-2''), 3.04 (dd, J = 12.0 and 4.6 Hz, 1H, H-2'), 2.44-2.63 (m, 4H, CH_2SCH_2), 2.34 (t, J = 7.4 Hz, 2H, CH_2CO), 1.50-1.79 (m, 4H, SCH_2CH_2, CH_2CH_2CO), 1.18-1.48 (br m, 17H, methylene protons); ^{13}C NMR (CD_3OD, 100 MHz, δ ppm): 173.36 (*C*OO), 166.01 (C-4), 155.60 (C-2 C=O), 140.49 (C-6), 95.35 (C-5), 87.73 (C-1'), 83.03 (C-4'), 64.55 (C-5'), 38.04 (C-2'), 34.20 (CH_2COO), 31.82, 29.80, 29.67, 29.58, 29.41, 29.62, 29.11, 28.90, 25.00, 22.88 (methylene carbons), 14.33 (CH_3); HR-MS (ESI-TOF) (m/z): $C_{22}H_{37}N_3O_4S_2$, calcd, 471.2225; found, 472.2418 $[M + H]^+$, 941.9318 $[2M + H]^+$.

5'-*O*-(Tetradecanoyl)-2',3'-didehydro-2',3'-dideoxythymidine (2.20), 5'-*O*-(12-azidododecanoyl)-2',3'-didehydro-2',3'-dideoxythymidine (2.21), 5'-*O*-(12-thioethyldodecanoyl)-2',3'-didehydro-2',3'-dideoxythymidine (2.22), and 5'-*O*-(12-bromododecanoyl)-2',3'-didehydro-2',3'-dideoxythymidine (2.23). Stavudine (2.19, 100 mg, 0.4 mmol) and DMAP (80 mg, 0.6 mmol) were dissolved in dry benzene (20 mL) and freshly prepared acid chloride (0.48 mmol) (as described above) was added to the mixture. The reaction mixture was refluxed at 100 °C for 4 h. The reaction mixture was cooled down to room temperature and neutralized with saturated sodium bicarbonate solution (100 mL). The benzene layer was separated and the aqueous layer was extracted with dichloromethane (3 × 100 mL). The organic layer was separated and mixed with the benzene layer and concentrated at reduced pressure. The residue was purified with silica gel column chromatography using dichloromethane and methanol (1 %) as eluents to yield **2.20-2.23**.

2.20. Yield (150 mg, 80%); ^{1}H NMR (400 MHz, $CDCl_3$, δ ppm): 9.29 (s, 1H, N*H*), 7.27 (s, 1H, H-6), 7.01-7.07 (br s, 1H, H-1'), 6.26-6.32 (m, 1H, H-2'), 5.91-5.95 (m, 1H, H-3'), 5.04-5.09 (m, 1H, H-4'), 4.44-4.55 (m, 1H, H-5''), 4.17-4.34 (m, 1H, H-5'), 2.34 (t, J = 7.4 Hz, 2H, CH_2CO), 1.95 (s, 3H, 5-CH_3), 1.61-1.67 (m, 2H, CH_2CH$_2$CO), 1.16-1.44 (br m, 20H, methylene protons), 0.90 (s, 3H, CH_3); ^{13}C NMR ($CDCl_3$, 100 MHz, δ ppm): 173.72 (*C*OO), 164.28 (C-4 C=O), 151.27 (C-2 C=O), 135.85 (C-6), 133.60 (C-3'), 127.72 (C-2'), 111.45 (C-5), 90.14 (C-1'), 84.69 (C-4'), 64,86 (C-5'), 34.51 (*C*H$_2$COO), 32.29, 30.02, 29.83, 29.73, 29.64, 29.50, 25.19, 23.07 (methylene carbons), 14.52 (5-

*C*H$_3$), 13.03 (*C*H$_3$); HR-MS (ESI-TOF) (m/z): $C_{24}H_{38}N_2O_5$, calcd, 434.5689; found, 456.9157 $[M + Na]^+$, 474.8787 $[M + K]^+$, 869.0358 $[2M + H]^+$, 891.0285 $[2M + Na]^+$.

2.21. Yield (120 mg, 70%); ^{1}H NMR (400 MHz, $CDCl_3$, δ ppm): 9.37 (s, 1H, N*H*), 7.24 (s, 1H, H-6), 6.99-7.03 (br s, 1H, H-1'), 6.27 (d, J = 5.7 Hz, 1H, H-2'), 5.90 (d, J = 5.7 Hz, 1H, H-3'), 5.02-5.06 (m, 1H, H-4'), 4.43 (dd, J = 12.4 and 3.8 Hz, 1H, H-5''), 4.22 (dd, J = 12.4 and 3.8 Hz, 1H, H-5'), 3.26 (t, J = 6.9 Hz, 2H, C*H*$_2$N$_3$), 2.32 (t, J = 7.5 Hz, 2H, C*H*$_2$COO), 1.92 (s, 3H, 5-C*H*$_3$), 1.50-1.70 (m, 4H, C*H*$_2$CH$_2$COO and C*H*$_2$CH$_2$N$_3$), 1.12-1.47 (br m, 14H, methylene protons); ^{13}C NMR ($CDCl_3$, 100 MHz, δ ppm): 173.71 (*C*OO), 164.35 (C-4 C=O), 151.31 (C-2 C=O), 135.89 (C-6), 133.61 (C-3'), 127.72 (C-2'), 111.45 (C-5), 90.16 (C-1'), 84.69 (C-4'), 64,86 (C-5'), 51.85 (C*H*$_2$N$_3$), 34.49 (*C*H$_2$COO), 29.81, 29.61, 29.48, 29.21, 26.30, 25.17 (methylene carbons), 13.03 (*C*H$_3$); HR-MS (ESI-TOF) (m/z): $C_{22}H_{33}N_5O_5$, calcd, 447.5279; found, 469.8802 $[M + Na]^+$, 485.8541 $[M + K]^+$.

2.22. Yield (110 mg, 65%); ^{1}H NMR (400 MHz, $CDCl_3$, δ ppm) 8.37 (s, 1H, N*H*), 7.25 (s, 1H, H-6), 6.99-7.04 (br s, 1H, H-1'), 6.29 (d, J = 5.8 Hz, 1H, H-2'), 5.92 (d, J = 5.8 Hz, 1H, H-3'), 5.04-5.08 (m, 1H, H-4'), 4.45 (dd, J = 12.4 and 4.0 Hz, 1H, H-5''), 4.24 (dd, J = 12.4 and 3.0 Hz, 1H, H-5'), 2.45-2.61 (m, 4H, C*H*$_2$SC*H*$_2$), 2.34 (t, J = 7.5, 2H, C*H*$_2$COO), 1.94 (s, 3H, 5-C*H*$_3$), 1.50-1.72 (m, 4H, C*H*$_2$CH$_2$COO and SCH$_2$C*H*$_2$), 1.18-1.42 (br m, 17H, methylene protons); ^{13}C NMR ($CDCl_3$, 100 MHz, δ ppm): 173.69 (*C*OO), 163.69 (C-4 C=O), 150.86 (C-2 C=O), 135.88 (C-6), 133.75 (C-3'), 127.64 (C-2'), 111.40 (C-5), 90.19 (C-1'), 84.74 (C-4'), 64.87 (C-5'), 34.52 (*C*H$_2$COO), 32.07, 30.11,

30.04, 29.90, 29.82, 29.74, 29.65, 29.58, 29.52, 29.46, 29.35, 26.32, 25.21 (methylene carbons), 15.24 (5-*C*H$_3$), 13.04 (*C*H$_3$); HR-MS (ESI-TOF) (m/z): $C_{24}H_{38}N_2O_5S$, calcd, 466.6339; found, 489.4530 $[M + Na]^+$, 505.4377 $[M + K]^+$ 955.8658 $[2M + Na]^+$.

2.23. Yield (150 mg, 80%); ^{1}H NMR (400 MHz, $CDCl_3$, δ ppm): 8.10 (s, 1H, N*H*), 7.24 (s, 1H, H-6), 7.00 (d, *J* = 1.7 Hz, 1H, H-1'), 6.28 (dd, *J* = 5.9 and 1.7 Hz, 1H, H-2'), 5.90 (d, *J* = 5.9 Hz, 1H, H-3'), 5.03-5.08 (m, 1H, H-4'), 4.43 (dd, *J* = 12.4 and 4.0 Hz, 1H, H-5'), 4.23 (dd, *J* = 12.4 and 2.9 Hz, 1H, H-5'), 3.54 and 3.42 (t, *J* = 6.8 and 6.4 Hz, 2H, C*H*$_2$Br isotopes), 2.33 (t, *J* = 7.50, 2H, C*H*$_2$COO), 1.93 (s, 3H, 5-C*H*$_3$), 1.73-1.88 (m, 2H, C*H*$_2$CH$_2$Br), 1.55-1.70 (m, 4H, C*H*$_2$CH$_2$COO), 1.36-1.48 (m, 2H, C*H*$_2$CH$_2$CH$_2$Br), 1.20-1.35 (br m, 12H, methylene protons); ^{13}C NMR ($CDCl_3$, 100 MHz, δ ppm): 173.70 (*C*OO), 164.30 (C-4 C=O), 151.28 (C-2 C=O), 135.87 (C-6), 133.61 (C-3'), 127.74 (C-2'), 111.45 (C-5), 90.16 (C-1'), 84.70 (C-4'), 64,88 (C-5'), 45.62 (*C*H$_2$Br), 34.51 (*C*H$_2$COO), 33.20, 29.82, 29.76, 29.62, 29.48, 29.45, 29.13, 28.54, 27.25, 25.18 (methylene carbons), 13.03 (5-*C*H$_3$); HR-MS (ESI-TOF) (m/z): $C_{22}H_{33}BrN_2O_5$, calcd, 485.4118; found 507.2254 $[M + Na]^+$and 509.1860 $[M + Na]^+$ (Bromo isotopes).

(-)-5'-*O*-(*t*-Butyldimethylsilyl)-5-fluoro-2',3'-dideoxy-3'-thiacytidine (2.25). Emtricitabine (**2.24**, 500 mg, 2.18 mmol), *tert*-butyldimethylsilyl chloride (1 g, 6.54 mmol), and imidazole (440 mg, 6.54 mmol) were dissolved in dry DMF (10 mL) and the reaction mixture was stirred for 18 h at room temperature. The solvent was concentrated at reduced pressure and the residue was purified with silica gel column chromatography using dichloromethane and methanol (0-5%) as eluents to yield **2.25**(700 mg, 90%).

^{1}H NMR (400 MHz, $CDCl_3$, δ ppm): 8.50-9.20 (br s, 2H, NH_2), 8.17 (d, J = 6.4 Hz, 1H, H-6), 6.25 (dd, J = 5.2 and 2.4 Hz, 1H, H-1'), 5.17-5.21 (t, J = 2.4 Hz, 1H, H-4'), 4.15 (dd, J = 11.8 and 2.4 Hz, 1H, H-5''), 3.90 (dd, J = 11.8 and 2.4 Hz, 1H, H-5'), 3.47 (dd, J = 12.4 and 5.2 Hz, 1H, H-2''), 3.14 (dd, J = 12.4 and 2.4 Hz, 1H, H-2'), 0.90 (s, 9H, $(CH_3)_3C$), 0.10 (s, 6H, CH_3Si); ^{13}C NMR ($CDCl_3$, 100 MHz, δ ppm): 158.24 (J = 14.5 Hz, C-4), 153.73 (C-2C=O), 136.32 (J = 240.7 Hz, C-5), 126.04 (J = 32.7 Hz, C-6), 88.22 (C-1'), 87.30 (C-4'), 63.66 (C-5'), 39.11 (C-2'), 25.85 , 18.56 $(CH_3)_3C$-Si), -5.47, -5.49 (CH_3-Si); HR-MS (ESI-TOF) (m/z): $C_{14}H_{25}FN_3O_3SSi$, calcd, 361.1292; found, 362.4160 $[M + H]^+$, 723.8098 $[2M + H]^+$.

(-)-5'-*O*-(*t*-Butyldimethylsilyl)-N_4-(4,4'-dimethoxytrityl)--5-fluoro-2',3'-dideoxy-3'-thiacytidine (2.26). Compound **2.25** (600 mg, 1.75 mmol) was dissolved in dry pyridine (10 mL). A solution of DMTr-Cl (700 mg, 1.2 equiv) in 10 mL pyridine was added to the reaction mixture dropwise at 0 °C. The reaction mixture was stirred for 30 min. The temperature was raised to room temperature and stirring was continued overnight. The reaction mixture was neutralized with saturated sodium bicarbonate solution (100 mL) and was extracted with dichloromethane (3 × 100 mL). The organic layer was separated and concentrated at reduced pressure. The residue was purified with silica gel column chromatography using dichloromethane and methanol (0-1%) as eluents to yield **2.26** (1.0 g, 86%).

^{1}H NMR (400 MHz, $CDCl_3$, δ ppm): 8.73-9.40 (br s, 1H, N*H*), 8.49 (d, J = 6.0, 1H, H-6), 7.27 (d, J = 3.6 Hz, 5H, DMTr protons), 7.17 (d, J = 8.7 Hz, 4H, DMTr protons), 6.83 (d, J = 8.7 Hz, 4H, DMTr protons), 6.26-6.29 (br s, 1H, H-1'), 5.23-5.25 (br s, 1H, H-4'),

4.25 (dd, J = 10.2 and 1.8 Hz, 1H, H-5''), 3.94 (d, J = 10.2 Hz, 1H, H-5'), 3.80 (s, 6H, DMTr-OCH_3), 3.53 (dd, J = 12.2, 4.6, 1H, H-2''), 3.24 (d, J = 12.2, 1H, H-2'), 0.94 (s, 9H, (CH_3)$_3$C), 0.15 (s, 6H, CH_3Si); ^{13}C NMR ($CDCl_3$, 100 MHz, δ ppm): 158.63 (C-4), 155.85 (C-2 C=O), 151.47, 147.33 (DMTr-*C*), 139.46 (C-5), 129.14, 127.86, 127.77 (DMTr-*C*), 127.09 (C-6), 113.17 (DMTr-*C*), 89.14 (C-1'), 87.26 (C-4'), 81.44 (DMTr-*C*-NH), 63.22 (C-5'), 55.26 (DMTr-OCH_3), 39.59 (C-2'), 25.86 (*C*H_3-C), 18.66 ((CH_3)$_3$*C*-Si), -5.46, -5.50 (*C*H_3-Si); HR-MS (ESI-TOF) (m/z): $C_{35}H_{43}FN_3O_5SSi$, calcd, 663.2598; found, 663.9596 $[M + H]^+$, 765.0250 $[M + TEA]^+$.

(-)-N_4-(4,4'-Dimethoxytrityl)--5-fluoro-2',3'-dideoxy-3'-thiacytidine (2.27).

Compound **2.26** (1 g, 1.55 mmol) was dissolved in 1M solution of tetrabutylammonium fluoride (4.5 ml, 1M, 3 equiv) and stirred for 3 h. The reaction mixture was concentrated at reduced pressure and the residue was purified with silica gel column chromatography using dichloromethane (2% triethylamine) and methanol (2 %) as eluents to yield 2.27 (750 mg, 90%).

^{1}H NMR (400 MHz, $CDCl_3$, δ ppm): 7.83-7.96 (m, 1H, H-6), 7.10-7.35 (m, 9H, DMTr protons), 6.80 (s, 4H, DMTr protons), 6.42-6.46 (br s, 1H, O*H*), 6.15-6.19 (br s, 1H, H-1'), 5.14-5.18 (br s, 1H, H-4'), 4.06-4.20 (m, 1H, H-5''), 3.93 (d, J = 12.5, 1H, H-5'), 3.78 (s, 6H, DMTr-OCH_3), 3.34-3.50 (m, 1H, H-2''), 2.98-3.15 (m, 1H, H-2'); HR-MS (ESI-TOF) (m/z): $C_{29}H_{29}FN_3O_5S$, calcd, 549.1734; found, 550.5078 $[M + H]^+$, 651.6923 $[M+TEA]^+$, 1122.0138 $[2M + Na]^+$.

(-)-N_4-(4,4′-Dimethoxytrityl)-5'-*O*-(tetradecanoyl)-5-fluoro-2',3'-dideoxy-3'-thiacytidine (2.28), (-)-5'-*O*-(12-azidododecanoyl)-N_4-(4,4′-dimethoxytrityl)-5-fluoro-2',3'-dideoxy-3'-thiacytidine (2.29), and (-)-(4,4′-dimethoxytrityl)-5'-*O*-(12-thioethyldodecanoyl)- 5-fluoro-2',3'-dideoxy-3'-thiacytidine (2.30). Compound **2.27** (250 mg, 0.45 mmol), the corresponding fatty acid (0.90 mmol) and HBTU (350 mg, 0.90 mmol) were dissolved in dry DMF (10 mL). DIPEA (2mL, 15 mmol) was added to the reaction mixture and stirring was continued overnight at room temperature. The reaction mixture was concentrated at reduced pressure and the residue was purified by reversed phase HPLC using C_{18} column and water/acetonitile as solvents as described above to afford **2.28-2.30**.

2.28. HR-MS (ESI-TOF) (m/z): $C_{43}H_{54}FN_3O_6S$, calcd, 759.3717; found, 760.3287 $[M + H]^+$, 861.4357 $[M+TEA]^+$, 1520.6604 $[2M + H]^+$.

2.29. Yield (250 mg, 71%); ^{1}H NMR (400 MHz, $CDCl_3$, δ ppm): 8.20-9.00 (br s, 1H, 4-N*H*), 8.07 (d, *J* = 6.1 Hz, 1H, H-6), 7.22-7.33 (m, 5H, DMTr protons), 7.17 (d, *J* = 8.8 Hz, 4H, DMTr protons), 6.83 (d, *J* = 8.8 Hz, 4H, DMTr protons), 6.27-6.31 (br s, 1H, H-1'), 5.34-5.39 (m, *J* = 3.1 Hz, 1H, H-4'), 4.65 (dd, *J* = 12.6 and 3.9 Hz, 1H, H-5''), 4.45 (dd, *J* = 12.6 and 2.6 Hz, 1H, H-5'), 3.71 (s, 6H, DMTr-OCH_3), 3.57 (dd, *J* = 5.1 and 12.6 Hz, 1H, H-2''), 3.20-3.31 (m, 3H, CH_2N_3, H-2'), 2.40 (t, *J* = 7.3 Hz, 2H, CH_2CO), 1.55-1.75 (m, 4H, CH_2CH_2N_3, CH_2CH_2CO), 1.23-1.41 (br m, 14H, methylene protons); ^{13}C NMR ($CDCl_3$, 100 MHz, δ ppm): 173.12 (*C*OO), 158.62 (C-4), 156.47 (C-2 C=O), 152.13, 147.33 (DMTr-*C*), 139.46 (C-5), 129.14, 127.86, 127.77 (DMTr-*C*), 127.09 (C-

6), 113.16 (DMTr-*C*), 87.25 (C-1'), 85.13 (C-4'), 81.44 (DMTr-*C*-NH), 62.91 (C-5'), 55.27 (DMTr-O*C*H$_3$), 51.49 (*C*H$_2$N$_3$), 39.16 (C-2'), 33.96, 29.44, 29.38, 29.21, 29.14, 29.07, 28.84, 26.71, 24.82 (methylene Carbons); HR-MS (ESI-TOF) (m/z): $C_{41}H_{49}FN_6O_6S$, calcd, 772.3418; found, 770.8986 $[M + H]^+$.

2.30. Yield (240 mg, 70%); ^{1}H NMR (400 MHz, $CDCl_3$, δ ppm): 8.50-9.40 (br s, 1H, 4-N*H*), 8.09 (d, *J* = 5.8 Hz, 1H, H-6), 7.23-7.34 (m, 5H, DMTr protons), 7.17 (d, *J* = 8.8 Hz, 4H, DMTr protons), 6.83 (d, *J* = 8.8 Hz, 4H, DMTr protons), 6.27-6.31 (br s, 1H, H-1'), 5.34-5.38 (br s, 1H, H-4'), 4.66 (dd, *J* = 12.7 and 3.8 Hz, 1H, H-5''), 4.45 (dd, *J* = 12.7 and 2.1 Hz, 1H, H-5'), 3.79 (s, 6H, DMTr-OC*H*$_3$), 3.58 (dd, *J* = 12.1 and 4.6 Hz, 1H, H-2''), 3.23 (d, *J* = 12.1, 1H, H-2'), 2.49-2.58 (m, 4H, C*H*$_2$SC*H*$_2$), 2.41 (t, *J* = 7.4 Hz, 2H, C*H*$_2$CO), 1.52-1.72 (m, 4H, SCH$_2$C*H*$_2$, C*H*$_2$CH$_2$CO), 1.23-1.43 (br m, 17H, methylene protons); ^{13}C NMR ($CDCl_3$, 100 MHz, δ ppm): 173.09 (*C*OO), 158.63 (C-4), 156.23 (C2 C=O), 151.71, 147.33 (DMTr-*C*), 139.46 (C-5), 129.14, 127.85, 127.77 (DMTr-*C*), 127.08 (C-6), 113.17 (DMTr-*C*), 87.24 (C-1'), 85.26 (C-4'), 81.44 (DMTr-*C*-NH), 62.84 (C-5'), 55.26 (DMTr-O*C*H$_3$), 39.23 (C-2'), 33.98, 31.69, 29.65, 29.51, 29.41, 29.26, 29.22, 29.18, 28.96, 25.96, 24.82 (methylene carbons), 14.84 (*C*H$_3$); HR-MS (ESI-TOF) (m/z): $C_{43}H_{54}FN_3O_6S_2$, calcd, 791.3438; found, 790.0172 $[M + H]^+$.

(-)-5'-*O*-(Tetradecanoyl)-5-fluoro-2',3'-dideoxy-3'-thiacytidine (2.31), (-)-5'-*O*-(12-azidododecanoyl)-5-fluoro-2',3'-dideoxy-3'-thiacytidine (2.32), and (-)-5-fluoro-5'-*O*-(12-thioethyldodecanoyl)-2',3'-dideoxy-3'-thiacytidine (2.33). AcOH (80%, 10 mL) was added to compounds **2.28-2.30** (0.3 mmol). The reaction mixture was heated at 80

°C for 30 min. The reaction mixture was concentrated at reduced pressure and the residue was purified by reversed phase HPLC using C_{18} column and water/acetonitile as solvents as described above to yield **2.31-2.33**.

2.31. Yield (120 mg, 87%); ^{1}H NMR (400 MHz, $CDCl_3$, δ ppm): 8.03 (d, J = 6.2 Hz, 1H, H-6), 6.25-6.29 (m, 1H, H-1'), 5.33-5.37 (m, 1H, H-4'), 4.63 (dd, J = 12.6 and 4.1 Hz, 1H, H-5''), 4.43 (dd, J = 12.6 and 2.2 Hz, 1H, H-5'), 3.56 (dd, J = 12.6 and 5.2 Hz, 1H, H-2''), 3.23 (d, J = 12.6 Hz, 1H, H-2'), 2.29-2.43 (m, , 2H, CH_2CO), 1.55-1.73 (m, 2H, CH_2CH$_2$CO), 1.15-1.49 (br m, 20H, methylene protons), 0.89 (s, J = 6.2 Hz, 3H, CH_3); ^{13}C NMR ($CDCl_3$, 100 MHz, δ ppm): 173.15 (*C*OO), 157.20 (J = 16.4 Hz, C-4), 152.07 (C-2 C=O), 135.94 (J = 240.1 Hz, C-5), 126.29 (J = 32.4 Hz, C-6), 87.26 (C-1'), 85.02 (C-4'), 63.00 (C-5'), 39.00 (C-2'), 34.22 (*C*H$_2$CO), 31.93, 29.65, 29.61, 29.46, 29.36, 29.28, 29.24, 29.11, 24.83, 22.70 (methylene carbons), 14.13 (*C*H$_3$); HR-MS (ESI-TOF) (m/z): $C_{22}H_{36}FN_3O_4S$, calcd, 457.2411; found, 458.0814 $[M + H]^+$, 915.1334 $[2M + H]^+$.

2.32. Yield (125 mg, 88%); ^{1}H NMR (400 MHz, $CDCl_3$, δ ppm) 8.90-9.70 (bs, 2H, 4-NH_2), 8.05 (d, J = 5.9 Hz, 1H, H-6), 6.25-6.29 (m, 1H, H-1'), 5.33-5.37 (m, 1H, H-4'), 4.62 (dd, J = 12.6 and 4.0 Hz, 1H, H-5''), 4.43 (dd, J = 12.6 and 1.8 Hz, 1H, H-5'), 3.56 (dd, J = 12.6 and 5.2 Hz, 1H, H-2''), 3.24 (t, J = 6.7 Hz, 3H, H-2', CH_2-N$_3$), 2.30-2.43 (m, 2H, CH_2CO), 1.53-1.69 (m, 4H, CH_2CH$_2$CO, CH_2CH$_2$N$_3$), 1.20-1.40 (br m, 14H, methylene protons); ^{13}C NMR ($CDCl_3$, 100 MHz, δ ppm): 173.13 (*C*OO), 156.96 (J = 16.0 Hz, C-4), 151.89 (C-2 C=O), 135.95 (J = 237.1 Hz, C-5), 126.45 (J = 32.7 Hz, C-6), 87.25 (C-1'), 85.05 (C-4'), 63.00 (C-5'), 51.47 (*C*H$_2$N$_3$), 38.90 (C-2'), 34.21 (*C*H$_2$CO),

29.42, 29.36, 29.23, 29.18, 29.11, 29.08, 29.04, 28.82, 26.69, 24.79, 24.76 (methylene carbons); HR-MS (ESI-TOF) (m/z): $C_{20}H_{31}FN_6O_4S$, Calcd, 470.2112; found, 471.0575 $[M + H]^+$, 941.0986 $[2M + H]^+$.

2.33. Yield (110 mg, 80%); ^{1}H NMR (400 MHz, $CDCl_3$) δ 8.07 (d, J = 6.1 Hz, 1H, H-6), 6.26-6.30 (m, 1H, H-1'), 5.37 (t, J = 2.4 Hz, 1H, H-4'), 4.65 (dd, J = 12.6 and 4.1 Hz, 1H, H-5"), 4.45 (dd, J = 12.6 and 2.4 Hz, 1H, H-5'), 3.58 (dd, J = 12.7 and 5.3 Hz, 1H, H-2"), 3.23 (dd, J = 12.7 and 2.1 Hz, 1H, H-2'), 2.49-2.58 (m, 4H, CH_2SCH_2), 2.30-2.45 (m, 2H, CH_2COO), 1.53-1.69 (m, 4H, SCH_2CH_2, CH_2CH_2CO), 1.24-1.42 (br m, 17H, methylene protons). ^{13}C NMR ($CDCl_3$, 100 MHz, δ ppm): 173.08 (*C*OO), 156.00 (J = 17.2 Hz, C-4), 150.87 (C-2 C=O), 135.67 (J = 239.3 Hz, C-5), 126.79 (J = 32.5 Hz, C-6), 87.20 (C-1'), 85.46 (C-4'), 62.75 (C-5'), 39.21 (C-2'), 33.96 (CH_2COO), 31.68, 29.65, 29.50, 29.40, 29.32, 29.24, 29.15, 29.07, 28.96, 28.88, 25.92, 24.80, 24.73 (methylene carbons), 14.83 (CH_3); HR-MS (ESI-TOF) (m/z): $C_{22}H_{36}FN_3O_4S_2$, calcd, 489.2131; found, 489.9879 $[M + H]^+$, 978.9209 $[2M + H]^+$.

(-)-5'-*O*-(12(N-Fmoc-aminododecanoyl)-N$_4$-(4,4'-dimethoxytrityl)-2',3'-dideoxy-3'-thiacytidine (2.34) and (-)-5'-*O*-(3(N-Fmoc-aminopropanoyl)-N$_4$-(4,4'-dimethoxytrityl)-2',3'-dideoxy-3'-thiacytidine (2.35). Compound **2.12** (320 mg, 0.60 mmol), the corresponding Fmoc-amino acid (1.2 mmoL), and HBTU (500 mg, 1.3 mmol) were dissolved in a mixture of dry DMF (10 mL) and DIPEA (2 mL, 15 mmol). The reaction mixture was stirred overnight at room temperature. The reaction mixture was

concentrated and dried under reduced pressure to afford crude 5′-*O*-Fmoc-amino acid derivatives of N_4-DMTr-2',3'-dideoxy-3'-thiacytidine, **2.34** and **2.35**.

2.34. HR-MS (ESI-TOF) (m/z): $C_{47}H_{44}N_4O_8S$, calcd, 824.288; found, 825.2218 $[M + H]^+$, 1650.0664 $[M + H]^+$.

2.35. HR-MS (ESI-TOF) (m/z): $C_{56}H_{62}N_4O_8S$, calcd, 950.4288; found, 951.8527 $[M + H]^+$.

(-)-5′-*O*-(3-Aminopropanoyl)-N_4-(4,4′-dimethoxytrityl)-2',3'-dideoxy-3'-thiacytidine (2.36) and (-)-5′-*O*-(12-aminododecanoyl)-N_4-(4,4′-dimethoxytrityl)-2',3'-dideoxy-3'-thiacytidine (2.37). The crude products were dissolved in THF (10 mL). To the reaction mixture was added piperidine (6 μL, 0.06 mmol) and 1-octanethiol (10 mmol solution in THF, 0.6 mL, 6 mmol). The reaction mixture was allowed to stir for 1 h at room temperature. The reaction solution was concentrated at reduced pressure. The residue was purified with reversed phase HPLC using C_{18} column and water/acetonitrile as solvents as described above to yield **2.36** and **2.37**.

2.36. Overall yield (200 mg, 55%); HR-MS (ESI-TOF) (m/z): $C_{32}H_{34}N_4O_6S$, calcd, 602.2199; found, 603.1806 $[M + H]^+$, 1205.0313 $[2M + H]^+$.

2.37. Overall yield = 210 mg, 52%); HR-MS (ESI-TOF) (m/z): $C_{41}H_{52}N_4O_6S$, calcd, 728.3608; found, 729.2265 $[M + H]^+$, 1458.1201 $[2M + H]^+$.

General procedure for the Synthesis of 5′-*O*-(5(6)-Carboxyfluorescein) Derivatives of 3TC (2.38 and 2.39). A mixture of 5(6)-carboxyfluroscein (430 mg, 1.15 mmol), the corresponding N_4-DMTr-**5′-*O*-**aminoacyl derivative of lamivudine (**2.36** or **2.37**, 0.29 mmoL), and HBTU (440 mg, 1.15 mmol) were dissolved in a mixture of dry DMF (10 mL) and DIPEA (2 mL, 15 mmol) and stirred overnight at room temperature. The reaction mixture was concentrated and dried under vacuum. ACOH (80%, 10 mL) was added to the reaction mixture and was heated at 80 °C for 30 min. The final compounds were purified with reversed phase HPLC using C_{18} column and using water/acetonitile as solvents as described above.

(-)-5′-*O*-(3-(N(5(6)-Carboxyfluorescein)aminopropanoyl)-2′,3′-dideoxy-3′-thiacytidine (2.38). Yield (40 mg, 20%); ^{1}H NMR (400 MHz, CD_3CN + D_2O, δ ppm) 8.41 (s, 0.5H, FAM-Ar-H, 5 or 6 isomer), 8.11 and 8.12 (two d, J = 8.0 Hz, 1H, H-6), 8.00-8.05 (m, 1H, FAM-Ar-H, 5 or 6 isomer), 7.93 (d, J = 8.0 Hz, 0.5H, FAM-Ar-H, 5 or 6 isomer), 7.53 (s, 0.5H, FAM-Ar-H, 5 or 6 isomer), 7.29 (d, J = 8.0 Hz, 0.5H, FAM-Ar-H, 5 or 6 isomer), 6.78-6.90 (m, 4H, FAM-Ar-H), 6.71 (dd, J = 2.4 and 8.9 Hz, 2H, FAM-Ar-H, 5 or 6 isomer), 6.10 and , 6.17 (two d, J = 8.0, 2H, H-1′, H-5), 5.36-5.42 and 5.25-5.31 (two m, J = 2.9 Hz, 1H, H-4′), 4.55 (dd, J = 12.6 and 4.4 Hz, 1H, H-5″), 4.32 (dd, J = 12.6 and 2.9 Hz, 1H, H-5′), 3.45-3.69 (m, 3H, H-2″ and CH_2NH), 3.13-3.21 (m, 1H, H-2′), 2.72 and 2.61 (two t, J = 6.5 Hz, 2H, CH_2CO); ^{13}C NMR (CD_3CN + D_2O, 100 MHz, δ ppm): 172.49, 172.32 (*C*OO), 168.80 (*C*ONH), 167.24, 167.11 (*C*OO-FAM), 160.71 (Ar-*C*-FAM), 159.78, 159.72 (C-4), 154.66 (C-2 C=O), 147.62, 147.55 (Ar-*C*-

FAM), 144.50, 144.39 (C-6), 136.44, 133.91, 130.70, 129.60, 128.39, 115.06, 111.93, 102.87 (FAM-*C*), 94.32, 94.26 (C-5), 87.38, 87.21 (C-1'), 85.17, 84.98 (C-4'), 63.93, 63.81 (C-5'), 49.09 (CH_2NH_2), 37.98, 37.87 (C-2'), 36.15, 36.06 (CH_2COO); HR-MS (ESI-TOF) (m/z): $C_{32}H_{26}N_4O_{10}S$, calcd, 658.137; found, 330.2546 $[M + 2H]^{2+}$, 659.2739 $[M + H]^+$, 1317.2294 $[2M + H]^+$.

(-)-5'-*O*-(12-(N(5(6)-Carboxyfluorescein)aminododecanoyl)-2',3'-dideoxy-3'-thiacytidine (2.39). Yield (30 mg, 16%);. ^1H NMR (400 MHz, $CD_3CN + D_2O$, δ ppm) 8.28-8.35 (m, 0.5H, FAM-Ar-H, 5 or 6 isomer), 8.11 and 8.12 (two d, *J* = 8.0 Hz, 1H, H-6), 7.96-8.04 (m, 1.5H, FAM-Ar-H), 7.52 (s, 0.5H, FAM-Ar-H, 5 or 6 isomer), 7.25 (d, *J* = 8.0 Hz, 0.5H, FAM-Ar-H, 5 or 6 isomer), 6.68-6.74 (m, 2H, FAM-Ar-H), 6.59-6.67 (m, 2H, FAM-Ar-H), 6.56 (dd, *J* = 2.3 and 8.8 Hz, 2H, FAM-Ar-H), 6.13-6.22 (m, 1H, H-1'), 6.08 and 6.09 (two d, *J* = 8.0, 2H, H-5), 5.33-5.40 (m, 1H, H-4'), 4.50 (dd, *J* = 12.5 and 4.8 Hz, 1H, H-5''), 4.38 (dd, *J* = 12.5 and 3.1 Hz, 1H, H-5'), 3.54 (dd, *J* = 5.5 and 12.6 Hz, 1H, H-2''), 3.34 (m, 3H, H-2' and CH_2NH), 2.25-2.34 (m, 2H, CH_2COO), 1.40-1.60 (m, 4H, CH_2CH_2CO, CH_2CH_2NH), 1.11-1.25 (br m, 16H, methylene protons); ^{13}C NMR (CD_3CN+D_2O, 100 MHz, δ ppm): 174.02 (*C*OO), 170.02 (*C*ONH), 167.21 (*C*OO-FAM), 160.84 (C-4), 153.67 (C-2 C=O), 148.19, 145.23 (Ar-*C*-FAM), 142.19 (C-6), 137.63, 135.24, 130.52, 130.39, 130.10, 128.11, 126.38, 125.50, 124.85, 123.85, 113.80, 110.95, 103.48 (FAM-*C*), 94.73 (C-5), 88.12 (C-1'), 85.72 (C-4'), 64.39 (C-5'), 49.69 (CH_2NH_2), 38.55 (C-2'), 34.54 (CH_2COO), 30.17, 30.13, 30.07, 30.01, 29.94, 29.87, 29.80, 29.71, 29.59 (methylene carbons), 27.58 ($CH_2CH_2NH_2$), 25.54

CH_2CH_2COO); HR-MS (ESI-TOF) (m/z): $C_{41}H_{44}N_4O_{10}S$, calcd, 784.2778; found, 393.0862 $[M + 2H]^{2+}$, 784.9019 $[M]^+$, 1569.4510 $[2M + H]^+$.

2.3.3. Anti-HIV Assays

Anti-HIV activities of the compounds were evaluated according to the previously reported procedure (Krebs et al., 1999). In summary, HeLa (Human cervical carcinoma: ATCC CCL-2.1) cell line was used to measure inactivation of both cell-free virus preparations and virus-infected cell preparations. Cells were plated in culture plates 24 h prior to each experiment. Cell-free viral preparations of HIV-1 strains IIIB (lymphocytotropic strain) and BaL (monocytotropic strain) were used for cell-free assay. For cell-associated assay, SulT1 cells were infected with IIIB virus 5 days prior to the experiment. Cell-free virus and virus-infected cells were mixed with different compounds and diluted to make different concentrations. The mixture was further diluted with the buffer and added to the HeLa cells. The cells were incubated at 37 °C for 48 h, stained for β-galctosidease expression and compared with β-galctosidease expression from the β-gal-positive cells in absence of any microbicidal compound to get IC_{50} values.

2.3.4. Cellular Uptake Study

All of the stock solutions for compounds FAM, **2.38**, and **2.39** were prepared in DMSO. The human T lymphoblastoid cells CCRF-CEM (ATCC No. CCL-119) were grown on 25 cm^2 cell culture flasks with RMPI-1640 medium containing 10% fetal bovine serum. Upon reaching about 70% confluency, the cells were treated as described below and incubated for 1 h or longer at 37 °C.

2.3.4.1. Cellular Uptake of FAM, 2.38 and 2.39 at Different Time Points

When the cells reached about 70% confluency, FAM, **2.38**, or **2.39** (1 mL, 20 μM) in RMPI-1640 medium were added to 1 mL of cells to make the final concentration as 10 μM. The cells were incubated for 0.5, 1, 2, 4, and 8 h at 37 °C. Then the flow cytometry assays were performed as described below.

2.3.4.2. Cellular Uptake of 2.39 at Different Concentrations

When the cells reached about 70% confluency, 1 mL of graded concentrations (0, 10, 20, 40, 80, and 200 μM in RMPI-1640) of **2.39** was added to 1 mL of cells to make the final concentration as 0, 5, 10, 20, 40, and 100 μM. The cells were incubated for 1 h at 37 °C. Then the flow cytometry assays were performed as described in General Information.

2.3.4.3. Cellular Uptake of 2.38 and 2.39 with Trypsin Treatment.

The assays were performed as previously described in section 2.3.4.1 at 1 h time point with the exception that the cells used were incubated with 0.25% trypsin/0.53 mM EDTA for 5 min before washing with PBS (pH 7.4).

2.3.4.4. Flow Cytometry

The cells were washed twice with PBS (pH 7.4) at 2000 rpm for 5 min. Then the cells were analyzed by flow cytometry (FACS Calibur: Becton Dickinson) using FITC

channel and CellQuest software. The data presented are based on the mean fluorescence signal for 10000 cells collected. All the assays were done in triplicate.

2.3.5. Cell Viability Assay

When the cells reached about 70% confluency, the cells were incubated with a solution of CCRF-CEM cell alone or 10 μM FAM, 2.38, or 2.39 for 24 h at 37 °C. Then 20 μL of the cells from each flask were treated with μl of trypan blue (0.1%) for 1 min. The cells were then transferred to a Cellometer® counting slide and analyzed using Cellometer Auto T.4 (Nexcelom Bioscience). All the assays were performed in triplicate.

2.3.6. Real Time Fluorescence Microscopy in Live CCRF-CEM Cell Line

The cellular uptake studies and intracellular localization of CCRE-CEM cell alone, or incubated with **2.38** and **2.39** were imaged using a ZEISS Axioplan 2 light microscope equipped with transmitted light microscopy with a differential-interference contrast method and an Achroplan 40X objective. The human T lymphoblastoid cells CCRF-CEM (ATCC No. CCL-119) were grown on 60 mm Petri Dishes with RPMI-1640 medium containing 10% fetal bovine serum. Upon reaching about 70% confluency, the cells were incubated with a solution of 10 μM of **2.38** and **2.39** for 1 h at 37 °C. They were then observed under the fluorescent microscope under bright field and FITC channels (480/520 nm).

2.4. Results and discussion

2.4.1. Chemistry

2.4.1.1. Fatty Acyl Ester Derivatives of 3TC, d4T, and FTC

A number of fatty acyl esters of 3TC, d4T and FTC were synthesized (Figure 2.1) to improve the cellular uptake, anti-HIV activity, and resistant profile of the parent nucleosides. Four fatty acids, myristic acid, 12-azidododecanoic acid, 12-thioethyldodecanoic acid, and 12-bromododecanoic acid, were used for the conjugation with nucleoside analogs.

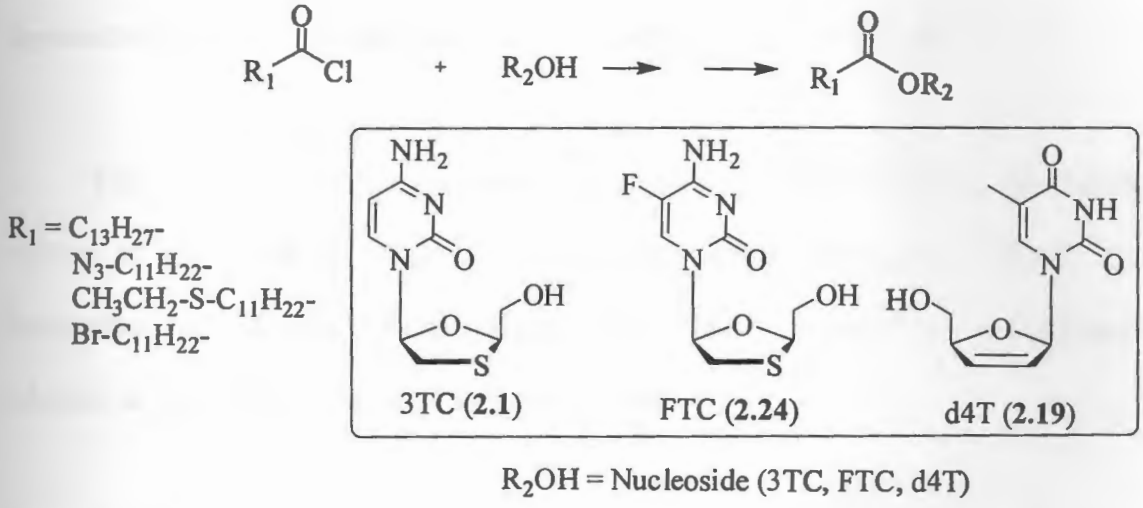

Figure 2.1. General structures of fatty acyl ester derivatives of nucleosides.

Scheme 2.1 depicts the synthesis of the fatty acyl ester derivatives of 3TC. 5'-Hydroxyl and/or 4-amino positions were substituted with the fatty acids to synthesize three classes of compounds: two 5',N_4-disubstituted (**2.2** and **2.3**), three N_4-substituted (**2.8-2.10**), and three 5'-*O*-ester (**2.16-2.18**) of 3TC. 5',N_4-Disubstituted derivatives (**2.2** and **2.3**) were synthesized by reacting 3TC with the appropriate fatty acyl chloride in

presence of DMAP as a base. N_4-substituted derivatives (**2.8-2.10**) were synthesized by selectively protecting 5′-hydroxyl group with *tert*-butyldimethylsilyl chloride in the presence of imidazole as a base to afford **2.4**, 5′-TBDMS protected 3TC was further reacted with the fatty acyl chloride followed by deprotection of TBDMS to afford N_4-substituted derivatives (**2.8-2.10**). 5′-*O*-Fatty acyl derivatives of 3TC (**2.16-2.18**) were synthesized by first protecting 4-amino group of **2.4** with DMTr protecting group to afford **2.11**. The TBDMS group was then removed from 5′-*O*-position by treatment of **2.11** with TBAF to yield N_4-DMTr derivative of 3TC (**2.12**). Compound **2.12** was then reacted with the fatty acids in the presence of HBTU and DIPEA followed by DMTr deprotection to afford 5′-*O*-(fatty acyl) ester derivatives of 3TC (**2.16-2.18**).

Four 5′-*O*-(fatty acyl) ester derivatives of d4T (**2.19-2.22**) were synthesized by reaction of d4T with the appropriate fatty acyl chloride (myristoyl chlroide, 12-azidododecanoyl chloride, 12-thiaethyldodecanoyl chloride, and 12-bromododecanoyl chloride) in the presence of DMAP as a base (Scheme 2.2).

Furthermore, three 5′-*O*-fatty acyl ester derivatives of FTC (**2.31-2.33**) were synthesized (Scheme 2.3) using a similar approach described above for the synthesis of 5′-*O*-(fatty acyl) ester derivatives of 3TC (**2.16-2.18**).

All compounds were synthesized at 100 mg scale and were tested for the anti-HIV and cytotoxicity assays. Compounds **2.8**, **2.16**, and **2.17** were further synthesized in larger

scale (5 g) for further biological evaluations. These three compounds were first purified by using silica gel column chromatography (>90% purity) and then HPLC (>99% purity).

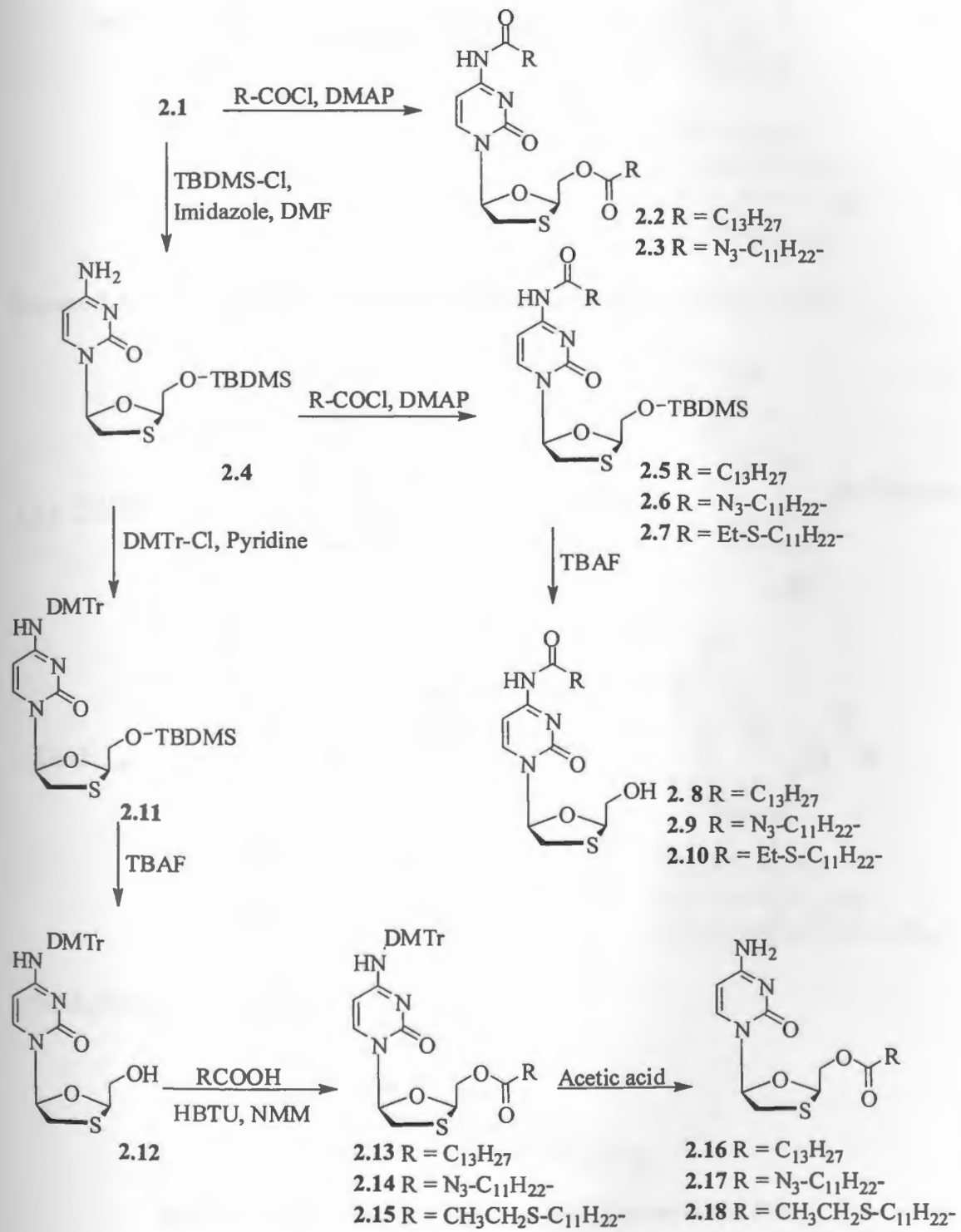

Scheme 2.1. Synthesis of fatty acyl ester derivatives of 3TC.

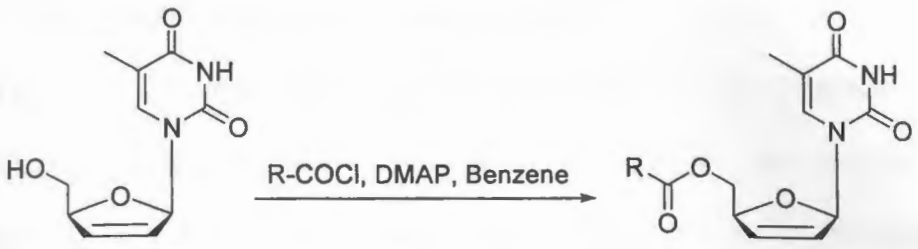

2.19

2.20 R = $C_{13}H_{27}$
2.21 R = N_3-$C_{11}H_{22}$-
2.22 R = Et-S-$C_{11}H_{22}$-
2.23 R = Br-$C_{11}H_{22}$-

Scheme 2.2. Synthesis of 5′-*O*-(fatty acyl) ester derivatives of Stavudine (d4T).

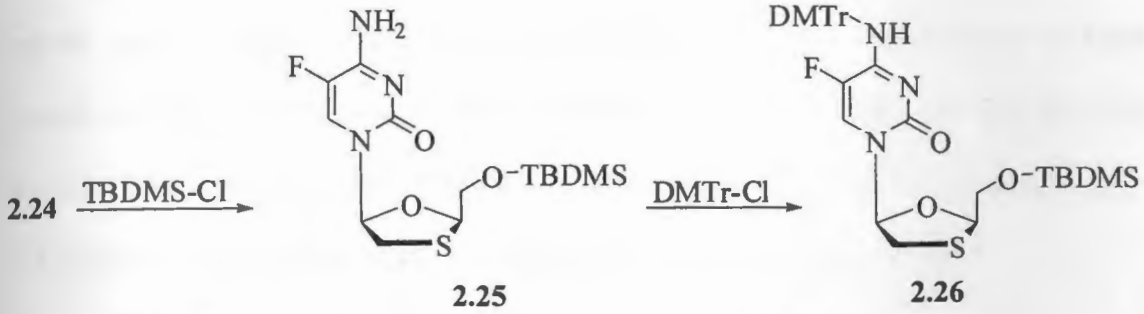

2.25 **2.26**

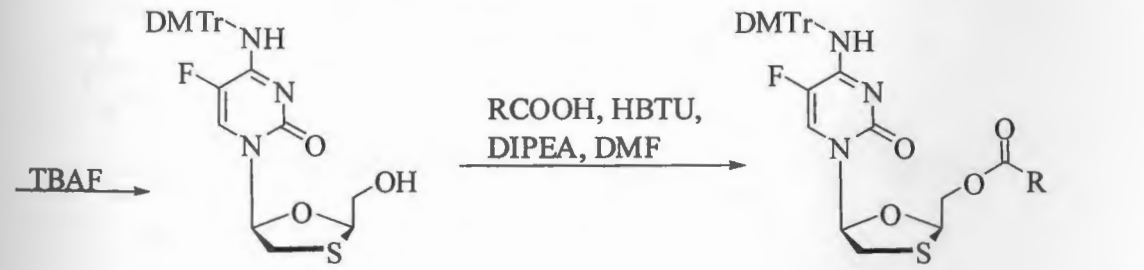

2.27

2.28 R = $C_{13}H_{27}$
2.29 R = N_3-$C_{11}H_{22}$-
2.30 R = CH_3CH_2S-$C_{11}H_{22}$-

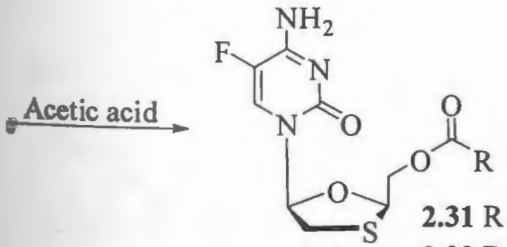

2.31 R = $C_{13}H_{27}$
2.32 R = N_3-$C_{11}H_{22}$-
2.33 R = CH_3CH_2S-$C_{11}H_{22}$-

Scheme 2.1. Synthesis of fatty acyl ester derivatives of FTC.

2.4.1.2. 5(6)-Carboxyfluorescein Derivatives of 3TC

3TC was attached to 5(6)-carboxyfluorescein using β-alanine and 12-aminododecanoic acid as linkers. First, 3TC-DMTr (**2.12**) was reacted with the corresponding Fmoc-amino acid in the presence of HBTU and DIPEA. Second, *N*-Fmoc deprotection to free amino group was achieved in the presence of piperidine. Finally, FAM was attached to free amino group in the presence of HBTU and DIPEA, followed by DMTr deprtotection to afford 5(6)-carboxyfluorescein derivatives of 3TC, **2.36** and **2.37** (Scheme 2.4). These compounds were used for cellular uptake studies to determine cellular uptake profile of fatty acyl ester derivatives of 3TC. 3TC attached to FAM through β-alanine (**2.36**) was used as a control 3TC analog. 3TC attached to FAM through 12-aminododecanoyl(**2.37**) was used as an analog of 5'-*O*-(12-azidododecanoyl)-2',3'-dideoxy-3'-thiacytidine (**2.17**) and other fatty acid ester analogs of 3TC.

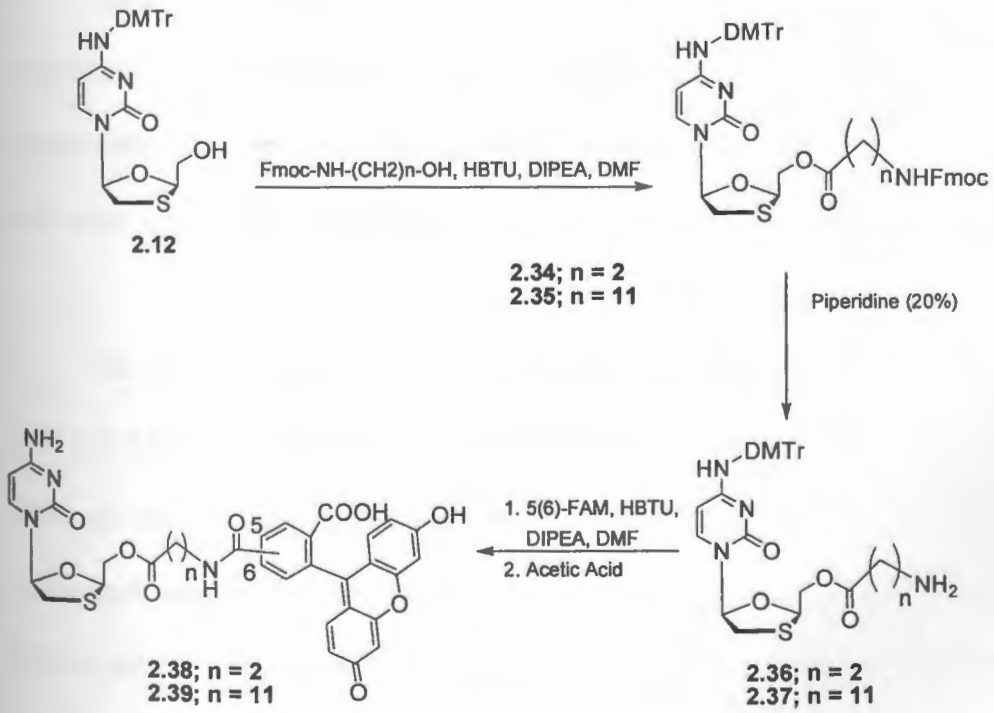

Scheme 2.4. Synthesis of 5'-carboxyfluorescein derivatives of 3TC (**2.38** and **2.39**) through different linkers.

2.4.2. Biological Activities

Although 3TC, FTC, and d4T are less potent than FLT against cell-free virus assays, but they exhibited a higher anti-HIV activity against cell-associated virus. Table 2.2 illustrates the anti-HIV-1 activities of the fatty acyl ester derivatives of 3TC, d4T, and FTC in comparison with 3TC, FTC, and d4T against cell-free and cell-associated virus.

The data provide structure-anti-HIV activity relationships for different fatty acyl ester derivatives of 3TC by comparing N_4-substituted, 5′-*O*-substituted, and 5′-*O*,N_4-disubstituted compounds. In general, when the N_4 and/or 5′-*O* positions were substituted with a fatty acid, minimal cytotoxicity was observed (EC_{50} > 200 μM).

Anti-HIV activity of the 3TC derivatives was dependent on the site of esterification. 5′-*O*,N_4-Disubstituted derivatives of 3TC, **2.2** and **2.3**, displayed significantly less activity against both cell-free and cell-associated HIV (EC_{50} = 73-> 154 μM) when compared with other fatty acyl derivatives of 3TC and 3TC.

On the other hand, all the N_4- or 5′-*O*-monosubstituted derivatives of 3TC (**2.8-2.10** and **2.16-2.18**) exhibited a higher potency than that of 3TC against cell-free virus. Although the 5′-*O*-monosubstituted ester derivatives (**2.16-2.18**) were the most potent compounds against cell-free virus (EC_{50} = 0.2-2.3 μM) among all 3TC derivatives as determined by the viral inhibition assays, they lost their effectiveness when used in the cell-to-cell transmission assay (EC_{50} > 212-228 μM).

On the other hand, N_4-myristoyl derivative of 3TC, **2.8**, exhibited the anti-HIV activity against cell-free (EC_{50} = 0.7-10.9 μM) and cell-associated virus (EC_{50} = 0.7 μM). Compound **2.8** was the most versatile analog in the cell-associated lymphocytotropic strain (CTC) based inhibition assay and showed 114-fold higher anti-HIV activity against cell-associated virus when compared with 3TC (EC_{50} = 80.3 μM) Furthermore, compound **2.8** was also more potent than FTC (EC_{50} = 88.6 μM) andd4T (EC_{50} = 136.1 μM) in cell-to cell transmission assay (Table 2.2).

In general, three of 5′-*O*-(fatty acyl) ester derivatives d4T (**2.21-2.23**) showed higher anti-HIV activities (EC_{50} = 2.3-14.9 μM) against cell-free virus when compared with d4T (EC_{50} = 26.8-28.1 μM), but were only moderately active when compared to other corresponding fatty acyl derivatives of 3TC and FTC. Among all fatty acyl ester derivatives of d4T, 12-azidododecanoyl ester **2.21** was the most potent compound and showed 4-9 fold higher anti-HIV activities against cell-free and cell-associated virus when compared with d4T (Table 2.2).

Unlike 3TC and d4T derivatives, 5′-*O*-(fatty acyl) ester derivatives of FTC, **2.31-2.33**, were consistently active against both cell-free and cell-associated virus (Table 2.2). These compounds exhibited the highest anti-HIV activity against cell-free virus (EC_{50} = 0.04-0.8 μM) among all the fatty acyl ester derivatives and their parent nucleoside analogs. 5′-*O*-Myristoyl derivative of FTC (**2.31**) displayed about 10-24 fold higher anti-HIV activities than those of FTC against cell-free and cell associated virus. 5′-*O*-12-

thioethyldodecanoyl derivative of FTC (**2.33**) displayed slightly higher anti-HIV activity than **2.31**, but showed higher toxicity against normal cells (EC_{50} = 93.6 μM).

In summary, structure-function analysis revealed that the anti-HIV activity of fatty acyl substituted derivatives of nucleosides was clearly dependent on the nature of the nucleoside and fatty acid analog. The rate of cellular uptake and the intracellular hydrolysis to parent nucleoside and fatty acids determine the overall anti-HIV activities of the conjugates.

Table 2.3 shows the anti-HIV activities (in μg/mL) of the 5′-*O*-fatty acyl ester derivatives of FTC compared with the corresponding physical mixtures. The equimolar (50:50) physical mixture of FTC with myristic acid (**2.34**) and 12-thioethyldodecanoic acid (**2.35**) showed significantly less anti-HIV activities (EC_{50} = 0.1-9.9 μM) than the corresponding 5′-*O*-fatty acyl ester derivatives, **2.31** and **2.33** (EC_{50} = 0.02-2.4 μM), respectively, against cell-free and cell-associated virus. The anti-HIV activity of the physical mixtures was only slightly higher than that of FTC. The results indicate that the conjugation of FTC with myristic acid analog is critical in improving the anti-HIV profile of the conjugate. The comparative studies of physical mixtures with the corresponding ester conjugate indicated that the esterification is important for the inhibitor activity, especially against cell-associated virus.

Table 2.2. In vitro assays of 3TC, d4T and FTC analogs for inhibition of HIV.

Compound	Solvent	Diluent	CTS[a] EC(50)[b] (μM)	VBI(IIIB [c] EC(50) (μM)	VBI(BaL)[d] EC(50) (μM)	CTC[e] EC(50) (μM)
2.1 (3TC)	DMSO	R10	> 200	32.7	11.3	80.3
2.2	DMSO	R10	> 200	> 154.0	135.2	> 154.0
2.3	DMSO	R10	> 200	> 148.1	72.7	> 148.1
2.8	dH_2O	DMSO	> 200	10.9	0.7	0.7
2.9	dH_2O	DMSO	> 200	29.4	3.8	14.6
2.10	DMSO	R10	> 200	5.3	0.4	> 212.2
2.16	DMSO	R10	> 200	0.5	> 0.2	> 227.7
2.17	DMSO	R10	> 200	0.9	0.7	> 221.1
2.18	DMSO	R10	> 200	2.3	0.2	> 212.2
2.19 (d4T)	DMSO	R10	> 200	26.8	28.1	136.1
2.20	DMSO	R10	> 200	78.3	12.4	> 230.3
2.21	DMSO	R10	> 200	6.7	3.1	22.4
2.22	DMSO	R10	> 200	14.4	5.8	46.5
2.23	dH_2O	DMSO	> 200	14.9	2.3	> 206.5
2.24 (FTC)	DMSO	R10	> 200	1.9	0.7	88.6
2.31	DMSO	R10	> 200	0.1	0.07	3.7
2.32	DMSO	R10	> 200	0.8	0.2	9.1
2.33	DMSO	R10	93.6	0.05	0.04	4.9
AZT	DMSO	R10	> 200	10.9	14.2	>375
FLT	DMSO	R10	> 200	0.8	0.4	>410
DMSO	DMSO	R10	> 200	>100	>100	>100

[a]Cytotoxicity assay; [b]50% Effective concentration; [c]Viral entry inhibition assay (lymphocytotropic strain); [d]Viral entry inhibition assay (monocytotropic strain); [e]Cell- to- cell transmission assay (IIIB).

In summary, the conjugation of RT inhibitor nucleoside analogs with selected long chain fatty acids (NMT inhibitors) exerted anti-HIV synergic effect. Among 3TC derivatives, **2.8**, **2.16**, and **2.17** exhibited the best anti-HIV profile. 5′-O-Myristoyl FTC derivative (**2.31**) showed consistent anti-HIV activity against cell-free (IIIB and BaL)

strains and cell-associated virus, and was the most potent compound among fatty acyl derivatives of FTC, 3TC, and d4T..Compounds **2.8**, **2.16**, and **2.17** are currently under further biological evaluations.

Table 2.3. Comparison of anti-HIV activities of fatty acyl derivatives of FTC with physical mixtures of FTC + fatty acids..

Compound	Chemical Name	CTS[a] EC(50)[b] (μg/ml)	VBI(IIIB[c] EC(50) (μg/ml)	VBI(BaL)[d] EC(50) (μg/ml)	CTC[e] EC(50) (μg/ml)
2.24	FTC	> 100	0.48	0.18	21.9
2.31	5′-*O*-Myristoyl FTC	> 100	0.056	0.033	1.7
2.33	5′-*O*-(12-thioethyldodecanoyl) FTC	45.8	0.024	0.02	2.4
2.34	Myristic acid + FTC (50:50)	> 100	0.6	0.1	9.9
2.35	12-thioethyldodecanoic acid + FTC (50:50)	> 100	0.1	0.2	9.8
DMSO	DMSO	> 100	>100	>100	>100

[a]Cytotoxicity assay; [b]50% Effective concentration; [c]Viral entry inhibition assay (lymphocytotropic strain); [d]Viral entry inhibition assay (monocytotropic strain); [e]Cell- to- cell transmission assay (IIIB).

2.4.3. Spermicidal Activity.

The spermicidal activities of several fatty acids have been previously reported (Brown-Woodman et al., 1985; Jianzhong et al., 1987). The spermicidal activities of 3TC (**2.1**), d4T (**2.19**), and their fatty acyl ester derivatives **2.2**, **2.3**, and **2.20-2.22** were compared with N-9, a marketed spermicidal product (Figures 2.2 and 2.3). In a dose-response study to evaluate spermicidal activity, none of these derivatives shows significant sperm immobilizing or spermicidal activity, even at their maximum concentrations (1 mg/mL).

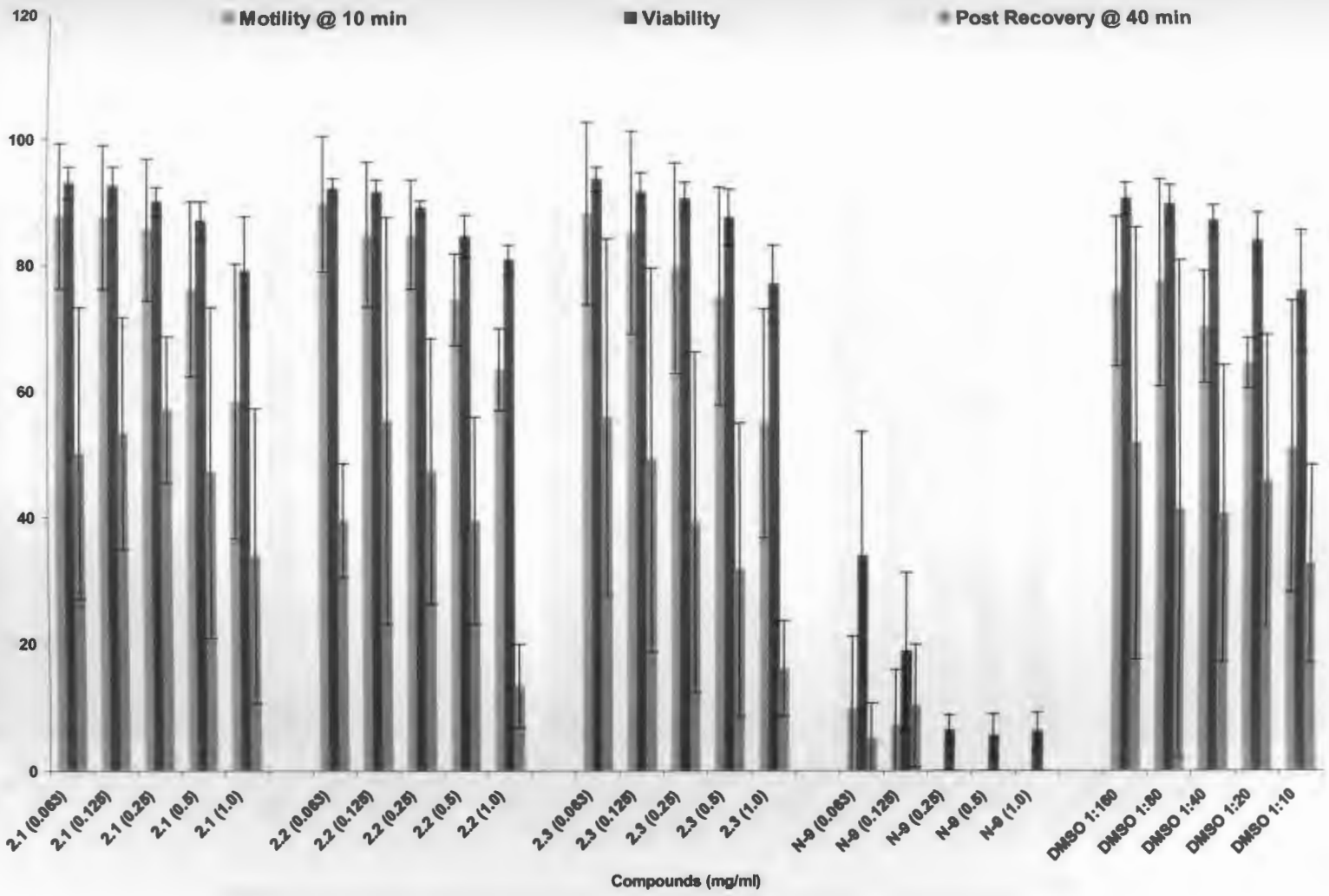

Figure 2.2. *In vitro* assays for spermicidal activity of 3TC (**2.1**), **2.2**, and **2.3**.

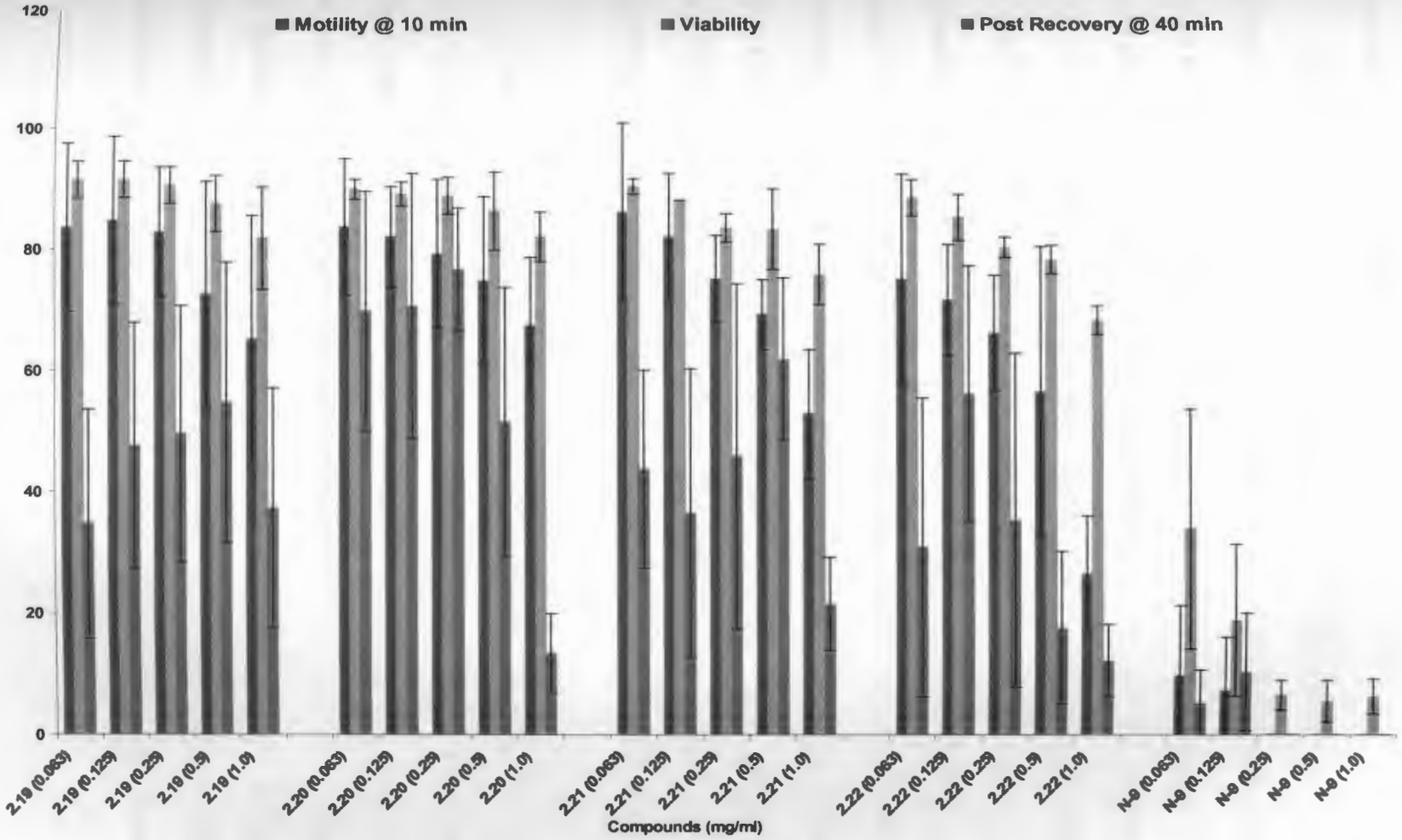

Figure 2.3. *In vitro* assays of for spermicidal activity of d4T (**2.19**), **2.20**, **2.21** and **2.22**.

2.4.4. Cellular Uptake Study

Studies were performed to understand cellular uptake profile of 5′-*O*-fatty acyl derivatives in comparison with 3TC. 3TC attached to FAM through β-alanine (**2.38**) was used as a control 3TC analog. 3TC attached to FAM through 12-aminododecanoic acid (**2.39**) was used as an analog of 5'-*O*-(12-azidododecanoyl)-2',3'-dideoxy-3'-thiacytidine (**2.16**) and other fatty acid ester analogues of 3TC. The human T lymphoblastoid cells (CCRF-CEM, ATCC No. CCL-119) were used for the study and were grown to the 70% confluency in the culture media. The cells were incubated with the fluorescein-substituted conjugates (**2.38** and **2.39**) in different time periods, concentrations, and in the presence or absence of trypsin (Figures 2.4-2.6), DMSO and FAM were used as control for the study. The cells were analyzed by flow cytometry (FACSCalibur: Becton Dickinson) using FITC channel and CellQuest software. The data presented are based on the mean fluorescence signal for 10000 cells collected. All the assays were carried out in triplicate.

First, cells were incubated with 10 μM of the compounds in different time periods (0.5 h, 1 h, 2 h, 4 h and 8 h, Figure 2.4). Compound **2.39** exhibited 3-6 fold higher cellular uptake than that of **2.38** and FAM alone. The results clearly indicate that presence of long chain enhances the cellular uptake of 3TC, by increasing lipophilicity. The continuous incubation of cells with compounds up to 8 h did not show significant difference in the cellular uptake, suggesting that most of the fatty acyl ester derivative is absorbed into cells within first 30 min and the cellular uptake was not time dependent.

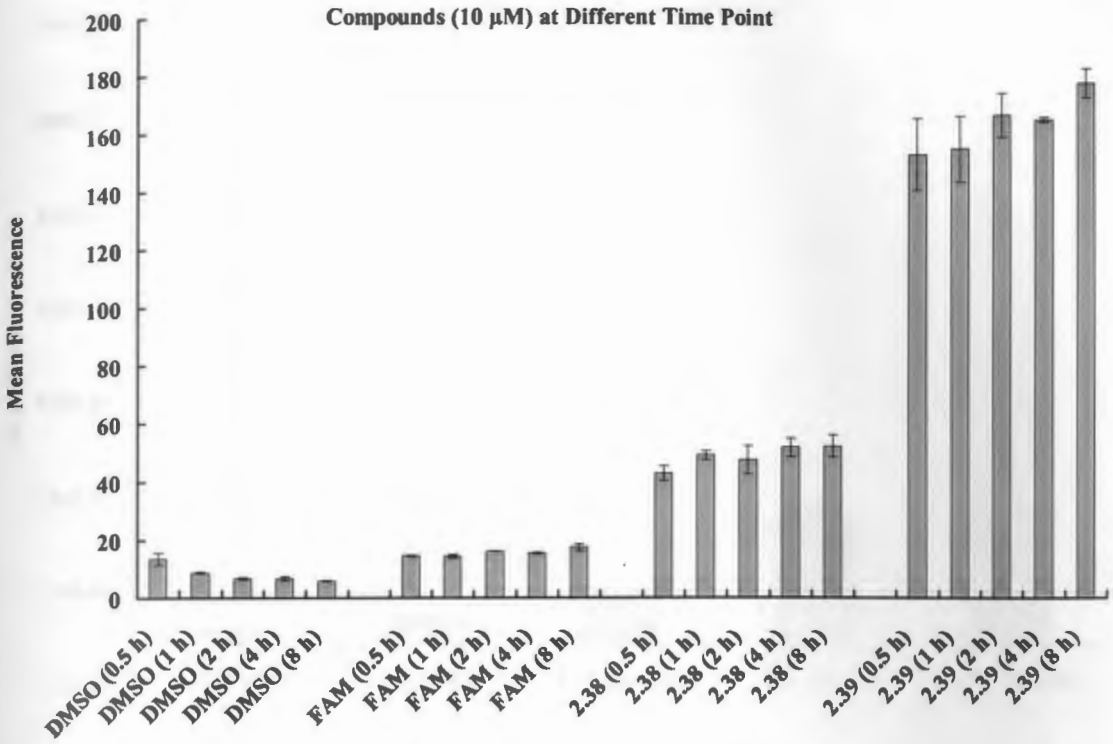

Figure 2.4. Cellular uptake studies for 5(6)-carboxyfluorescein derivatives of 3TC (**2.38** and **2.39**) along with FAM and DMSO as controls at different time intervals.

Cells were then incubated with different concentrations (5, 10, 20, 40 and 100 μM) of carboxyfluorescein derivatives of 3TC, **2.38** and **2.39** for 1 h (Figure 2.5). The data suggest that the cellular uptake was concentration dependent.

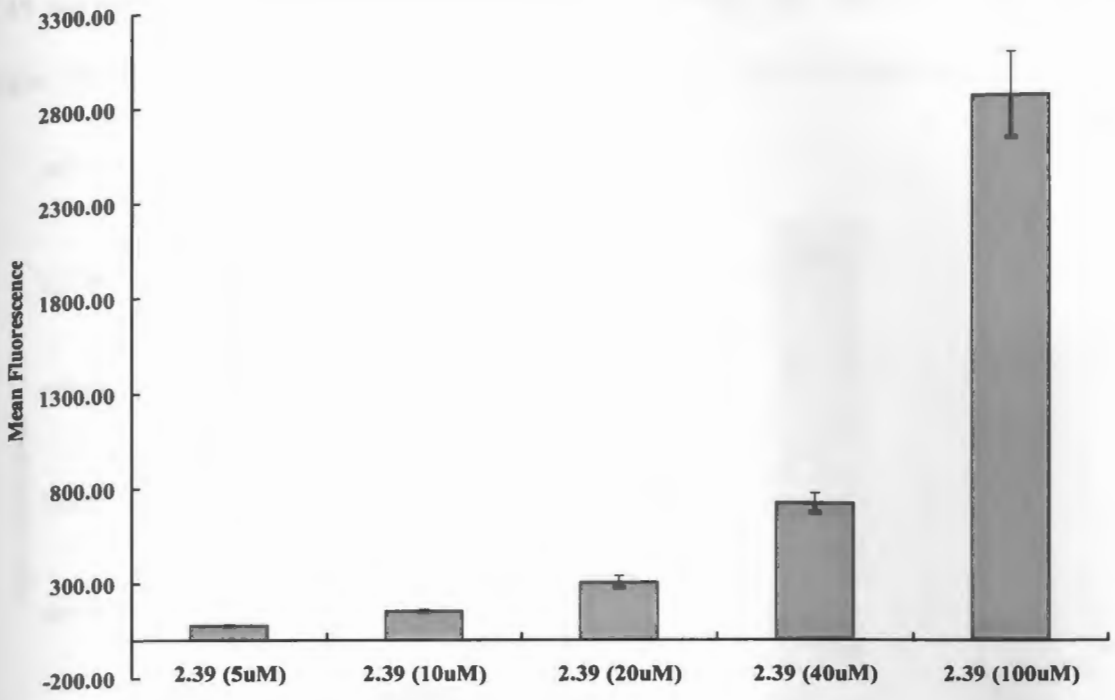

Figure 2.5. Cellular uptake studies for 5(6)-carboxyfluorescein derivative of 3TC (**2.39**) at different concentrations.

To confirm that the enhanced uptake of 5(6)-carboxyfluorescein derivative of 3TC, **2.39**, is not due to the absorption on the cell membrane surface, cells were incubated with 10 μM of DMSO, **2.38**, and **2.39** for 1 h and then half of the cells were finally treated with trypsin for 5 min to wash the adsorbed molecules (if any) from the cell membrane. The comparison of the data between trypsin treated and untreated cells indicates that only small amount of the fluorescence was due to the absorption on the cell membrane surface. The cellular uptake studies after trypsin treatment showed that the cellular uptake of **2.39** was still much higher than those of control compounds and **2.38** (Figure 2.6). Cellular uptake for the trypsin-treated cells with **2.39** was approximately 7 times higher than that of **2.38**. On the other hand, trypsin-untreated cells incubated with

2.39 showed only 4-fold higher cellular uptake than **2.38**. The results suggest that the higher cellular uptake of **2.39** is not due to artificial absorption to the cell membrane.

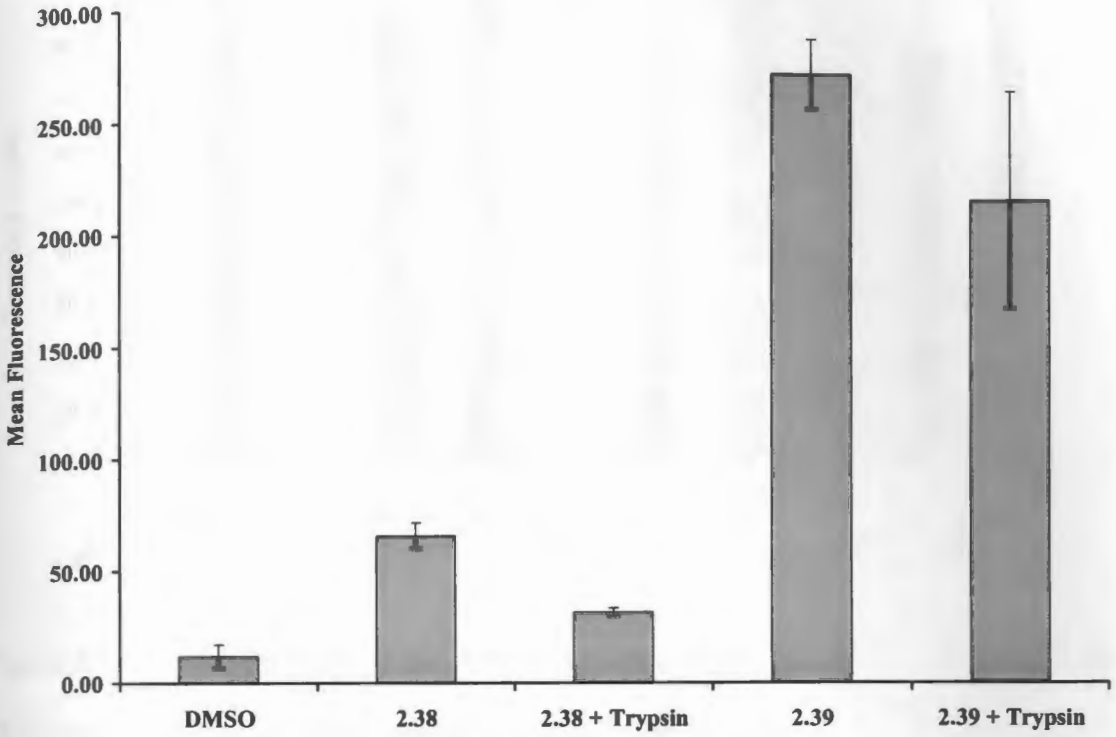

Figure 2.6. Cellular uptake studies for **2.38** and **2.39** with DMSO as controls with and without treatment with trypsin.

2.4.5. Cell Viability Study

Cell viability study was performed to analyze the effect of FAM, **2.38** and **2.39** on the live cells. CCRF-CEM cells were incubated with 10 μM of the compounds and mixed with trypan blue (0.1%) to color the dead cells. The percentage of viability was calculated using Cellometer Auto T.4 (Nexcelom Bioscience). It was observed that at least 80% of the cells were viable in presence of the compounds in 24 h incubation period (Figure 2.7).

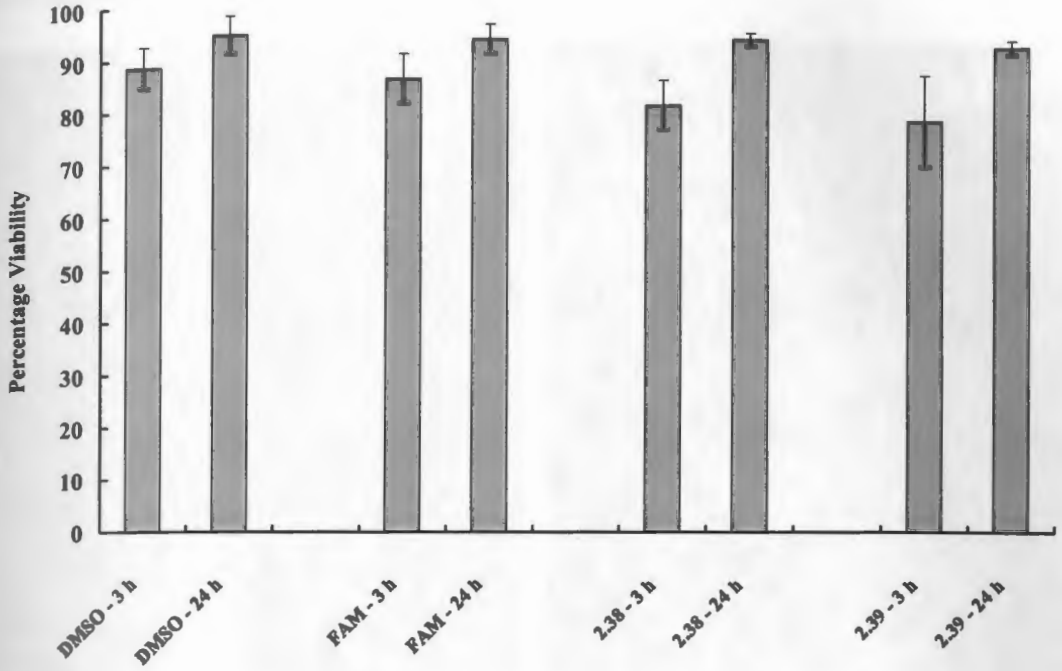

Figure 2.7. Cell viability assay after 3h and 24 h incubation of **2.38** and **2.39** with CCRF-CEM cells. DMSO and FAM were used as positive controls.

2.4.6. Real Time Fluorescence Microscopy in Live CCRF-CEM Cells

CCRF-CEM cells were incubated with 10 μM of DMSO, FAM, **2.38** and **2.39** for 1 h and were imaged using light microscope (ZEISS Axioplan 2) equipped with transmitted light microscopy with a differential-interference contrast method and an Achroplan 40X objective. Cells showed no significant fluorescence when incubated with DMSO, FAM, and **2.38** (Figure 2.8). On the other hand, cells incubated with **2.39** showed fluorescence. The results further confirm the higher cellular uptake of **2.39**, a fatty acyl derivative of 3TC, in comparison to **2.38** and FAM alone. In general, these data

indicate that the fatty acyl derivatives of nucleosides have better cellular uptake than their parent nucleosides.

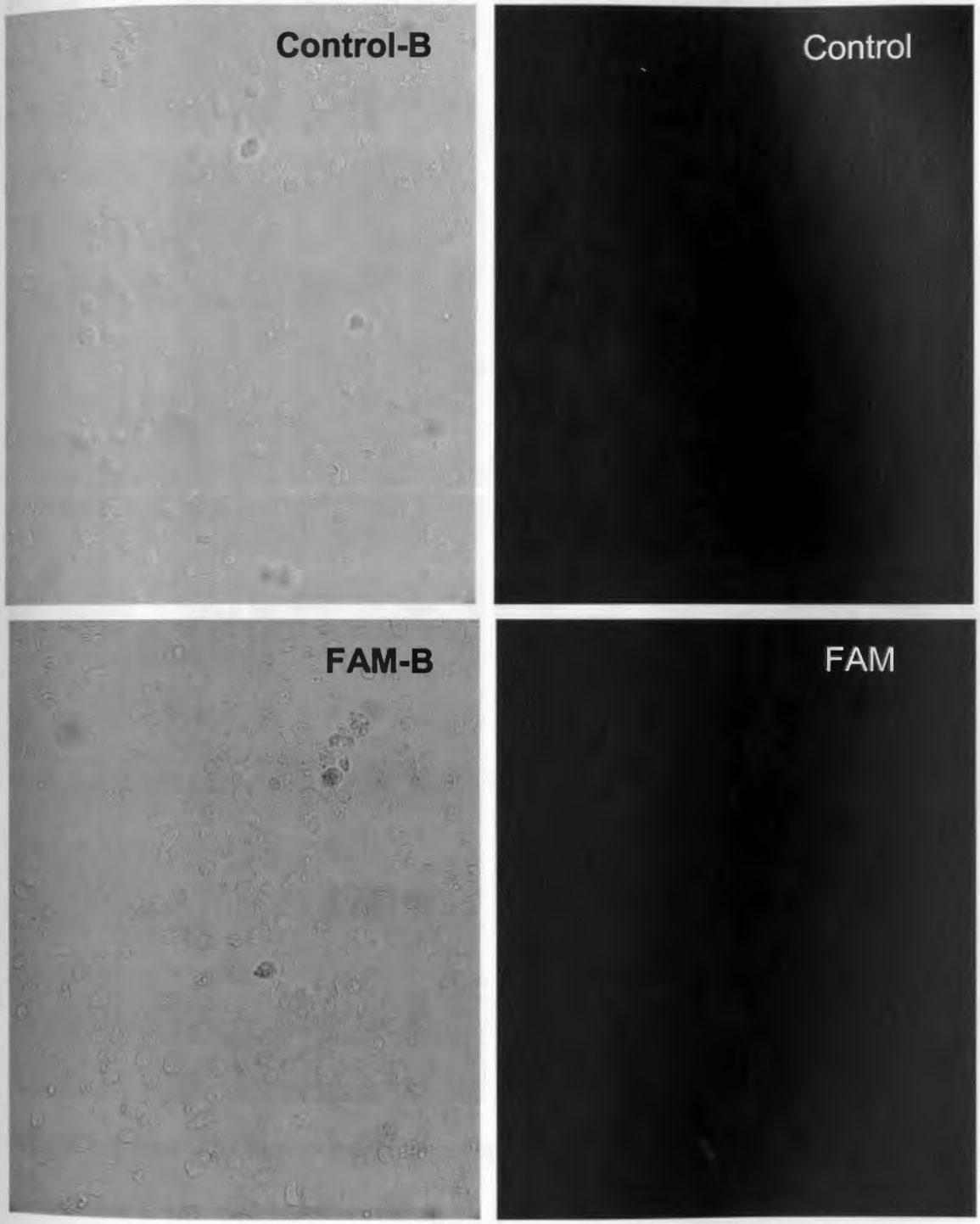

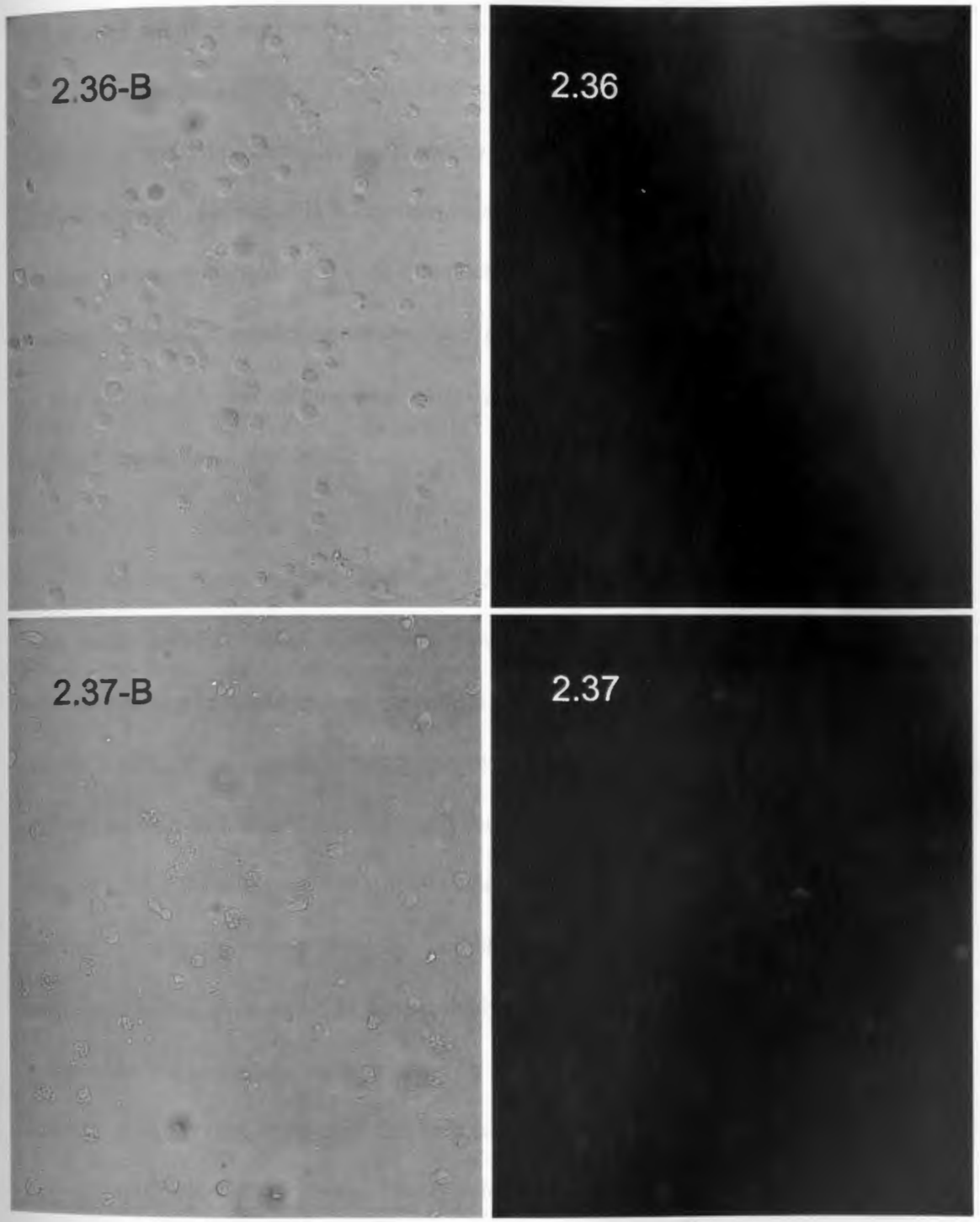

Figure 2.8. Real time fluorescence microscopy in live CCRF-CEM cell line. Control = DMSO, FAM = 5(6)-carboxyfluorescein.

2.5. Conclusions.

Several bifunctional 5′-*O*-substituted or N_4-substituted fatty acyl derivatives of 3TC, d4T, and FTC were designed and synthesized as prodrugs and their biological activities, such as anti-HIV activities, spermicidal properties, and cellular uptake studies. In general, the conjugation of selected fatty acids with RT inhibitor nucleoside analogs resulted in activity better anti-HIV profile because of improved cellular uptake of the conjugates and intracellular hydrolysis of the conjugates yielding two parent analogs targeting RT and NMT.

Among all the ester derivatives, **2.31**, **2.32**, **2.8**, **2.16**, and **2.17** were found to have better anti-HIV activity profile in comparison to 3TC, d4T, FTC and other fatty acyl derivatives. 5′-*O*-Myrsitoyl derivative of FTC (**2.31**), was found to be the most potent anti-HIV compound among the tested compounds and displayed consistent activity against cell-free (IIIB and BaL) stains and cell-associated virus. The physical mixtures of FTC with myristic acid (**2.34**) and 12-thioethyldodecanoic acid (**2.35**) showed significantly less anti-HIV activity than the corresponding 5′-*O*-fatty acyl ester derivatives, **2.31** and **2.33**, respectively.. The data indicate that conjugation of the nucleoside with myristic acid analogs is important in achieving a higher anti-HIV activity possibly by improving the cellular uptake. The significant enhancement of cellular uptake cannot be obtained by physically mixing the nucleoside and fatty acid.

3TC derivatives, **2.8**, **2.16** and **2.17**, exhibited higher anti-HIV activities than other 3TC derivatives. Furthermore, N_4-myristoyl derivative of 3TC, **2.8**, showed the

highest anti-HIV activities against cell-associated virus when compared with all tested fatty acyl ester derivatives of nucleosides here.

The presence of long chain fatty acid at 5′-position enhanced the lipophilicity of 3TC and the cellular uptake as was shown by cellular uptake studies of 5′-carboxyfluroscein derivatives of FLT containing short chain (**2.38**) and long chain (**2.39**) alkyl ester groups. FACS experiments showed that **2.39** had at least 3-5 fold higher cellular uptake in CCRF-CEM cells than **2.38**. Fluorescence microscopy of the cells incubated with these compounds further confirmed the FACS results as cells incubated with **2.39** showed significantly higher fluorescence when compared with cells incubated with FAM and **2.38**. These results suggest that the increased inhibition by the fatty acyl ester derivatives of 3TC, FTC, and d4T may be due to their increased rate of uptake and intracellular hydrolysis yielding two antiviral agents with different targets, parent nucleoside and fatty acid analog. These data provided insights for more rational design of additional potent and safe anti-HIV microbicides using the 3TC or FTC as the parent nucleosides. When taken together, the results will have significant implications for the design of more potent and innovative anti-HIV agents.

2.6. Acknowledgments.

Support for this subproject (MSA-03-367) was provided by CONRAD, Eastern Virginia Medical School under a Cooperative Agreement (HRN-A-00-98-00020-00) with the United States Agency for International Development (USAID). The views expressed by the authors do not necessarily reflect the views of USAID or CONRAD.

2.7. References

Bryant, M. L., McWherter, C. A., Kishore, N. S., Gokel, G. W., Gordon, J. I. MyristoylCoA:protein *N*-myristoyltransferase as a therapeutic target for inhibiting replication of human immunodeficiency virus-1. *Perspect. Drug Dis. Des.*, **1993**, 1, 193-209.

Das, K., Xiong, X., Yang, H., Westland, C. E., Gibbs, C. S., Sarafianos, S. G., and Arnold, E. Molecular modeling and biochemical characterization reveal the mechanism of hepatitis b virus polymerase resistance to lamivudine (3TC) and emtricitabine (FTC). *J. Virol.*, **2001**, 75, 4771–4779.

Diallo, K., Götte, M., Wainberg1, M. A. Molecular impact of the M184V mutation in human immunodeficiency virus type 1 reverse transcriptase. *Antimicrob. Agents Chmother.*, **2003**, 47, 3377–3383.

Farazi, T. A., Waksman, G., Gordon, J. I. The biology and enzymology of protein *N*-myristoylation. *J.Biol. Chem.*, **2001**, 276, 39501–39504.

Gallant, J. E., DeJesus, E., Arras, J. R., et al. Tenofovir DF, Emtricitabine, and Efavirenz vs Zidovudine, and Efavirenz for HIV. *N. Engl. J. Med.*, **2006**, 354, 251-260.

García-Lerma, J. G., MacInnes, H., Bennett, D., Reid, P., Nidtha, S., Weinstock, H., Kaplan, J. E., Heneine, W. A novel genetic pathway of human immunodeficiency virus type 1 resistance to stavudine mediated by the K65R mutation. *J. Virol.*, **2003**, 77, 5685–5693.

Hurst, M and Noble, S. Stavudine, an update of its use in the treatment of HIV infection. *Drugs*, **1999**, 58, 919-949.

Krebs, F. C., Miller, S. R., Malamud, D., Howett, M. K., Wigdahl, B. Inactivation of human immunodeficiency virus type 1 by nonoxynol-9, C21G, or an alkyl sulfate, sodium dodecyl sulfate. *Antiviral Res.*, **1999**, 43, 147-163.

Mansuri, M. M., Hitchcock, M. J. M., Buroker, R. A., Bregman, C. L., Ghazzouli, I., Desiderio, J. V., Starrett, J. E., Sterzycki, R. Z. and Martin, J. C. Comparison of in vitro biological properties and mouse toxicities of three thymidine analogs active against human immunodeficiency virus. *Antimicrob. Agents Chemother.*, **1990**, 34, 637-641.

Masho, S. W., Wang, C. L., Nixon, D. E. Review of tenofovir-emtricitabine. *Ther.Clin. Risk Manag.*, **2007**, 3, 1097-1104.

Mulder, L. C. F., Harari, A., Simon, V. Cytidine deamination induced HIV-1 drug resistance. *Proc. Natl. Acad. Sci. U. S. A.*, **2008**, 105, 5501–5506.

Parang, K., Wiebe, L. I., Knaus, E. E., Huang, J.-S., Tyrrell, D. L., Csizmadia, F. *In vitro* antiviral activities of myristic acid analogs against human immunodeficiency and hepatitis B viruses. *Antiviral Res.*, **1997**, 34, 75-90.

Pozniak, A. L., Gallant, J. E., DeJesus, E., Arribas, J. R., Gazzard, B., Campo, R. E., Chen, S. S., McColl, D., Enejosa, J., Toole, J. J, Cheng, A. K._Tenofovir disoproxil fumarate, emtricitabine, and efavirenz versus fixed-dose zidovudine/lamivudine and efavirenz in antiretroviral-naive patients: virologic, immunologic, and morphologic changes – a 96-week analysis. *J. Acquir. Immune. Defic. Syndr.*, **2006**, 43, 535-540.

Sarafianos, S. G., Das, K., Clark, Jr., A. D., Ding, J., Boyer, P. L., Hughes, S. H., Arnold, E. Lamivudine (3TC) resistance in HIV-1 reverse transcriptase involves steric hindrance with b-branched amino acids. *Proc. Natl. Acad. Sci. U. S. A.*, **1999**, 96, 10027–10032.

Skalaski, V., Chang, C. N., Dutachman, G., Cheng, Y. C. The biochemical basis for the differential anti-human immunodeficiency virus activity of two cis enantiomers of 2',3'-dideoxy-3'-thiacytidine. *J. Biol. Chem.*, **1993**, 268, 23234-23238.

Takamune, N., Hamada, H. Misumi, S. And Shoji, S. Novel strategy for anti-HIV-1 action: selective cytotoxic effect of *N*-myristoyltransferase inhibitor on HIV-1 infected cells. *FEBS letters.*, **2002**, 527, 138-142.

Wu, Z., Alexandratos, J., Ericksen, B., Lubkowshi, J., Gallo, R. C., Lu, W. Total chemical synthesis of N-myristoylated HIV-1 matrix protein p17: Structural and mechanistic implications of p17 myristoylation. *Proc. Natl. Acad. Sci. U. S. A.*, **2004**, 101, 11587-11592.

Chapter 3

Synthesis and Anti-HIV Activities of Succinate, Suberate, Glutamate, and Peptide Derivatives of 3′-Fluoro-2′,3′-Dideoxythymidine , 3′-Azido-2′,3′-Dideoxythymidine , and 2',3'-Dideoxy-3'-Thiacytidine

Hitesh K. Agarwal,[a] Megrose Quiterio,[a] Gustavo F. Doncel,[b] Keykavous Parang[a]

[a]Department of Biomedical and Pharmaceutical Sciences, University of Rhode Island, Kingston, RI, USA, 02881;[b]CONRAD, Department of Obstetrics and Gynecology, Eastern Virginia Medical School, Norfolk, VA, USA 23507

3.1. Abstract

Three classes of mono- di-, or trinucleoside conjugated on multivalent scaffolds (e.g., dicarboxylic acids, amino acids, and peptides) were synthesized to generate broad-spectrum anti-HIV agents with higher barrier to drug resistance, and/or higher cellular uptake: (i) Unsymmetrical and symmetrical dinucleoside conjugates of succinic acid or suberic acid; (ii) Peptides containing one nucleoside and one myristoyl group; and (iii) Dinucleoside- and trinucleoside glutamic acid derivatives with or without myristoyl moiety. Unsymmetrical dinucleoside succinate derivatives were synthesized by reacting nucleoside succinate derivatives with 3′-azido-2′,3′-dideoxythymidine (AZT), 3′-fluoro-2′,3′-dideoxythymidine (FLT), or 2′,3′-dideoxy-3′-thiacytidine (3TC) in the presence of HBTU. Symmetrical dinucleoside suberate derivatives were synthesized from the reaction of suberic acid with the corresponding nucleoside in the presence of HBTU. Small peptides containing one nucleoside and one myristoyl group attached to the amino acid side chains were synthesized by using Fmoc-solid phase protocol. Dinucleoside- and trinucleoside glutamate derivatives containing different nucleosides attached on carboxylic groups and myristoyl or acetyl groups at amino group were synthesized by using multi-step solution phase methods. The anti-HIV activities of several synthesized compounds were determined against cell-free virus and compared with the corresponding physical mixtures. Among all the tested compounds, a glutamate derivative containing three different nucleosides, AZT, FLT, and 3TC, (**3.37**; EC_{50} = 0.96 μM), was found to be the most potent conjugate, and exhibited 35-fold higher anti-HIV activity than both AZT (EC_{50} = 34.4 μM) and 3TC (EC_{50} = 32.7 μM). Compound **3.37** had a comparable anti-HIV activity to FLT

(EC_{50} = 0.8 μM). *N*-Myristoylated conjugates of the glutamic acid showed 1.5-6 higher anti-HIV activities than the corresponding *N*-acetylated conjugates. In general, when compared with the corresponding conjugated derivatives, the physical mixtures demonstrated higher anti-HIV activity. In addition, the physical mixtures containing myristic acid exhibited 2-3 fold higher anti-HIV activity than those without myristic acid. These data suggest that the presence of myristic acid plays an important role in improving anti-HIV activity of the conjugated compounds or the physical mixtures.

3.2 Introduction

Scaffolds are defined as skeleton, core, or template of the structure to which multiple functional groups and moieties may be attached. The scaffolds may have multiple positions for multivalent linkages. Some examples of scaffolds include polycarboxylic acid derivatives, amino acids, and peptides. Herein, we compared the anti-HIV activities of nucleosides conjugated on small peptides with those conjugated on dicarboxylic acid derivatives (i.e., suberic acid, succinic acid) and glutamic acid. For example, diversity in the structure and physicochemical properties of peptides allow their applications in targeted drug delivery, enzyme inhibitors, and scaffolds.

Peptides-based prodrugs are commonly used in drug delivery. Peptides have been used as linkers to deliver drugs at desired site where they undergo site specific enzymatic hydrolysis to deliver the active molecules. For example, Chau et al. have used a specific peptide sequence of matrix metalloproteinase, an enzyme overexpressed in cancer cells, to deliver anti-cancer drugs, such as methotrexate to the cancer cells (Chau et al., 2004, Chau et al., 2005, and Chau et al., 2006). Peptides with

different chain lengths have also been used as spacers to deliver active drugs after lysosomal hydrolysis of the peptide conjugates (Penugonda et al., 2007, Subr et al., 1992, Soyez et al., 1996).

Peptide esters have been previously used to improve the bioavailability of the active drugs. Peptide prodrugs of lopinavir showed higher oral bioavailability than lopinavir itself (Agarwal et al., 2008). Peptide conjugates of 5-aminolaevulinic acid showed improved pharmacological response as a result of better cellular uptake (Bourre et al., 2008).

Furthermore, peptide derivatives are also being used to produce direct pharmacological activity against some targeted enzymes. Ramipril, enalapril, and captopril are peptide-based compounds that are used as angiotensin converting enzyme inhibitors (Acharya et al., 2003). Enfuvirtide is a recently approved anti-HIV drug that acts as the anti-HIV entry blocker, and is a peptide structure based derivative (Lazzarin, 2005). Several HIV protease inhibitors, such as lopinavir, saquinavir, are also peptide-based drugs (Agarwal et al., 2008, Cvetkovic et al., 2003).

Although the introduction of highly active antiretroviral therapy (HAART) in the mid-1990s has resulted in a decrease of the morbidity and mortality in the HIV-1 patient population that has access to treatment, therapy failure still occurs. A combination of reverse transcriptase (RT) inhibitor nucleoside analogs is used in HAART to reduce the viral load. Each nucleoside analog has different cellular uptake rate and pharmacokinetics. Several of nucleoside analogs succumb to newly developed resistant virus. For example, Lamivudine is a (-)-2',3'-dideoxy-3'-thiacytidine analog that is used in the treatment of both HIV-1 and hepatitis disease (Skalski et al., 1993)..

Although Lamivudine has good activity against wild type HIV, a single point mutation at 184 residue results in 3TC-resistant mutant virus (M184V/I) (Mulder et al., 2008, Sarafianos et al., 1999, Diallo et al., 2003). Several studies have provided different reasons for resistance development, such as cytidine deamination and the generation of steric hindrance at 184 amino acid residues. Similar to the HIV, mutation at Met552 with Val and Ile (M552V/I) results in 3TC and FTC resistant HBV strains (Das et al., 2001). Nucleoside analogs are also very polar and have limited cellular uptake. Therefore it is logical to develop new and more potent multi-nucleoside conjugates, with major advantages to HAART therapy that display broad-spectrum activity against drug-resistant HIV, have higher cellular uptake, and can deliver several RT nucleoside inhibitors simultaneously to the HIV-infected cells.

The objective of this research was to design multi-nucleoside conjugates substituted on a multivalent scaffold. The conjugates may have application in delivery of several nucleosides to the infected cells, broad-spectrum activity, and a higher barrier to drug resistance. Herein, we report the synthesis and anti-HIV evaluation of, three classes of nucleoside analog (AZT, FLT, or 3TC) conjugates. In the first class, combinations of two similar or different nucleosides, (AZT, FLT, or 3TC) were attached to the carboxylic acid groups of succinic acid and suberic acid. Second class of compounds includes myristoyl or acetyl derivatives of di- or trinucleoside-glutamic acid conjugates containing more than one nucleoside. In the third class of compounds, peptide derivatives containing nucleosides and myristoyl group on the side chain were synthesized.

Nucleoside-scaffold conjugates were designed with the expectation that the attachment of more than one nucleoside analog to the scaffold will generate a prodrug capable of delivering different nucleosides to the HIV-infected cells . Myristic acid was attached to the scaffolds to improve the lipophilicity of the conjugates and their cellular uptake. It was expected that once the conjugate enters the cells, it will be hydrolyzed by esterase and/or peptidases to generate parent nucleoside analogs. The release of different nucleosides will help to increase the barrier to resistance to the individual compounds. The combined conjugates may have also the benefits of synergistic antiviral effects on HIV-1 and HIV-2, increased antiviral spectrum, dosing simplicity, and favorable pharmacokinetic properties.

3.3 Materials and Methods

3.3.1 Materials

Succinic acid, succinyl chloride, suberic acid, pyridine, acetonitrile, and diisopropylethylamine (DIPEA) were purchased from Fisher Scientific. Fmoc protected amino acids (Fmoc-Glu-OtBu, Fmoc-Ser-OH, Fmoc-Lys(Mtt)-OH, Fmoc-β-Ala-OH, Fmoc-Gly-OH, and 2-(1H-benzotriazole-1-yl)-1,1,3,3-tetramethyluronium hexafluorophosphate (HBTU) were purchased from Novabiochem. Lamivudine, Zidovudine, and Alovudine were purchased from Euro Asia Tran Continental (Bombay, India). All the other reagents including solvents were purchased from Fisher Scientific.

The products were purified on a Phenomenex®Gemini 10 μm ODS reversed-phase column (2.1 × 25 cm) with Hitachi HPLC system using a gradient system at constant flow rate of 17 ml/min (Table 3.1).

Table 3.1. HPLC method used for the purification of the compounds.

Time (minutes)	Water Concentration A (%)	Acetonitrile Concentration B (%)	Flow rate (mL/min)
0.00	100.0	0.0	1.0
1.0	100.0	0.0	17.0
45.0	0.0	100.0	17.0
55.0	0.0	100.0	17.0
59.0	100.0	0.0	17.0
60.0	100.0	0.0	1.0

PS3 automated peptide synthesizer (Rainin Instrument Co., Oakland, CA) was used to synthesize peptides. In general, all peptides were synthesized by the solid-phase synthesis strategy employing *N*-(9-fluorenyl)methoxycarbonyl (Fmoc)-based chemistry and Fmoc-L-amino acid building blocks. 2-(1H–Benzotriazole-1-yl)-1,1,3,3-tetramethyluronium hexafluorophosphate (HBTU) and NMM in *N,N*-dimethylformamide (DMF) were used as coupling and activating reagents, respectively. Wang resin, Fmoc-amino acid Wang resins, coupling reagents, and Fmoc-amino acid building blocks were purchased from Novabiochem.

The chemical structures of final products were characterized by nuclear magnetic resonance spectrometry (^{1}H NMR and ^{13}C NMR) determined on a Bruker NMR spectrometer (400 MHz). Chemical shifts are reported in parts per millions

(ppm). The chemical structures of final products were confirmed by a high-resolution PE Biosystems Mariner API time-of-flight electrospray mass spectrometer.

3.3.2. Chemistry

3.3.2.1. Synthesis of Unsymmetrical and Symmetrical Dinucleoside Conjugates of Succinic acid or Suberic acid. FLT, AZT, and 3TC were attached to succinic acid and suberic acid to synthesize dinucleoside derivatives of succinic acid and suberic acid respectively.

5′-*O*-(Succinate)-3′-fluoro-2′,3′-dideoxythymidine (3.1) and 5′-*O*-(succinate)-3′-azido-2′,3′-dideoxythymidine (3.2). Succinic anhydride (290 mg, 2.90 mmol) and nucleoside (AZT or FLT) (1.45 mmol) were dissolved in dry pyridine (15.0 mL). The reaction mixture was stirred at room temperature overnight. The solvent was evaporated under reduced pressure and the crude product was purified with reversed phase HPLC using a C_{18} column and water/acetonitrile as solvents as described above in Table 3.1.

3′-Fluoro-2′,3′-dideoxy-5′-*O*-(succinate)thymidine (3.1). Yield (350 mg, 70%); ^{1}H NMR (400 MHz, $CDCl_3$, δ ppm): 10.73 (s, 1H, N*H*), 7.41 (s, 1H, H-6), 6.06 (dd, J = 4.5 and 9.7 Hz, 1H, H-1′), 5.36 (dd, J = 4.6 and 53.4 Hz, 1H, H-3′), 4.99 (d, J = 12.7 Hz, 1H, H-5″), 4.38-4.54 (m, 1H, H-4′), 4.14 (dd, J = 3.5 and 12.7 Hz, 1H, H-5′), 2.53-2.97 (m, 4H, succinate protons), 2.40-2.51 (m, 1H, H-2″), 2.01-2.23 (m, 1H, H-2′), 1.86 (s, 3H, 5-C*H*$_3$); ^{13}C NMR ($CDCl_3$, 100 MHz, δ ppm): 178.40 (*C*OOH),

173.26 (*C*OOFLT), 167.11 (C-4 *C*=O), 149.52 (C-2 *C*=O), 138.20 (C-6), 109.96 (C-5), 93.81 (J = 176.9 Hz, C-3′), 86.05 (C-1′), 83.88 (J = 26.9 Hz, C-4′), 63.79 (J = 10.9 Hz, C-5′), 39.22 (J = 20.1 Hz, C-2′), 29.03 (succinate *C*H_2), 28.82 (succinate *C*H_2), 12.70 (5-*C*H_3); HR-MS (ESI-TOF) (m/z): $C_{14}H_{17}FN_2O_7$: calcd, 344.1020; found, 345.4061 $[M + H]^+$, 689.5581 $[2M + H]^+$.

5′-*O*-(Succinate)-3′-azido-2′,3′-dideoxythymidine (3.2). Yield (350 mg, 70%); ^{1}H NMR (400 MHz, CD_3OD, δ ppm): 11.37 (br s, 1H, N*H*), 7.51 (s, 1H, H-6), 6.14 (t, J = 6.5 Hz, 1H, H-1′), 4.49 (dd, J = 5.9 and 13.4 Hz, 1H, H-3′), 4.32 (dd, J = 4.5 and 12.1 Hz, 1H, H-5″), 4.19 (dd, J = 3.7 and 12.1 Hz, 1H, H-5′), 3.96 (dd, J = 4.5 and 9.5 Hz, 1H, H-4′), 2.27-2.52 (m, 6H, succinate protons, H-2″, H-2′), 1.80 (s, 3H, 5-C*H*$_3$); HR-MS (ESI-TOF) (m/z): $C_{14}H_{17}N_5O_7$: calcd, 367.1128; found, 368.1823 $[M + H]^+$, 390.1566 $[M + Na]^+$, 735.3566 $[2M + H]^+$, 757.3207 $[2M + Na]^+$, 789.2567 $[2M + 2Na]^+$.

[5′-*O*-(3′-Azido-2′,3′-dideoxythymidinyl)][5′-*O*-(3′-fluoro-2′,3′-dideoxythymidineyl)]-1,4-succinate (3.3). Compound **3.1** (100 mg, 0.29 mmol), AZT (100 mg, 0.37 mmoL), HBTU (440 mg, 1.15 mmol), and DIPEA (2 mL, 15 mmol) were dissolved in dry DMF (10 mL) and stirred overnight at room temperature. The reaction mixture was concentrated and dried under vacuum. The residue was purified with reversed phase HPLC using a C_{18} column and water/acetonitrile as solvents as described above to yield **3.3** (110 mg, 65%).

^{1}H NMR (400 MHz, CD_3CN, δ ppm): 7.35, 7.34 (s, 2H, AZT H-6, FLT H-6), 6.18 (dd, J = 5.7 and 53.4 Hz, 1H, FLT H-1′), 6.05 (t, J = 6.3 Hz, 1H, AZT H-1′), 5.21 (dd, J = 5.1 and 9.0 Hz, 1H, FLT H-3′), 4.04-4.42 (m, 6H, AZT H-3′, AZT H-5′, AZT H-5″, FLT H-5′, FLT H-5″, FLT H-4′), 3.97 (dd, J = 4.6 and 9.2 Hz, 1H, AZT H-4′), 2.09-2.73 (m, 8H, succinate protons, AZT H-2″, AZT H-2′, FLT H-2″, FLT H-2′), 1.80 (s, 6H, 5-C*H*$_3$); ^{13}C NMR (CD_3CN, 100 MHz, δ ppm): 173.58, 173.56 (*C*OOFLT, *C*OOAZT), 165.96, 165.92 (FLT C-4 *C*=O, AZT C-4 *C*=O), 151.74, 151.68 (FLT C-2 *C*=O, AZT C-2 *C*=O), 137.41, 136.96 (FLT C-6, AZT C-6), 111.88, 111.76 (FLT C-5, AZT C-5), 94.80 (J = 175.1 Hz, FLT C-1′), 85.97 (FLT C-3′), 85.60 (AZT C-1′), 83.05 (J = 26.4 Hz, FLT C-4′), 83.14 (AZT C-4′), 64.68, 64.37 (AZT C-5′, FLT C-5′), 61.8 (AZT C-3′), 38.05 (J = 20.6 Hz, FLT C-2′), 37.15 (AZT C-2′), 29.5 (succinate *C*H$_2$), 12.5, 12.45 (FLT 5-*C*H$_3$, AZT 5-*C*H$_3$); HR-MS (ESI-TOF) (m/z): $C_{24}H_{28}FN_7O_{10}$: calcd, 593.1882; found, 594.0366 $[M + H]^+$.

[5′-*O*-(3′-Fluoro-2′,3′-dideoxythymidineyl)][(-)-5′-*O*-(2′,3′-dideoxy-3′-thiacytidinyl)]-1,4-succinate (3.4). The synthesis of (-)-N_4-(4,4′-dimethoxytrityl)-2′,3′-dideoxy-3′-thiacytidine was previously described in Chapter 2. Compound **3.1** (100 mg, 0.29 mmol), **2.12** (100 mg, 0.37 mmoL), HBTU (440 mg, 1.15 mmol), and DIPEA (2 mL, 15 mmol) were dissolved in dry DMF (10 mL) and stirred overnight at room temperature. The reaction mixture was concentrated, and acetic acid (80%, 10 mL) was added to the residue. The mixture was stirred at 80 °C for 30 min. The reaction mixture was concentrated and dried under vacuum. The residue was purified

with reversed phase HPLC using a C_{18} column and water/acetonitrile as solvents as described above to yield **3.4** (80 mg, 50 %).

^{1}H NMR (400 MHz, CD_3CN, δ ppm): 7.98 (d, J = 7.9 Hz, 1H, 3TC H-6), 7.37 (s, 1H, FLT H-6), 6.16-6.23 (m, 2H, 3TC H-1′, FLT H-1′), 6.12 (d, J = 7.9 Hz, 1H, 3TC H-5), 5.36 (t, J = 4.2 Hz, 1H, 3TC H-4′), 5.23 (dd, J = 5.2 and 53.4 Hz, 1H, FLT H-3′), 4.18-4.46 (m, 5H, 3TC H-5′, 3TC H-5″, FLT H-4′, FLT H-5′, FLT H-5″), 3.53 (dd, J = 5.6 and 12.2 Hz, 1H, 3TC H-2′), 3.22 (dd, J = 3.0 and 12.2 Hz, 1H, 3TC H-2″), 2.48-2.68 (m, 5H, succinate protons, FLT H-2″), 2.14-2.24 (m, 1H, FLT-H-2′), 1.80 (s, 3H, FLT-5-C*H*$_3$); ^{13}C NMR (CD_3CN, 100 MHz, δ ppm): 173.64 (*C*OOFLT), 173.40 (-*C*OO 3TC), 165.98 (3TC C-4 *C*=O), 160.28 (FLT C-4 *C*=O), 151.78 (3TC C-2 *C*=O), 148.20 (FLT C-2 *C*=O), 145.05 (3TC C-6), 137.03 (FLT C-6), 111.94 (FLT C-5), 95.01 (3TC C-5), 94.85 (J = 175.0 Hz, FLT C-3′), 87.95 (3TC C-1′), 86.03 (FLT C-1′), 85.03 (3TC C-4′), 83.10 (J = 26.5 Hz, FLT C-4′), 64.88, 64.77 (FLT C-5′, 3TC C-5′), 38.14 (J = 20.4 Hz, FLT C-2′), 38.09 (3TC C-2′), 29.54, 29.44 (succinate *C*H$_2$), 12.50 (FLT 5-*C*H$_3$); HR-MS (ESI-TOF) (m/z): $C_{22}H_{26}FN_5O_9S$: calcd, 555.1435; found, 556.0964 $[M + H]^+$.

[5′-*O*-(3′-Azido-2′,3′-dideoxythymidinyl)][(-)-5′-*O*-(2′,3′-dideoxy-3′-thiacytidinyl)]-1,4-succinate (3.5). Compound **3.2** (100 mg, 0.29 mmol), **2.12** (100 mg, 0.37 mmoL), HBTU (440 mg, 1.15 mmol), and DIPEA (2 mL, 15 mmol) were dissolved in dry DMF (10 mL) and stirred overnight at room temperature. The reaction mixture was concentrated and acetic acid (80%, 10 mL) was added to the residue. The mixture was stirred at 80 °C for 30 min. The reaction mixture was

concentrated and dried under vacuum. The residue was purified with reversed phase HPLC using a C_{18} column and water/acetonitile as solvents as described above to yield **3.5** (80 mg, 50 %).

^{1}H NMR (400 MHz, CD_3CN, δ ppm): 7.99 (d, J = 7.9 Hz, 1H, 3TC H-6), 7.35 (s, 1H, AZT H-6), 6.21 (dd, J = 3.2 and 5.5 Hz, 1H, 3TC H-1′), 6.13 (d, J = 7.9 Hz, 1H, 3TC H-5), 6.06 (t, J = 6.4 Hz, 1H, 1H, AZT H-1′,) 5.36 (t, J = 4.1 Hz, 1H, 3TC H-4′), 4.43 (d, J = 4.0 Hz, 1H, AZT H-3′), 4.23-4.29 (m, 4H, 3TC H-5′, 3TC H-5″, AZT H-5′, AZT H-5″), 3.87-4.05 (m, 1H, AZT H-4′), 3.53 (dd, J = 5.5 and 12.2 Hz, 1H, 3TC H-2′), 3.22 (dd, J = 3.2 and 12.2 Hz, 1H, 3TC H-2″), 2.64 (s, 4H, succinate protons), 2.38 (t, J = 6.4 Hz, 2H, AZT H-2′ and H-2″), 1.80 (s, 3H, AZT 5-C*H*$_3$); ^{13}C NMR (CD_3CN, 100 MHz, δ ppm): 173.60 (*C*OOAZT), 173.38 (*C*OO 3TC), 165.92 (3TC C-4 *C*=O), 160.34 (AZT C-4 *C*=O), 151.67 (3TC C-2 *C*=O), 148.20 (AZT C-2 *C*=O), 145.02 (3TC C-6), 137.42 (AZT C-6), 111.76 (AZT C-5), 95.00 (3TC C-5), 87.96 (3TC C-1′), 85.60 (AZT C-1′), 85.07 (3TC C-4′), 82.25 (AZT C-4′), 64.85, 64.30 (AZT C-5′, 3TC C-5′), 60.85 (AZT C-3′), 38.13 (3TC C-2′), 37.20 (AZT C-2′), 29.54, 29.44 (succinate *C*H$_2$), 12.48 (AZT 5-*C*H$_3$); HR-MS (ESI-TOF) (m/z): $C_{22}H_{26}N_8O_9S$: calcd, 578.1543; found, 579.0164 $[M + H]^+$.

Di[5′-*O*-(3′-azido-2′,3′-dideoxythymidinyl)]-1,4-succinate (3.6) and di[5′-*O*-(3′-fluoro-2′,3′-dideoxythymidinyl)]-1,4-succinate (3.7). FLT or AZT (0.45 mmol) and DMAP (110 mg, 0.90 mmoL) were dissolved in dry benzene (10 mL). Succinyl chloride (22 μL, 0.2 mmoL) was added to the reaction mixture. The reaction mixture was stirred overnight at room temperature, concentrated at reduced pressure, and dried

under vacuum. The residue was purified with reversed phase HPLC using a C_{18} column and water/acetonitile as solvents as described above to yield **3.6** or **3.7**.

3.6. Yield (100 mg, 80%); ^{1}H NMR (400 MHz, CD_3OD, δ ppm): 7.40 (s, 2H, H-6), 6.09 (t, J = 6.4 Hz, 2H, H-1′), 4.40 (dd, J = 4.8 and 9.0 Hz, 2H, H-3′), 4.23-4.36 (m, 4H, H-5′ and H-5″,), 4.00 (dd, J = 4.8 and 9.0 Hz, 2H, H-4′), 2.70 (s, 4H, succinate protons), 2.34-2.51 (m, 4H, H-2′ and H-2″), 1.87 (s, 3H, 5-CH_3); ^{13}C NMR (CD_3OD, 100 MHz, δ ppm): 173.30 (*C*OOAZT), 165.87 (C-4 *C*=O), 151.70 (C-2 *C*=O), 137.36 (C-6), 111.78 (C-5), 86.23 (C-1′), 82.63 (C-4′), 64.46 (C-5′), 61.37 (C-3′), 37.68 (C-2′), 29.56 (succinate *C*H_2), 12.68 (5-*C*H_3); HR-MS (ESI-TOF) (m/z): $C_{24}H_{28}N_{10}O_{10}$: calcd, 616.199; found, 617.1990 $[M + H]^+$, 1233.1624 $[M + H]^+$.

3.7. Yield (100 mg, 80%); ^{1}H NMR (400 MHz, CD_3OD, δ ppm): 7.43 (s, 2H, H-6), 6.27 (dd, J = 6.5 and 8.9 Hz, 2H, H-1′), 5.24 (dd, J = 4.9 and 53.6 Hz, 2H, H-3′), 4.35-4.48 (m, 4H, H-4′, H-5″), 4.27 (dd, J = 2.8 and 10.9 Hz, 2H, H-5′), 2.70 (s, 4H, succinate protons), 2.50-2.641 (m, 1H, H-2″), 2.18-2.44 (m, 1H, H-2′), 1.89 (s, 3H, 5-CH_3); ^{13}C NMR (CD_3OD, 100 MHz, δ ppm): 173.68 (*C*OOFLT), 166.41 (C-4 *C*=O), 152.36 (C-2 *C*=O), 137.40 (C-6), 112.50 (C-5), 95.11 (J = 177.2 Hz, C-3′), 86.90 (C-1′), 83.97 (J = 26.2 Hz, C-4′), 65.28 (C-5′), 38.90 (J = 21.1 Hz, C-2′), 30.02 (succinate *C*H_2), 13.25 (5-*C*H_3); HR-MS (ESI-TOF) (m/z): $C_{24}H_{28}F_2N_4O_{10}$: calcd, 570.1773; found, 571.2164 $[M + H]^+$, 1141.1336 $[M + H]^+$.

Di[5′-*O*-(3′-azido-2′,3′-dideoxythymidinyl)]-1,8-suberate (3.8) and di[5′-*O*-(3′-fluoro-2′,3′-dideoxythymidinyl)]-1,8-suberate (3.9). AZT or FLT (0.58 mmol),

suberic acid (50 mg, 0.29 mmol), HBTU (440 mg, 1.15 mmol), and DIPEA (2 mL, 15 mmol) were dissolved in dry DMF (10 mL). The reaction mixture was stirred overnight at room temperature, concentrated, and dried under vacuum. The residue was purified with reversed phase HPLC using a C_{18} column and water/acetonitile as solvents as described above to yield **3.8** and **3.9**.

3.8. Yield (60 mg, 30 %); ^{1}H NMR (400 MHz, CD_3OD, δ ppm): 7.33 (s, 2H, H-6), 6.07 (t, J = 6.3 Hz, 2H, H-1′), 4.11-4.34 (m, 6H, H-3′, H-5′, and H-5″), 4.23-4.36 (m, 4H, H-4′), 2.33 (dt, 8H, CH_2COO, H-2′ and H-2″), 1.80 (s, 6H, 5-CH_3), 1.52 (t, J = 6.2 Hz, 4H, CH_2CH$_2$COO), 1.18-1.30 (br m, 4H, suberate methylene); ^{13}C NMR (CD_3OD, 100 MHz, δ ppm): 174.78 (*C*OOAZT), 165.78 (C-4 *C*=O), 151.66 (C-2 *C*=O), 137.24 (C-6), 111.65 (C-5), 85.59 (C-1′), 83.28 (C-4′), 64.04 (C-5′), 61.08 (C-3′), 37.34 (C-2′), 34.44 (*C*H$_2$COO), 29.03 (*C*H$_2$CH$_2$COO), 25.13 (suberate *C*H$_2$), 12.52 (5-*C*H$_3$); HR-MS (ESI-TOF) (m/z): $C_{28}H_{36}N_{10}O_{10}$: calcd, 672.2616; found, 673.1400 $[M + H]^+$.

3.9. Yield (60 mg, 30%); ^{1}H NMR (400 MHz, CD_3OD, δ ppm): 7.36 (s, 2H, H-6), 6.18 (dd, J = 5.6 and 8.9 Hz, 2H, H-1′), 5.24 (dd, J = 5.1 and 53.1 Hz, 2H, H-3′), 4.39 (dt, J = 3.5 and 26.6 Hz, 2H, H-4′), 4.27 (dd, J = 3.5 and 12.1 Hz, 2H, H-5′), 4.17 (dd, J = 3.5 and 12.1 Hz, 2H, H-5″), 2.46 (m, 2H, H-2″), 2.13-2.33 (m, 6H, CH_2COO, H-2′), 1.79 (s, 6H, 5-CH_3), 1.44-1.55 (m, 4H, CH_2CH$_2$COO), 1.15-1.27 (m, 4H, suberate methylene); ^{13}C NMR (CD_3OD, 100 MHz, δ ppm): 174.86 (*C*OOFLT), 165.88 (C-4 C=O), 151.74 (C-2 *C*=O), 136.86 (C-6), 111.77 (C-5), 94.96 (J = 175.0 Hz, C-3′), 86.05 (C-1′), 83.22 (J = 26.3 Hz, C-4′), 64.30 (C-5′), 38.41, 38.20 (J = 178.3 Hz, C-2′), 34.38 (*C*H$_2$COO), 28.97 (*C*H$_2$CH$_2$COO), 25.06 (suberate *C*H$_2$), 12.54 (5-*C*H$_3$);

HR-MS (ESI-TOF) (m/z): $C_{28}H_{36}F_2N_4O_{10}$: calcd, 626.2399; found, 627.1035 $[M + H]^+$, 1253.4346 $[M + H]^+$.

Di[(-)-5′-*O*-(2′,3′-dideoxy-3′-thiacytidinyl)-1,8-suberate (3.10). Compound **2.12** (310 mg, 0.58 mmol), suberic acid (50 mg, 0.29 mmol) HBTU (440 mg, 1.15 mmol), and DIPEA (2 mL, 15 mmol) were dissolved in dry DMF (10 mL). The mixture was stirred overnight at room temperature and was concentrated at reduced pressure. Acetic acid (80%, 10 mL) was added to the residue and the reaction mixture was stirred at 80 °C for 30 min. The reaction mixture was concentrated and dried under vacuum. The residue was purified with reversed phase HPLC using a C_{18} column and water/acetonitile as solvents as described above to yield **3.10** (50 mg, 30%).

^{1}H NMR (400 MHz, CD_3OD, δ ppm): 8.02 (d, J = 7.9 Hz, 2H, H-6), 6.20 (dd, J = 5.4 and 3.1 Hz, 2H, H-1′), 6.10 (d, J = 7.9 Hz, 2H, H-5), 5.35-5.45 (m, 1H, H-4′), 4.31-4.54 (m, 4H, H-5′ and H-5″), 3.54 (dd, J = 5.4 and 12.6 Hz, 2H, H-2″), 3.20-3.27 (m, 2H, H-2′), 2.20-2.36 (m, 4H, CH_2COO), 1.38-1.60 (m, 4H, CH_2CH$_2$COO), 1.12-1.32 (m, 4H, suberate methylene); ^{13}C NMR (CD_3OD, 100 MHz, δ ppm): 174.78 (*C*OO3TC), 160.63 (C-4 *C*=O), 148.60 (C-2 *C*=O), 144.99 (C-6), 94.80 (C-5), 88.01 (C-1′), 85.45 (C-4′), 64.30 (C-5′), 38.30 (*C*H$_2$COO), 34.38 (*C*H$_2$CH$_2$COO), 29.04 (C-2′), 25.17 (suberate *C*H$_2$); HR-MS (ESI-TOF) (m/z): $C_{24}H_{32}N_6O_8S_2$: calcd, 596.1723; found, 597.0920 $[M + H]^+$, 1193.4381 $[M + H]^+$.

3.3.2.2. Synthesis of Peptide-Nucleosides Conjugates (Peptides Containing one nucleoside and one Myristoyl Group)

Several peptide conjugates of AZT, FLT, 3TC, and myristic acid were synthesized employing a PS3 automated peptide synthesizer and Fmoc solid-phase peptide synthesis using Fmoc-L-amino acid building blocks. The peptide-nucleoside conjugates were assembled on Wang resin solid support at room temperature. The building blocks, Fmoc-Glu(nucleoside)-OH and Fmoc-Ser(myristoyl)-OH, were synthesized from Fmoc-Glu(OH)-tBu and Fmoc-Ser-OH, respectively, as described below:

Fmoc-Glu(3′-fluoro-2′,3′-dideoxythymidine-5′-yl)-OH (3.12) and Fmoc-Glu(3′-azido-2′,3′-dideoxythymidine-5′-yl)-OH. Fmoc-Glu(OH)O*t*Bu (5 g, 11.8 mmol), FLT or AZT (3.5 g, 14.1 mmol), and HBTU (6.67 g, 17.6 mmol) were dissolved in DMF (25 mL). DIPEA (5 mL, **38 mmol**) was added to the solution and the reaction mixture was stirred at room temperature overnight. The solvent was removed at reduced pressure to yield crude Fmoc-Glu(3′-fluoro-2′,3′-dideoxythymidine-5′-yl)O*t*Bu (**3.11**) or Fmoc-Glu(3′-azido-2′,3′-dideoxythymidine-5′-yl)O*t*Bu (**3.13**).

3.11. HR-MS (ESI-TOF) (m/z): $C_{34}H_{38}FN_3O_9$: calcd, 651.2592; found, 652.1312 $[M + H]^+$; 1303.2873. $[2M + H]^+$; **3.13.** HR-MS (ESI-TOF) (m/z): calcd, $C_{34}H_{38}N_6O_9$; found,: 674.27 $[M + H]^+$, 697.0440. $[M + Na]^+$.

TFA (20 mL) was added to the reaction mixture containing **3.11** or **3.12**. The reaction mixture was stirred for 1 h to remove *t*-butyl protecting group at *C*-terminal. TFA was

removed at reduced pressure and the residue was purified with HPLC using a C_{18} column and water/acetonitile as a solvents using method as described above to yield **3.12** and **3.14.**

3.12. Overall yield (5.0 g, 70%); ^{1}H NMR (400 MHz, CD_3OD, δ ppm): 7.78 (d, *J* = 7.4 Hz, 2H, Fmoc Ar-H), 7.60-7.69 (m, 2H, Fmoc Ar-H), 7.35-7.42 (m, 3H, H-6, Fmoc Ar-H), 7.31 (dt, *J* = 7.4 and 3.3 Hz, 2H, Fmoc Ar-H), 6.23 (dd, *J* = 6.4 and 9.3 Hz, 1H, H-1′), 5.27 (dd, *J* = 5.9 and 53.3 Hz, 1H, H-3′), 4.34-4.51 (m, 5H, H-4′, H-5″, Glu C*H*(α), and Fmoc NHCOOC*H*$_2$), 4.28 (dd, *J* = 5.9 and 9.1 Hz, 1H, H-5′), 4.22 (t, *J* = 6.7 Hz, 1H, Fmoc NHCOOCH$_2$C*H*), 2.10-2.58 (m, 6H, Glu C*H*$_2$C*H*$_2$COO (β and γ methylene), H-2″, and H-2′), 1.87 (s, 3H, C*H*$_3$); HR-MS (ESI-TOF) (m/z): $C_{30}H_{30}FN_3O_9$: calcd, 595.1966; found, 596.2122 $[M + H]^+$, 1191.4197 $[2M + H]^+$.

3.14. Overall yield (5.2 g, 70%); ^{1}H NMR (400 MHz, CD_3OD, δ ppm): 7.78 (d, *J* = 7.4 Hz, 2H, Fmoc Ar-H), 7.35-7.70 (m, 2H, Fmoc Ar-H), 7.44 (s, 1H, H-6), 7.37 (t, *J* = 7.4 Hz, 2H, Fmoc Ar-H), 7.30 (t, *J* = 7.4 Hz, 2H, Fmoc Ar-H), 6.10 (t, *J* = 6.4 Hz, 1H, H-1′), 4.15-4.45 (m, 7H, H-3′, H-5′, H-5″, Glu-α-C*H*, Fmoc NHCOOC*H*$_2$C*H*), 4.05 (dd, *J* = 4.8 and 9.0 Hz, 1H, H-4′), 2.52 (t, *J* = 7.2 Hz, 2H, Glu-C*H*$_2$COO (β-methylene), 2.32-2.48 (m, 2H, Glu-C*H*$_2$CH$_2$COO (γ-methylene), 2.14-2.30 (m, 1H, H-2′), 1.90-2.05 (m, 1H, H-2″), 1.85 (s, 3H, 5-C*H*$_3$); ^{13}C NMR (CD_3OD, 100 MHz, δ ppm): 175.27 (*C*OOH), 173.97 (*C*OOAZT), 162.39 (C-4 *C*=O), 152.25 (C-2 *C*=O), 145.40, 142.73 (Fmoc Ar-C), 137.85 (C-6), 128.95, 128.33, 126.42, 121.08 (Fmoc Ar-C), 112.02 (C-5), 86.70 (C-1′), 83.176 (C-4′), 68.16 (*C*H$_2$OCONH), 64.88 (C-5′),

62.15 (Glu *C*H(α), 54.57 ((C-3′), 37.88 (C-2′), 31.47 (Glu γ-CH_2), 27.99 (Glu β-CH_2), 12.73 (5-*C*H_3); HR-MS (ESI-TOF) (m/z): $C_{30}H_{30}N_6O_9$: calcd, 618.2074; found, 619.5564 $[M + H]^+$.

Fmoc-Ser(O-Myristoyl)OH (3.15). Fmoc-Ser(OH)OH (5 g, 15.3 mmol) and DIPEA (10 mL, 75 mmol) were dissolved in DMF (20 mL). Myristic chloride (10 g, 23 mmol) was added to the solution. The reaction mixture was stirred for overnight. The solvent was removed at reduced pressure and the residue was purified using silica gel column chromatography using dichloromethane (DCM)/methanol (0-5%) as eluents. The compound was eluted at 5% methanol in DCM to yield **3.15** (5.3 g, 63%).

^{1}H NMR (400 MHz, $CDCl_3$, δ ppm): 7.70 (d, *J* = 7.4 Hz, 2H, Fmoc Ar-H), 7.53 (d, *J* = 6.9 Hz, 2H, Fmoc Ar-H), 7.34 (t, *J* = 7.4 Hz, 2H, Fmoc Ar-H), 7.25 (t, *J* = 7.4 Hz, 2H, Fmoc Ar-H), 5.50 (d, *J* = 8.0 Hz, serine C*H*(α)), 4.65-4.71 (m, 1H, serine C*H*″ (β)), 4.45 (dd, *J* = 3.9 and 11.4 Hz, 1H, serine C*H*′ (β)), 4.32-4.39 (m, 2H, Fmoc NHCOOCH_2), 4.17 (t, *J* = 6.9 Hz, 1H, Fmoc NHCOOCH_2C*H*), 2.26 (t, *J* = 7.5 Hz, 2H, CH_2COO), 1.54 (t, *J* = 6.3 Hz, 2H, CH_2CH_2COO), 1.13-1.25 (br m, 20H, Methylene protons), 0.80 (t, *J* = 6.6 Hz, 3H, CH_3); HR-MS (ESI-TOF) (m/z): $C_{32}H_{43}NO_6$: calcd, 537.309; found, 538.2673 $[M + H]^+$, 1075.5442 $[2M + H]^+$.

Myristoyl-Glu(3′-fluoro-2′,3′-dideoxythymidine-5′-yl)-Lys(myristoyl)OH [My-Glu(FLT)-Lys(My)-OH, 3.16]. Fmoc-Lys(Mtt)-Wang resin (300 mg, 0.45 mmol/g) was swelled in DMF for 30 min and Fmoc-Glu(FLT)-OH (320 mg, 0.54 mmol), HBTU (200 mg, 0.54 mmol), and NMM (0.54 mmol) were added to the swelled resin suspension in DMF. The mixture was shaken overnight at room temperature. The resin

was filtered and washed two times with DMF (10 mL). Fmoc deprotection was carried out using piperidine in DMF (20%,10 mL). The resin was washed with DMF (3 × 10 mL). To the resin was added TFA:DCM mixture (5%, 10 mL) to remove methyltrityl protecting group (Mtt) at lysine side chain. The mixture was shaken for 1 h at room temperature. The resin was washed with DCM (3 × 10 mL) and DMF (10 mL) and swelled in DMF (10 mL). Myristic anhydride (100 mg, 1.08 mmol) and DIPEA (2 mL, 15 mmol) were added to the swelled resin. The mixture was shaken for 2 h at room temperature. The resin was washed with DMF (2 × 10 mL). A mixture of TFA/anisole/water (95:2.5:2.5, 10 mL) was added to the resin and the mixture was shaken for 1 h. After filtration, the solution was concentrated and dried under reduced pressure. The crude peptide conjugates were purified with reversed phase HPLC using a C_{18} column and water/acetonitile as solvents as described above and were lyophilized to yield 3.16 (10 mg, 8.0%).

HR-MS (ESI-TOF) (m/z): $C_{49}H_{84}FN_5O_{10}$: calcd, 921.6202; found, 922.9989 $[M + H]^+$, 1845.9558 $[2M + H]^+$.

Acetyl-Glu(3′-fluoro-2′,3′-dideoxythymidine-5′-yl)-β-Ala-Lys(myristoyl)OH [Ac-Glu(FLT)-βAla-Lys(My)-OH, 3.17] and Acetyl-Glu(3′-azido-2′,3′-dideoxythymidine-5′-yl)-βAla-Lys(myristoyl)OH [Ac-Glu(AZT)-βAla-Lys(My)-OH, 3.18]. The peptide was assembled on Fmoc-Lys(Mtt)-Wang resin (600 mg, 0.45 mmol/g) by Fmoc solid-phase peptide synthesis strategy on a PS3 automated peptide synthesizer at room temperature using Fmoc protected amino acids [Fmoc-β-Ala-OH (C + 1) and Fmoc-Glu(nucleoside)-OH (C + 2) (3.12 or 3.14, 1.08 mmol)]. HBTU

(1.08 mmol) and NMM (1.08 mmol) in DMF were used as coupling and activating reagents, respectively. Fmoc deprotection at each step was carried out using piperidine in DMF (20%). NH_2-Glu(FLT)-βAla-Lys(Mtt)-Wang resin or NH_2-Glu(AZT)-βAla-K(Mtt)-Wang resin was transferred to the reaction vessel and swelled in DMF (2 mL) for 30 min. Acetic anhydride (2 mL) and DIPEA (2 mL, 15 mmol) were added to the mixture. The reaction was shaken at room temperature for 30 min to cap the *N*-terminal with acetyl group. *N*-Acetylated resin was washed with DMF (2 × 10 mL). To the resin was added TFA:DCM (5%, 10 mL). The mixture was shaken for 1 h at room temperature. The resin was washed with DCM (3 × 10 mL) and DMF (10 mL) and swelled in DMF (10 mL). Free amino group at lysine side chain was further myristoylated by adding myristic anhydride (100 mg, 1.08 mmol) and DIPEA (2 mL, 15 mmol) to the swelled resin. The mixture was shaken for 2 h at room temperature. The resin was washed with DMF (3 × 10 mL). A mixture of TFA/anisole/water (95:2.5:2.5 v/v/v, 10 mL) was added to the resin and the mixture was shaken for 1 h. After filtration, the solution was concentrated and dried under reduced pressure. The crude peptide conjugates were purified with reversed phase HPLC using a C_{18} column and water/acetonitile as solvents as described above and were lyophilized to yield 3.17 and 3.18.

3.17. Overall yield (20 mg, 8%); ^{1}H NMR (400 MHz, CD_3OD, δ ppm): 7.48 (s, 1H, FLT H-6), 6.28 (dd, J = 5.6 and 8.8 Hz, 1H, FLT H-1′), 5.29 (dd, J = 53.5 and 4.4 Hz, 1H, FLT H-3′), 4.20-4.70 (m, 6H, FLT H-4′ and FLT H-5″, Ser COC*H*NH (CH(α), Ser CH_2O (CH(β), Glu COC*H*NH (CH(α)), 4.07 (dd, J = 3.9 and 17.8 Hz, 1H,

FLT H-5′), 3.72-3.92 (m, 2H, Gly COC*H*$_2$NH (CH(α)), 3.38-3.58 (m, 2H, β-Ala C*H*$_2$NH), 2.24-2.64 (m, 8H, FLT H-2′, FLT H-2″, β-Ala C*H*$_2$COO, Glu C*H*$_2$C*H*$_2$COO), 2.16 (t, J = 7.2 Hz, 3H, myristate C*H*$_2$COO), 1.94-2.08 (m, 3H, Ac C*H*$_3$), 1.88 (s, 3H, FLT 5-C*H*$_3$), 1.52-1.66 (m, 2H, myristate C*H*$_2$CH$_2$COO), 1.22-1.38 (br m, 20H, methylene protons), 0.90 (t, J = 6.3 Hz, 3H, myristate C*H*$_3$); HR-MS (ESI-TOF) (m/z): $C_{40}H_{65}FN_6O_{11}$: calcd, 824.4695; found, 825.6640 $[M + H]^+$, 1651.2282 $[2M + H]^+$.

3.18. Overall yield (20 mg, 8%); ^{1}H NMR (400 MHz, CD_3OD, δ ppm): 7.48 (s, 1H, H-6 AZT), 6.14 (t, J = 6.6 Hz, 1H, AZT H-1′), 4.20-4.70 (m, 6H, AZT H-5′, AZT H-5″, AZT H-3′, Ser COC*H*NH (CH(α), Ser C*H*$_2$O (CH(β), Glu COC*H*NH) (CH(α), 4.07 (dd, J = 4.9 and 8.9 Hz, 1H, AZT H-4′), 3.84-4.05 (m, 2H, Gly COC*H*$_2$NH (CH(α)), 3.44 (dd, J = 6.6 and 12.5 Hz, 2H, β-Ala C*H*$_2$NH), 2.10-2.66 (m, 10H, FLT H-2′, FLT H-2″, β-Ala C*H*$_2$COO, Glu C*H*$_2$C*H*$_2$COO, myristate C*H*$_2$COO), 1.92-2.09 (m, 3H, Ac C*H*$_3$), 1.89 (s, 3H, 5-C*H*$_3$-AZT), 1.52-1.72 (m, 2H, myristate-C*H*$_2$CH$_2$COO), 1.24-1.50 (br m, 20H, methylene protons), 0.90 (t, J = 6.5 Hz, 3H, myristate C*H*$_3$); HR-MS (ESI-TOF) (m/z): $C_{40}H_{65}N_9O_{11}$: calcd, 847.4804; found, 848.9452 $[M + H]^+$.

Acetyl-Ser(myristoyl)-β-Ala-Glu(3′-fluoro-2′,3′-dideoxythymidine-5′-yl)-Gly-OH [Ac-Ser(My)-βAla-Glu(FLT)Gly-OH, 3.19] and Acetyl-Ser(myristoyl)-β-Ala-Glu(3′-azido-2′,3′-dideoxythymidine-5′-yl)-Gly-OH [Ac-Ser(My)-βAla-Glu(AZT)Gly-OH, 3.20]. The peptide was assembled on Fmoc-Gly-Wang resin (600 mg, 0.45 mmol/g) by Fmoc solid -phase peptide synthesis strategy using Fmoc

protected amino acids [Fmoc-Glu(nucleoside)-OH (C + 1) (3.12 or 3.14), Fmoc-β-Ala-OH (C + 2) and Fmoc-Ser(Myristoyl)-OH (C + 3) (3.15), each 1.08 mmol]. HBTU (1.08 mmol) and NMM (1.08 mmol) in DMF were used as coupling and activating reagents, respectively. Fmoc deprotection at each step was carried out using piperidine in DMF (20%). NH_2-Ser(My)-βAla-Glu(FLT)Gly-Wang resin or NH_2-Ser(My)-βAla-Glu(AZT)-Gly-Wang resin was transferred to the reaction vessel and swelled in DMF (2 mL) for 30 min. Acetic anhydride (2 mL) and DIPEA (2 mL, 15 mmol) were added to the mixture. The reaction was shaken at room temperature for 30 min to cap *N*-terminal with acetyl group. *N*-Acetylated resin was washed DMF (2 × 10 mL). To the resin was added the peptide was cleaved from the resin by a mixture of TFA/anisole/water (95:2.5:2.5 v/v/v, 10 mL) and the mixture was shaken for 1 h. After filtration, the solution was concentrated and dried under reduced pressure. The crude peptide conjugates were purified with reversed phase HPLC using a C_{18} column and water/acetonitile as solvents as described above and were lyophilized to yield 3.19 and 3.20.

3.19. Overall yield (20 mg, 8%); HR-MS (ESI-TOF) (m/z): $C_{39}H_{61}FN_6O_{13}$: calcd, 841.4281; found, 842.0071 $[M + H]^+$, 1683.8930 $[2M + H]^+$.

3.20. Overall yield (20 mg, 8 %); HR-MS (ESI-TOF) (m/z): $C_{39}H_{61}N_9O_{13}$: calcd, 863.4389; found, 864.9022 $[M + H]^+$, 1729.8398 $[2M + H]^+$.

3.3.2.3. Synthesis of Dinucleoside- and Trinucleoside Glutamic Acid Derivatives With or Without Myristoyl Moiety Glutamate-nucleoside conjugates containing more than one nucleoside with or without myristoyl group were synthesized by using solution phase synthesis.

Fmoc-Glu(FLT)-3TC-DMTr (3.21) Compounds **3.12** (500 mg, 0.84 mmol), **2.12** (535 mg, 1 mmol), and HBTU (650 mg 1.7 mmol) were dissolved in DMF (10 mL). DIPEA (5 mL, 37 mmol) was added to the solution and the reaction mixture was stirred overnight at room temperature. The solvent was removed and the residue was dried under reduced pressure. The residue was purified with reversed phase HPLC using a C_{18} column and water/acetonitile as solvents as described above and was lyophilized to yield **3.21** (820 mg, 75%).

^{1}H NMR (400 MHz, $CDCl_3$, δ ppm): 8.99 (s, 1H, FLT N*H*), 7.74 (d, J = 7.5 Hz, 1H, Fmoc Ar-H), 7.55 (d, J = 7.6 Hz, 1H, 3TC H-6), 7.38 (t, J = 7.5 Hz, Fmoc Ar-H), 7.06-7.33 (m, 13H, DMTr Ar-H, Fmoc Ar-H, and FLT H-6), 6.76-6.87 (m, 4H, DMTr Ar-H protons), 6.34 (m, 1H, 3TC H-1′), 6.14-6.22 (m, 1H, FLT H-1′), 5.64 (d, J = 7.6 Hz, 1H, 3TC H-5), 5.05-5.27 (m, 2H, FLT H-3′ and 3TC H-4′), 4.24-4.45 (m, 8H, 3TC H-5′, 3TC H-5″, Fmoc NHCOOCH_2C*H*, FLT H-4′, FLT H-5′, FLT H-5″), 4.17 (t, J = 6.7 Hz, 1H, Glu HN-C*H*-COO CH(α)), 3.75 and 3.78 (two s, 6H, DMTr CH_3O), 3.46 (dd, J = 11.8 and 5.3 Hz, 1H, 3TC H-2″), 2.97 (dd, J = 11.8 and 5.3 Hz, 1H, 3TC H-2′), 1.97-2.67 (m, 6H, FLT H-2′, FLT H-2″, and Glu CH_2CH_2COO), 1.86 (s, 3H, 5-CH_3); ^{13}C NMR ($CDCl_3$, 100 MHz, δ ppm): 172.00 (FLT *C*OO), 171.25 (3TC *C*OO), 165.06 (3TC C-4), 163.50 (FLT C-4 *C*=O), 158.69 (DMTr Ar-*C*-OCH_3), 156.00 (3TC

DMTr Ar-C), 111.41 (FLT C-5), 95.17 (3TC C-5), 93.20 (J = 178.3 Hz, FLT C-3′), 87.64 (3TC C-1′), 86.01 (FLT C-1′), 83.16 (3TC C-4′), 82.16 (J = 26.9 Hz, FLT C-4′), 81.69 (DMTr Ph_3C-NH), 70.34 (Fmoc CH_2-OCONH), 67.15 (FLT C-5′), 65.76 (3TC C-5′), 55.28 (DMTr OCH_3), 53.40 (CH(α)), 47.04 (Fmoc CH-CH_2-OCONH), 38.16 (FLT C-2′), 37.36 (3TC C-2′), 29.86, (Glu γ-CH_2), 27.16 (Glu β-CH_2), 12.64 (FLT 5-CH_3); HR-MS (ESI-TOF) (m/z): $C_{59}H_{57}FN_6O_{13}S$: calcd, 1108.3688; found, 1109.4804 $[M + H]^+$, 1131.4395$[M + Na]^+$, 1147.4739 $[M + K]^+$, 2218.5704 $[2M + H]^+$.

NH_2-Glu(FLT)-3TC-DMTr (3.22). Compound **3.21** (800 mg, 0.72 mmol) was dissolved in THF (10 mL). Piperidine (7.18 µl, 0.072 mmol) and 1-octanethiol (7.3 mmol, 10 mM solution in THF, 0.73 mL) were added to the reaction mixture. The mixture was stirred for 1 h at room temperature. The solvent was removed and the residue was dried under reduced pressure. The residue was purified with reversed phase HPLC using a C_{18} column and water/acetonitile as solvents as described above and lyophilized to yield **3.22** (300 mg, 50%).

^{1}H NMR (400 MHz, $CDCl_3$, δ ppm): 7.44 (d, J = 7.8 Hz, 1H, 3TC H-6), 7.25-7.33 (m, 4H, DMTr Ar-H), 7.18-7.21 (m, 2H, DMTr Ar-H and FLT H-6), 7.12 (d, J = 8.8 Hz, 4H, DMTr Ar-H), 6.84 (d, J = 8.8 Hz, 4H, DMTr Ar-H), 6.20 (dd, J = 5.7 and 8.6 Hz, 1H, FLT H-1′), 6.13 (t, J = 5.2 Hz, 1H, 3TC H-1′), 5.33 (dd, J = 4.0 and 6.0 Hz, 1H, 3TC H-4′), 5.10-5.31 (m, 2H, FLT H-3′ and 3TC H-5), 4.28-4.45 (m, 4H, 3TC H-5′, 3TC H-5″, FLT H-5′, and FLT H-5″), 4.18-4.26 (m, 1H, FLT H-4′), 4.07 (t, J = 6.6 Hz, 1H, HN-CH(CH_2)-COO (CH(α)), 3.77 (s, 6H, DMTr-CH_3O), 3.41 (dd, J = 11.9 and 5.2 Hz, 1H, 3TC H-2″), 3.05 (dd, J = 11.9 and 5.2 Hz, 1H, 3TC H-2′), 2.10-2.66

(m, 6H, FLT H-2′, FLT H-2″, and Glu CH_2CH_2COO), 1.85 (s, 3H, 5-CH_3); ^{13}C NMR ($CDCl_3$, 100 MHz, δ ppm): 172.56 (FLT *C*OO), 169.13 (3TC *C*OO), 165.55 (3TC C-4, FLT C-4 *C*=O), 159.68 (DMTr Ar-*C*-OCH_3), 159.16 (3TC C-2 *C*=O), 151.51 (FLT C-2 *C*=O), 145.56 (3TC C-6), 136.96 (FLT C-6), 130.77, 130.72, 129.30, 129.09 128.86, 128.41, 127.35, 114.33, 113.70 (DMTr Ar-C), 111.90 (FLT C-5), 96.74 (3TC C-5), 94.11 (J = 177.9 Hz, FLT C-3′), 88.58 (3TC C-1′), 86.72 (FLT C-1′), 82.92 (J = 26.6 Hz, FLT C-4′), 82.78 (3TC C-4′), 71.72 (DMTr Ph_3C-NH), 67.15 (FLT C-5′), 64.53 (3TC C-5′), 55.66 (DMTr OCH_3), 52.36 (*C*H(α)), 37.85 (J = 21.1 Hz, FLT C-2′), 37.27 (3TC C-2′), 29.70, (Glu γ-CH_2), 25.80 (Glu β-CH_2), 12.73 (FLT 5-CH_3); HR-MS (ESI-TOF) (m/z): $C_{44}H_{47}FN_6O_{11}S$: calcd, 886.3008; found, 887.4078 $[M + H]^+$, 1817.4315 $[2M + H]^+$.

$C_{13}H_{27}$-CONH-Glu(FLT)-3TC (3.24). Compound **3.22** (100 mg, 0.12 mmol) and myristic anhydride (100 mg, 0.24 mmol) were dissolved in DMF (10 mL). DIPEA (5 mL, 37 mmol) was added to the solution. The mixture was stirred for 2 h at room temperature. The solvent was removed under reduced pressure to yield $C_{13}H_{27}$-CONH-Glu(FLT)-3TC-DMTr **(3.23)**.

3.23. HR-MS (ESI-TOF) (m/z): $C_{58}H_{73}FN_6O_{12}S$: calcd, 1096.4991; found, 1097.2874 $[M + H]^+$, 2193.8167 $[2M + H]^+$.

Compound **3.23** was dissolved in acetic acid (80% in water, 10 mL) and was heated at 80 °C for 30 min to remove DMTr protection. Acetic acid was removed under reduced pressure and the residue was purified with reversed phase HPLC using a C_{18} column

and water/acetonitrile as solvents as described above and was lyophilized to yield **3.24** (40 mg, 45%).

3.24. ^{1}H NMR (400 MHz, $CDCl_3$, δ ppm): 8.13 (d, J = 7.8 Hz, 1H, 3TC H-6), 7.45 (s, 1H, FLT H-6), 6.28 (dd, J = 3.6 and 5.4 Hz, 1H, FLT H-1′), 6.22 (dd, J = 5.7 and 8.8 Hz, 1H, 3TC H-1′), 6.17 (d, J = 7.8 Hz, 1H, 3TC H-5), 5.43 (dd, J = 3.2 and 4.9 Hz, 1H, 3TC H-4′), 5.25 (dd, J = 5.2 and 53.7 Hz, 1H, FLT H-3′), 4.59 (dd, J = 4.9 and 12.4 Hz, 1H, 3TC H-5″), 4.31-4.55 (m, 4H, 3TC H-5′, FLT H-5′, FLT H-5″, FLT H-4′-), 4.27 (dd, J = 3.0 and 10.8 Hz, 1H, Glu HN-C*H*-COO CH(α)), 3.54-3.65 (m, 2H, 3TC H-2′ and H-2″), 2.11-2.65 (m, 8H, FLT H-2′, FLT H-2″, myristate CH_2COO, and Glu CH_2CH_2COO), 1.86 (s, 3H, 5-CH_3), 1.58 (t, J = 6.8 Hz, 2H, CH_2CH$_2$COOH), 1.20-1.35 (br m, 20H, methylene protons), 0.85 (t, J = 6.6 Hz, 3H, CH_3); ^{13}C NMR (CD_3OD, 100 MHz, δ ppm): 175.92, 172.97 (FLT *C*OO , 3TC *C*OO), 172.13 (*C*ONH), 165.61 (3TC C-4), 160.80 (FLT C-4 *C*=O), 151.57 (3TC C-2 *C*=O), 147.96 (FLT C-2 *C*=O), 145.21 (3TC C-6), 136.97 (FLT C-6), 111.34 (FLT C-5), 97.92 (3TC C-5), 93.27 (J = 179.4 Hz, FLT C-3′), 87.99 (3TC C-1′), 86.32 (FLT C-1′), 82.19 (J = 26.6 Hz, FLT C-4′), 81.68 (3TC C-4′), 64.96 (FLT C-5′), 64.14 (3TC C-5′), 54.23 (*C*H(α)), 37.59 (J = 20.8 Hz, FLT C-2′), 36.96 (3TC C-2′), 36.40 (*C*H$_2$COO), 31.93, 26.34, 30.34, 30.21, 30.09, 29.91, 29.76, 29.69, 26.80, 23.16 (methylene carbons, Glu γ-CH_2, Glu β-*C*H$_2$), 13.88 (myristate *C*H$_3$), 12.10 (FLT 5-*C*H$_3$); HR-MS (ESI-TOF) (m/z): $C_{37}H_{55}FN_6O_{10}S$: calcd, 794.3684; found, 795.1608 $[M + H]^+$, 1590.3674 $[2M + H]^+$.

CH_3-CONH-Glu(FLT)-3TC (3.26). Compound **3.22** (100 mg, 0.12 mmol) and acetic anhydride (2 mL, 20 mmol) were dissolved in DMF (10 mL). DIPEA (5 mL, 37 mmol) was added to the solution. The reaction mixture was stirred for 2 h at room temperature. The solvent was removed under reduced pressure to yield CH_3-CONH-Glu(FLT)-3TC-DMTr **(3.25).**

3.25. HR-MS (ESI-TOF) (m/z): $C_{46}H_{49}FN_6O_{12}S$: calcd, 928.3113; found, 929.1423 [M + H]$^+$.

Compound **3.25** was dissolved in acetic acid (80% in water, 10 mL) and was heated at 80 °C for 30 min to remove DMTr protection. Acetic acid was removed under reduced pressure and the residue was purified with reversed phase HPLC using a C_{18} column and water/acetonitile as solvents as described above and was lyophilized to yield **3.26** (30 mg, 40%).

3.26. ^{1}H NMR (400 MHz, CD_3OD, δ ppm): 8.13 (d, *J* = 7.8 Hz, 1H, 3TC H-6), 7.46 (s, 1H, FLT H-6), 6.28 (dd, *J* = 3.7 and 5.4 Hz, 1H, FLT H-1′), 6.23 (dd, *J* = 5.7 and 8.8 Hz, 1H, 3TC H-1′), 6.16 (d, *J* = 7.8 Hz, 1H, 3TC H-5), 5.44 (dd, *J* = 3.1 and 4.9 Hz, 1H, 3TC H-4′), 5.25 (dd, *J* = 5.2 and 53.7 Hz, 1H, FLT H-3′), 4.60 (dd, *J* = 4.9 and 12.4 Hz, 1H, 3TC H-5″), 4.32-4.55 (m, 4H, 3TC H-5′, FLT H-5′, FLT H-5″, and FLT H-4′), 4.26 (dd, *J* = 3.3 and 11.4 Hz, 1H, Glu HN-C*H*-COO CH(α)), 3.71 (dd, *J* = 5.7 and 12.6 Hz, 1H, 3TC H-2″), 3.58 (dd, *J* = 5.7 and 12.6 Hz, 1H, 3TC H-2′), 2.11-2.63 (m, 6H, FLT H-2′, FLT H-2″, and Glu C*H*$_2$C*H*$_2$COO), 1.96 (s, 3H, acetyl *CH*$_3$), 1.86 (s, 3H, 5-C*H*$_3$); ^{13}C NMR (CD_3OD, 100 MHz, δ ppm): 173.71, 173.65 (FLT *C*OO, 3TC *C*OO), 172.86 (*C*ONH), 161.46 (3TC C-4), 161.21 (3TC C-2 *C*=O), 152.33 (FLT C-2 *C*=O), 146.00 (3TC C-6), 137.69 (FLT C-6), 112.06 (FLT C-5),

95.23 (J = 176.4 Hz, FLT C-3′), 95.14 (3TC C-5), 88.73 (3TC C-1′), 87.13 (FLT C-1′), 85.55 (3TC C-4′), 84.03 (J = 26.0 Hz, FLT C-4′), 65.69 (FLT C-5′), 64.99 (3TC C-5′), 53.03 (*C*H(α)), 38.64 (FLT C-2′), 38.42 (3TC C-2′), 31.04 (Glu γ-*C*H_2), 27.55 (Glu β-*C*H_2), 22.48 (acetyl *C*H_3), 12.78 (FLT 5-*C*H_3); HR-MS (ESI-TOF) (m/z): $C_{25}H_{31}FN_6O_{10}S$: calcd, 626.1806; found, 627.6073 $[M + H]^+$, 1254.9359 $[2M + H]^+$.

Fmoc-Glu(FLT)-AZT (3.27). Compound **3.12** (500 mg, 0.84 mmol), AZT (269 mg, 1 mmol), and HBTU (650 mg 1.7 mmol) were dissolved in DMF (10 mL). DIPEA (5 mL, 37 mmol) was added to the solution and the reaction mixture was stirred over night. The solvent was removed and the residue was dried under reduced pressure. The residue was purified with reversed phase HPLC using a C_{18} column and water/acetonitile as solvents as described above and was lyophilized to yield **3.27** (620 mg, 85%).

^{1}H NMR (400 MHz, $CDCl_3$, δ ppm): 9.24 (s, 1H, FLT N*H*), 9.09 (s, 1H, AZT N*H*), 7.75 (d, J = 7.2 Hz, 1H, Fmoc Ar-H), 7.57 (d, J = 3.6 Hz, 1H, Fmoc Ar-H), 7.38 (t, J = 7.2 Hz, Fmoc Ar-H), 7.29 (t, J = 7.2 Hz, 2H, Fmoc Ar-H), 7.15 (s, 1H, FLT H-6), 7.07 (s, 1H, AZT H-6), 6.14 (t, J = 8.1 Hz, 1H, FLT H-1′), 5.80 (t, J = 6.9 Hz, 1H, AZT H-1′), 5.17 (dd, J = 2.0 and 55.6 Hz, 1H, FLT H-3′), 4.23-4.60 (m, 6H, AZT H-5′, AZT H-5″, AZT H-3′, FLT H-4′ , FLT H-5′, and FLT H-5″), 4.19 (t, J = 6.7 Hz, 1H, Glu HN-C*H*-COO CH(α)), 3.95-4.05 (m, 1H, AZT H-4′), 2.16-2.69 (m, 8H, AZT H-2′, AZT H-2″, FLT H-2′, FLT H-2″, and Glu CH_2CH_2COO), 1.88 (br s, 6H, FLT 5-CH_3 and AZT 5-CH_3); ^{13}C NMR ($CDCl_3$, 100 MHz, δ ppm): 172.3, 171.4 (FLT *C*OO, AZT *C*OO), 163.85, 163.72 (FLT C-4 *C*=O, AZT C-4 *C*=O), 156.23 (Fmoc OCONH),

150.10, 149.98 (AZT C-2 *C*=O and FLT C-2 *C*=O), 143.74, 143.55, 141.31(Fmoc Ar-C), 137.23, 135.88 (AZT C-6, FLT C-6), 127.88, 127.10, 125.05, 125.00, 120.08, (Fmoc Ar-C), 111.37, 111.28 (AZT C-5, FLT C-5), 93.23 (J = 177.8 Hz, FLT C-3′), 87.82 (FLT C-1′), 86.53 (AZT C-1′), 82.21 (J = 26.3 Hz, FLT C-4′), 81.72 (AZT C-4′), 68.00 (Fmoc *C*H_2-OCONH), 63.82 (FLT C-5′), 60.29 (AZT C-5′), 53.48, 53.31 (AZT C-3′, *C*H(α)), 47.04 (Fmoc *C*H-CH_2-OCONH), 37.58 (J = 20.1 Hz, FLT C-2′), 36.94 (AZT C-2′), 29.72 (Glu γ-*C*H_2), 25.60 (Glu β-*C*H_2), 12.57, 12.43 (AZT 5-*C*H_3, FLT 5-*C*H_3); HR-MS (ESI-TOF) (m/z): $C_{40}H_{41}FN_8O_{12}$: calcd, 844.2828; found, 845.0241 $[M + H]^+$.

NH_2-Glu(FLT)-AZT (3.28). Compound **3.27** (610 mg, 0.72 mmol) was dissolved in THF (10 mL). Piperidine (7.18 µl, 0.072 mmol) and 1-octanethiol (7.3 mmol, 10 mM solution in THF, 0.73 mL) were added to the reaction mixture. The mixture was stirred at room temperature for 1 h. The solvent was removed and the residue was dried under reduced pressure. The residue purified with reversed phase HPLC using a C_{18} column and water/acetonitile as solvents as described above and lyophilized to yield **3.28** (225 mg, 50%).

^{1}H NMR (400 MHz, CD_3OD, δ ppm): 7.44 (s, 1H, FLT H-6), 7.38 (s, 1H, AZT H-6), 6.22 (dd, J = 8.1 Hz, 1H, FLT H-1′), 6.02 (t, J = 6.9 Hz, 1H, AZT H-1′), 5.23 (dd, J = 2.0 and 55.6 Hz, 1H, FLT H-3′), 4.20-4.55 (m, 6H, AZT H-5′, AZT H-5″, AZT H-3′, FLT H-4′, FLT H-5′, and FLT H-5″), 4.15 (t, J = 6.7 Hz, 1H, Glu HN-C*H*-COO CH(α)), 3.98-4.04 (m, 1H, AZT H-4′), 2.16-2.69 (m, 8H, AZT H-2′, AZT H-2″, FLT H-2′, FLT H-2″, CH_2CH_2COO), 1.87 (br s, 6H, FLT 5-CH_3, AZT 5-CH_3); ^{13}C NMR

(CD_3OD, 100 MHz, δ ppm): 173.29, 170.17 (FLT *C*OO, AZT *C*OO), 166.40, 163.72 (FLT C-4 *C*=O, AZT C-4 *C*=O), 152.33 , 152.19 (AZT C-2 *C*=O, FLT C-2 *C*=O), 139.13, 137.89 (AZT C-6, FLT C-6), 114.03, 112.08 (AZT C-5, FLT C-5), 95.07 (J = 176.7 Hz, FLT C-3′), 88.12 (FLT C-1′), 87.34 (AZT C-1′), 83.86 (J = 27.3 Hz, FLT C-4′), 82.72 (AZT C-4′), 66.90 (FLT C-5′), 61.99 (AZT C-5′), 53.23, 52.28 (AZT C-3′, *C*H(α)), 38.26 (J = 21.2 Hz, FLT C-2′), 37.10 (AZT C-2′), 30.14 (Glu γ-*C*H_2), 26.63 (Glu β-*C*H_2), 12.73, 12.53 (AZT 5-*C*H_3, FLT 5-*C*H_3); HR-MS (ESI-TOF) (m/z): $C_{25}H_{31}FN_8O_{10}$: calcd, 622.2147; found, 622.9532 $[M + H]^+$, 1244.9406 $[2M + H]^+$.

$C_{13}H_{27}$-CONH-Glu(FLT)-AZT (3.29). Compound **3.28** (75 mg, 0.12 mmol) and myristic anhydride (100 mg, 0.24 mmol) were dissolved in DMF (10 mL). DIPEA (5 mL, 37 mmol) was added to the solution. The mixture was stirred for 2 h at room temperature. The solvent was removed under reduced pressure and the residue was purified with reversed phase HPLC using a C_{18} column and water/acetonitile as solvents as described above and was lyophilized to yield **3.29** (40 mg, 40%).

^{1}H NMR (400 MHz, CD_3OD, δ ppm): 7.45, 7.44 (two s, 2H, AZT H-6, FLT H-6), 6.23 (dd, J = 8.9 and 5.6 Hz, 1H, FLT H-1′), 6.09 (t, J = 6.7 Hz, 1H, AZT H-1′), 5.24 (dd, J = 5.0 and 53.6 Hz, 1H, FLT H-3′), 4.32-4.48 (m, 6H, AZT H-5′, AZT H-5″, AZT H-3′, FLT H-4′, FLT H-5′, and FLT H-5″), 4.22 (dd, J =3.8 and 11.4 Hz, 1H, Glu HN-C*H*-COO CH(α)), 4.06 (dd, J = 4.8 and 8.6 Hz, 1H, AZT H-4′), 2.15-2.60 (m, 10H, AZT H-2′, AZT H-2″, FLT H-2′, FLT H-2″, myristate CH_2COO, Glu CH_2CH_2COO), 1.87 (s, 6H, FLT 5-CH_3, AZT 5-CH_3), 1.58 (t, J = 6.6 Hz, 2H, CH_2CH_2COO), 1.23-1.33 (br m, 20H, methylene protons), 0.87 (t, J = 6.7 Hz, 3H, 5-

CH_3); ^{13}C NMR ($CDCl_3$, 100 MHz, δ ppm): 173.78, 172.37, 171.56 (FLT *C*OO, AZT *C*OO, *C*ONH), 164.01 (FLT C-4 *C*=O and AZT C-4 *C*=O), 150.27 (AZT C-2 *C*=O, FLT C-2 *C*=O), 137.14, 135.77 (AZT C-6, FLT C-6), 111.37 (AZT C-5, FLT C-5), 93.27 (J = 179.4 Hz, FLT C-3′), 87.56 (FLT C-1′), 86.32 (AZT C-1′), 82.19 (J = 26.6 Hz, FLT C-4′), 81.68 (AZT C-4′), 63.83 (FLT C-5′), 60.33 (AZT C-5′), 51.48, 51.35 (AZT C-3′, *C*H(α)), 37.59 (J = 20.8 Hz, FLT C-2′), 36.96 (AZT C-2′), 36.39 (*C*H_2COO), 34.14, (Glu γ-*C*H_2), 31.93 (Glu β-*C*H_2), 30.04, 29.90, 29.83, 29.66, 29.60, 29.51, 29.46, 29.36, 29.31, 29.16, 27.27 25.59, 24.97, 22.70 (methylene carbons), 14.15 (My-*C*H_3) 12.73, 12.53 (5-*C*H_3-AZT, 5-*C*H_3-FLT); HR-MS (ESI-TOF) (m/z): $C_{39}H_{57}FN_8O_{11}$: calcd, 832.4131; found, 832.8583 $[M + H]^+$, 1665.8057 $[2M + H]^+$.

CH_3-CONH-Glu(FLT)-AZT (3.30). Compound **3.28** (75 mg, 0.12 mmol) was dissolved in DMF (10 mL). DIPEA (5 mL, 37 mmol) and acetic anhydride (2 mL, 20 mmol) were added to the solution. The reaction mixture was stirred for 2 h at room temperature. The solvent was removed under reduced pressure and the residue was purified with reversed phase HPLC using a C_{18} column and water/acetonitile as solvents as described above and was lyophilized to yield **3.30** (30 mg, 35%).

^1H NMR (400 MHz, CD_3CN, δ ppm): 7.45, 7.43 (two s, 2H, AZT H-6, FLT H-6), 6.23 (dd, J = 8.8 and 5.6 Hz, 1H, FLT H-1′), 6.09 (t, J = 6.6 Hz, 1H, AZT H-1′), 5.24 (dd, J = 5.0 and 53.6 Hz, 1H, FLT H-3′), 4.33-4.47 (m, 6H, AZT H-5′, AZT H-5″, AZT H-3′, FLT H-4′, FLT H-5′, FLT H-5″), 4.22 (dd, J =3.2 and 11.0 Hz, 1H, Glu HN-C*H*-COO CH(α)), 4.07 (dd, J = 4.6 and 8.8 Hz, 1H, AZT H-4′), 2.11-2.61 (m, 8H, AZT H-2′, AZT H-2″, FLT H-2′, FLT H-2″, and Glu CH_2CH_2COO), 1.96 (s, 3H,

acetyl CH_3), 1.87 (s, 6H, FLT 5-CH_3, AZT 5-CH_3); ^{13}C NMR (CD_3OD, 100 MHz, δ ppm): 172.17, 172.10, 171.40 (FLT *C*OO, AZT *C*OO, *C*ONH), 164.93, 164.82 (FLT C-4 *C*=O, AZT C-4 *C*=O), 150.93, 150.73 (AZT C-2 *C*=O, FLT C-2 *C*=O), 136.57, 136.07 (AZT C-6, FLT C-6), 110.55 (AZT C-5, FLT C-5), 93.69 (J = 176.6 Hz, FLT C-3′), 85.80 (FLT C-1′), 85.51 (AZT C-1′), 82.42 (J = 26.0 Hz, FLT C-4′), 81.55 (AZT C-4′), 64.31 (FLT C-5′), 60.94 (AZT C-5′), 51.75 (AZT C-3′, *C*H(α)), 36.96 (J = 20.6 Hz, FLT C-2′), 36.14 (AZT C-2′), 29.39 (Glu γ-CH_2), 26.04 (Glu β-CH_2), 20.88 (acetyl CH_3), 12.73, 12.53 (AZT 5-CH_3, FLT 5-CH_3); HR-MS (ESI-TOF) (m/z): $C_{37}H_{55}FN_6O_{10}S$: calcd, 794.3684; found, 795.1608 $[M + H]^+$, 1590.3674 $[2M + H]^+$.

Fmoc-Glu(AZT)-3TC-DMTr (3.31). Compound **3.14** (520 mg, 0.84 mmol), **2.12** (535 mg, 1 mmol), and HBTU (650 mg 1.7 mmol) were dissolved DMF (10 mL). DIPEA (5 mL, 37 mmol) was added to the solution and to the reaction mixture was stirred overnight at room temperature. The solvent was removed and the residue was dried reduced pressure. The residue purified with reversed phase HPLC using a C_{18} column and water/acetonitile as solvents as described above and was lyophilized to yield **3.31** (840 mg, 87%).

HR-MS (ESI-TOF) (m/z): $C_{59}H_{57}FN_6O_{13}S$: calcd, $C_{59}H_{57}N_9O_{13}S$; found, 1131.3797 $[M + H]^+$, 1132.3485 $[M + H]^+$, 2265.1887 $[2M + H]^+$.

NH_2-Glu(AZT)-3TC-DMTr (3.32). Compound **3.31** (815 mg, 0.72 mmol) was dissolved in THF (10 mL). Piperidine (7.18 µl, 0.072 mmol) and 1 and 1-octanethiol (7.3 mmol, 10 mM solution in THF, 0.73 mL) were added to the reaction mixture. The

mixture was stirred for 1 h at room temperature. The solvent was removed at reduced pressure and the residue was purified with HPLC using a C_{18} column and water/acetonitile as a solvent as described above to yield **3.32** (325 mg, 50%).

^{1}H NMR (400 MHz, $CDCl_3$, δ ppm): 8.04 (d, J = 7.8 Hz, 1H, 3TC H-6), 7.02-7.47 (m, 10H, DMTr Ar-H and AZT H-6), 6.82 (d, J = 8.8 Hz, 4H, DMTr Ar-H), 6.18-6.35 (m, 1H, 3TC H-1′), 6.15 (d, J = 7.8 Hz, 1H, 3TC H-5), 6.07 (t, J = 6.5 Hz, 1H, AZT H-1′), 5.30-5.55 (m, 1H, 3TC H-4′), 4.66 (dd, J = 6.4 and 12.1 Hz, 1H, 3TC H-5′), 4.57 (dd, J = 3.2 and 12.1 Hz, 1H, 3TC H-5″), 4.26-4.46 (m, 3H, AZT H-3′ , AZT H-5′, and AZT H-5″), 4.21 (t, J = 6.6 Hz, 1H, Glu HN-C*H*-COO CH(α)), 3.93-4.07 (m, 1H, AZT H-4′), 3.75 (s, 6H, DMTr CH_3O), 3.63-3.70 (m, 1H, 3TC H-2″), 3. 75 (dd, J = 12.3 and 5.5 Hz, 1H, 3TC H-2′), 2.67 (t, J = 7.0 Hz, 2H, CH_2COO), 2.07-2.56 (m, 4H, AZT H-2′, AZT H-2″ , Glu CHCH_2CH_2COO), 1.85 (s, 3H, AZT 5-CH_3); ^{13}C NMR ($CDCl_3$, 100 MHz, δ ppm): 173.20 (AZT *C*OO), 169.95 (3TC *C*OO), 166.25 (3TC C-4, AZT C-4 *C*=O), 161.54 (DMTr Ar-*C*-OCH_3), 160.03 (3TC, C-2 *C*=O), 148.70 (AZT C-2 *C*=O), 145.48 (3TC C-6), 138.34 (AZT C-6), 137.37, 131.25, 129.32, 128.7, 127.69, 114.00 (DMTr Ar-C), 111.86 (AZT C-5), 95.32 (3TC C-5), 88.88 (AZT C-1′), 87.15 (3TC C-1′), 84.02 (AZT C-4′), 82.93 (3TC C-4′), 67.30 (AZT C-5′), 65.16 (3TC C-5′), 62.06 (DMTr OCH_3), 55.69 (AZT C-3′), 53.03 (*C*H(α)), 37.48 (AZT C-2′), 37.38 (3TC C-2′), 30.15 (Glu γ-*C*H_2), 26.53 (Glu β-*C*H_2), 12.54 (AZT 5-*C*H_3); HR-MS (ESI-TOF) (m/z): $C_{44}H_{47}N_9O_{11}S$; calcd, 909.3116; found, 910.4154 $[M + H]^+$, 1821.5154 $[2M + H]^+$.

$C_{13}H_{27}$-CONH-Glu(AZT)-3TC (3.34). Compound **3.32** (100 mg, 0.12 mmol) and myristic anhydride (100 mg, 0.24 mmol) were dissolved in DMF (10 mL). DIPEA (5 mL, 37 mmol) was added to the solution. The mixture was stirred for 2 h at room temperature. The solvent was removed under reduced pressure to yield $C_{13}H_{27}$-CONH-Glu(AZT)-3TC-DMTr **(3.33).**

3.33. HR-MS (ESI-TOF) (m/z): $C_{58}H_{73}N_9O_{12}S$: calcd, 1119.5099; found, 1120.3183 $[M+H]^+$.

Acetic acid (80% in water, 10 mL) was added to compound **3.33**. The mixture was heated at 80 °C for 30 min to remove DMTr protection. Acetic acid was removed under reduced pressure and the residue was purified with reversed phase HPLC using a C_{18} column and water/acetonitile as solvents as described above to yield **3.34** (35 mg, 50%).

3.34. ^{1}H NMR (400 MHz, $CDCl_3$, δ ppm): 7.91 (d, *J* = 7.8 Hz, 1H, 3TC H-6), 7.17 (s, 1H, AZT H-6), 6.20 (dd, *J* = 3.7 and 5.2 Hz, 1H, 3TC H-1′), 6.14 (d, *J* = 7.8 Hz, 1H, 3TC H-5), 5.94 (t, *J* = 6.5 Hz, 1H, AZT H-1′), 5.31 (dd, *J* = 4.3 and 3.6 Hz, 1H, 3TC H-4′), 4.32-4.58 (m, 4H, 3TC H-5′, 3TC H-5″, AZT H-3′), 4.21-4.29 (m, 3H, AZT H-5′, AZT H-5″, Glu HN-C*H*-COO (CH(α)), 3.94 (dd, *J* = 3.7 and 5.1 Hz, 1H, AZT H-4′), 3.47 (dd, *J* = 5.2 and 12.6 Hz, 1H, 3TC H-2″), 3.13 (dd, *J* = 3.7 and 12.6 Hz, 1H, 3TC H-2′), 2.07-2.51 (m, 8H, AZT H-2′, AZT H-2″, myristate C*H*$_2$COO, and Glu C*H*$_2$C*H*$_2$COO), 1.81 (s, 3H, AZT 5-C*H*$_3$), 1.40-1.58 (m, 2H, *CH*$_2$CH$_2$COOH), 1.04-1.27 (br m, 20H, methylene protons), 0.78 (t, *J* = 7.0 Hz, 3H, *CH*$_3$); ^{13}C NMR (CD_3OD, 100 MHz, δ ppm): 175.92, 172.79 (AZT *C*OO, 3TC *C*OO), 171.70 (*C*ONH), 164.82 (3TC C-4), 160.74 (AZT C-4 *C*=O), 150.67 (3TC C-2 *C*=O), 148.15 (AZT C-2

C=O), 143.44 (3TC C-6), 136.83 (AZT C-6), 111.32 (AZT C-5), 94.90 (3TC C-5), 87.07 (AZT C-1′), 86.45 (3TC C-1′), 84.35 (AZT C-4′), 81.86 (3TC C-4′), 64.38 (AZT C-5′), 63.75 (3TC C-5′), 60.80 (AZT C-3′), 51.54 (*C*H(α)), 38.22 (AZT C-2′), 37.05 (*C*H_2COO), 36.24 (3TC C-2′), 32.11, 30.11, 29.99, 29.83, 29.55, 29.47, 29.40, 25.80 (methylene carbons), 26.77 (Glu γ-*C*H_2), 22.85 (Glu β-*C*H_2), 14.19 (myristate *C*H_3), 12.40 (AZT 5-*C*H_3); HR-MS (ESI-TOF) (m/z): $C_{37}H_{55}N_9O_{10}S$: calcd, 817.3793; found, 818.2535 $[M + H]^+$, 1636.0917 $[2M + H]^+$.

CH_3-CONH-Glu(AZT)-3TC (3.36). To compound **3.32** (110 mg, 0.12 mmol) in DMF (10 mL) was DIPEA (5 mL, 37 mmol) and acetic anhydride (2 mL, 20 mmol). The reaction mixture was stirred for 2 h at room temperature. The solvent was removed under reduced pressure to yield CH_3-CONH-Glu(AZT)-3TC-DMTr **(3.35).**

3.35. HR-MS (ESI-TOF) (m/z): $C_{46}H_{49}N_9O_{12}S$: calcd, 951.3221; found, 952.2062 $[M + H]^+$, 1903.9995 $[2M + H]^+$.

Acetic acid (80% in water, 10 mL) was added to compound **3.35**. The reaction mixture was heated at 80 °C to remove DMTr protection. Acetic acid was removed under reduced pressure and the residue was purified with reversed phase HPLC using a C_{18} column and water/acetonitile as a solvents as described above to yield **3.36** (35 mg, 55%).

3.36. ^{1}H NMR (400 MHz, CD_3OD, δ ppm): 8.02 (d, J = 7.9 Hz, 1H, 3TC H-6), 7.33 (s, 1H, FLT H-6), 6.20-6.30 (m, 1H, 3TC H-1′), 6.03-6.16 (m, 2H, AZT H-1′ and 3TC H-5), 5.42 (t, J = 3.7 Hz, 1H, 3TC H-4′), 4.43-4.62 (m, 3H, 3TC H-5″, 3TC H-5′, and

AZT H-3′), 4.25-4.35 (m, 3H, AZT H-5′, AZT H-5″, Glu HN-C*H*-COO (CH(α)), 4.02 (dd, J = 4.5 and 9.1 Hz, 1H, AZT H-4′), 3.57 (dd, J = 5.5 and 12.4 Hz, 1H, 3TC H-2″), 3.24 (dd, J = 3.4 and 12.4 Hz, 1H, 3TC H-2′), 2.11-2.53 (m, 6H, AZT H-2′, AZT H-2″, Glu C*H*$_2$C*H*$_2$COO), 1.96 (s, 3H, acetyl *CH*$_3$), 1.87 (s, 3H, 5-C*H*$_3$); ^{13}C NMR (CD_3OD, 100 MHz, δ ppm): 173.22, 172.50 (AZT *C*OO, 3TC *C*OO), 172.24 (*C*ONH), 165.41 (3TC C-4), 161.32 (AZT C-4 *C*=O), 151.49 (3TC C-2 *C*=O), 148.53 (AZT C-2 *C*=O), 144.96 (3TC C-6), 137.32 (AZT C-6), 111.56 (AZT C-5), 95.03 (3TC C-5), 87.92 (AZT C-1′), 86.03 (3TC C-1′), 84.92 (AZT C-4′), 82.40 (3TC C-4′), 65.19 (AZT C-5′), 64.42 (3TC C-5′), 61.36 (AZT C-3′), 52.36 (*C*H(α)), 38.29 (AZT C-2′), 37.36 (3TC C-2′), 30.65 (Glu γ-*C*H$_2$), 27.06 (Glu β-*C*H$_2$), 22.60 (acetyl *C*H$_3$), 12.60 (FLT 5-*C*H$_3$); HR-MS (ESI-TOF) (m/z): $C_{25}H_{31}N_9O_{10}S$: calcd, 649.1915; found, 650.2228 [M + H]$^+$, 1299.0050 [2M + H]$^+$.

FLT-Succ-NH-Glu(AZT)-3TC (3.37). Compound **3.32** (110 mg, 0.12 mmol), DIPEA (5 mL, 37 mmol), and FLT-Succinate (100 mg, 0.30 mmol) were dissolved in DMF (10 mL). The reaction mixture was stirred for 2 h at room temperature. The solvent was removed under reduced pressure. Acetic acid (80% in water, 10 mL) was added to the residue. The reaction mixture was heated at 80 °C to remove DMTr protection. Acetic acid was removed under reduced pressure and the residue was purified with HPLC using a C_{18} column and water/acetonitile as a solvent as described above to yield **3.37** (55 mg, 50 %).

^{1}H NMR (400 MHz, CD_3CN, δ ppm): δ 10.7 (s, 1H, N*H*), 9.59 (s, 2H, N*H*), 7.97 (d, *J* = 7.6 Hz, 1H, 3TC H-6), 7.77 (s, 1H, N*H*), 7.36 (s, 1H, FLT H-6), 7.29 (s, 1H, AZT H-6), 6.96 (d, 1H, N*H*), 6.17-6.26 (m, 2H, 3TC H-1′ and FLT H-1′), 6.14 (d, *J* = 7.6 Hz, 1H, 3TC H-5), 6.06 (t, *J* = 6.3 Hz, 1H, AZT H-1′), 5.40 (t, *J* = 3.6 Hz, 1H, 3TC H-4′), 5.24 (dd, *J* = 4.8 and 53.7 Hz, 1H, FLT H-3′), 4.16-4.59 (m, 9H, 3TC H-5′, 3TC H-5″, FLT H-5′, FLT H-5″, FLT H-4′, AZT H-5′, AZT H-5″, AZT H-3′, Glu HN-C*H*-COO (CH(α)), 4.00 (dd, *J* = 6.6 Hz, 1H, AZT H-4′), 3.56 (dd, *J* = 11.9 and 5.2 Hz, 1H, 3TC H-2″), 3.24 (dd, *J* = 11.9 and 5.2 Hz, 1H, 3TC H-2′), 2.05-2.66 (m, 12H, Succinate OOCC*H*$_2$C*H*$_2$CON, FLT H-2′, FLT H-2″, AZT H-2′, AZT H-2″, and Glu C*H*$_2$C*H*$_2$COO), 1.83 (s, 6H, FLT 5-C*H*$_3$ and AZT 5-C*H*$_3$); ^{13}C NMR (CD_3CN, 100 MHz, δ ppm): 174.50, 173.95, 172.95 (3TC *C*OO, FLT *C*OO, AZT *C*OO), 166.38 (3TC C-4), 161.62 (AZT C-4 *C*=O and FLT C-4 *C*=O), 152.38, 152.27, 148.86 (AZT C-2, FLT C-2, 3TC C-2 *C*=O), 145.83, 138.25, 137.50 (FLT C-6, AZT C-6, 3TC C-6), 112.22, 112.04 (FLT C-5, AZT C-5), 95.43 (*J* = 176.5 Hz, FLT C-3′), 96.42 (3TC C-5), 88.78 (3TC C-1′), 86.85 (FLT C-1′), 86.81 (AZT C-1′), 86.81 (3TC C-4′), 84.11 (*J* = 26.0 Hz, FLT C-4′), 83.16 (AZT C-4′), 65.93, 65.05, 64.99 (3TC C-5′, FLT C-5′, AZT C-5′), 62.20 (AZT C-3′), 52.64 (*C*H(α)), 38.79 (3TC C-2′), 38.48 (*J* = 19.0 Hz, FLT C-2′), 37.76 (AZT C-2′), 31.86, 31.06, (succinate two-*C*H$_2$), 30.24 (Glu γ-*C*H$_2$), 27.71 (Glu β-*C*H$_2$), 12.89, 12.75 (AZT 5-*C*H$_3$ and FLT 5-*C*H$_3$); HR-MS (ESI-TOF) (m/z): $C_{37}H_{44}FN_{11}O_{15}S$: calcd, 933.2723; found, 934.2864 $[M + H]^+$, 1867.6791 $[2M + H]^+$.

3.4. Results and discussion

3.4.1. Chemistry

3.4.1.1. Unsymmetrical and Symmetrical 5′,5′-Dinucleoside Conjugates of Succinic Acid or Suberic Acid

Several 1,4-dinucleoside succinate and 1,8-dinucleoside suberate ester derivatives were synthesized (Schemes 3.1-3.3).

Unsymmetrical dinucleoside succinate derivatives were synthesized in two-step synthesis. First, nucleoside succinates, FLT succinate (**3.1**) and AZT succinate (**3.2**), were synthesized by the reaction of FLT or AZT with succinic anhydride in presence of pyridine as the base (Scheme 3.1). FLT succinate was then reacted with AZT in the presence of HBTU and DIPEA as a base and 3TC-DMTr (**2.12**) in the presence of HBTU and DIPEA, followed by acetic acid to give FLT-AZT 1,4-succinate (**3.3**) and FLT-3TC 1,4-succinate (**3.4**), respectively. Similarly, AZT-succinate was reacted with 3TC-DMTr (**2.12**) followed by DMTr removal to give AZT-3TC 1,4-succinate (**3.5**).

Symmetrical dinucleoside 1,4-succinate derivatives of AZT (**3.6**) and FLT (**3.7**) were synthesized by reaction of nucleosides with succinyl chloride in the presence of DMAP as the base (Scheme 3.2). Symmetrical dinucleoside 1,8-suberate were synthesized by reaction of two equivalents of nucleosides, FLT, AZT, or DMTr-3TC, with one equivalent of suberic acid in presence of HBTU and DIPEA. Acetic acid cleavage was used to deprotect the DMTr group in 3TC conjugate (Scheme 3.3).

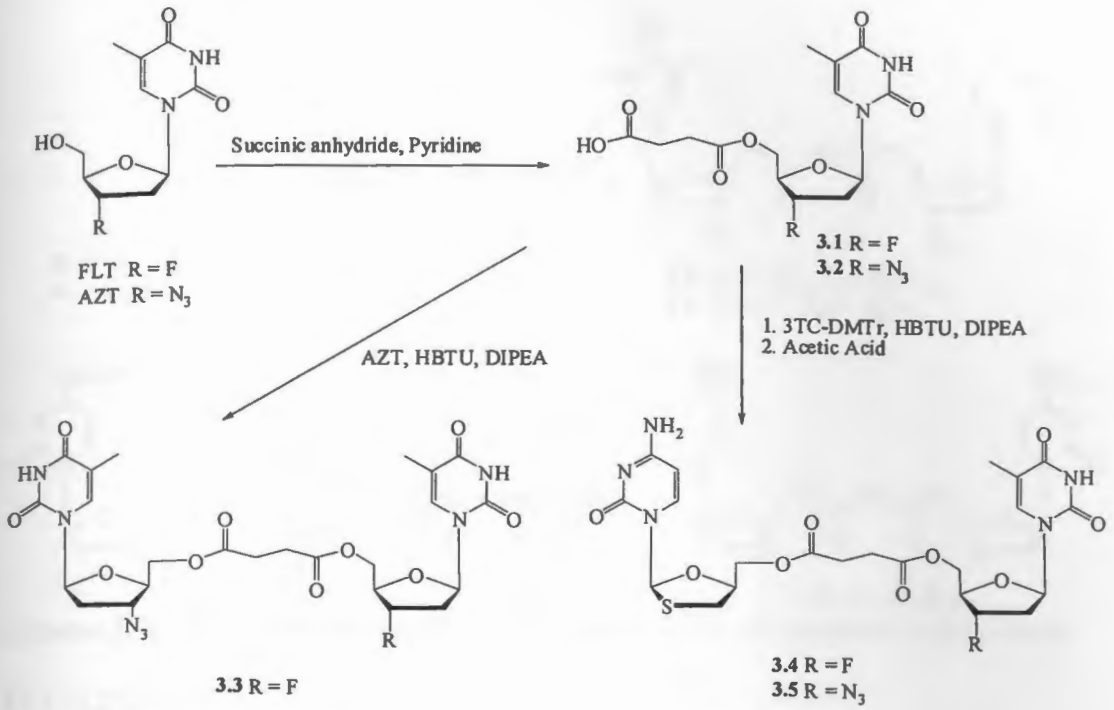

Scheme 3.1. Synthesis of unsymmetrical 5',5'-dinucleoside 1,4-succinate derivatives of FLT, AZT, and 3TC.

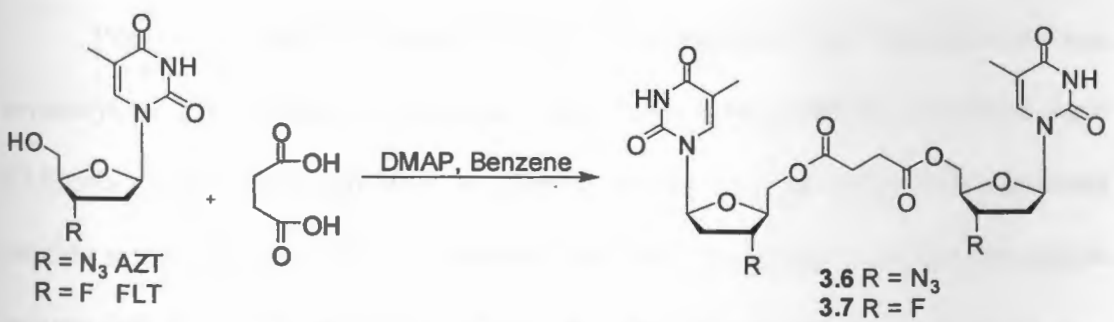

Scheme 3.2. Synthesis of symmetrical 5',5'-dinucleoside 1,4-succinate derivatives of FLT and AZT.

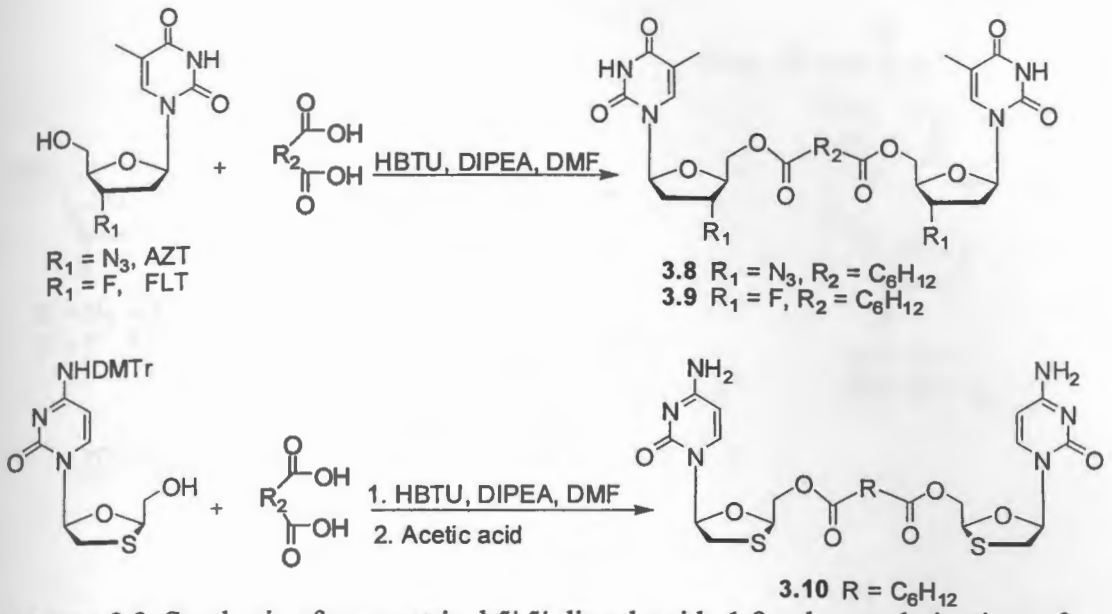

Scheme 3.3. Synthesis of symmetrical 5′,5′-dinucleoside 1,8-suberate derivatives of FLT, AZT, and 3TC.

3.4.1.2. Synthesis of Peptide-Nucleoside Conjugates (Peptides Containing One Nucleoside and One Myristoyl Group).

Peptide-nucleoside derivatives (**3.16-3.20**) containing one nucleoside and one myristoyl moiety attached in the peptide side chains were synthesized in three steps: (i) Fmoc-building block synthesis; (ii) Peptide assembly on the resin using automated peptide synthesizer; and (iii) Deprotection followed by acylation of the free amino groups. Step-by-step synthetic procedures are shown in the schemes 3.6-3.8.

Fmoc-Glu(nucleoside)-OH were synthesized by reaction of Fmoc-Glu(OH)-*t*Bu with the corresponding nucleoside (AZT or FLT) in the presence of HBTU and DIPEA, followed by the deprotection of *t*Bu group with TFA (Scheme 3.4).

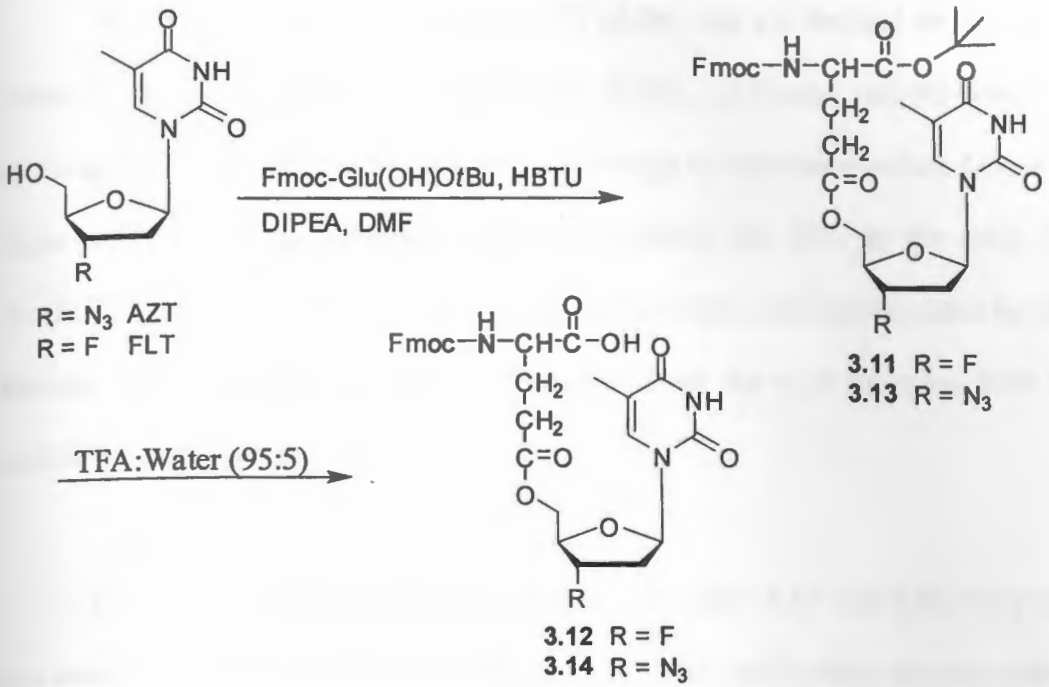

Scheme 3.4. Synthesis of Fmoc-Glu(FLT)-OH (**3.12**) and Fmoc-Glu(AZT)-OH (**3.14**).

Fmoc-Ser(OMys)OH (**3.15**), a fatty acid building block, was synthesized by the reaction of Fmoc-Ser(OH)-OH with myristoyl chloride in the presence of DIPEA (Scheme 3.5).

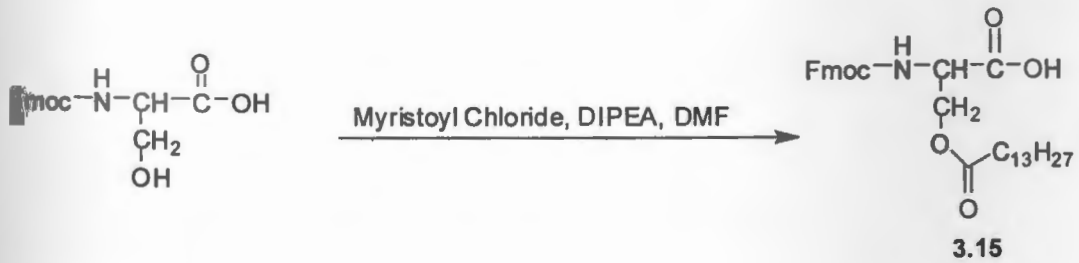

Scheme 3.5. Synthesis of Fmoc-Ser(OMys)OH (**3.15**).

Dipeptide My-Glu(FLT)-Lys(My)-OH (**3.16**) was synthesized by assembling Fmoc protected building block, Fmoc-Glu(FLT)-OH, on Fmoc-Lys(Mtt)-Wang resin by using Fmoc solid phase peptide synthesis strategy at room temperature Lysine side chain protecting group Mtt was removed by adding 5% TFA to the resin NH_2-Glu(FLT)-Lys(Mtt)-Wang resin. The free amino groups were myristoylated by using myristic anhydride and the peptide was cleaved from the resin by using 95% TFA cocktail to yield **3.16** (Scheme-3.6).

For the synthesis of peptide-nucleoside conjugates **3.17** and **3.18**, the peptide was assembled on Fmoc-Lys(Mtt)-Wang resin by Fmoc solid-phase peptide synthesis strategy on a PS3 automated peptide synthesizer at room temperature using Fmoc protected amino acids [Fmoc-β-Ala-OH and Fmoc-Glu(nucleoside)-OH (**3.12** or **3.14**)], followed by acetylation. After acidic removal of lysine Mtt group, the *N*-terminal was myrisotylated using myristic anhydride in the presence of DIPEA as the base to afford **3.17** and **3.18** (Scheme 3.7).

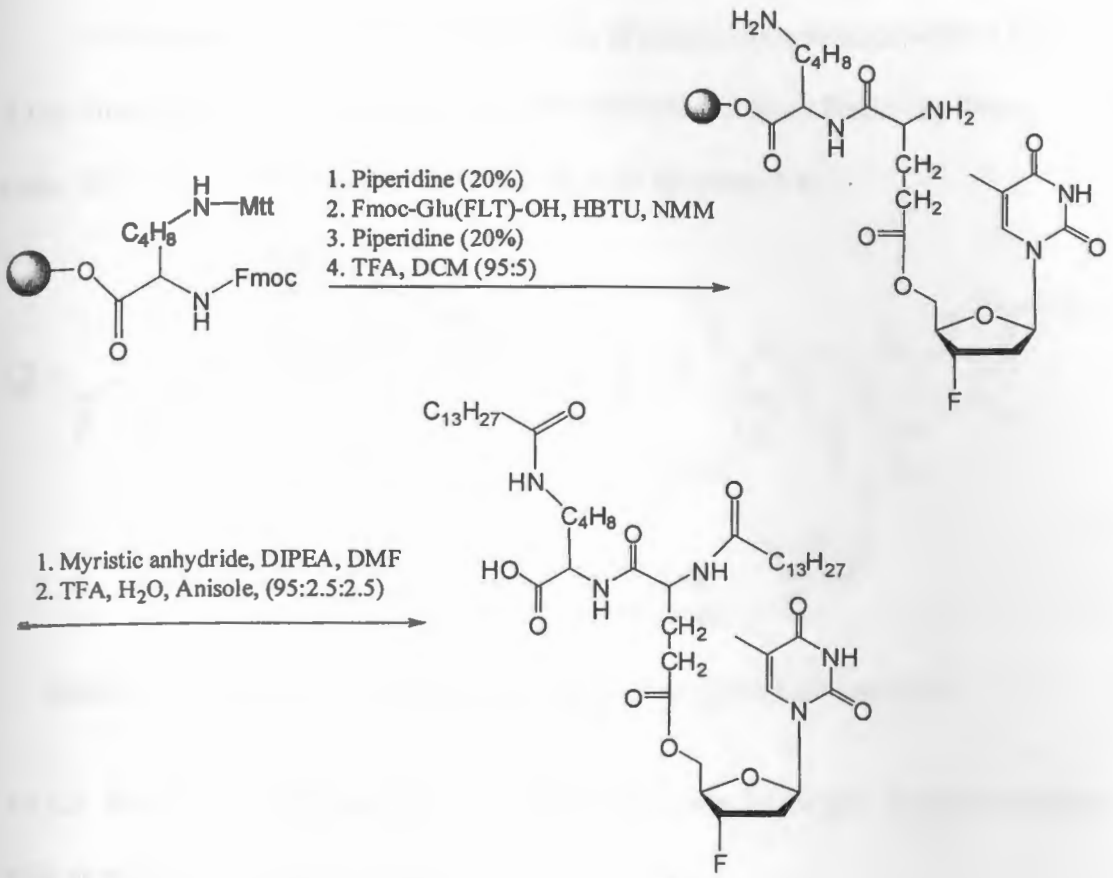

Scheme 3.6. Solid phase synthesis of My-Glu(FLT)-Lys(My)-OH (**3.16**).

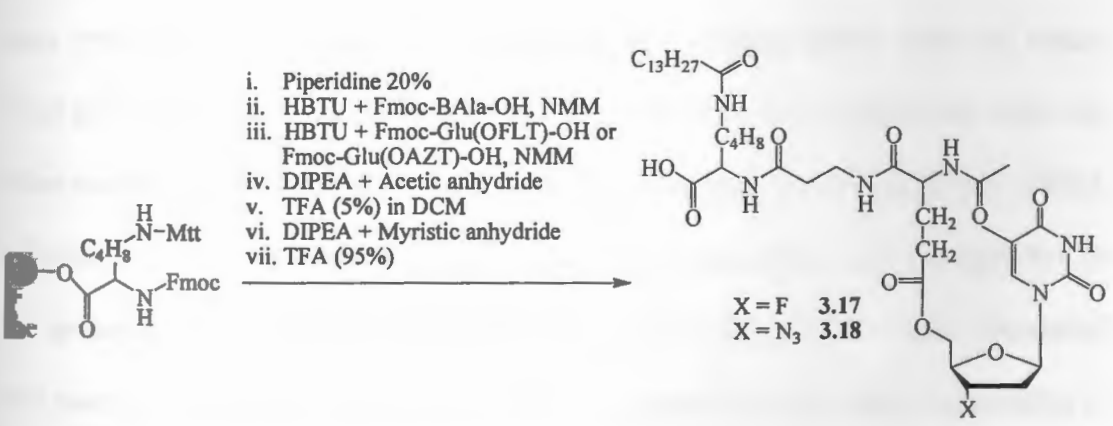

Scheme 3.7. Solid phase synthesis of peptide-nucleoside conjugates **3.17** and **3.18**.

Solid-phase reaction of building blocks, [Fmoc-Glu(nucleoside)-OH (**3.12** or **3.14**), Fmoc-β-Ala-OH, and Fmoc-Ser(Myristoyl)-OH (**3.15**) on Fmoc-Gly-Wang resin, followed by cleavage afforded **3.19** and **3.20** (Scheme 3.8).

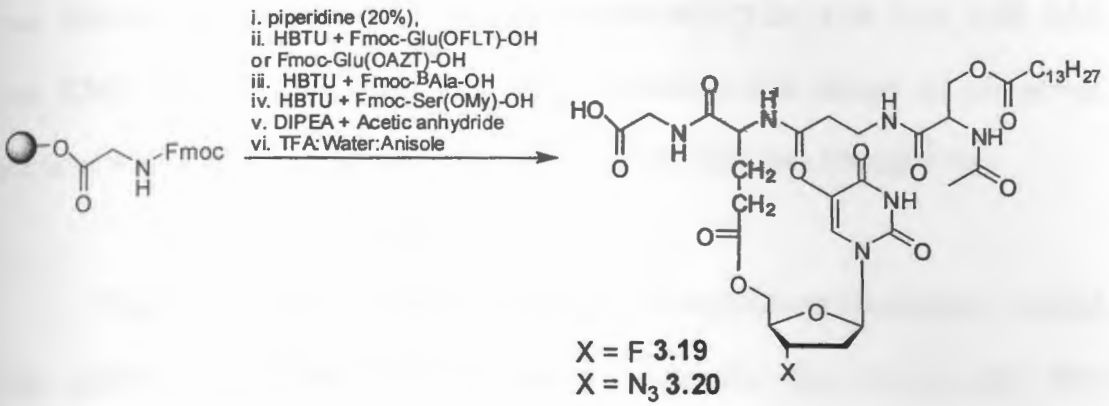

Scheme 3.8. Synthesis of Peptide-nucleoside conjugates **3.19** and **3.20**.

3.4.1.3. Synthesis of Dinucleoside- and Trinucleoside Glutamic Acid Derivatives with or without Myristoyl Moiety

The synthesis of glutamate esters containing two to three nucleosides, with or without myristic acid, was accomplished by solution phase synthesis. The conjugates were synthesized by reaction of an appropriate building block, such as Fmoc-Glu(FLT)-OH (**3.12**) or Fmoc-Glu(AZT)-OH (**3.14**) as at free α-carboxylic acid with other nucleosides, such as 3TC-DMTr or AZT, in the presence of HBTU and DIPEA afforded **3.21**, **3.27** or **3.31**. In the next step, Fmoc deprotection was accomplished in the presence of piperidine and octanethiol to afford **3.22**, **3.28**, or **3.32**. Octanethiol was used in excess as a scavenger since the conjugates were not stable to piperidine or other bases like DMAP. The use of piperidine in proportions more than 0.1 equivalent or the increase in the cleavage reaction time resulted in the loss of nucleoside from side chain of glutamate at δ-carboxylic acid. After the removal of Fmoc protection

from amino group, *N*-terminal was reacted with myristic anhydride or acetic anhydride in the presence of DIPEA. Deprotection of DMTr group was accomplished with acetic acid reaction. This strategy provided the synthesis of the glutamate ester containing two different nucleosides with or without myristic acid (**3.24**, **3.26**, **3.29**, **3.30**, **3.34**, and **3.36**). Myristoyl and acetyl capping at *N*-terminal was carried out to provide peptides with high and low lypophilicity, respectively (Schemes 3.9 and 3.10).

Finally, a glutamate conjugate containing three different nucleosides attached was synthesized (Scheme 3.10). In this molecule, the first, second, and third nucleosides were attached to *C*-terminal, to the side chain, amino group, respectively. A glutamate conjugate containing two different nucleosides, 3TC and AZT, at α and δ-carboxylic acids (NH_2-Glu(AZT)-3TC-DMTr) (**3.32**) was first reacted with FLT-succinate in the presence of DIPEA followed by acetic acid cleavage to afford a glutamate conjugate containing three nucleosides (**3.37**).

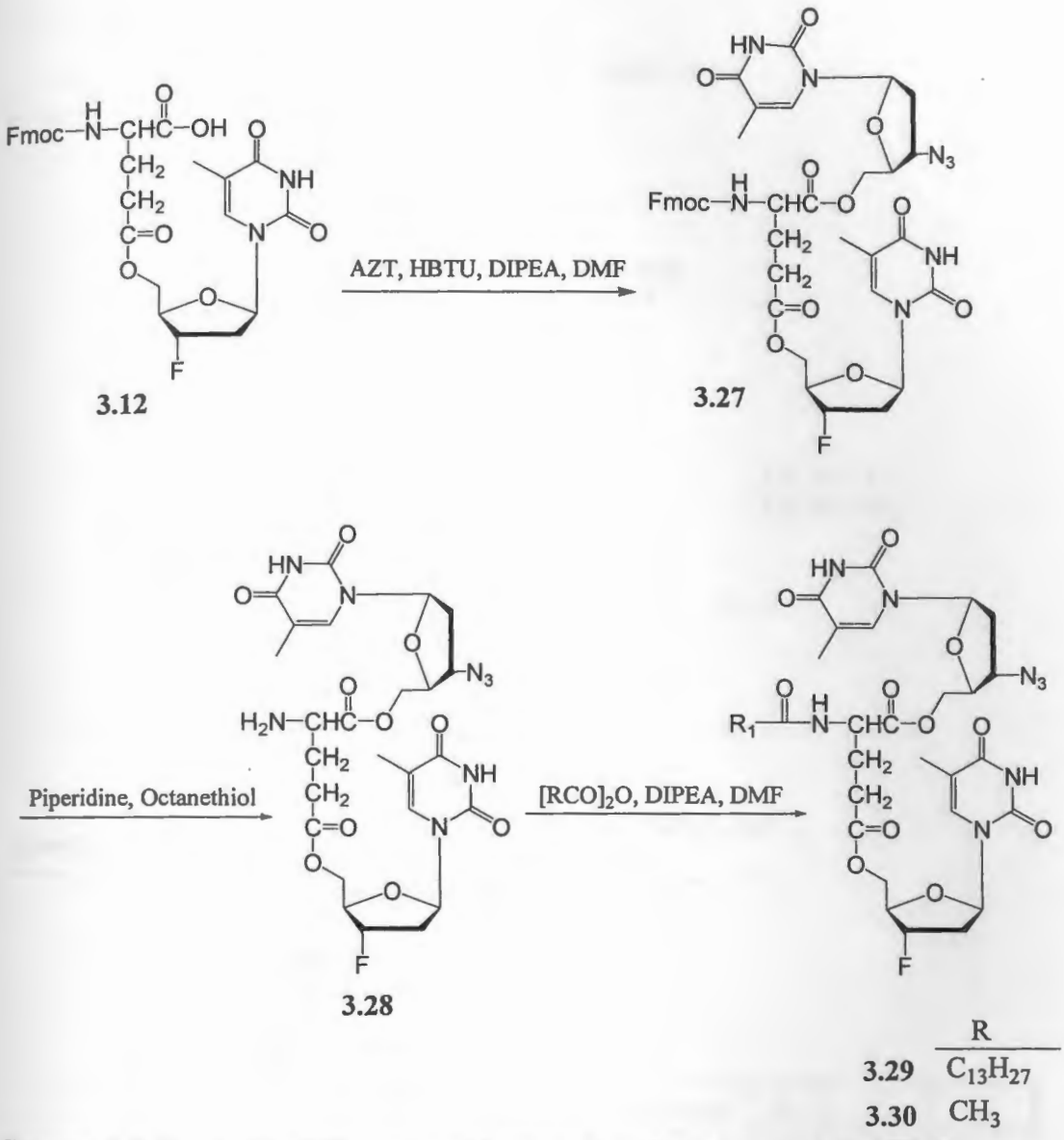

Scheme 3.9. Synthesis of Glutamic acid esters of nucleosides (AZT and FLT)

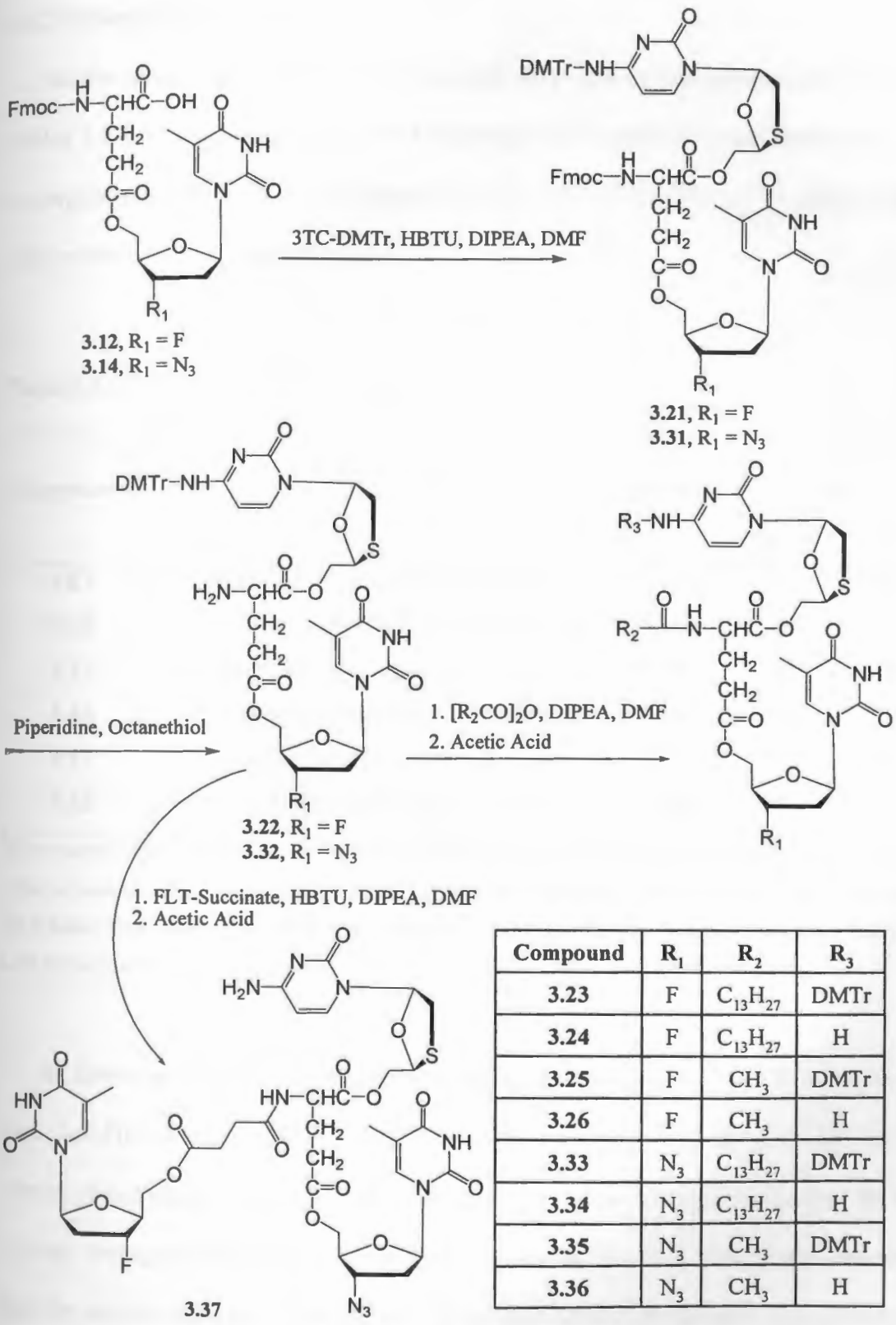

Compound	R_1	R_2	R_3
3.23	F	$C_{13}H_{27}$	DMTr
3.24	F	$C_{13}H_{27}$	H
3.25	F	CH_3	DMTr
3.26	F	CH_3	H
3.33	N_3	$C_{13}H_{27}$	DMTr
3.34	N_3	$C_{13}H_{27}$	H
3.35	N_3	CH_3	DMTr
3.36	N_3	CH_3	H

Scheme 3.10. Synthesis of Glutamic acid esters of nucleosides (AZT, FLT and 3TC).

3.4.2 Biological evaluation

All the compounds were tested for their anti-HIV activity and cytotoxicity profile. Tables 3.2-3.4 illustrate the anti-HIV-1 activities of the selected compounds and the corresponding physical mixtures against cell-free virus (IIIB) strain. The compounds are currently under evaluation against other strains of virus.

Table 3.2. Anti HIV Activity of peptide-nucleoside conjugates

Compound	Chemical Name	CTS[a] (μg/mL)	Cell-free HIV-1 (IIIB)[b]	
		[a]	(μg/mL)	(μM)
AZT	3'-azido-2',3'-dideoxythymidine (AZT)	>100	9.2	34.4
FLT	3'-fluoro-2',3'-deoxythymidine (FLT)	>100	0.2	0.8
3.19	FLT(Glutamyl)-myrsitoyllysine	>100	8.7	10.4
3.16	FLT(myristoylglutamyl)-mysritoyllysine	>100	24.7	26.8
3.17	Myristoylserine-FLT(glutamyl)glycine	>100	9.3	11.1
3.18	Myristoylserine-AZT(glutamyl)glycine	>100	54.5	63.1

[a]Cytotoxicity assay; [b]Viral entry inhibition assay (lymphocytotropic strain); Data represent EC_{50} (50% effective concentration). Single-round infection assay where compounds, virus and cells were incubated for 2 hours. Cells were then washed and cultured for additional 48h. Infection was measured by HIV-LTR driven Galactosidase expression.

As shown in Table 3.2, all the peptide-nucleoside conjugates (**3.16-3.19**) displayed poor anti-HIV activity (EC_{50} >10 μM when compared to FLT (EC_{50} = 0.8 μM). Myristoylated peptide-AZT conjugate **3.18** was almost two fold less active than AZT. Peptide conjugates were nearly 13-79 folds less active than FLT. The results indicate that the peptides may not be an appropriate scaffold for the attachment of nucleosides and attachment of myristic acid did not improve the ant-HIV profile of the

nucleosides. This may be due to the low cellular uptake of compounds containing peptide backbone.

The anti-HIV activities for glutamate esters of two different nucleosides were evaluated against monocytotropic stain of virus and compared with the physical mixture of the corresponding nucleosides with or without myristic acid (Table 3.3). The data showed improved anti-HIV activity for molecules containing myristic acid when compared to the molecules without the fatty acid. Glutamate ester of FLT and 3TC with myristic acid (**3.24**) exhibited 8.5-fold higher activity than the corresponding conjugate without myristic acid (**3.26**). Furthermore, compound **3.24** was the most active conjugate among glutamic ester of two nucleosides. However, the anti-HIV activity for all the compounds was less than that of FLT.

Surprisingly, the physical mixtures of nucleosides and glutamic acid with myristic acid showed higher potency than the corresponding conjugates. This result indicates that attachment of nucleosides to the amino acid backbone is deleterious, possibly because of poor cellular uptake.

In general, the presence of the myristic acid in the conjugates or physical mixtures improved the anti-HIV activity. The possible reason for the better activity could be the improved lypophilicity, which ultimately results in higher cellular uptake of the active compounds and higher solubility of the physical mixtures in the presence

of myristic acid in tested solutions. More investigations are required to confirm these hypotheses.

Table 3.3. Dinucleoside-Glutamic Acid Derivatives with or without Myristoyl Moiety

Compound	Chemical Name	CTS[a] (μg/mL)[a]	Cell-free HIV-1 (IIIB)[b]	
			(μg/mL)	μM
AZT	3'-azido-2',3'-dideoxythymidine (AZT)	>100	9.2	34.4
FLT	3'-fluoro-2',3'-deoxythymidine (FLT)	>100	0.2	0.8
3TC	2',3'-dideoxy-3'-thiacytidine (lamivudine, 3TC)	>100	7.5	32.7
3.26	FLT(acetylglutamyl)-3TC	>100	10.7	17.1
3.24	FLT(mysristoylglutamyl)-3TC	>100	1.6	2.0
3.38	FLT + 3TC + Glutamic acid	>100	0.6	
3.39	FLT + 3TC + Glutamic acid + Myristic acid	>100	0.3	
3.30	FLT(acetylglutamyl)-AZT	>100	9.0	13.5
3.29	FLT(mysristoylglutamyl)-AZT	>100	2.0	2.4
3.40	FLT + AZT + Glutamic acid	>100	1.0	
3.41	FLT + AZT + Glutamic acid + Myristic acid	>100	0.3	
3.36	AZT(acetylglutamyl)-3TC	>100	7.8	12.0
3.34	AZT(mysristoylglutamyl)-3TC	>100	4.9	6.0
3.42	AZT + 3TC + Glutamic acid	>100	1.7	
3.43	AZT + 3TC + Glutamic Acid + Myristic Acid	>100	1.9	

[a]Cytotoxicity assay; [c]Viral entry inhibition assay (lymphocytotropic strain); Data represent EC_{50} (50% effective concentration). Single-round infection assay where compounds, virus and cells were incubated for 2 hours. Cells were then washed and cultured for additional 48h. Infection was measured by HIV-LTR driven Galactosidase expression.

Table 3.4 displays the anti-HIV activity of a glutamate derivative with three different nucleosides (**3.37**). Compound **3.37** showed 35-fold higher anti-HIV activity that AZT and 3TC, , but had a comparable activity to FLT against IIIB strain of virus EC_{50} = 0.8 μM. Compound **3.37** was >10 folds better active than the corresponding molecule with two nucleosides (**3.26**) indicating that the addition of three nucleosides to the glutamate improves the anti-HIV activity. Compound **3.37** exhibited 4-17 times better anti-HIV activity when compared with disubstituted succinate derivatives of AZT and FLT (**3.6** and **3.7**).

The activity of **3.37** was also compared to the corresponding physical mixtures either with or without myristic acid (Table 3.4). The data showed higher anti-HIV activity for the physical mixture **3.45** than **3.37**. Physical mixture containing FLT, AZT, 3TC, and glutamic acid (**3.45**) showed comparable activity to **3.37**. Replacing FLT with FLT-succinate in the physical mixture (**3.46**) resulted in decrease in anti-HIV activity by 2 fold, possibly because of slow hydrolysis of FLT-succinate to FLT. This data is consistent with our earlier results suggesting that glutamate and peptides are not appropriate scaffolds for improving anti-HIV profile.

Addition of myristic acid in equivalent ratio to the physical mixture (**3.46**) improved the activity by three fold in comparison with **3.37** and the physical mixture **3.45**. These data were consistent with those obtained for the physical mixtures of two nucleosides and myristic acid described above.

Table 3.4. Anti HIV Activity of glutamic acid ester of three different Nucleosides in comparison with succinate derivatives of nucleosides

Compound	Chemical Name	CTS[a] µg/mL.	Cell-free HIV-1 (IIIB)	
			µg/mL	µM
AZT	3'-azido-2',3'-dideoxythymidine (AZT)	>100	9.2	34.4
FLT	3'-fluoro-2',3'-deoxythymidine (FLT)	>100	0.2	0.8
3TC	2',3'-dideoxy-3'-thiacytidine (3TC)	>100	7.5	32.7
3.6	AZT-succinate-AZT	>100	8.6	13.9
3.7	FLT-succinate-FLT	>100	2.1	3.7
3.37	FLT-Succinate-AZT(glutamyl)-3TC	>100	0.9	0.96
3.44	FLT-Succinate + AZT + 3TC + Glutamic acid	>100	1.8	
3.45	FLT + AZT + 3TC + Glutamic acid	>100	0.8	
3.46	FLT + AZT + 3TC + Glutamic acid + Myristic acid	>100	0.3	

[a]Cytotoxicity assay; [c]Viral entry inhibition assay (lymphocytotropic strain); Data represent EC_{50} (50% effective concentration). Single-round infection assay where compounds, virus and cells were incubated for 2 hours. Cells were then washed and cultured for additional 48h. Infection was measured by HIV-LTR driven Galactosidase expression.

3.5. Conclusions

Three classes of mono- di-, or trinucleoside conjugated on multivalent scaffolds (e.g., polycarboxylic acids, amino acids, and peptides) were synthesized with the expectation to improve the cellular uptake profile of the nucleosides, to exert synergistic effect by delivering different ant-HIV nucleosides at the same time to the infected cells, and to generate broad-spectrum anti-HIV agents with higher barrier to drug resistance.

Peptides or glutamate conjugated with myristic acid and nucleosides exhibited higher anti-HIV activities when compared with those substituted only with nucleosides. Increasing the number of anti-HIV nucleosides to 2 or 3 on the peptide chain enhanced the anti-HIV potency. Physical mixtures of nucleosides with amino acids and fatty acids used in the conjugation also showed significantly higher potency. The presence of one myristic acid in the conjugates or physical mixtures improved the anti-HIV activity, but addition of two myristic acids to the conjugates was not beneficial.

Glutamate-nucleoside derivatives showed higher anti-HIV activity than dinucleoside succinate derivatives. The glutamate conjugate with three different nucleosides (**3.37**) was found to be the most potent compound in three classes of compounds evaluated here. Compound **3.37** had higher anti-HIV activity than AZT and 3TC, and showed comparable activity to FLT (EC_{50} = 0.8 μM). Although glutamate conjugates containing two nucleosides exhibited higher activity than AZT and 3TC, but they were less active than FLT. Presence of myristic acid in the glutamic acid conjugates and their corresponding physical mixtures improved the anti-HIV activity.

The advantages of these compounds will be more clearly defined with further evaluation against multiple drug resistant strains. Selected compounds are currently under further biological evaluations for their broad-spectrum anti-HIV properties.

3.6. Acknowledgments

Support for this subproject (MSA-03-367) was provided by CONRAD, Eastern Virginia Medical School under a Cooperative Agreement (HRN-A-00-98-00020-00) with the United States Agency for International Development (USAID). The views expressed by the authors do not necessarily reflect the views of USAID or CONRAD.

3.7. References

Acharya, K.R., Sturrock, E.D., Riodan, J.K., Ehlers, M.R. ACE revisited: A New Target for Structure-Based Dug Design. *Nat. Rev. Drug Discov.*, 2003, 2, 891-902

Agarwal, S., Boddu, S.H.S., Jain, R., Samanta, S., Pal, D., Mitra, A. K. Peptide prodrugs: Improved oral absorption of lopinavir, anti- HIV protease inhibitor. *Intl. J. Pharm.*, **2008**, 359, 7–14.

Bourre, L., Giuntini, F., Eggleston, I. M., Wilson, M. W., MacRobert, A. J. 5-Aminolaevulinic acid peptide prodrugs enhance photosensitization for photodynamic therapy. *Mol. Cancer Ther.*, **2008**, 7, 1720-1729.

Chau, Y., Dang, N. M., Tan, F. E., Langer, R. Investigation of Targeting Mechanism of New Dextran-Peptide-Methotrexate Conjugates Using Biodistribution Study in Matrix-Metalloproteinase-Overexpressing Tumor Xenograft Model. *J. Pharm. Sci.*, **2006**, 95, 542-551.

Chau, Y., Padera, R. F., Dang1, N. M., Langer, R. Antitumor efficacy of a novel polymer–peptide–drug conjugate in human tumor xenograft models. *Int. J. Cancer*, **2006**, 118, 1519–1526.

Chau, Y., Tan, F. E., Langer, R. Synthesis and Characterization of Dextran-Peptide-Methotrexate Conjugates for Tumor Targeting via Mediation by Matrix Metalloproteinase II and Matrix Metalloproteinase IX. *Bioconjug. Chem.*, **2004**, 15, 931-941.

Cvetkovic, R.S., Goa, K.L. Lopinavir/ritonavir: a review of its use in the management of HIV infection. *Drugs*, **2003**, 63, 769-802.

Das, K., Xiong, X., Yang, H., Westland, C. E., Gibbs, C. S., Sarafianos, S. G., and Arnold, E. Molecular modeling and biochemical characterization reveal the mechanism of hepatitis b virus polymerase resistance to lamivudine (3TC) and emtricitabine (FTC). *J. Virol.*, **2001**, 75, 4771–4779.

Diallo, K., Götte, M., Wainberg1, M. A. Molecular Impact of the M184V Mutation in Human Immunodeficiency Virus Type 1 Reverse Transcriptase. *Antimicrob. Agents Chemother.*, **2003**, 47, 3377–3383.

Krebs, F. C., Miller, S. R., Malamud, D., Howett, M. K., Wigdahl, B. Inactivation of human immunodeficiency virus type 1 by nonoxynol-9, C21G, or an alkyl sulfate, sodium dodecyl sulfate. *Antiviral Res.*, **1999**, 43, 147-163.

Lazzarin, A. Enfuvirtide: The first HIV fusion Inhibitor. *Expert Opin. Pharmacother.*, **2005**, 6, 453-464.

Mulder, L. C. F., Harari, A., Simon, V. Cytidine deamination induced HIV-1 drug resistance. *Proc. Natl. Acad. Sci. U. S. A.*, **2008**, 105, 5501–5506.

Penugonda, S., Kumar, A., Agarwal, H. K., Parang, K., Mehvar, R. Synthesis and in vitro characterization of novel dextran-methylprednisolone conjugates with peptide linkers: Effects of linker length on hydrolytic and enzymatic release of methylprednisolone and its peptidyl intermediates. *J. Pharm. Sci.*, **2008**, 97, 2649–2664.

Sarafianos, S. G., Das, K., Clark, Jr., A. D., Ding, J., Boyer, P. L., Hughes, S. H., Arnold, E. Lamivudine (3TC) resistance in HIV-1 reverse transcriptase involves steric hindrance with b-branched amino acids. *Proc. Natl. Acad. Sci. U. S. A.*, **1999**, 96, 10027–10032.

Skalaski, V., Chang, C. N., Dutachman, G., Cheng, Y. C. The biochemical basis for the differential anti-human immunodeficiency virus activity of two cis enantiomers of 2',3'-dideoxy-3'-thiacytidine. *J. Biol. Chem.*, **1993**, 268, 23234-23238.

Soyez, H., Schacht, E., Vanderkerken, S. The crucial role of spacer groups in macromolecular prodrug design. *Adv. Drug Deliv. Rev.*, **1996**, 21, 81–106.

Subr, V., Strohalm, J., Ulbrich, K., Duncan, R., Hume, I. C. Polymers containing enzymatically degradable bonds, XII. Effect of spacer structure on the rate of release of daunomycin and adriamaycin from poly [N-(2-hydroxypropyl)-methylacrylamide] copolymer drug carriers in vitro and antitumor activity measured in vivo. *J. Control Release*, **1992**, 18, 123–132.

Chapter 4

Application of Solid-Phase Chemistry for the Synthesis of 3'-Fluoro-3'-deoxythymidine

Hitesh K. Agarwal, Keykavous Parang

Department of Biomedical and Pharmaceutical Sciences, University of Rhode Island, Kingston, RI, USA, 02881

Published in *Nucleosides, Nucleotides, and Nucleic Acids*, **2007**, 26, 317-322.

4.1. Abstract

Reported solution-phase methods for the synthesis of 3′-fluoro-3′-deoxythymidine (FLT) are cumbersome, require purification of intermediates, and include several protecting/deprotecting steps. To circumvent these problems, a solid-phase strategy was designed for the synthesis of FLT. Thymidine was immobilized on trityl resin via the 5′-hydroxyl group. The subsequent mesylation of the free 3′-hydroxyl group in the presence of methanesulfonyl chloride afforded the polymer-bound 3′-*O*-mesylthymidine. Nucleophilic substitution of the mesyl moiety by hydroxyl group in the presence of sodium hydroxide produced the polymer-bound threothymidine. Fluorination with diethylaminosulfur trifluoride followed by acidic cleavage of the polymer-bound FLT in the presence of trifluoroacetic acid afforded FLT.

4.2. Introduction

3′-Fluoro-3′-deoxythymidine (FLT, alovudine) is a nucleoside analogue structurally related to 3′-azido-3′-deoxythymidine (AZT), a commercially available anti-human immunodeficiency virus type 1 (HIV-1) drug. FLT has a substitution of fluorine for the hydroxyl group at the 3′ position of the ribose ring of thymidine, and has been reported to be one of the most active inhibitors of HIV *in vitro*. FLT is up to 10-fold more potent than AZT *in vitro* (Pan et al., 1992, Kong et al., 1992) and is at least 10 times more active than AZT in monkeys infected with simian immunodeficiency virus (Lundgren et al., 1991). Further investigations of this compound (Matthes et al., 1987, Cheng et al., 1987) showed that FLT-5'-triphosphate (FLT-TP) is a potent and selective inhibitor of HIV-1 reverse transcriptase.

HIV isolates with mutations resulting in multidrug resistance against all currently available reverse transcriptase inhibitors including AZT had no evidence of cross resistance to FLT (Kim et al., 1994). American Cyanamid Co discontinued the development of FLT in 1994 because of the observed hematological toxicity (Hoshi et al., 1994). However, Medivir continued to test FLT for the treatment of patients with multidrug-resistant HIV infection. The phase IIa clinical trials of FLT was successfully completed in July 2002. All patients underwent treatment without any serious side effects (Calvez et al., 2002, Rusconi, 2003). FLT is currently undergoing further clinical tests.

Recently 3′-[^{18}F]fluoro-3′-deoxythymidine ([^{18}F]FLT) has been proposed as a new marker for imaging tumor proliferation by positron emission tomography (PET) (Seitz et al., 2002, Wagner et al., 2003). The introduction of ^{18}F at the ribose rather than labelling the nucleotide with ^{18}F enhanced the metabolic stability of the marker (Shields et al., 1998). [^{18}F]FLT was predominantly taken up by proliferating cells. Further phosphorylation of [^{18}F]FLT by thymidine kinase 1 (TK-1) resulted in intracellular trapping of the metabolite, [^{18}F]FLT-monophosphate (Shields et al., 1998, Wodarski et al., 2000).

The synthesis of FLT in solution phase has been carried out by using several protecting and deprotecting steps (Herdewijn et al., 1987, Sahlberg et al., 1992, Hager et al., 1992, Kumar et al., 2004, Yun et al., 2003). These reactions are cumbersome and the intermediates need to be purified in each step. Furthermore, the overall yield is

not satisfactory. Because of revival of research interest for using FLT as anti-HIV agent or as a marker in tumor imaging by PET, there is a need for an alternative facile and effective synthesis of this compound. We designed a solid-phase strategy for the synthesis of FLT using unprotected thymidine to circumvent some of the problems associated with the solution-phase methods.

4.3. Materials and Methods

4.3.1. Materials

All the chemicals and solvents were purchased from fisher scientific. Trityl resin was purchased from Novabiochem. All reactions were carried out in Bio-Rad polypropylene columns by shaking and mixing using a Glass-Col small tube rotator in dry conditions at room temperature unless otherwise stated. Trityl chloride resin (1.6 mmol/g) was purchased from Novabiochem. Other chemicals and reagents were purchased from Sigma-Aldrich Chemical Co. (Milwaukee, WI). The chemical structure of FLT was confirmed by nuclear magnetic resonance spectrometry (^{1}H NMR, ^{13}C NMR) on a NMR spectrometer (400 MHz) and a high-resolution PE Biosystems Mariner API time-of-flight mass spectrometer.

4.3.2. Synthesis

Polymer-bound thymidine (4.3). The reaction vessel containing trityl chloride resin (**4.2**, 1.6 mmol/g, 0.36 mmol, 225 mg), thymidine (**4.1**, 350 mg, 1.44 mmol) and anhydrous pyridine (10 mL) was shaken at room temperature for 48 h. The resin was collected by filtration and washed with DMF (2 × 25 mL), DCM (2 × 25 mL), and

anhydrous MeOH (2 × 25 mL), respectively, and dried under vacuum to give **4.3** (272 mg, 91% yield). IR (cm^{-1}): 3382 (O-H), 3056 (N-H), 3019 (N-H), 1683 (C=O amide), 1654 (C=O amide).

Polymer-bound 3'-*O*-mesylthymidine (4.4). Methanesulfonyl chloride (166 μL, 2.14 mmol) was added to swelled resin **3** (272 mg) in dry pyridine (10 mL). The reaction mixture was shaken for 48 h at room temperature. The resin was collected by filtration and washed with DMF (2 × 25 mL), DCM (2 × 25 mL), and anhydrous MeOH (2 × 25 mL), respectively. The resin was dried under vacuum to afford **4.4** (290 mg, 98% yield). IR (cm^{-1}): 3056 (N-H), 3019 (N-H), 1687 (C=O amide), 1654 (C=O amide), 1356 (SO_2), 1173 (SO_2).

The completion of reaction was confirmed by cleaving a small amount of resin **4.4** with 2% TFA in DCM. The spectral properties were identical with those of 3'-*O*-mesylthymidine. HR-MS (ESI-TOF) (*m/z*): $C_{11}H_{16}N_2O_7S$ calcd, 320.3189; found, 321.2275 $[M + H]^+$, 343.2270 $[M + Na]^+$.

Polymer-bound threothymidine (4.5). Sodium hydroxide solution (0.5 mL, 1N) was added to the swelled resin **4.4** (290 mg) in DMF (20 mL). The mixture was shaken for 24 h. Additional amount of NaOH solution (1 mL, 1N) was added, and the reaction mixture was refluxed for 24 h. The resin was collected by filtration and washed with water (2 × 25 mL), DMF (2 × 25 mL), DCM (2 × 25 mL), and anhydrous MeOH (2 ×

25 mL), respectively, and dried under vacuum to yield **4.5** (262 mg, 98%). IR (cm^{-1}): 3407 (O-H), 3056 (N-H), 3019 (N-H), 1686 (C=O amide).

Polymer-bound 3′-fluoro-3′-deoxythymidine (4.6). Completely dried resin **4.5** (262 mg) was swelled in dry benzene (10 mL) and THF (1 mL) and cooled to 0 °C. DAST (135 μL, 1.02 mmol) was added to the reaction vessel. The reaction mixture was shaken for 72 h at room temperature. The resin was collected by filtration and washed with water (2 × 25 mL), DMF (2 × 25 mL), DCM (2 × 25 mL), and anhydrous MeOH (2 × 25 mL), and dried under vacuum to afford **4.6** (248 mg, 95%). IR (cm^{-1}): 3056 (N-H), 3017 (N-H), 1683 (C=O amide), 1659 (C=O amide).

3′-Fluoro-3′-deoxythymidine (4.7). Resin **4.6** (248 mg) was suspended in DCM containing 3% TFA (10 mL) and was shaken at room temperature for 1 h. The resin was collected by filtration. The filtrate was concentrated under reduced pressure and purified by silica-gel column chromatography using DCM and methanol as eluents (98:2, v/v) to afford FLT (39 mg, 55%). ^{1}H NMR, ^{13}C NMR, and high resolution time-of-flight electrospray mass spectrometry confirmed the structure of the compound. Melting point (177-178 °C) (reported mp 176-177 °C) (Herdewijn et al., 1987) and the NMR data corresponded to those reported in the literature (Herdewijn et al., 1987, Sahlberg et al., 1992, Hager et al., 1992, Kumar et al., 2004, Yun et al., 2003). High resolution ESI-MS for FLT **(4.7)** ($C_{10}H_{13}FN_2O_4$) cacld, 244.2196; found, 267.2051 $[M + Na]^+$.

4.4. Results and Discussion

Recent phase IIa clinical trials of FLT for the treatment of patients with multidrug-resistant human immunodeficiency virus infection showed promising results without any serious side effects. Furthermore, [^{18}F] FLT has been proposed as a new marker for imaging tumor proliferation by PET. Thus, there is an increased research interest in studying the biological properties of FLT. We designed a solid-phase method for the synthesis of FLT.

Scheme 4.1 displays the solid-phase synthesis of FLT. 5'-Hydroxyl group of thymidine (**4.1**) was immobilized on trityl chloride resin (**4.2**) in the presence of pyridine to yield polymer-bound thymidine (**4.3**, 91%). Resin **4.3** was subjected to reaction with methanesulfonyl chloride in the presence of pyridine to afford polymer-bound 3'-*O*-mesylthymidine (**4.4**, 98%). The reaction of **4.4** with sodium hydroxide in DMF for 48 h gave polymer-bound threothymidine (**4.5**, 98%). Diethylaminosulfur trifluoride (DAST) was added to the suspension of resin **4.5** in anhydrous benzene and THF to produce polymer-bound FLT (**4.6**, 95%). The reaction was continued for 72 h. Washing and acidic cleave of trityl resin with TFA/DCM (3%) afforded FLT (**4.7**, 55%) (overall yield 45%) (Scheme 1).

Scheme 4.2 shows the solution-phase synthesis of FLT according to the modified reported procedure (Yun et al., 2003). Thymidine was converted to 5′-*O*-(4,4′-dimethoxytrityl)thymidine **4.8** (90%) in the presence of 4,4′-dimethoxytrityl chloride and dry pyridine. Subsequent mesylation of 3′-hydroxyl group in **4.8** with

methanesulfonyl chloride in the presence of pyridine afforded 5′-*O*-(4,4′-dimethoxytrityl)-3′-*O*-mesylthymidine **4.9** (94%). Basic hydrolysis of **4.9** with ethanolic sodium hydroxide afforded 5′-*O*-(4,4′-dimethoxytrityl)threothymidine **4.10**, which was fluorinated with DAST and sequential acidic deprotection to afford FLT (**4.7**, 23%) (overall yield 19%).

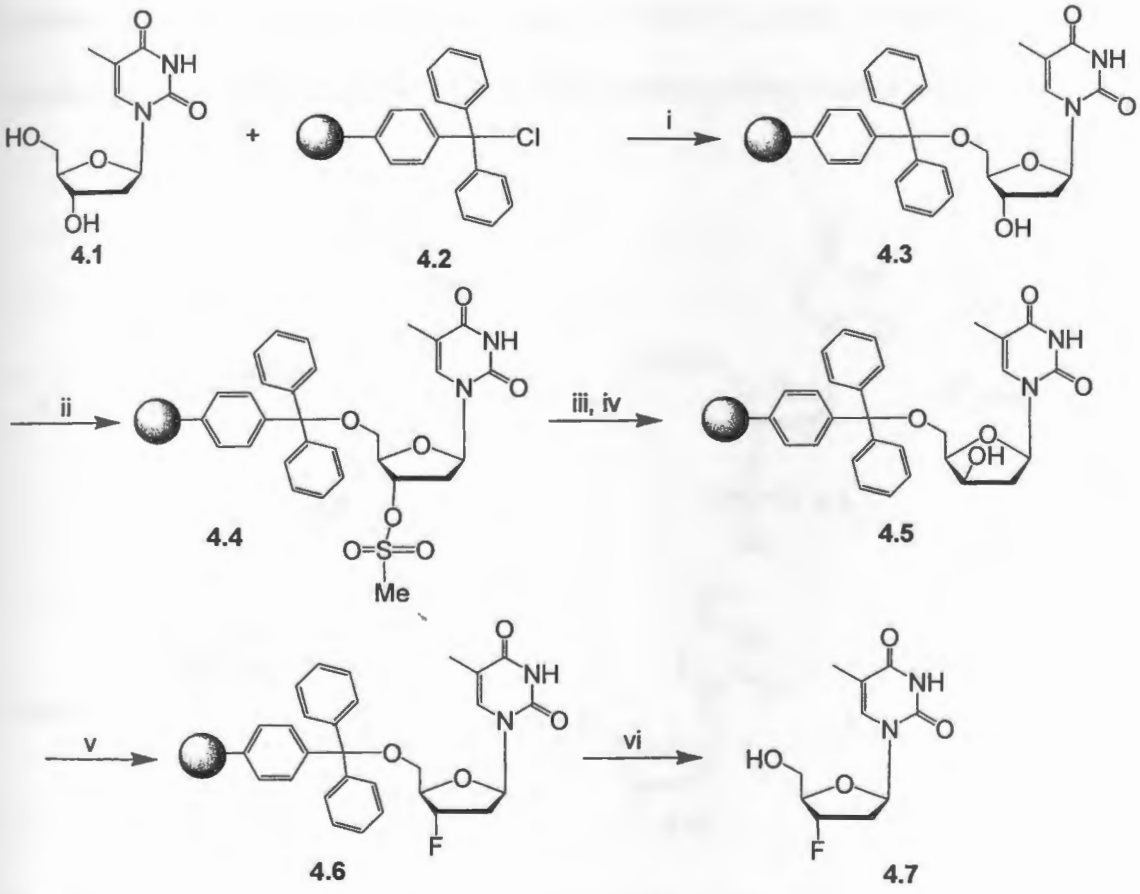

Scheme 4.1. Solid-phase synthesis of FLT. Reagents: (i) pyridine, 48 h; (ii) MsCl, pyridine, 48 h; (iii) NaOH (1N), DMF, H_2O, 24 h; (iv) NaOH (1N), reflux, 24 h; (v) DAST, benzene, THF, 72 h; (vi) TFA/DCM (3%), 1 h.

The novelty of the method lies in its simplicity. Thymidine is mixed with trityl chloride and is thereby "captured" as an immobilized compound through the 5′-hydroxyl group. Washing the support allows for the recovery of an excess of thymidine and removal of unreacted reagents, and guarantees that no unreacted starting materials remain. This makes the method very economical and cost-effective. Trityl chloride resin has a hindered structure, thereby allowing for the regioselective reaction. The most reactive hydroxyl group (5′-hydroxyl group) of thymidine reacts selectively with hindered resin when an excess amount of thymidine (4 eq) is used.

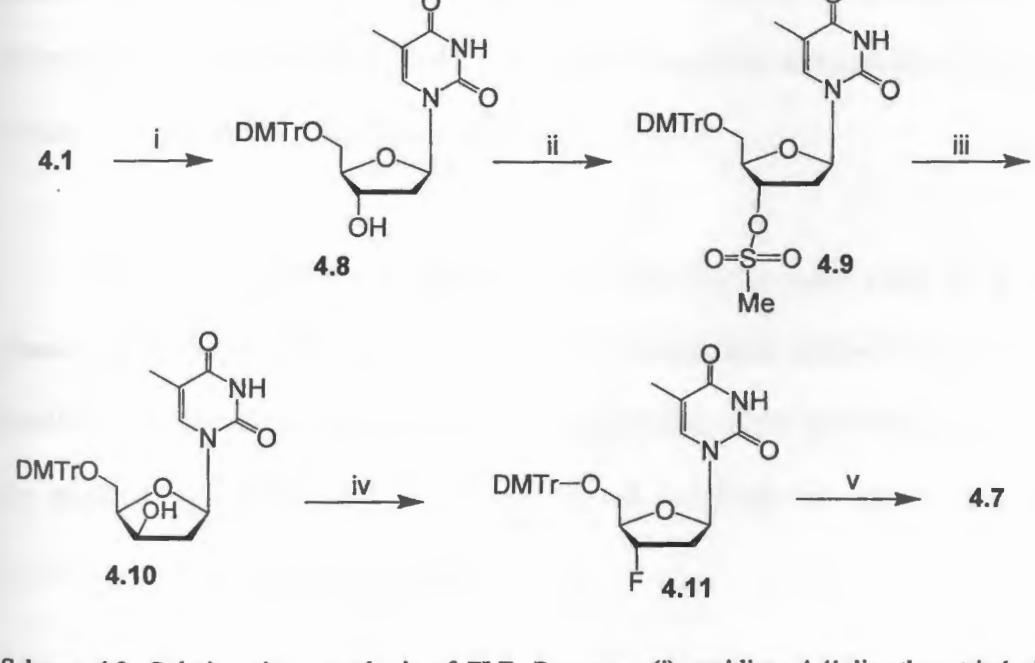

Scheme 4.2. Solution-phase synthesis of FLT. Reagents: (i) pyridine, 4,4′-dimethoxytrityl chloride (DMTrCl), 3 h; (ii) MsCl, pyridine, 3 h; (iii) NaOH (1 N), EtOH, 12 h (RT), 3 h (reflux); (iv) DAST, benzene, THF, 2 h; (vi) CH_3COOH (80%), 15 min, reflux.

This solid-phase strategy allowed the synthesis of FLT in a short time when compared to the solution-phase approaches. The synthesis was accomplished without

the need for purification of intermediates. The intermediates and the final compound remained trapped on the resin, which facilitated the separation of any unreacted reagent by washing and filtration. The solid-phase method allowed facile isolation and recovery of the final product.

Reported solution-phase approaches to the synthesis of FLT include a variety of protecting groups (Herdewijn et al., 1987, Sahlberg et al., 1992, Hager et al., 1992, Kumar et al., 2004). For example, in a parallel modified solution-phase method, (Yun et al., 2003) 5′-hydroxyl group of thymidine was protected by 4,4′-dimethoxytrityl group to afford **4.8**. Subsequent mesylation, basic hydrolysis, fluorination, and acidic cleavage reactions afforded FLT (**4.7**). All the intermediates were purified by silica gel column chromatography in a time consuming process.

FLT was synthesized in a higher overall yield (45% overall yield) by the solid-phase method when compared to that for the solution-phase method[18] carried out in parallel (19% overall yield). The successful application of the solid-phase strategy for the synthesis of FLT provides insight for the synthesis of other 3′-substituted nucleosides using a similar methodology.

4.5. References

Calvez, V.; Tubiana, R.; Ghosn, J.; Wirden, M.; Marcelin, A. G.; Westling, C.; Shoen, H.; Harmenberg, J.; Mardh, G.; Oberg, B.; Katlama, C. MIV-310 reduces markedly viral load in patients with virological failure despite multiple-drug therapy: Results from a 4-week phase II study. *Antivir. Ther.*, **2002**, 7, Abs S4.

Cheng, Y.C.; Dutschman, G.E.; Baston, K.F.; Sarngadharan, M.G.; Ting R.Y.C. Human immunodeficiency virus reverse transcriptase: general properties and its interactions with nucleotide triphosphate analogs. *J. Biol. Chem.* **1987**, 262, 2187–2189.

Hager, M. W.; Liotta, D. C. An efficient synthesis of 3'-fluoro-3'-deoxythymidine (FLT). *Tet. Lett.*, **1992**, 33, 7083–7086.

Herdewijn, P.; Balzarini, J.; De Clercq, E.; Pauwels, R.; Baba, M.; Broder, S.; Vanderhaeghe, H. 3'-Substituted 2',3'-dideoxynucleoside analogues as potential anti-HIV (HTLV-III/LAV) agents. *J. Med. Chem.*, **1987**, 30, 1270–1278.

Hoshi, A.; Castaner, J. Alovudine. *Drugs Future*, **1994**, 19, 221–224.

Kong, X. B.; Zhu, Q.-Y.; Vidal, P.M.; Watanabe, K.A.; Polsky, B.; Armstrong, D.; Ostrander, M.; Lang, S.A.; Muchmore, E.; Chou, T.-C. Comparisons of anti-human immunodeficiency virus activities, cellular transport, and plasma and intracellular pharmacokinetics of 3′-fluoro-3′-deoxythymidine. *Antimicrob. Agents Chemother.*, **1992**, 36, 808–818.

Kim, E.Y.; Vrang, L.; Oberg, B.; Merigan, T.C. Anti-HIV type 1 activity of 3′-fluoro-3′-deoxythymidine for several different multi-drug-resistant mutants. *AIDS Res. Hum. Retroviruses.*, **2001**, 17, 401–407.

Kumar, P.; Ohkura, K.; Balzarini, J.; De Clercq, E.; Seki, K.; Wiebe, L. I. Synthesis and antiviral activity of novel fluorinated 2',3'-dideoxynucleosides. *Nucleosides Nucleotides Nucleic Acids,* **2004**, 23, 7–29.

Lundgren, B.; Bottiger, D.; Ljungdahl-Stahle, E.; Norrby, E.; Stahle, L.; Wahren, B.; Orberg, B. Antiviral effects of 3′-fluorothymidine and 3′-azidothymidine in cynomolgus monkeys infected with simian immunodeficiency virus. *J. Acquir. Immune Defic. Syndr.*, **1991**, 4, 489–498.

Matthes, E.; Lehmann, C.H.; Scholz, D.; Von Janta-Lipinski, M.; Gaerther, K.; Rosenthal, H.A.; Langen, P. Inhibition of HIV-associated reverse transcriptase by sugar-modified derivatives of thymidine 5'-triphosphate in comparison to cellular DNA polymerases A and B. *Biochem. Biophys. Res. Commun.*, **1987**, 148, 78–85.

Pan, X.-Z.; Qui, Z.-D.; Baron, P.A.; Gold, J.W. M.; Polsky, B.; Chou, T.-C.; Armstrong, D. Three-drug synergistic inhibition of HIV-1 replication in vitro by 3′-

fluoro-3′-deoxythymidine, recombinant soluble CD4 and recombinant interferon-alpha. *AIDS Res. Hum. Retroviruses*, **1992**, 8, 589–595.

Rusconi, S. Alovudine Medivir. *Curr. Opin. Invest. Drugs*, **2003**, 4, 219–223.

Sahlberg, C. Synthesis of 3'-ethynylthymidine, 3'-vinylthymidine and 3'-bromovinylthymidine as potential antiviral agents. *Tet. Lett.*, **1992**, 33, 679–682.

Seitz, U.; Wagner, M.; Neumaier, B.; Wawra, E.; Glatting, G.; Leder, G.; Schmid, R. M.; Reske, S. N. Evaluation of pyrimidine metabolising enzymes and in vitro uptake of 3'-[(18)F]fluoro-3'-deoxythymidine ([(18)F]FLT) in pancreatic cancer cell lines. *Eur. J. Nucl. Med. Mol. Imaging*, **2002**, 29, 1174–1181.

Shields, A. F.; Grierson, J. R.; Dohmen, B. M.; Machulla, H. J.; Stayanoff, J. C.; Lawhorn-Crews, J. M.; Obradovich, J. E.; Muzik, O.; Mangner, T. J. Imaging proliferation in vivo with [F-18]FLT and positron emission tomography. *Nature Med.*, **1998**, 4, 1334–1336.

Wagner, M.; Seitz, U.; Buck, A.; Neumaier, B.; Schultheiss, S.; Bangerter, M.; Bommer, M.; Leithauser, F.; Wawra, E.; Munzert, G.; Reske, S. N. 3'-[^{18}F]fluoro-3'-deoxythymidine ([^{18}F]-FLT) as positron emission tomography tracer for imaging proliferation in a murine B-Cell lymphoma model and in the human disease. *Cancer Res.*, **2003**, 63, 2681–2687.

Wodarski, C.; Eisenbarth, J.; Weber, K.; Henze, M.; Haberkorn, U.; Eisenhut, M. Synthesis of 3′-deoxy-3′-[^{18}F]fluoro-thymidine with 2,3′-*O*-anhydro-5′-*O*-(4,4′-dimethoxy-trityl)thymidine. *J. Lab. Compds. Radiopharm.*, **2000**, 43, 1211–1218.

Yun, M.; Oh, S. J.; Ha, H.-J.; Ryu, J. S., Moon, D. H. High radiochemical yield synthesis of 3′-deoxy-3′-[^{18}F]fluorothymidine using (5′-*O*-dimethoxytrityl-2′-deoxy-3′-*O*-nosyl-β-D-*threo* pentofuranosyl)thymine and its 3-*N*-BOC-protected analogue as a labeling precursor. *Nucl. Med. Biol.*, **2003**, 30, 151–157.

Chapter 5

Synthesis and Anti-HIV Activities of Phosphate Triester Derivatives of 3′-Fluoro-2′,3′-dideoxythymidine and 3′-Azido-2′,3′-dideoxythymidine

Hitesh K. Agarwal,[a] Gustavo F. Doncel,[b] Keykavous Parang[a]

[a]Department of Biomedical and Pharmaceutical Sciences, University of Rhode Island, Kingston, RI, 02881, USA; [b]CONRAD, Department of Obstetrics and Gynecology, Eastern Virginia Medical School, Norfolk, VA 23507, USA.

Published in *Tetrahedron Letters*, **2008**, 49, 4905-4907.

5.1. Abstract

Fatty acyl-glycol phosphate triester conjugates of 3′-fluoro-2′,3′-dideoxythymidine (FLT) were prepared in three steps from the reaction of diisopropylphoramidous dichloride with fatty acyl-substituted glycols, followed by a coupling reaction with FLT and oxidation with *tert*-butyl hydroperoxide (*t*-BuOOH). Additionally, a number of fatty alcohols were reacted with diisopropylphoramidous dichloride to produce the phosphitylating intermediates, which underwent coupling reactions with 3′-azido-2′,3′-dideoxythymidine (AZT) and FLT followed by oxidation with *t*-BuOOH to yield fatty alcohol phosphate triester derivatives of AZT and FLT.

5.2. Introduction

2′,3′-Dideoxynucleoside analogs are used clinically against the human immunodeficiency virus (HIV). There are numerous reasons to utilize nucleotide prodrug strategy in order to make anti-HIV nucleosides more effective against the virus. Bypassing the first rate-limiting phosphorylation step (Van et al., 1990), increasing the lipophilicity, and enhancing the cellular uptake and half-life in blood are some of them (Parang et al., 2000).

On entering the cell, the majority of anti-HIV nucleoside analogs, such as 3′-fluoro-2′,3′-dideoxythymidine (FLT, alovudine) and 3′-azido-2′,3′-dideoxythymidine (AZT, zidovudine), are phosphorylated to monophosphates, diphosphates, and

triphosphates forms by host cellular kinases to show antiviral activity. Negatively-charged nucleoside monophosphates cannot be directly used because of their high polarity and poor cellular uptake. Furthermore, they are readily dephosphorylated on cell surfaces and in extracellular fluids by non-specific phosphohydrolases. In order to bypass the first rate-limiting phosphorylation step in the metabolic conversion of nucleoside analogs, numerous prodrugs of 5′-monophosphate types, such as neutral species of phosphotriester derivatives of nucleosides have been proposed (Parang et al., 2000, Meier et al., 2004, Rose et al., 2005, Thumann et al., 2996, Meier et al., 2002, Meier et al., 2006, Farquhar et al., 1994, Jochum et al., 2005) with the hope that these prodrugs would release the corresponding nucleoside-monophosphates intracellularly. The phosphotriesters must have acceptable stability prior to cellular uptake and selective intracellular biotransformation of the active species. Furthermore, extensive efforts have been carried out to synthesize lipophilic prodrugs of anti-HIV nucleosides by esterification strategy (Parang et al., 2000, Parang et al., 1998, Parang et al., 1998, Parang et al., 1998). Both strategies have not yet provided an anti-HIV prodrug agent with a clear-cut therapeutic advantage for clinical use. The major challenge of developing nucleotide prodrugs has been in the selection of a suitable phosphate-masking group. By judicious choice of the alcohols used in triester formation, it may be possible to improve cellular uptake and to direct intracellular hydrolysis to nucleoside monophosphates. Thus, further research to identify prodrugs containing both phosphotriester and lipophilic groups with distinct advantages, relative to parent anti-HIV nucleosides is warranted.

Herein, we report the synthesis of uncharged fatty acyl and fatty alcohol phosphotriester derivatives of AZT and FLT (Figure 5.1). The lipophilic moieties, fatty acyls or fatty alcohols, were incorporated into the structure with the aim of improving interaction with membrane bilayers and cellular uptake of anti-HIV nucleoside phosphotriester derivatives and to release nucleoside monophosphates intracellularly, bypassing the first phosphorylation step (Figure 5.2).

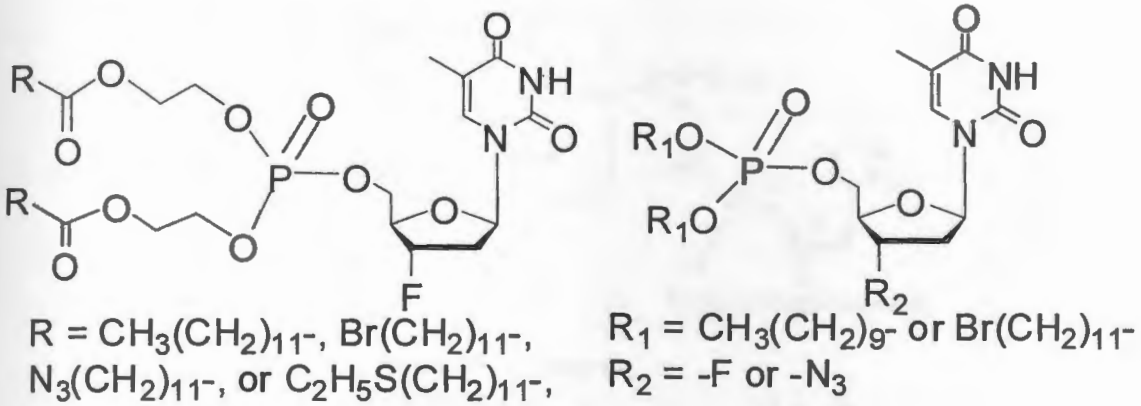

Figure 5.1. Fatty acyl and fatty alcohol phosphotriester derivatives of AZT and FLT.

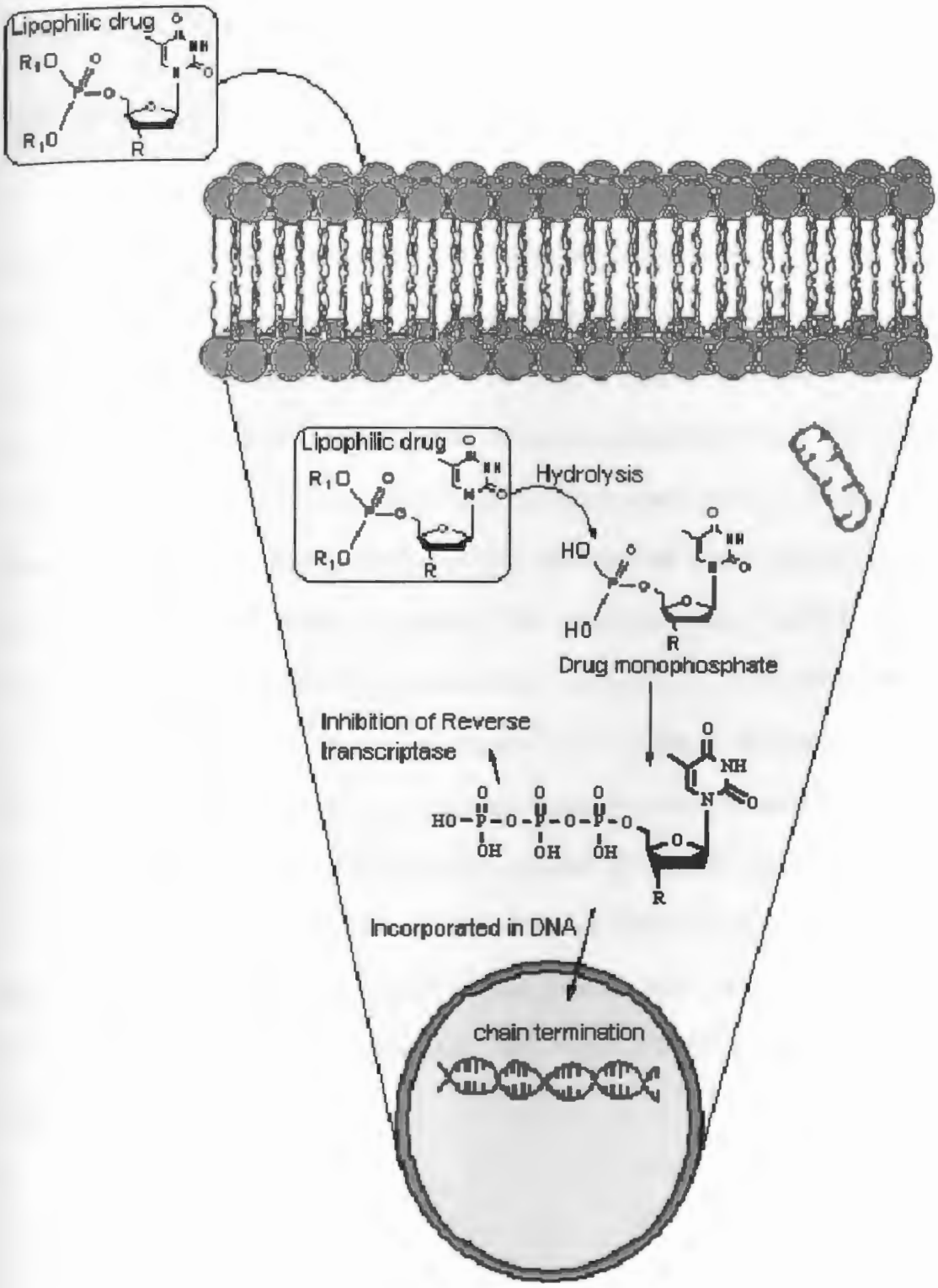

Figure 5.2. Proposed mechanism for cellular uptake and intracellular hydrolysis of uncharged phosphotriester derivatives of nucleosides.

5.3. Materials and Methods

5.3.1. Materials

Alovudine (FLT) was synthesized according to the previously reported method (Herdewijn et al., 1987). Zidovudine (AZT) was purchased from Euro Asia Tran Continental (Bombay, India). 12-Bromododecanoic acid and 5-ethyl-1*H*-tetrazole were purchased from Sigma Aldrich. All the other chemicals including myristoyl chloride, glycol, *tert*-butyl hydroperoxide, diisopropylphosphoramidous dichloride, sodium hydride, sodium iodide, ethanethiol, dimethylamino pyridine (DMAP), 12-crown-4-ether, *N*,*N*-dimethylformamide (DMF), benzene and tetrahydrofuran (THF) were purchased from Fisher scientific. The products were purified on a Phenomenex®Jupiter 10 μm ODS reversed-phase column (2.1 × 25 cm) with Hitachi HPLC L-7150 system with diode array detector. The chemical structures of final desalted products were characterized by nuclear magnetic resonance spectrometry (^{1}H NMR, ^{13}C NMR, ^{31}P NMR) determined on a Bruker DPX NMR spectrometer (400 MHz). ^{13}C NMR spectra are fully decoupled. Chemical shifts are reported in parts per millions (ppm). The chemical structures of final products were confirmed by a high-resolution PE Biosystems Mariner API 2000 time-of-flight electrospray mass spectrometer.

5.3.2. Chemistry

2-Hydroxyethyl tetradecanoate (5.1) and 2-hydroxyethyl 12-bromododecanoate (5.2). A mixture of ethylene glycol (1 mL, 18 mmol) and fatty acyl chloride (4 mmol) were refluxed for 3 h in the presence of DMAP (600 mg, 5 mmol) as a base in dry benzene (10 mL) and DMF (10 mL). The reaction mixture was cooled down to room temperature and neutralized with sodium bicarbonate solution (5%). The organic layer was separated and the aqueous layer was extracted with DCM (3 x 100 mL). The organic layers were mixed together, dried with anhydrous sodium sulfate, and evaporated under vacuum. Crude products were purified by using silica gel column chromatography and hexane and dichloromethane (50:50) as eluting solvents to afford **5.1** and **5.2** in 70% yield.

2-Hydroxyethyl tetradecanoate (5.1). ^{1}H NMR (400 MHz, $CDCl_3$, δ ppm): δ 4.16 (t, J = 4.8 Hz, 2H, COOCH_2), 3.76 (t, J = 4.8 Hz, 2H, CH_2OH), 2.78-2.89 (br s, 1H, O*H*), 2.30 (t, J = 7.6 Hz, 2H, CH_2COO), 1.59-1.70 (m, 2H, CH_2CH$_2$COO), 1.20-1.41 (br m, 20H, methylene envelope), 0.84 (t, J = 6.8 Hz, 3H, CH_3); ^{13}C NMR ($CDCl_3$, 100 MHz, δ ppm): 174.72 (*C*OO), 66.20 (COO*C*H$_2$), 61.35 (*C*H$_2$OH), 34.54 (*C*H$_2$COO), 32.23, 30.06, 30.03, 29.94, 29.84, 29.74, 29.66, 29.52, 25.27, 23.06 (methylene carbons), 14.48 (*C*H$_3$); HR-MS (ESI-TOF) (m/z): $C_{16}H_{32}O_3$: calcd. 272.2351; found 273.6315 $[M + H]^+$.

2-Hydroxyethyl 12-bromododecanoate (5.2). ^{1}H NMR (400 MHz, $CDCl_3$, δ ppm): δ 4.16 (t, J = 4.7 Hz, 2H, COOCH_2), 3.78 (t, J = 4.7 Hz, 2H, CH_2OH), 3.37 (t, J = 6.9

Hz, 2H, CH_2Br), 2.40-2.52 (br s, 1H, OH), 2.31 (t, J = 7.7 Hz, 2H, CH_2COO), 1.78-1.87 (m, 2H, BrCH$_2$CH_2), 1.53-1.65 (m, 2H, CH_2CH$_2$CO), 1.35-1.45 (m, 2H, BrCH$_2$CH$_2$CH_2), 1.20-1.35 (please give a range) (br m, 12H, methylene envelope); ^{13}C NMR ($CDCl_3$, 100 MHz, δ ppm): 174.36 (*C*OO), 65.96 (COO*C*H$_2$), 61.20 (*C*H$_2$OH), 34.25 (*C*H$_2$COO, *C*H$_2$Br), 32.90, 29.52, 29.47, 29.31, 29.19, 28.82, 28.23, 24.97 (methylene carbons); HR-MS (ESI-TOF) (m/z): $C_{14}H_{27}BrO_3$: calcd. 322.1144; found 323.5677 $[M + H]^+$.

2-Hydroxyethyl 12-iododododecanoate (5.3). Compound **5.2** (1.7 g, 5.3 mmol) was mixed with sodium iodide (1.6 g, 10.7 mmol) in dry acetone (100 mL) and the reaction mixture was stirred for 18 h at room temperature. After filtration, water (250 mL) was added to the filtrate and extracted with dichloromethane (3 x 100 mL). The organic layers were mixed together, dried with anhydrous sodium sulfate, concentrated under vacuum, and dried overnight to give **5.2** (95% yield).

^{1}H NMR (400 MHz, $CDCl_3$, δ ppm): δ 4.20-4.27 (m, 2H, COOCH_2), 3.80-3.86 (m, 2H, CH_2OH), 3.17 (t, J = 7.0 Hz, 2H, CH_2I), 2.33 (t, J = 7.5 Hz, 2H, CH_2COO), 2.15-2.30 (br s, 1H, OH), 1.74-1.84 (m, 2H, ICH$_2$CH_2), 1.58-1.69 (m, 2H, CH_2CH$_2$CO), 1.35-1.42 (m, 2H, ICH$_2$CH$_2$CH_2), 1.22-1.35 (br m, 12H, methylene protons); ^{13}C NMR ($CDCl_3$, 100 MHz, δ ppm): 174.17 (*C*OO), 65.82 (COO*C*H$_2$), 61.17 (*C*H$_2$OH), 34.10 (*C*H$_2$COO), 33.46, 30.41, 29.36, 29.29, 29.14, 29.03, 28.43, 24.82 (methylene carbons), 7.31 (*C*H$_2$I); HR-MS (ESI-TOF) (m/z): $C_{14}H_{27}IO_3$: calcd. 370.1005; found 393.0269 $[M + Na]^+$.

2-Hydroxyethyl 12-azidododecanoate (5.4). Compound **5.3** (1.8 g, 4.9 mmol) was mixed with sodium azide (1 g, 15.4 mmol) and 12-crown-4 ether (2.6 mL, 15.9 mmol) in DMF (100 mL). The reaction mixture was stirred overnight at room temperature. The solvent was evaporated using reduced pressure and the crude product was purified using silica gel column chromatography and hexane and dichloromethane (50:50) as eluting solvents to afford **5.4** (55% yield).

^{1}H NMR (400 MHz, $CDCl_3$, δ ppm): δ 4.18 (t, J = 4.7 Hz, 2H, COOCH_2), 3.79 (t, J = 4.7 Hz, 2H, CH_2OH), 3.23 (t, J = 7.0 Hz, 2H, CH_2N_3), 2.23 (t, J = 7.7 Hz, 2H, CH_2COO), 1.50-1.64 (m, 4H, $N_3CH_2CH_2$, CH_2CH_2CO), 1.15-1.45 (br m, 14H, methylene envelope); ^{13}C NMR ($CDCl_3$, 100 MHz, δ ppm): 174.17 (*C*OO), 65.77 (COO*C*H_2), 61.05 (*C*H_2OH), 51.34 (*C*H_2N_3), 34.05 (*C*H_2COO), 29.31, 29.26, 29.11, 28.98, 28.70, 26.57, 24.77 (methylene carbons); HR-MS (ESI-TOF) (m/z): $C_{14}H_{27}N_3O_3$: calcd. 285.2052; found 308.1454 $[M + Na]^+$.

2-Hydroxyethyl 13-thiapentadecanoate (5.5). 2-Hydroxyethyl-12-bromododecanoate **(5.2)** (2.0 g, 6.2 mmol) was added to a mixture containing sodium hydride (200 mg, 8.3 mmol) and ethanethiol (470 mg, 7.6 mmol) in dry THF (50 mL). The mixture was stirred at room temperature for 1 h and then refluxed for 16 h. The reaction mixture was cooled down to the room temperature and water (200 mL) was added to it. The solution was extracted with dichloromethane (3 x 100 mL). The organic layer was separated, dried with anhydrous sodium sulfate, and evaporated under vacuum. The crude product was purified using silica gel column

chromatography and hexane and dichloromethane (50:50) as eluting solvents to afford **5.5** (60% yield).

^{1}H NMR (400 MHz, $CDCl_3$, δ ppm): δ 4.16 (t, J = 4.7 Hz, 2H, COOCH_2), 3.78 (t, J = 4.7 Hz, 2H, CH_2OH), 2.56-2.64 (br s, 1H, O*H*), 2.40-2.56 (m, 4H, CH_2SCH_2), 2.31 (t, J = 7.7 Hz, 2H, CH_2COO), 1.50-1.65 (m, 4H, SCH_2CH_2, and CH_2CH_2CO), 1.14-1.40 (br m, 17H, methylene envelope, CH_3CH_2S); ^{13}C NMR ($CDCl_3$, 100 MHz, δ ppm): 174.66 (*C*OO), 66.24 (COO*C*H_2), 61.42 (*C*H_2OH), 34.54 (*C*H_2COO), 31.90, 29.99, 29.66, 29.78, 29.61, 29.49, 29.31, 26.42, 25.26 (methylene carbons), 15.19 (*C*H_3); HR-MS (ESI-TOF) (m/z): $C_{16}H_{32}O_3S$: calcd. 304.2072; found 327.2986 $[M + Na]^+$, 343.2708 $[M + K]^+$.

Synthesis of fatty acyl-glycol ester conjugates 5.14-5.17. Diisopropylphosphoramidous dichloride (0.5 equivalent, 300 mg, 1.5 mmol) and DMAP (1 equiv., 360 mg, 3 mmol) were dissolved in THF (100 mL) and cooled down to -80 °C. Solution of **5.1-5.5** (800 mg, 3 mmol) in THF (20 mL) was added dropwise to the reaction mixture with constant stirring during 1 h period. The reaction mixture was continued to stir for 3 h to yield intermediates **5.6-5.9**. DMAP hydrochloride was filtered out and FLT (0.5 equiv, 350 mg, 1.5 mmol) and 5-ethyl-1*H*-tetrazole (585 mg, 4.5 mmol) were added to the reaction mixture and stirred overnight to produce **5.10-5.13**. *t*-BuOOH in decane (5-6 M) (450 µL, 4.5 mmol) was added to the reaction mixture and stirring was continued for 4 h. To the reaction mixture was added water (100 mL) and the solution extracted with dichloromethane (3 x 50 mL). The organic layer was dried with anhydrous sodium sulfate and evaporated under vacuum. The

crude products were purified using reverse-phase HPLC and acetonitrile (100%) as the eluting solvent to afford **5.14-5.17** in 7-17% overall yield (70-180 mg).

3′-Fluoro-2′,3′-dideoxythymidine-5′-[(bis(2-tetradecanoylglycolyl]phosphate (5.14). ^{1}H NMR (400 MHz, $CDCl_3$, δ ppm): δ 8.27 (s, 1H, N-*H*), 7.41 (s, 1H, H-6), 6.42 (dd, *J* = 9.2 and 5.4 Hz, 1H, H-1′), 5.30 (dd, *J* = 53.2 and 4.9 Hz, 1H, H-3′), 4.40 (dd, *J* = 26.6 and 2.5 Hz, 1H, H-4′), 4.25-4.34 (br m, 10H, H-5′ and H-5″, $COOCH_2CH_2O$), 2.53-2.67 (m, 1H, H-2′), 2.30-2.38 (m, 4H, CH_2CO), 2.09-2.28 (m, 1H, H-2″), 1.95 (s, 3H, 5-CH_3), 1.56-1.66 (m, 4H, CH_2CH_2CO), 1.21-1.35 (br m, 40H, methylene envelope), 0.89 (t, *J* = 6.80 Hz, 3H, CH_3); ^{13}C NMR ($CDCl_3$, 100 MHz, δ ppm): 173.38 (*C*OO), 163.08 (C-4 *C*=O), 152.99 (C-2 *C*=O), 135.01 (C-6), 112.20 (C-5), 93.35 (*J* = 178.6 Hz, C-3′), 84.93 (C-1′), 82.71 (*J* = 27.1 Hz, C-4′), 66.84 (CH_2-OP), 66.07 ($COOCH_2$), 62.44 (C-5′), 37.93 (*J* = 20.7 Hz, C-2′), 33.99 (CH_2COO), 31.91, 29.65, 29.61, 29.47, 29.35, 29.28, 29.13, 24.80, 22.69 (methylene carbons), 14.12 (CH_3), 12.41 (5-CH_3); ^{31}P NMR ($CDCl_3$, H_3PO_4 85% in water as external standard, 162 MHz, δ ppm): 4.79; HR-MS (ESI-TOF) (m/z): $C_{42}H_{74}FN_2O_{11}P$: calcd. 832.5014; found 855.4673 $[M + Na]^+$.

3′-Fluoro-2′,3′-dideoxythymidine-5′-[(bis(2-(12-bromododecanoyl)glycolyl)]phosphate (5.15). ^{1}H NMR (400 MHz, $CDCl_3$, δ ppm): δ 8.30 (s, 1H, N-*H*), 7.41 (s, 1H, H-6), 6.42 (dd, *J* = 9.2 and 5.4 Hz, 1H, H-1′), 5.25 (dd, *J* = 53.4 and 5.1 Hz, 1H, H-3′), 4.40 (dd, *J* = 26.6 and 2.5 Hz, 1H, H-4′), 4.25-4.33 (br m, 10H, H-5′, H-5″, and $COOCH_2CH_2O$), 3.54 (t, *J* = 6.8 Hz, 2H, $BrCH_2$),

3.42 (t, J = 6.8 Hz, 2H, BrCH_2), 2.55-2.67 (m, 1H, H-2′), 2.29-2.38 (m, 4H, CH_2CO), 2.09-2.28 (m, 1H, H-2″), 1.95 (s, 3H, 5-CH_3), 1.73-1.89 (m, 4H, CH_2CH$_2$Br), 1.57-1.67 (m, 4H, CH_2CH$_2$CO), 1.36-1.47 (m, 4H, CH_2CH$_2$CH$_2$CO), 1.20-1.35 (br m, 24H, methylene envelope); ^{13}C NMR ($CDCl_3$, 100 MHz, δ ppm): 173.81 (*C*OO), 163.79 (C-4 *C*=O), 150.61 (C-2 *C*=O), 135.44 (C-6), 112.20 (C-5), 93.79 (J = 178.0 Hz, C-3′), 85.33 (C-1′), 83.07 (J = 26.8 and 7.6 Hz, C-4′), 67.30 (J = 10.9 and 6.0 Hz, *C*H$_2$-OP), 66.54 (COO*C*H$_2$), 62.90 (J = 6.8 Hz, C-5′), 45.63 (*C*H$_2$Br), 38.32 (J = 21.2 Hz, C-2′), 34.45 (*C*H$_2$COO), 33.21, 30.10, 29.86, 29.79, 29.66, 29.50, 29.27, 29.15, 28.55, 27.26, 27.19 (methylene carbons), 12.85 (5-*C*H$_3$); ^{31}P NMR ($CDCl_3$, H_3PO_4 85% in water as external standard, 162 MHz, δ ppm): 4.78; HR-MS (ESI-TOF) (m/z): $C_{38}H_{64}Br_2FN_2O_{11}P$: calcd. 932.2599; found 955.4436 $[M + Na]^+$, 976.3518, $[M + 2Na]^+$.

3′-Fluoro-2′,3′-dideoxythymidine-5′-[(bis(2-(12-azidododecanoyl)glycolyl)]phosphate (5.16). ^{1}H NMR (400 MHz, $CDCl_3$, δ ppm): δ 9.37 (s, 1H, N-*H*), 7.39 (s, 1H, H-6), 6.41 (dd, J = 9.2 and 5.4 Hz, 1H, H-1′), 5.23 (dd, J = 53.4 and 5.1 Hz, 1H, H-3′), 4.38 (dd, J = 26.5 and 2.5 Hz, 1H, H-4′), 4.22-4.29 (br m, 10H, H-5′, H-5″, and COOCH_2CH_2O), 3.23 (t, J = 7.0 Hz, 4H, N_3CH_2), 2.53-2.70 (m, 1H, H-2′), 2.29-2.35 (m, 4H, CH_2CO), 2.10-2.30 (m, 1H, H-2″), 1.92 (s, 3H, 5-CH_3), 1.52-1.68 (m, 8H, N_3CH$_2$CH_2), 1.20-1.45 (br m, 28H, methylene envelope); ^{13}C NMR ($CDCl_3$, 100 MHz, δ ppm): 173.80 (*C*OO), 164.06 (C-4 *C*=O), 150.80 (C-2 *C*=O), 135.41 (C-6), 112.20 (C-5), 93.80 (J = 178.4 Hz, C-3′), 85.31 (C-1′), 83.55 (J = 26.8 and 7.9 Hz, C-4′), 67.27 (J = 5.7 and 10.9 Hz, *C*H$_2$-OP), 66.52 (COO*C*H$_2$),

62.91 (J = 5.0 Hz, C-5′), 51.85 (CH_2N_3), 38.31 (J = 20.9 Hz, C-2′), 34.36 (CH_2COO), 29.78, 29.72, 29.64, 29.62, 29.51, 29.21, 27.01, 25.18 (methylene carbons), 12.83 (5-CH_3); ^{31}P NMR ($CDCl_3$, H_3PO_4 85% in water as external standard, 162 MHz, δ ppm): 2.81; HR-MS (ESI-TOF) (m/z): $C_{38}H_{64}FN_8O_{11}P$: calcd. 858.4416; found 859.3552 $[M + H]^+$, 881.3245 $[M + Na]^+$, 897.2941 $[M + K]^+$.

3′-Fluoro-2′,3′-dideoxythymidine-5′-[(bis(2-(12-thioethyldodecanoyl)glycolyl)]phosphate (5.17). ^{1}H NMR (400 MHz, $CDCl_3$, δ ppm): δ 8.65 (s, 1H, N-H), 7.41 (s, 1H, H-6), 6.42 (dd, J = 9.2 and 5.4 Hz, 1H, H-1′), 5.25 (dd, J = 53.4 and 5.1 Hz, 1H, H-3′), 4.40 (dd, J = 26.5 and 2.5 Hz, 1H, H-4′), 4.25-4.35 (br m, 10H, H-5′, H-5″, and $COOCH_2CH_2O$), 2.59-2.75 (m, 1H, H-2′), 2.49-2.59 (m, 8H, CH_2SCH_2), 2.29-2.38 (m, 4H, CH_2CO), 2.09-2.29 (m, 1H, H-2″), 1.95 (s, 3H, 5-CH_3), 1.53-1.72 (m, 8H, CH_2CH_2S, CH_2CH_2CO), 1.20-1.39 (br m, 34H, methylene envelope, CH_3CH_2S); ^{13}C NMR ($CDCl_3$, 100 MHz, δ ppm): 173.80 (COO), 163.72 (C-4 C=O), 150.55 (C-2 C=O), 135.45 (C-6), 112.19 (C-5), 93.77 (J = 178.6 Hz, C-3′), 85.35 (C-1′), 83.07 (J = 26.8 and 7.8 Hz, C-4′), 67.28 (J = 11.1 and 5.6 Hz, CH_2-OP), 66.58 ($COOCH_2$), 62.90 (J = 5.1 Hz, C-5′), 38.34 (J = 21.1 Hz, C-2′), 34.40 (CH_2COO), 32.33, 32.06, 30.13, 30.05, 29.91, 29.84, 29.78, 29.65, 29.53, 29.36, 26.31, 26.31, 25.20 (methylene carbons), 15.23 (CH_3), 12.84 (5-CH_3); ^{31}P NMR ($CDCl_3$, H_3PO_4 85% in water as external standard, 162 MHz, δ ppm): 2.82; HR-MS (ESI-TOF) (m/z): $C_{42}H_{74}FN_2O_{11}PS_2$: calcd. 896.4456; found 897.3566 $[M + H]^+$.

Synthesis of fatty alcohol phosphotriester derivatives of AZT and FLT (5.23-5.25). Diisopropylphosphoramidous dichloride (0.5 equiv., 300 mg, 1.5 mmol) and DMAP (1 equiv., 360 mg, 3 mmol) were dissolved in THF (100 mL). The reaction mixture was cooled down to -80 °C. Solution of alcohols (800 mg, 3 mmol) in THF (20 mL) was added dropwise with constant stirring during 1 h period. The reaction mixture was continued to stir for 3 h to afford **5.18-5.19**. DMAP hydrochloride was filtered out and FLT or AZT (1.5 mmol) and 5-ethyl-1*H*-tetrazole (585 mg, 4.5 mmol) was added to the reaction mixture and stirred overnight to yield **5.20-5.22**. *t*-BuOOH in decane (5-6 M) (450 μL, 4.5 mmol) was added to the reaction mixture and stirring was continued for 4 h. To the reaction mixture was added water (100 mL) and the solution was extracted with dichloromethane (3 x 50 mL). The organic layer was dried with anhydrous sodium sulfate and evaporated under vacuum. The crude products were purified using reverse-phase HPLC and acetonitrile (100%) as the eluting solvent to afford **5.23-5.25** in 6-20% overall yield (45-180 mg).

3′-Fluoro-2′,3′-dideoxythymidine-5′-bis(decanoyl)-phosphate (5.23). ^{1}H NMR (400 MHz, $CDCl_3$, δ ppm): δ 9.71 (s, 1H, N-*H*), 7.44 (s, 1H, H-6), 6.44 (dd, J = 9.2 and 5.4 Hz, 1H, H-1′), 5.27 (dd, J = 53.2 and 4.9 Hz, 1H, H-3′), 4.37 (dd, J = 26.9 and 2.4 Hz, 1H, H-4′), 4.18-4.30 (m, 2H, H-5′ and H-5″), 4.00-4.09 (m, 4H, C*H*$_2$OP), 2.51-2.65 (m, 1H, H-2′), 1.95-2.19 (m, 1H, H-2″), 1.92 (s, 3H, 5-C*H*$_3$), 1.62-1.72 (m, 4H, C*H*$_2$CH$_2$OP), 1.17-1.38 (br m, 32H, methylene envelope), 0.85 (t, J = 6.7 Hz, 3H, C*H*$_3$); ^{13}C NMR ($CDCl_3$, 100 MHz, δ ppm): 164.32 (C-4 *C*=O), 150.98 (C-2 *C*=O), 135.32 (C-6), 112.20 (C-5), 94.09 (J = 178.0 Hz, C-3′), 85.06 (C-1′), 83.26 (J = 27.0

and 6.9 Hz, C-4′), 68.80 (*C*H$_2$OP), 66.89 (J = 11.3 and 4.8 Hz, C-5′), 38.54 (J = 20.7 Hz, C-2′), 32.25, 30.70, 30.10, 29.87, 29.66, 29.49, 25.79, 23.05 (methylene carbons), 14.49 (*C*H$_3$), 12.86 (5-*C*H$_3$); ^{31}P NMR (CDCl$_3$, H$_3$PO$_4$ 85% in water as external standard, 162 MHz, δ ppm): 5.09. HR-MS (ESI-TOF) (m/z): $C_{30}H_{54}FN_2O_7P$: calcd. 604.3653; found 605.0470 $[M + H]^+$, 642.9381 $[M + K]^+$.

3′-Fluoro-2′,3′-dideoxythymidine-5′-bis(11-bromoundecanoyl)phosphate (5.24): ^{1}H NMR (400 MHz, CDCl$_3$, δ ppm): δ 8.95 (s, 1H, N-*H*), 7.45 (s, 1H, H-6), 6.42 (dd, J = 9.2 and 5.4 Hz, 1H, H-1′), 5.25 (dd, J = 53.4 and 5.1 Hz, 1H, H-3′), 4.35 (dd, J = 26.6 and 2.5 Hz, 1H, H-4′), 4.18-4.28 (m, 2H, H-5′ and H-5″), 4.00-4.10 (m, 4H, C*H*$_2$OP), 3.35 (t, J = 6.8 Hz, 4H, BrC*H*$_2$), 2.52-2.65 (m, 1H, H-2′), 2.01-2.19 (m, 1H, H-2″), 1.92 (s, 3H, 5-C*H*$_3$), 1.80-1.89 (m, 4H, BrCH$_2$C*H*$_2$), 1.63-1.71 (m, 4H, C*H*$_2$CH$_2$OP), 1.33-1.44 (m, 4H, C*H*$_2$CH$_2$CH$_2$OP), 1.21-1.33 (br m, 24H, methylene envelope); ^{13}C NMR (CDCl$_3$, 100 MHz, δ ppm): 163.89 (C-4 *C*=O), 150.69 (C-2 *C*=O), 135.38 (C-6), 112.16 (C-5), 94.97 (J = 178.0 Hz, C-3′), 85.08 (C-1′), 83.56 (J = 27.0 Hz, C-4′), 68.79 (*C*H$_2$OP), 63.85 (C-5′), 53.43 (*C*H$_2$Br), 38.56 (J = 20.0 Hz, C-2′), 34.51, 33.18, 30.73, 30.66, 30.09, 29.95, 29.83, 29.80, 29.77, 29.48, 29.12, 28.53, 26.15, 25.80 (methylene carbons), 12.87 (5-*C*H$_3$); ^{31}P NMR (CDCl$_3$, H$_3$PO$_4$ 85% in water as external standard, 162 MHz, δ ppm): 5.03. HR-MS (ESI-TOF) (m/z): $C_{32}H_{56}Br_2FN_2O_7P$: calcd. 788.2176; found 789.9278 $[M + H]^+$.

3′-Azido-2′,3′-dideoxythymidine-5′-bis(decanoyl) phosphate (5.25): ^{1}H NMR (400 MHz, CDCl$_3$, δ ppm): δ 9.92 (s, 1H, N-*H*), 7.39 (s, 1H, H-6), 6.20 (t, J = 6.6 Hz, 1H,

H-1′), 4.26-4.33 (m, 1H, H-3′), 4.15-4.28 (m, 2H, H-5′ and H-5″), 3.95-4.05 (m, 5H, CH_2OP, H-4′), 2.34-2.42 (m, 1H, H-2′), 2.22-2.29 (m, 1H, H-2″), 1.87 (s, 3H, 5-CH_3), 1.55-1.68 (m, 4H, CH_2CH_2OP), 1.10-1.33 (br m, 40H, methylene envelope), 0.80 (t, J = 6.7 Hz, 3H, CH_3); ^{13}C NMR ($CDCl_3$, 100 MHz, δ ppm): 163.82 (C-4 C=O), 150.31 (C-2 C=O), 134.96 (C-6), 111.31 (C-5), 84.45 (C-1′), 82.14 (C-4′), 66.84 (CH_2OP), 59.98 (C-5′), 52.71 (C-3′), 37.33 (C-2′), 31.65, 30.11, 30.05, 29.47, 29.30, 29.15, 29.06, 28.90, 25.20, 22.45 (methylene carbons), 13.90 (CH_3), 12.28 (5-CH_3). ^{31}P NMR ($CDCl_3$, H_3PO_4 85% in water as external standard, 162 MHz, δ ppm): 5.08; HR-MS (ESI-TOF) (m/z): $C_{30}H_{54}N_5O_7P$: calcd. 627.3761; found 628.3108 $[M + H]^+$.

5.3.3. Anti-HIV assays

Anti-HIV activities of the compounds were evaluated according to the previously reported procedure (Krebs et al., 1999). In summary, HeLa (Human cervical carcinoma: ATCC CCL-2.1) cell line was used to measure inactivation of both cell-free virus preparations and virus-infected cell preparations. Cells were plated in culture plates 24 hrs prior to each experiment. Cell-free viral preparations of HIV-1 strains IIIB (lymphocytotropic strain) and BaL (monocytotropic strain) were used for cell-free assay. For cell-associated assay, SulT1 cells were infected with IIIB virus 5 days prior to the experiment. Cell-free virus and virus-infected cells were mixed with different compounds and diluted to make different concentrations. The mixture was further diluted with the buffer and added to the HeLa cells. The cells were incubated at 37°C for 48 h, stained for β-galctosidease expression and compared with β-

galctosidease expression from the β-gal-positive cells in absence of any microbicidal compound to get IC_{50} values.

5.4. Results and Discussion

In the first class of compounds, two identical fatty acids were linked through a glycol linker to a phosphate group, which was attached to 5'-*O*-position of FLT to afford bis(fatty acyl-glycol)phosphate triester derivatives. The selection of fatty acids was based on the previously reported moderate anti-HIV activities of 12-bromododecanoic acid, 12-azidododecanoic acid, and 12-thioethydodecanoic acid (Parang et al., 1997). In the second class of compounds, fatty alcohols and nucleosides, FLT and AZT, were directly attached to phosphotriester group.

The synthetic procedures used for the synthesis of phosphotriester derivatives of nucleosides were based on P(III) chemistry using phosphoramidite approach and consisted of three steps: (i) the derivatization of diisopropylphosphoramidous dichloride with fatty-acyl-glycols or fatty alcohols to afford phosphoramidites, (ii) the reaction of resulting phophoramidates with FLT or AZT in the presence of ethyl-1*H*-tetrazole, and (iii) oxidation of P(III) to P(V).

For the synthesis of compounds in the first class, fatty acid-glycol ester conjugates **5.1-5.5** (Scheme 5.1) were prepared. 2-Hydroxyethyl tetradecanoate **(5.1)**

and 2-hydroxyethyl 12-bromododecanoate **(5.2)** were synthesized (70% yield) from the treatment of the corresponding fatty acyl chloride (4 mmol) and ethylene glycol (18 mmol) in the presence of dimethylaminopyridine (DMAP) (5 mmol) in benzene and DMF (Scheme 5.1).

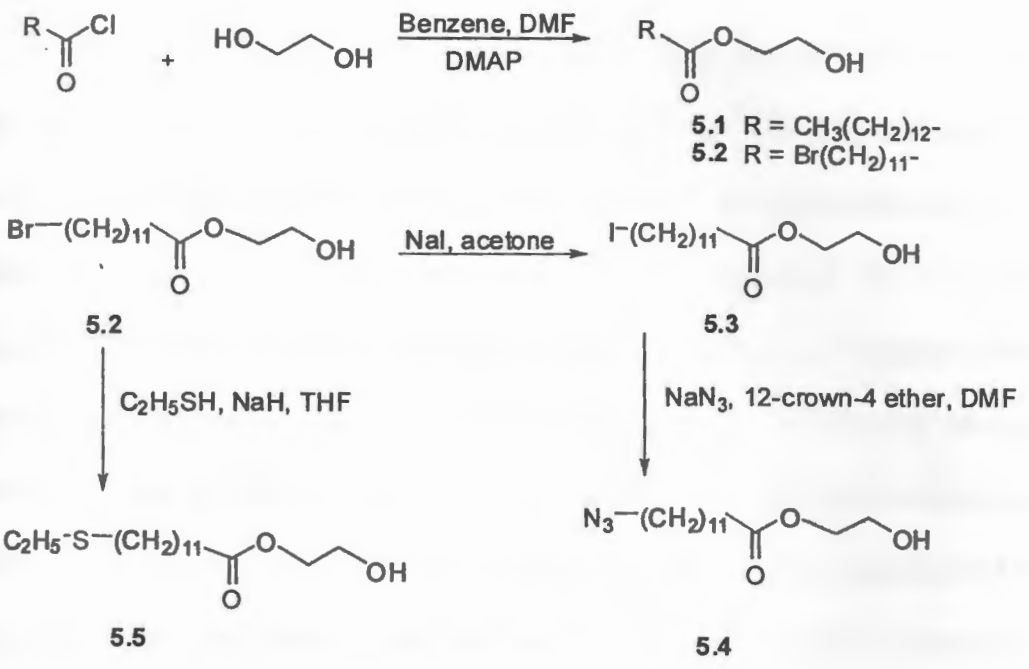

Scheme 5.1. Synthesis of fatty acid-glycol ester conjugates **5.1-5.5**.

2-Hydroxyethyl 12-bromododecanoate **(5.2)** was used for the synthesis of 2-hydroxyethyl 12-azidododecanoate **(5.4)** and 2-hydroxyethyl 13-thiapenatadecanoate **(5.5)**. Bromosubstituted ester conjugate **5.2** (5.3 mmol) was treated first with sodium iodide (10.7 mmol) in acetone to yield the corresponding iodosubstituted glycol ester **5.3** (95%). Compound **5.3** (4.9 mmol) was reacted with sodium azide (15.4 mmol) in the presence of 12-crown-4 ether (15.9 mmol) in DMF to yield **5.4** in 55% yield.

Similarly, nucleophilic reaction of ethanethiol (7.6 mmol) with **5.2** (6.2 mmol) in the presence of sodium hydride (8.3 mmol) afforded 12-thioethyl substituted analog **5.5** in 60% yield (Scheme 5.1).

Scheme 5.2 outlines the synthesis of bis(fatty acyl-glycol)phosphotriester derivatives of FLT (**5.14-5.17** using P(III) chemistry. In general, fatty acyl-glycol ester conjugates **5.1-5.5** (3 mmol) were treated in THF with diisopropylphosphoramidous dichloride (1.5 mmol) in the presence of DMAP (3 mmol) at -80 °C to afford intermediate bis(fatty acyl-glycol) diisopropyl phosphoramidite conjugates (**5.6-5.9**). Low temperature proved to be important for the success of this coupling reaction as shown by the failure of the reaction of **5.1** with diisopropylphosphoramidous dichloride in the presence of pyridine at room temperature. The intermediates **5.6-5.9** should be used immediately in the next reaction without purification because of the activity of the phosphorous in trivalent form in these compounds. Subsequent conversion of phosphoramidite intermediates to phosphotriesters was accomplished by treatment with FLT (1.5 mmol) in presence of 5-ethyl-1*H*-tetrazole (4.5 mmol) followed by in situ oxidation with *tert*-butyl hydroperoxide (*t*-BuOOH, 4.5 mmol) to obtain bis(fatty acyl-glycol)phosphotriester derivatives of FLT (**5.14-5.17**). The chemical structures of **5.14-5.17** were determined by ^{1}H NMR, ^{13}C NMR, ^{31}P NMR, and high-resolution ESI mass spectrometry (Table 5.1).

Table 5.1. The physicochemical characteristics and anti-HIV activities of compounds **5.14-5.17** and **5.23-5.25**.

Compd. No.	^{31}P NMR (δ, ppm)[a]	HR-MS (ESI-TOF)	Anti-HIV IC_{50} (uM)[b]	Overall Yield (%)
5.14	4.79	855.4673 $[M + Na]^+$	>100	6.3
5.15	4.78	955.4436 $[M + Na]^+$, 976.3518, $[M + 2Na]^+$.	63	7.7
5.16	2.81	859.3552 $[M + H]^+$, 881.3245 $[M + Na]^+$, 897.2941 $[M + K]^+$	76	6.5
5.17	2.82	897.3566 $[M + H]^+$	87	12.5
5.23	5.09	605.0470 $[M + H]^+$, 642.9381 $[M + K]^+$	>100	14.1
5.24	5.03	789.9278 $[M + H]^+$	33	7.0
5.25	5.08	628.3108 $[M + H]^+$	>100	19.8

[a]The spectra were measured on a 400 MHz spectrometer using $CDCl_3$ as the solvent (H_3PO_4 85% in water as external standard);

[b]IC_{50}: 50% inhibitory concentration.

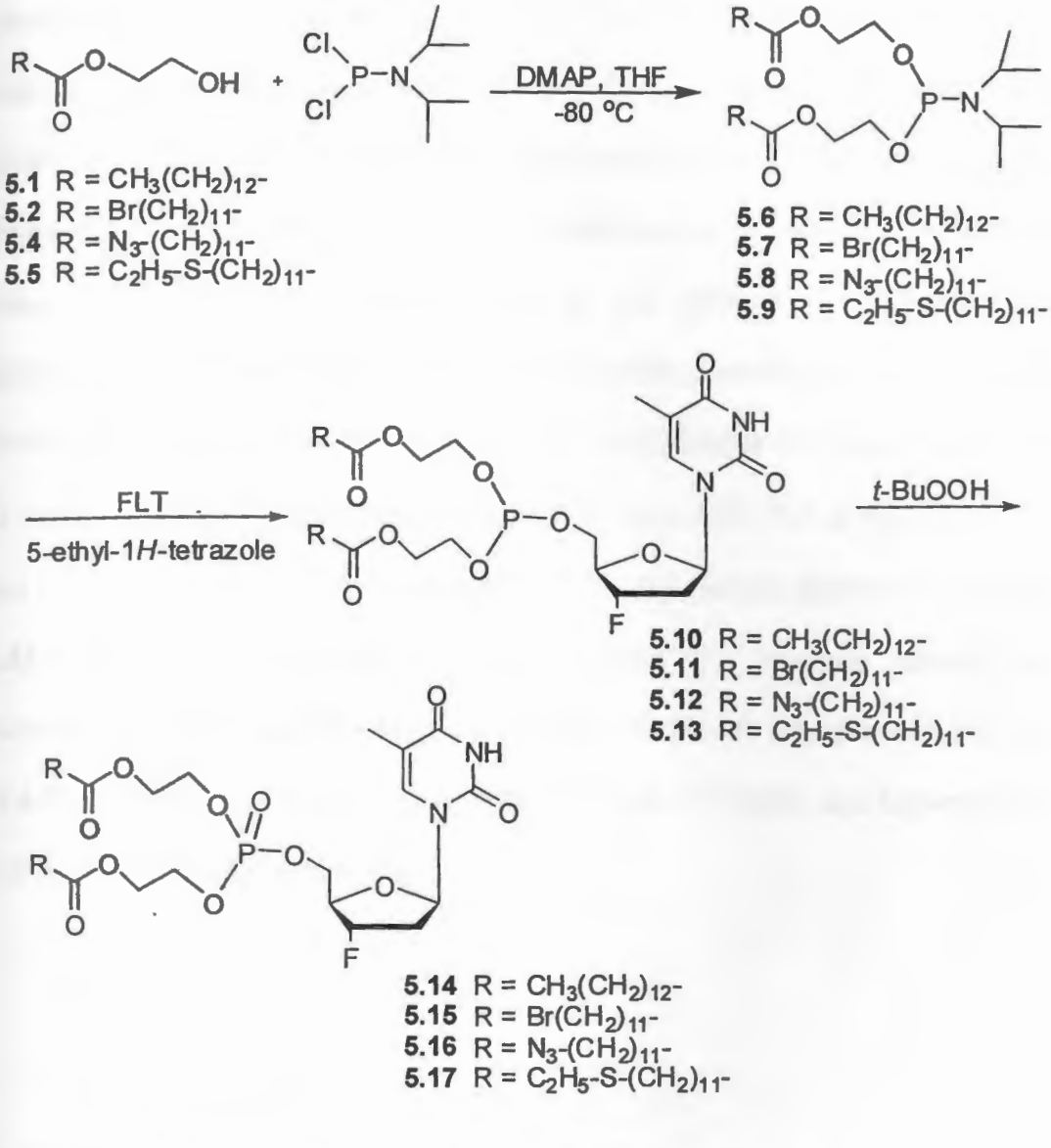

Scheme 5.2. Synthesis of fatty acyl-glycol ester conjugates **5.14-5.17**.

For the synthesis of fatty alcohol phosphotriester derivatives of the nucleosides, AZT was first attached to bis(diisopropyl-amino)chlorophosphine in the presence of pyridine. However, the intermediate was not stable during purification by silica gel column chromatography. Alternatively, the synthesis of fatty alcohol

phosphotriester derivatives of AZT and FLT **(5.20-5.22)** was accomplished by the reaction of dialkoxy substituted phosphitylating reagents, diisopropylamino dialkoxyphosphine, with AZT and FLT in the presence of 5-ethyl-1*H*-tetrazole in THF (Scheme 5.3). First dialkoxy substituted phosphitylating reagents were synthesized using diisopropylphosphoramidous dichloride and different fatty alcohols (i.e., decanol and 11-bromoundecanol). Solution of alcohols (3 mmol) in THF (20 mL) was added to a mixture of diisopropylphosphoramidous dichloride (1.5 mmol) and DMAP (3 mmol) in THF (100 mL) at -80 °C to afford **5.18** and **5.19**. FLT or AZT (1.5 mmol) and 5-ethyl-1*H*-tetrazole (4.5 mmol) were added to the reaction mixture to yield **5.20-5.22**. Oxidation of phosphite triesters **5.20-5.22** to phosphate triesters was accomplished with *t*-BuOOH (4.5 mmol) to afford **5.23-5.25**. The chemical structures of **5.23-5.25** were determined by ^{1}H NMR, ^{13}C NMR, ^{31}P NMR, and high-resolution ESI mass spectrometry (Table 5.1).

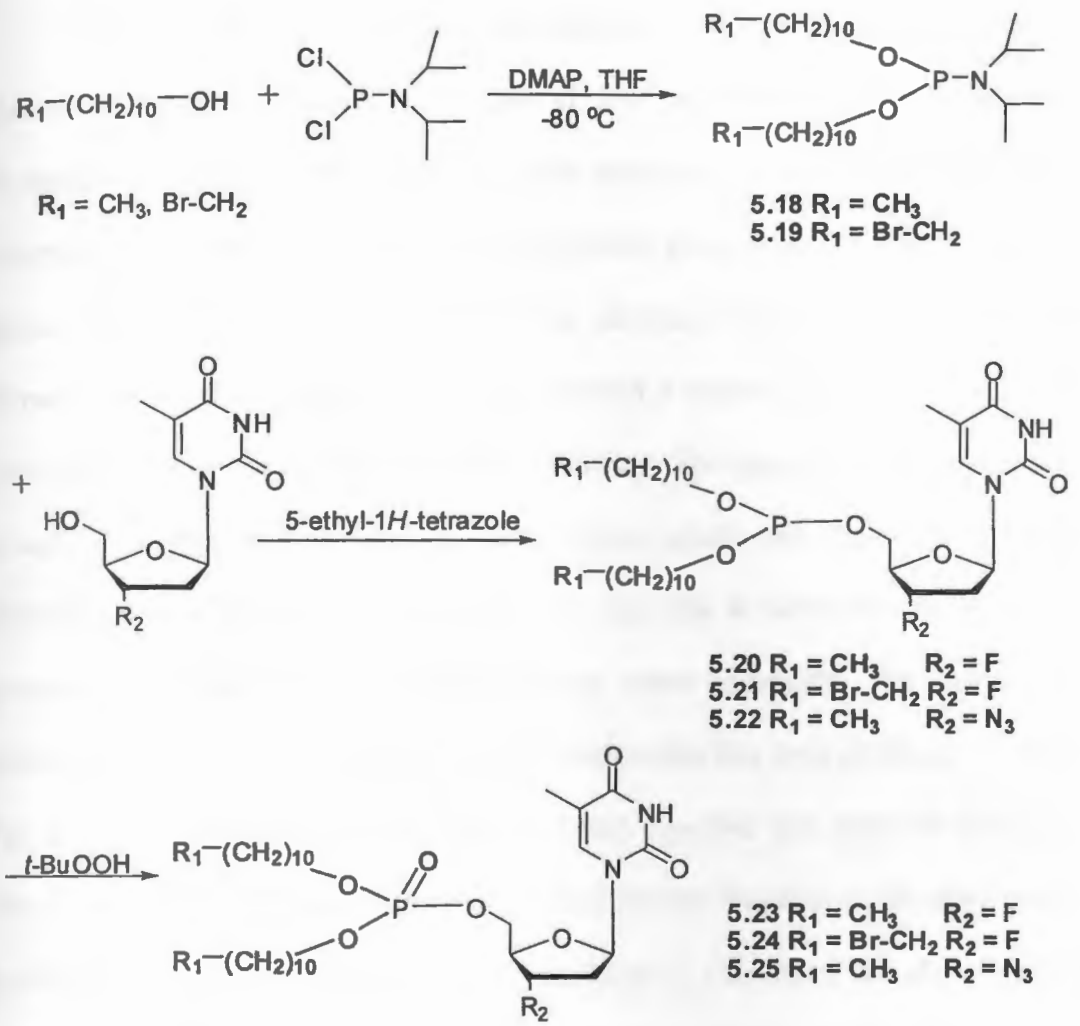

Scheme 5.3. Synthesis of fatty alcohol phosphotriester derivatives of AZT and FLT **(5.23-5.25)**.

Using a single-round infection assay (Krebs et al., 1999) with HIV-1 IIIB and transformed HeLa cells expressing HIV receptors (CD4) and coreceptors (CXCR4 and CCR5), the newly synthesized triester derivatives showed only modest antiviral activity, significantly lower than that of their parent nucleosides, AZT and FLT (IC_{50}= 10 and 0.8 μM, respectively).

In summary, the results presented herein show that the synthesis of different classes of lipophilic phosphate triesters of FLT and AZT can be successfully accomplished by using P(III) chemistry. The extension of this methodology should prove to be useful for the development of lipophilic phosphotriester prodrugs of other nucleosides. The premature hydrolysis of the phosphate-masking group bond in the extracellular medium, however, may have yielded a negatively-charged diester with low cellular uptake and reduced antiviral potency. The phosphotriesters must have acceptable stability in cell culture prior to cellular uptake and selective intracellular transformation of the active species. We were not able to determine the stability of compounds because of their extremely low water solubility. The extracellular hydrolysis of phosphotriester derivatives of nucleosides has been previously reported. For example, McGuigan et al. (1990 and 1994) reported that some of dialkyl and diaryl phosphotriester derivatives of AZT were inactive because of the rapid in vitro hydrolysis to release the nucleotide extracellularly. The utility of phosphotriester derivatives of nucleosides will be enhanced by a clearer understanding of the mechanisms pertaining to their bioconversion, uptake, and cellular incorporation.

5.5. References

Farquhar, D., Khan, S., Srivastva, D. N., Saunders, P. P. Synthesis and Antitumor Evaluation of Bis[(pivaloyloxy)methyl] 2'-Deoxy-5-fluorouridine 5'-Monophosphate (FdUMP): A Strategy To Introduce Nucleotides into Cells. *J. Med. Chem.*, **1994**, 37, 3902–3909.

Herdewijn, P., Balzarini, J., De Clercq E., Pauwels, R., Baba, M., Broder, S., Vanderhaeghe, H. 3'-Substituted 2',3'-dideoxynucleoide analogues as potential anti-HIV (HTLV-III/LAV) agents. *J. Med. Chem.*, **1987**, 30, 1270-1278.

Jochum, A., Schlienger, N., Egron, D., Peyrottes, S., Périgaud, C. Biolabile constructs for pronucleotide design. *J. Organometallic Chem.*, **2005**, 690, 2614–2625.

Krebs F. C., Miller, S. R., Malamud, D., Howett, M. K.; Wigdahl, B. Inactivation of human immunodeficiency virus type 1 by nonoxynol-9, C21G, or an alkyl sulfate, sodium dodecyl sulfate. *Antiviral Res.*, **1999**, 43, 157–173.

McGuigan, C., Nicholls, S. R., O'Connor, T. J., Kinchington, D. Synthesis and anti-HIV activity of some novel substituted dialkyl phosphate derivatives of AZT and ddCyd. *Antiviral Chem. Chemother.*, **1990**, 1, 25–33.

McGuigan, C., Pathirana, R. N., Davis, M. P. H., Balzarini, J., De Clercq, E. Diaryl phosphate derivatives act as pro-drugs of AZT with reduced cytotoxicity compared to the parent nucleoside. *Bioorg. Med. Chem. Lett.*, **1994**, 4, 427–430.

Meier, C. CycloSal-Pronucleotides – Design of Chemical Trojan Horses *Mini-Rev. Med. Chem.*, **2002**, 2, 219–234.

Meier, C., Ruppel, M. F., Vukadinovic, D., Balzarini, J. "Lock-in"-cycloSal-Pronucleotides - A New Generation of Chemical Trojan Horses? *Mini-rev. Med. Chem.*, **2004**, 4, 383–394.

Meier, C., Balzarini, J. Application of the *cyclo*Sal-prodrug approach for improving the biological potential of phosphorylated biomolecules. *Antiviral Res.*, **2006**, 71, 282–292.

Parang, K., Wiebe, L. I., Knaus, E. E., Huang, J. S., Tyrrell, D. L. In Vitro Anti-Hepatitis B Virus Activities of 5'-O-Myristoyl Analogue Derivatives of 3'-Fluoro-2',3'-dideoxythymidine (FLT) and 3'-Azido-2',3'-dideoxythymidine (AZT). *J. Pharm. Pharmaceut. Sci.*, **1998**, 1, 107–113.

Parang, K., Wiebe, L. I., Knaus, E. E. Novel Approaches for Designing 5'-O-Ester Prodrugs of 3'-Azido-2'3'-dideoxythymidine (AZT). *Current Med. Chem.*, **2000**, 7, 995–1039.

Parang, K., Knaus, E. E., Wiebe, L. I. Synthesis, in vitro anti-human immunodeficiency virus structure–activity relationships and biological stability of 5'-O-myristoyl analogue derivatives of 3'-azido-2'3'-dideoxythymidine (AZT) as potential prodrugs. *Antiviral. Chem. Chemother.*, **1998**, 9, 311–323.

Parang, K., Knaus, E. E., Wiebe, L. I. Synthesis, *In Vitro* Anti-HIV Activity, and Biological Stability of 5'-*O*-Myristoyl Analogue Derivatives of 3'-Fluoro-2',3'-Dideoxythymidine (FLT) as Potential Bifunctional Prodrugs of FLT. *Nucleosides & Nucleotides*, **1998**, 17, 987–1008.

Parang, K., Wiebe, L. I., Knaus, E. E., Huang, J. S., Tyrrell, D. L., Csizmadia, F. In vitro antiviral activities of myristic acid analogs against human immunodeficiency and hepatitis B viruses. *Antiviral Res.*, **1997**, 34, 75–90.

Rose, J. D., Parker, W. B., Secrist III, J. A. bis(*t*BuSATE) Phosphotriester Prodrugs of 8-Azaguanosine and 6-Methylpurine Riboside; bis(POM) Phosphotriester Prodrugs of 2'-Deoxy-4'-Thioadenosine and Its Corresponding 9α Anomer. *Nucleoside Nucleotides Nucleic Acids*, **2005**, 24, 809–813.

Thumann-Schweitzer, C., Gosselin, G., Périgaud, C., Benzaria, S., Girardet, J. L., Lefebvre, I., Imbach, J. L., Kirn, A., Aubertin, A. M. Anti-human immunodeficiency virus type 1 activities of dideoxynucleoside phosphotriester derivatives in primary monocytes/macrophages. *Res Virol.*, **1996**, 147,155–163.

Van Roey, J. P., Taylor, E. W., Chu, C. K., Shinazi, R. F. Correlation of molecular conformation and activity of reverse transcriptase inhibitors. *Ann. N. Y. Acad. Sci.*, **1990**, 616, 29–40.

Chapter 6

Synthesis, Analysis, in Vitro Characterization and in Vivo Disposition of a Lamivudine-Dextran Conjugate for Selective Antiviral Delivery to the Liver

Krishna C. Chimalakonda,[a] Hitesh K. Agarwal,[b] Anil Kumar,[b] Keykavous Parang,[b] and Reza Mehvar[a]

[a]Department of Pharmaceutical Sciences, School of Pharmacy, Texas Tech University Health Sciences Center, 1300 Coulter, Amarillo, Texas 79106, [b]Department of Biomedical and Pharmaceutical Sciences, University of Rhode Island, Kingston, RI, USA, 02881.

Published in *Bioconjugate Chem.* **(2007)** 18, 2097-2108.

6.1. Abstract

A liver-selective prodrug (3TCSD) of the antiviral drug lamivudine (3TC) was developed and characterized. 3TC was coupled to dextran (~25 kDa) using a succinate linker and the in vitro and in vivo behavior of the conjugate were studied using newly-developed size-exclusion and reversed-phase analytical methods. Synthesized 3TCSD had a purity of > 99% with a degree of substitution of 6.5 mg 3TC per 100 mg of the conjugate. Furthermore, the developed assays were precise and accurate in the concentration ranges of 0.125-20, 0.36-18, and 1-50 μg/mL for 3TC, 3TC succinate (3TCS), and 3TCSD, respectively. In vitro, the conjugate slowly released 3TC in the presence of rat liver lysosomes, whereas it was stable in the corresponding buffer. In vivo in rats, conjugation of 3TC to dextran resulted in forty- and seven-fold decreases in the clearance and volume of distribution of the drug, respectively. However, the accumulation of the conjugated 3TC in the liver was fifty-fold higher than that of the parent drug. The high accumulation of the conjugate in the liver was associated with a gradual and sustained release of 3TC in the liver. These studies indicate the feasibility of the synthesis of 3TC-succinate-dextran and its potential use for the selective delivery of 3TC to the liver.

6.2. Introduction

Lamivudine (β-L-2',3'-dideoxy-3'-thiacytidine, 3TC) is a deoxycytidine nucleoside analog that inhibits hepatitis B virus (HBV) replication and is used in the treatment of chronic hepatitis B infection (Jarvis et al., 1999). In addition to the efficacy of antiviral drugs against HBV, treatment of HBV infection is significantly

dependent on the pharmacokinetics of these drugs, in particular their distribution and accumulation in the liver. To be effective, 3TC needs to enter liver cells and be phosphorylated to its active form 3TC 5'-triphosphate intracellularly before incorporation into DNA of HBV by DNA polymerase (Shaw et al., 1999, Younger et al., 2004). Therefore, strategies that direct the drug to its site of action (liver) may increase the effectiveness of the drug and decrease its potential side effects in other non-target organs. Indeed, several studies (Bijsterbosch et al., 1996, Rensen et al., 1996, Fiume et al., 1997, DeVrueh et al., 2000, Tu et al., 2004, Erion et al., 2005, Reddy et al., 2005) have attempted to target antiviral drugs to the liver for the treatment of HBV infection.

Dextrans are glucose polymers, which are under investigation as macromolecular carriers for delivery of drugs and other therapeutic agents, such as proteins, after the systemic administration of the dextran-drug conjugates (Larsen et al., 1989, Takakura et al, 1995, Mehvar, 2000, Mehvar, 2003). Additionally, conjugates of dextrans with non-steroidal (Harboe, et al.,1989, Larsen et al., 1989) and steroidal (McLeod et al., 1993, McLeod et al., 1994) anti-inflammatory drugs have been studied for local delivery of these drugs to the colon. In a series of studies (Mehvar, 1997, Mehvar et al., 1995, Mehvar et al., 1994), we previously showed that the plasma kinetics and tissue distribution of dextran carriers are dependent on the M_w of the polymer. Therefore, dextrans of different M_w's may be useful for the delivery of drugs to different tissues after the systemic administration of the conjugate. For example, dextrans with M_w's of 20 kDa to 70 kDa showed a high degree of selectivity

for the liver when liver:plasma area under the concentration-time curve (AUC) ratio was considered (Mehvar et al., 1994). The liver selectivity of these dextrans was attributed to their sizes, which restrict their passage through most vascular bed pores, while allowing unrestricted passage through the substantially larger pore sizes of the liver sinusoids (Mehvar et al., 1994, Mehvar et al., 1987).

In addition to the molecular weight, both the electric charge (Nakane et al., 1987, Nishida et al., 1990) and chemical modification (Vansteenkiste et al., 1991, Nishikawa et al., 1993) of dextrans may affect their organ and cellular distribution. For example, it has been reported that positively charged dextrans are taken up by the liver more rapidly and extensively than neutral or negatively charged dextrans (Nakane et al., 1987, Nishida et al., 1990). Additionally, whereas unmodified dextrans distribute to both parenchymal and non-parenchymal cells of the liver (Nishikawa et al, 1992), galactosylation or mannosylation of dextrans results in selective delivery of the macromolecule to the parenchymal and non-parenchymal cells, respectively (Vansteenkiste et al., 1991, Nishikawa et al., 1993). Because electrical or chemical modifications of dextrans may alter their safety profiles (Yamaoka et al., 1995), we have recently used unmodified neutral dextrans for delivery of methylprednisolone to the liver for local immunosuppression (Mehvar et al., 2000, Zhang et al., 2001, Chimalakonda et al., 2006, Chimalakonda et al., 2003). These studies showed that after systemic administration, the conjugate selectively accumulates in the liver, where it gradually releases the active drug, resulting in more intense and sustained pharmacologic effects. Collectively, the above studies suggest that both unmodified

and glycosylated dextrans may be suitable for systemic delivery of therapeutic agents to the liver.

The aim of the present study was to synthesize and characterize a conjugate of 3TC with dextran ~25 kDa, intended for selective delivery of the anti-HBV drug to the liver. The conjugation of 3TC to dextran was achieved through a succinate linker, resulting in a macromolecular prodrug, potentially releasing 3TC and 3TC succinate (3TCS). Therefore, analytical methods were also developed for quantitation of the intact prodrug and simultaneous quantitation of its potential release products (3TC and 3TCS) in biological samples. In addition to in vitro characterization, the plasma pharmacokinetics and tissue disposition of the prodrug and parent drug were also studied in rats, a species which has recently been used as a model for human HBV infection (Wu et al., 2003, Takahashi et al., 1995, Wu et al., 2001). To the best of our knowledge, this is the first report of designing a macromolecular prodrug of anti-HBV drug lamivudine for targeted delivery to the liver.

6.3. Material and Methods

6.3.1. Materials

Dextran with an average M_w of ~25 kDa (actual M_w=23,500 Dalton) was purchased from Dextran Products (Scarborough, Ontario, Canada). Lamivudine (3TC) was purchased from Kemprotec (Middlesbrough, U.K.). Stavudine and kits for liver lysosomal isolation and acid phosphatase were purchased from Sigma Chemical (St. Louis, MO). For Chromatography, HPLC grade acetonitrile (Mallinckrodt Chromar

HPLC) was obtained from VWR Scientific (Minneapolis, MN). All other reagents were analytical grade and obtained through commercial sources.

6.3.2. Animals

Adult, male Sprague-Dawley rats were used in this study for in vitro blood and liver lysosome and in vivo disposition studies as outlined in the subsequent sections. All the procedures involving animals in this study were consistent with the "Principles of Laboratory Animal Care" (NIH publication Vol. 25, No. 28, revised 1996) and approved by the Texas Tech University Health Sciences Center Institutional Animal Care and Use Committee.

6.3.3. Synthesis of 3TC-Succinate-Dextran (3TCSD) Conjugate

The complete procedure for the synthesis of 3TCSD conjugate is depicted in Schemes 6.1 and 6.2 and described in detail below. The chemical structures of final desalted products were characterized by nuclear magnetic resonance spectrometry (^{1}H NMR, ^{13}C NMR, ^{31}P NMR) determined on a Bruker DPX NMR spectrometer (400 MHz). ^{13}C NMR spectra are fully decoupled. Chemical shifts are reported in parts per millions (ppm). The chemical structures of final products were confirmed by a high-resolution PE Biosystems Mariner API 2000 time-of-flight electrospray mass spectrometer.

(-)-4-N-(4,4'-Dimethoxytrityl)-5'-*O*-(succinate)-2',3'-dideoxy-3'-thiacytidine (6.1). 4-Dimethylaminopyridine (DMAP, 100 mg, 0.82 mmol) and succinic anhydride (290

mg, 2.90 mmol) were added to a solution of (-)-N_4-(4,4′-dimethoxytrityl)-2′,3′-dideoxy-3′-thiacytidine (**2.12**, 770 mg, 1.45 mmol) in dry pyridine (15.0 mL). Compound **2.12** was synthesized as described above in Chapter 2. The reaction mixture was stirred at room temperature overnight. After completion of the reaction, the solvent was evaporated under reduced pressure and the crude compound was purified by column chromatography over silica gel using dichloromethane/methanol containing 1% triethylamine as the eluents to yield **6.1** (0.82 g, 90%). ^{1}H NMR (400 MHz, DMSO-d_6, δ ppm): 8.56 (br s, 1H, NH), 7.60-7.70 (d, J = 7.8 Hz, 1H, H-6), 7.14-7.24 (m, 9H, aromatic hydrogens, DMTr), 6.72-6.84 (m, 4H, aromatic hydrogens, DMTr), 6.30-6.38 (m, 1H, H-1′), 6.10 (d, J = 7.8 Hz, 1H, H-5), 5.25-5.35 (m, 1H, H-4′), 4.22-4.34 (m, 2H, H-5′ and H-5″), 3.71 (s, 6H, DMTr-OCH_3), 3.58-3.63 (m, 2H, H-2′ and H-2″), 3.00-3.10 (m, 4H, CH_2CH_2); HR-MS (ESI-TOF) (*m/z*): $C_{33}H_{33}N_3O_8S$ calcd, 631.1988; found 632.1715 $[M + H]^+$, 654.1472 $[M + Na]^+$.

(-)-5′-O-(Succinate)-2′,3′-dideoxy-3′-thiacytidine (3TCS, 6.2). Acetic acid (AcOH, 10 mL, 80%) was added to compound **6.1** (100 mg, 0.16 mmol). The reaction mixture was heated at 80 °C for 30 min. The solvent was removed under reduced pressure and the crude compound was purified by HPLC (acetonitrile/water gradient) to yield **6.2** (47 mg, 90%). ^{1}H NMR (400 MHz, DMSO-d_6, δ ppm): 12.29 (s, 1H, COOH), 9.50-9.80 (br s, 2H, NH_2), 7.60-7.70 (m, 1H, H-6), 6.20-6.32 (m, 1H, H-1′), 5.81-5.93 (m, 1H, H-5), 5.30-5.36 (m, 1H, H-4′), 4.30-4.40 (m, 2H, H-5′ and H-5″), 3.71-3.80 (m, 2H, H-2′), 3.00-3.200 (m, 5H, H-2″ and CH_2CH_2); HR-MS (ESI-TOF) (*m/z*): $C_{12}H_{15}N_3O_6S$ calcd, 329.0682; found 330.3316 $[M + H]^+$, 658.3471 $[2M]^+$.

(-)-Dextran-5'-O-(succinate)-2',3'-dideoxy-3'-thiacytidine (3TC-succinate-dextran conjugate, 3TCSD, 6.3). DMAP (70.0 mg, 0.57 mmol), *N,N'*-diisopropylethylamine (DIPEA, 100 µL, 0.61 mmol), and N,N'-diisopropylcarbodiimide (DIC) (50 µL, 0.32 mmol) were added to a solution of compound **6.1** (275.0 mg, 0.44 mmol) and dextran 20 kDa (130 mg) in dry dimethylsulfoxide (DMSO, 3.0 mL) under nitrogen atmosphere. The reaction mixture was stirred at 40 °C for 48 h. After the completion of reaction, the reaction mixture was cooled to room temperature and cold diethyl ether: ethanol (45 mL, 50:50 v/v) was added. The mixture was washed twice with cold ethanol:diethyl ether (50:50, v/v) and finally with cold ethanol:acetonitrile (70:30, v/v) and centrifuged. The precipitate was dried under vacuum to give (-)-dextran-4-*N*-(4,4'-dimethoxytrityl)-*5'-O*-(succinate)-2',3'-dideoxy-3'-thiacytidin [4-*N*-(4'-dimethoxytrityl)-lamivudine-succinate-dextran conjugate, **6.3**].

Acetic acid (AcOH, 10 mL, 80%) was added to compound **6.3**. The reaction mixture was stirred at room temperature for 3 h and then heated at 80 °C for 30 min. The solvent was removed under reduced pressure and the residue was washed three times with cold diethyl ether:ethanol (45 mL, 50:50 v/v) and centrifuged to give 3TC-succinate-dextran conjugate (3TCSD, **6.4**). ^{1}H NMR (400 MHz, D_2O, δ ppm): 7.88-8.04 (br s, 1H, H-6), 6.25-6.35 (m, 1H, H-1'), 6.05-6.15 (br s, 1H, H-5), 5.41-5.50 (m, 1H, H-4'), 4.85-5.05 (m, anomeric hydrogen of dextran, H-1), 4.28-4.58 (m, 2H, H-5' and H-5''), 3.40-4.10 (m, H-2' and H-2'' of 3TC, H-2, H-3, H-4, H-5, and H6 of dextran), 3.30-3.38 (m, 4H, CH_2CH_2 of succinate).

6.3.4. Further Characterization of 3TC-Succinate-Dextran Conjugate (3TCSD, 6.4)

The purity of the powder was determined using both the size exclusion (SEC) and reversed-phase (RPC) chromatographic methods. The degree of substitution of 3TC in 3TCSD was determined by hydrolysis of the conjugate under basic conditions. To 1 mg of the conjugate were added 1 mL of 0.1 N NaOH and 0.6 mL of methanol. After leaving at room temperature for 5 min, 30 min, and 24 h, 100 μL of the sample was micropipetted into a microcentrifuge tube containing 100 μL of 0.1 M HCl. An aliquot (50 μL) was then injected into HPLC. The concentration of the released 3TC was determined using a reversed-phase method based on 3TC standard solutions as described below.

6.3.4.1. High Performance Liquid Chromatography

Size-exclusion (SEC) and reversed-phase (RPC) chromatographic methods were developed and validated for quantitation of the conjugate 3TCSD and its potential hydrolysis products (3TC and 3TCS), respectively, in buffers or biological samples.

6.3.4.1.1. Size-Exclusion Liquid Chromatography (SEC)

Lamivudine-succinate-dextran conjugate (3TCSD) was analyzed in non-biological and biological (plasma and tissue) samples at ambient temperature using a 30 cm x 7.8 mm analytical, gel chromatography column (PolySep-GFC 3000;

Phenomenex, Torrance, CA). The mobile phase consisted of water:acetonitrile:acetic acid (75:25:0.2, v/v/v) and was pumped at a flow rate of 1.0 mL/min.

6.3.4.1.2. Reversed-Phase Liquid Chromatography (RPC)

A reversed-phase chromatographic method was developed to quantitate the concentrations of 3TC and 3TCS in aqueous and biological samples. The separation of 3TC, 3TCS, and internal standard (stavudine, IS) was achieved on a 250 mm x 4.6 mm C18 column (Microsorb-MV, Varian, Lake Forest, CA) preceded by a 5-cm guard column. The mobile phase consisted of KH_2PO_4 (50 mM):methanol:triethylamine (90:10:0.1, v/v, pH 7.0), which was pumped at a flow rate of 1 mL/min.

6.3.4.2. HPLC System

The HPLC instrument consisted of a 510 pump (Waters; Milford, MA), a 717 plus auto sampler (Waters; Milford, MA), and a 486 UV detector (Waters) set at a wavelength of 276 nm. The chromatographic data was managed using Empower version 2 software. Calibration curves were constructed by plotting the peak areas of 3TCSD or peak area ratios of 3TC or 3TCS over IS against the concentration in the sample using a weight of 1/concentration.

6.3.4.3. Sample Preparation

For the size exclusion chromatography, to 100 µL of plasma in microcentrifuge tubes were added 20 µL of methanol and 20 µL of 20% (w/v) trichloroacetic acid. After vortex mixing for 5 s, the samples were centrifuged in a

microcentrifuge at 16,000 rpm for 5 min. A 100 μL aliquot of the supernatant was mixed with 50 μL of 0.5 M phosphate buffer (pH 6.0), and a 75-μL aliquot was injected into the HPLC.

To determine the concentrations of 3TCSD in the tissues by the SEC method, tissues were homogenized in 3 volumes of water using a homogenizer at a rate of 10,000 rpm. To 100 μL of the whole homogenate in siliconized microcentrifuge tubes were added 50 μL of 0.5 M phosphate buffer (pH 7.0) and 50 μL of cold methanol. Samples were then briefly vortex-mixed and 40 μL of trichloroacetic acid (40%) was added to precipitate proteins. After vortex-mixing for 5 s, the samples were centrifuged in a microcentrifuge at 10,000 rpm for 3 min. A 100 μL aliquot of the supernatant was mixed with 50 μL of 1 M sodium acetate, and a 75-μL aliquot was injected into the HPLC.

The preparation of plasma samples for reversed-phase chromatography was similar to that for the SEC method with one exception; for the reversed-phase system, 50 μL of 50 μg/mL stavudine was added as internal standard to the plasma sample before protein precipitation. Similarly, the tissue samples for reversed-phase chromatography were prepared as described above for the SEC method, but without the addition of 0.5 M phosphate buffer.

6.3.4.4. Validation of Assays

The inter-run precision (%CV) and accuracy (%error) of the assays were determined from the analysis of quality control samples (n = 5) based on reported guidelines (Shah et al., 1992). The concentrations of quality control samples were 1.0, 10, or 50 μg/mL for 3TCSD (SEC method), 0.125, 5.0, and 20 μg/mL for 3TC (RPC method), and 0.36, 5.4, and 18 μg/mL for 3TCS (RPC method). Calibration curves for SEC of 3TCSD contained 0, 1, 2, 5, 10, 15, 25, or 50 μg/mL of the prodrug (3TC equivalent). For RPC, calibration curves consisted of 0.0, 0.125, 0.25, 0.5, 1.0, 2.0, 5.0, 10, or 20 μg/mL of 3TC and 0.0, 0.36, 0.72, 1.80, 3.6, 5.4, 9.0, or 18 μg/mL of 3TCS as 3TC equivalents.

To determine the recovery of 3TCSD, 3TC, and 3TCS from plasma after protein precipitation, plasma samples (n = 5) containing 5 or 100 μg/mL 3TCSD, 5 or 50 μg/mL 3TC, or 1.8 or 18 μg/mL 3TCS were subjected to the above assays and the peak areas were determined. The peak areas of these samples were then compared with those containing an equal concentration of each analyte in distilled water, injected directly into the HPLC. Similarly, the recoveries of 3TCSD and 3TC from the liver samples (n = 5) containing 5 μg/mL 3TCSD or 0.5 μg/mL of 3TC were determined.

6.3.5. In Vitro Release Characterization.

6.3.5.1. Release Characteristics in Buffers.

The prodrug (3TCSD), at a concentration equivalent to 100 μg/mL 3TC, was dissolved in 10 mM KH2PO4 (pH 4.4) or phosphate buffer (pH 7.4). The solutions were then incubated at 37 °C (n = 3). Samples (100 μL) were taken at 0, 3, 6, 12, and 24 h and subjected to the above HPLC methods for the quantitation of intact 3TCSD (SEC method) and released 3TC or 3TCS (RPC method).

6.3.5.2. Release Characteristics in Rat Blood

Blood was obtained from rats by cardiac puncture. Approximately 4 IU of heparin was added to each mL of blood to prevent coagulation. Immediately after the collection of blood, 3TCSD conjugate (in 10 mM isotonic phosphate buffer at pH 7.4) was added to produce a blood concentration of 100 μg/mL (3TC equivalent) (n = 3). The solution was then incubated at 37 °C. Blood samples (1 mL) were collected at 0, 3, 6, and 12 h in heparinized microcentrifuge tubes. After centrifugation of the blood, the plasma samples (100 μL) were subjected to the assays described above for the determination of 3TC, 3TCS, and/or intact 3TCSD.

6.3.5.3. Release Characteristics in Rat Liver Lysosomes

Crude lysosomal fractions were prepared from the liver of untreated rats according to the procedure described in the lysosome isolation kit (Sigma). Briefly, the rat livers were perfused with ice-cold PBS before removal of the livers. The livers

were then homogenized in 4 volumes of the extraction buffer, followed by differential centrifugation for isolating the lysosomal fraction. The protein concentrations in lysosomal preparations were determined by Bio-Rad protein assay (Bio-Rad, Herecules, CA, USA). The activity of acid phosphatase, a lysosomal marker, in the preparation was tested using a commercial kit (Sigma). The specific enzyme activity in the lysosomal fraction was >9-fold that in the liver homogenate.

For lysosomal hydrolysis studies, 3TCSD (100 μg/mL, 3TC equivalent) was incubated at 37 °C in 50 mM acetate buffer (pH 4.0) in the presence of 5 mM reduced glutathione and 5 mg/mL lysosomal protein (n = 3). Samples (100 μL) were then taken at 0, 3, 6, 9, 12, and 24 h and treated as described above before reversed-phase and size-exclusion HPLC analysis.

6.3.6. In Vivo Disposition

A total of 42 adult male Sprague-Dawley rats were divided equally into two groups of 21 rats each, treated with 3TCSD or 3TC. The mean ± S.D. of the body weights of rats were 241 ± 8 and 240 ± 6 g for the 3TCSD- and 3TC-injected groups, respectively. The animals had free access to drinking water and rat chow before and during the course of experiments.

Single iv bolus doses (5 mg/kg; 3TC equivalent) of 3TCSD or the parent drug 3TC were injected into the penile vein of the animals under isoflurane anesthesia. Different groups of rats (n = 3/group/time point) were euthanized at 0 (before drug administration), 5, 15, 60, 120, or 180 min following drug administration, and tissues

(liver, spleen, kidneys, heart, lungs, and brain?) and blood (cardiac puncture) were collected. Additionally, total urine output was collected from zero to 180 min or to 24 h for the 3TC- or D3TCS-injected group (n = 3/group).

Immediately after excision, the tissues were rinsed in ice-cold saline solution to remove excess blood. Afterwards, the tissues were blotted dry and kept frozen until analysis. After centrifugation of the blood in a pre-chilled and heparin-coated microcentrifuge tube, the plasma was collected. To prevent in vitro hydrolysis of 3TCSD during storage, plasma (500 μL) was mixed with a 10% acetic acid solution (100 μL). Plasma, tissue, and urine samples were kept frozen at – 80 °C until analysis.

6.3.7. Pharmacokinetic Analysis

Non-compartmental analysis was performed by using WinNonlin™5.0.1 computer program (Pharsight Co.; Mount View, California). Terminal elimination rate constant (λ_z) was estimated from the log-linear portion of the plasma or tissue concentration-time courses. Area under the plasma or tissue concentration-time curve (AUC) was estimated from the average plasma or tissue concentrations at different time points using linear trapezoidal rule with extrapolation to infinity only for the plasma profiles. For tissues, AUCs were not extrapolated beyond the quantifiable samples because of uncertainty about the terminal half lives. Other estimated pharmacokinetic parameters included: apparent total body clearance (CL), renal clearance (CL_R), volume of distribution at steady-state (V_{ss}), terminal volume of distribution (V_z), fraction of the drug excreted unchanged in urine (f_e), mean residence

time (MRT), and maximum observed drug concentration (C_{max}). The maximum concentrations of 3TCSD or 3TC in plasma (C_0) after the injection of the conjugate or parent drug were estimated by the program. The concentrations of drugs in the tissues were corrected (Mehvar et al., 1994) for the residual blood using the blood volume fraction of different tissues.

6.3.8. Statistical Analysis

Because of destructive sampling procedure used for the collection of blood and tissues from different animals at each time point, the composite kinetic parameter AUC could not be obtained for individual rats (Mehvar et al., 1994). Therefore the variance of AUC was estimated by a reported (Bailer et al., 1988, Yuan et al., 1993) procedure based on the standard error of mean and number of samples at each time point. The pairwise comparison of AUCs was then carried out at an α level of 0.05 and a Bonferroni-adjusted α of 0.05 or 0.0167 for pairwise comparison of two (1 comparison) or three (3 comparison) means, respectively. The critical values of Z (Z_{crit}) for the two-sided test using the Bonferroni-adjusted α of 0.05 and 0.0167 were 1.96 and 2.39, respectively, and the observed Z (Z_{obs}) was calculated as reported before (Bailer et al., 1988, Yuan et al., 1993). A Z_{obs} value > Z_{crit} was used as an indication of a significant difference between the AUCs.

The differences between groups in their kinetic parameters that could be estimated for individual rats (e.g., C_{max} and CL_R) were determined using a two-tailed unpaired t test at a significance level (α) of 0.05. When possible, data are presented as mean ± S.D.

6.4. Results and Discussion

Targeted delivery of anti-HBV drugs to the liver, for the treatment of viral hepatic diseases, has attracted the attention of scientists for several years. In one of the first publications on this subject, Balboni et al. showed that conjugation of cytosine arabinoside and 5-fluorodeoxyuridine to albumin resulted in accumulation of these antiviral drugs in the mouse liver cells, increasing the effectiveness of the drugs in comparison with the free drugs (Balboni et al, 1976). Further works by Fiume and colleagues (Fiume et al., 1997) modified this strategy by the use of lactosaminated albumin as the carrier, selectively targeting the asialoglycoprotein receptors on the hepatocytes with the galactose moiety of lactose. Additionally, conjugates of antiviral drugs with galactosylated poly-L-lysine, instead of albumin, have been synthesized and tested by the same group (Fiume et al., 1986, Fiume et al., 1997). Others have used arabinogalactan (Enriquez et al., 1995) or glycosylated lipoproteins (Bijsterbosch et al., 1996, DeVrueh et al., 2000), as liver-accumulating carriers, or prodrugs that release the active drug based on metabolism by hepatic cytochrome P450 (Erion et al., 2005, Reddy et al., 2005) for targeted delivery of antiviral drugs to the liver. These studies support the general concept that targeted delivery of antiviral drugs to the liver potentially increases the efficacy of these drugs in the treatment of viral liver infections while, at the same time, decreasing their toxic effects in other tissues. However, the choice of carrier and targeting moieties need optimization to reduce carrier-related side effects, such as increased alkaline phosphatase levels seen with lactosylated human serum albumin (Fiume et al., 1997), or to improve drawbacks

associated with variability in density and affinity seen with the asialoglycoprotein receptors (Rensen et al., 1996).

6.4.1. Synthesis and Characterization of 3TCSD

In addition to our study, we are aware of only one other study that used dextran as a macromolecular prodrug of antiviral agents (Tu et al., 2004). In that study, acyclovir was conjugated to dextran with a M_w of 40 kDa. However, to synthesize the conjugate, dextran was first oxidized to dextran aldehyde before direct reaction of the aldehyde groups of dextran with the amine group of acyclovir to produce a Schiff's base, without any spacer between acyclovir and dextran. Modification of dextrans, including their oxidation, may alter the degradation and safety profiles of native dextrans, which have been used clinically for almost six decades as plasma volume expanders (Thoren, 1981). Therefore, we designed this strategy for conjugation of 3TC to dextran to minimize changing the structure of native dextran molecule. Consequently, 3TC was coupled to dextran through a succinate linker, thus avoiding a need for oxidation of dextran as previously reported (Tu et al., 2004).

In the present study, we used dextran with a M_w of ~25 kDa as an alternative to the currently studied carriers for the selective delivery of 3TC to the liver in HBV treatment. The synthesis of the conjugate was challenging because of the presence of free *N*4-amino group in the structure of 3TC, which had to be protected before the reaction of 3TC with succinic anhydride for the synthesis of 3TCS. Lamivudine (3TC) was conjugated to dextran using a succinate linker in two major steps by synthesis of

5′-*O*-succinate ester of the drug (Scheme 6.1), followed by the reaction of the ester conjugate with dextran (Scheme 6.2).

In this study, Lamivudine was initially reacted with TBDMS-Cl in the presence of imidazole to yield 5′-*O*-TBDMS-lamivudine (**2.4**). The protection of *N*4-amino group of 5′-*O*-protected lamivudine was carried out in the presence of DMTr-Cl and pyridine to give N_4-DMTr-5′-*O*-TBDMS-lamivudine (**2.11**). The deprotection of 5′-*O*-TBDMS in the presence of tetrabutylammonium fluoride (TBAF) afforded N_4-DMTr derivative of lamivudine (**2.12**). This strategy was described in detail in Chapter 2.

Compound **2.12** was used in the reaction with succinic anhydride to generate N_4-DMTr-5′-*O*-succinate ester conjugate of lamivudine (**6.1**) (Scheme 6.1). Compound **6.1** was reacted with dextran in the presence of DIC and DMAP to afford N_4-(DMTr)lamivudine-succinate-dextran conjugate (**6.3**) that was deprotected in the presence of acetic acid to afford lamivudine-succinate-dextran conjugate (3TCSD, **6.4**) with a reasonable degree of 3TC substitution (6.5%, w/w) (Scheme 6.2).

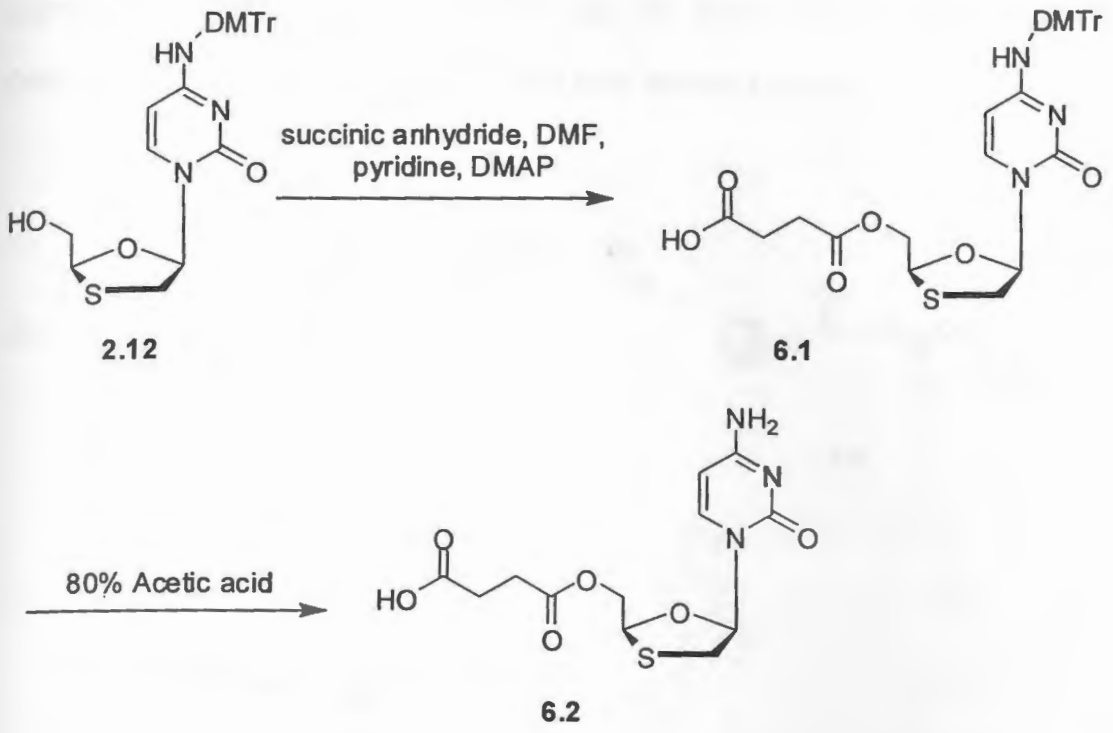

Scheme 6.1. Synthesis of 4-*N*-(4,4′-Dimethoxytrityl)-5′-*O*-(succinate)-2′,3′-dideoxy-3′-thiacytidine **(6.4)**.

The purity of the conjugate was > 99% as determined by the reversed phase analysis of a 100-μg/mL solution of the conjugate (n = 3), which contained only 0.296 ± 0.041 μg/mL of 3TC without any measurable peak of 3TCS. The degree of substitution of the final product, which was obtained by the base hydrolysis of 3TCSD to 3TC followed by reversed-phase quantitation of the released 3TC, was 6.5 mg lamivudine in 100 mg of 3TCSD powder. The complete hydrolysis of 3TCSD was confirmed by a complete disappearance of the 3TCSD peak in the SEC method. Additionally, the area of the unhydrolyzed 3TCSD peak in the SEC method was the same as the area of the released 3TC peak in the reversed-phase method after

appropriate volume correction, indicating that the degree of substitution may be determined directly from the area of 3TCSD peak without hydrolysis.

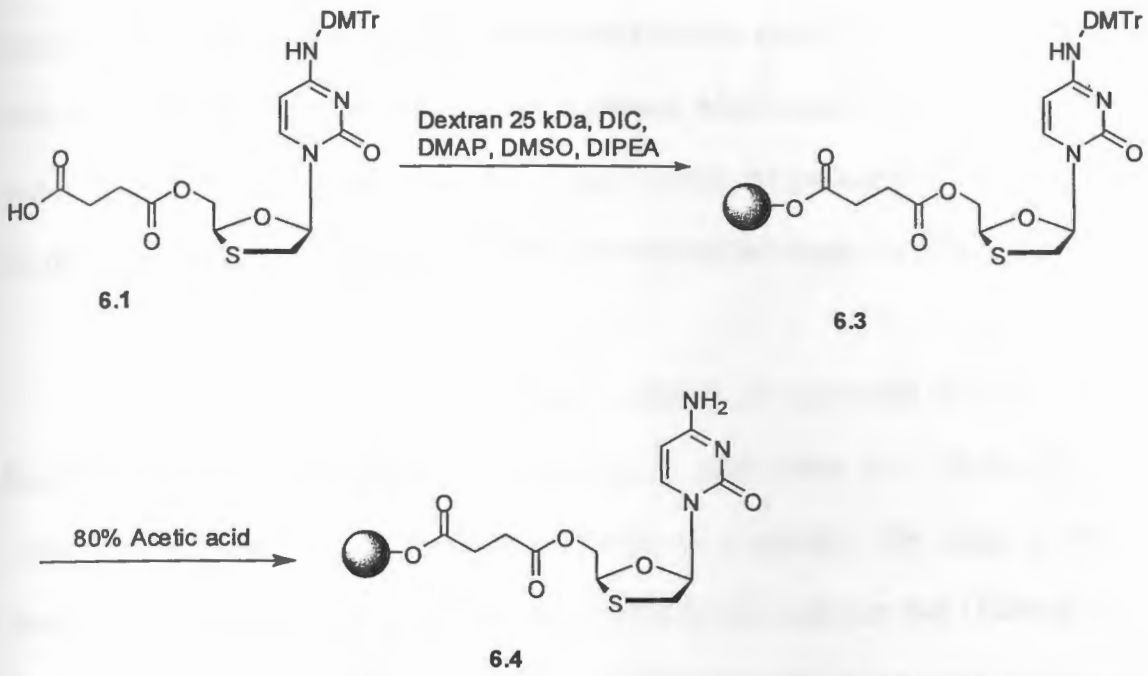

Scheme 6.2. Synthesis of 3TCS–Dextran (3TCSD, **6.4**).

6.4.2. Size-Exclusion Chromatographic Method

Lamivudine-succinate-dextran (3TCSD) has two ester bonds in its structure (Scheme 6.2), whose hydrolysis potentially releases 3TC or 3TCS. Therefore, to completely determine the fate of the conjugate and its potential release products in both in vitro and in vivo experiments, analytical methods capable of measurement of all three moieties are needed. To quantitate 3TCSD in both aqueous and biological samples, a SEC assay was developed. The method is capable of separating the conjugate peak from the endogenous peaks (Figure 6.1) and accurately and precisely quantitating the conjugate (Table 6.2).

Chromatograms of plasma samples taken from a rat before (blank) and 180 min after the administration of a single 5-mg/kg dose (3TC equivalent) of 3TCSD are demonstrated in Figure 6.1. Dextran-lamivudine succinate eluted at ~5.3 min and was well separated from the endogenous peaks in plasma, which eluted after the conjugate peak (Figure 6.1). Additionally, the relationship between the peak area of 3TCSD and the detector response was linear ($r^2 \geq 0.998$) over the studied range 1 to 50 μg/mL.

The results of the assay validation in plasma are presented in Table 6.1. Excellent accuracy of the assay is demonstrated by error values of < 1% for all the concentrations (even at the lowest concentration of 1 μg/mL). The assay is also deemed precise because the C.V. values are < 13% for the inter-run data (Table 6.1). Based on the data presented in Table 1, the limit of quantitation of the assay is at least equal to 1 μg/mL.

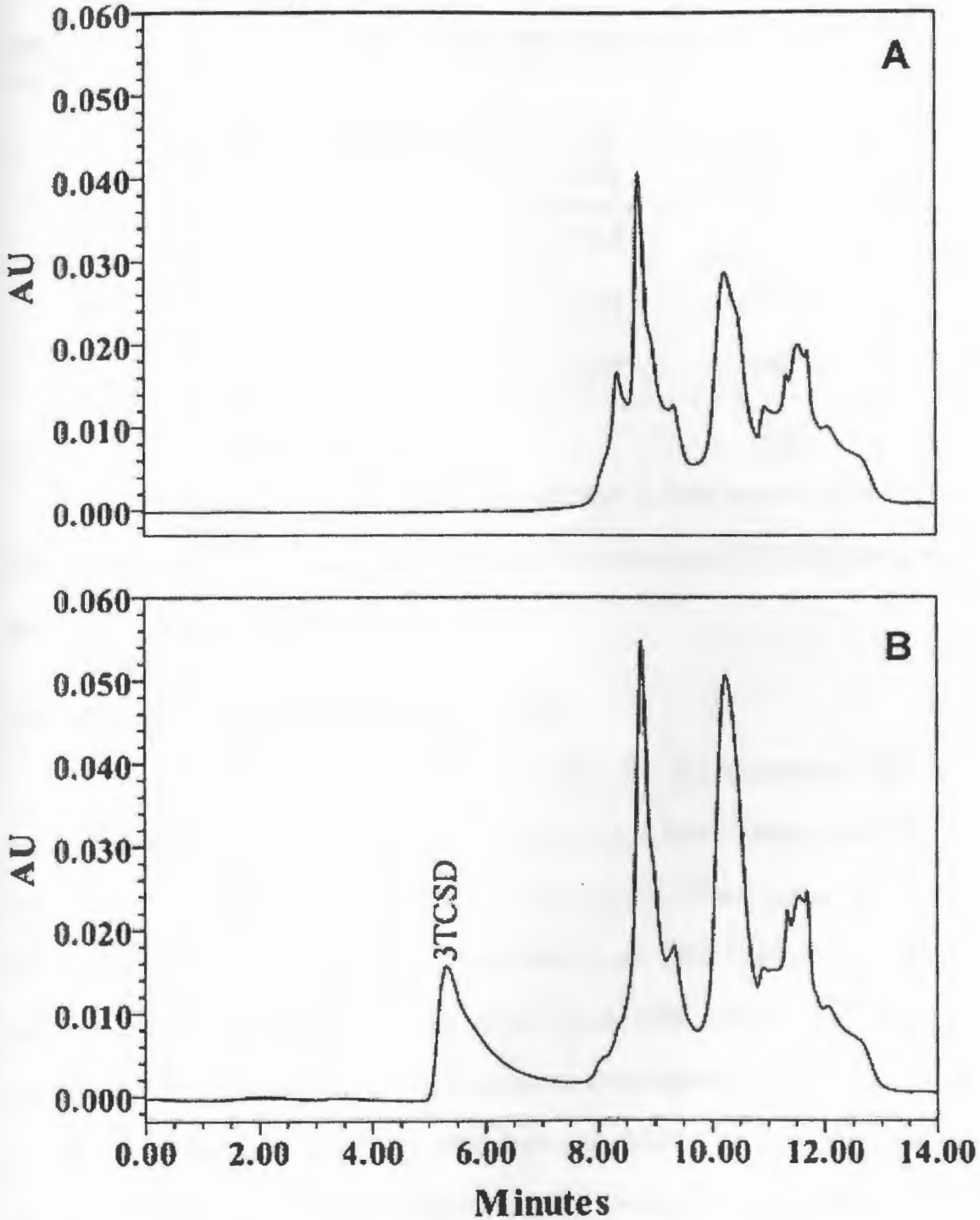

Figure 6.1. Chromatograms of plasma samples taken from a rat before (A) and 180 min after (B) the administration of a single 5 mg/kg dose (3TC equivalent) of 3TCSD, subjected to the size-exclusion chromatographic method. The 180 min sample contained 9.70 μg/mL 3TCSD.

Table 6.1. Inter-Run Accuracy and Precision for Quantitation of 3TCSD using the SEC Assay ($n = 5$)

Added Conc. (μg/mL)	Calculated Conc. (μg/mL)	CV (%)	Error (%)
1	0.992	12.8	-0.84
10	10.1	2.34	0.70
50	49.6	1.60	-0.80

The recovery of 3TCSD from plasma was 88.0 ± 4.2% and 94.1 ± 4.6% at concentrations of 5 and 50 μg/mL, respectively. The recovery of 3TCSD from liver was 94.2 ± 9.5% at a concentration of 5 μg/mL.

6.4.3. Reversed-Phase Chromatographic Method.

Several HPLC assays are currently available for determination of 3TC in plasma and/or tissues (Zhou et al., 1997, Kenney et al., 2000, Zheng et al., 2001, Alnouti et al., 2004, Bezy et al., 2005, Kano et al., 2005). These assays use either solid-phase extraction (Kenney et al., 2000, Zheng et al., 2001, Bezy et al., 2005) or protein precipitation (Zhou et al., 1997, Alnouti et al., 2004, Kano et al., 2005) for sample preparation. Additionally, all of them use reversed-phase chromatography with C_{18} (Zhou et al., 1997, Kenney et al., 2000, Bezy et al., 2005), C_8 (Kano et al., 2005), or phenyl (Zheng et al., 2001, Alnouti et al., 2004) columns for separation of 3TC from the endogenous peaks. To quantitate both 3TC and 3TCS simultaneously in our samples, we had to modify these assays. We found that a protein precipitation method with a combination of methanol and trichloroacetic acid resulted in the highest

recovery (≥ 86%) for both 3TC and 3TCS from biological samples. Additionally, our chromatographic conditions resulted in complete separation of 3TC, 3TCS, and IS from the endogenous peaks (Figure 6.2) and accurate and precise quantitation of 3TC and 3TCS (Table 6.2).

Figure 6.2 depicts the chromatograms of plasma samples at zero (blank) and 15 min after the administration of a single 5-mg/kg dose of 3TC to rats and at 3 h after the in vitro incubation of 3TCSD in blood. Lamivudine, internal standard (stavudine), and 3TCS eluted at ~11, 17, and 26 min, respectively and were well separated from the endogenous peaks in plasma (Figure 6.2). Additionally, the relationship between the peak area ratios of 3TC and 3TCS and the sample concentrations was linear ($r^2 \geq$ 0.998) over the studied concentration range of 0.125 to 20 μg/mL for 3TC and 0.36 to 18 μg/mL (3TC equivalent) for 3TCS.

Validation results for the reversed-phase assay of 3TC and 3TCS in plasma are presented in Table 6.2. Excellent accuracy of the assay is demonstrated by error values of < 11% for all the concentrations. The assay is also deemed precise because the C.V. values are < 9% for all the concentrations except for the lowest concentration of 3TC, which showed an acceptable C.V. of 16.8% (Table 6.2). Based on the data presented in Table 6.2, the limit of quantitation of the assay is 0.125 and 0.36 μg/mL for 3TC and 3TCS, respectively.

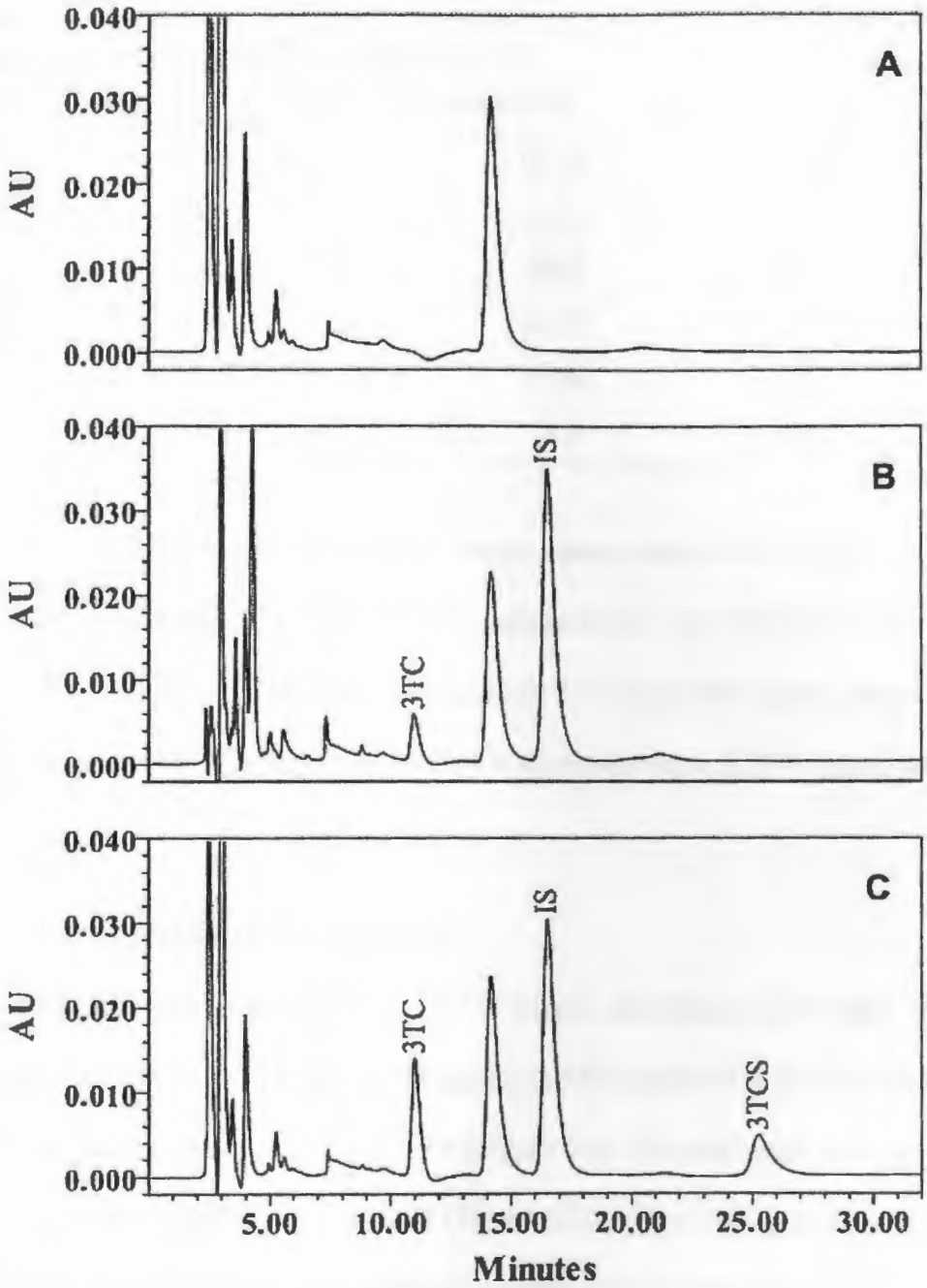

Figure 6.2. Chromatograms of plasma samples taken from a rat before (A) and 15 min after (B) the administration of a single 5 mg/kg dose of 3TC to rats and at 3 h after in vitro incubation of 3TCSD with rat blood (C), subjected to the reversed-phase chromatographic method. Sample B contained 1.84 μg/mL 3TC, and sample C contained 3.97 and 5.12 μg/mL 3TC and 3TCS, respectively.

Table 6.2. Inter-Run Accuracy and Precision for Quantitation of 3TC and 3TCS in Plasma using the Reversed-Phase Assay (n = 5)

Analyte	Added Conc. (μg/mL)	Calculated Conc. (μg/mL)	CV (%)	Error (%)
3TC	0.125	0.138	16.8	10.9
3TC	5.0	4.75	3.15	-5.04
3TC	20	20.8	5.83	4.00
3TCS	0.36	0.378	8.33	5.14
3TCS	5.4	5.18	4.18	-3.73
3TCS	18	18.8	3.93	4.32

For 3TC, the degrees of recovery from plasma were 101 ± 1.8% and 104 ± 1.8% at concentrations of 5 and 50 μg/mL, respectively. For 3TCS, the values were 89.7 ± 8.5% and 85.7 ± 2.6% at concentrations of 1.8 and 18 μg/mL, respectively. The recovery of 3TC from the liver samples at a concentration of 0.5 μg/mL was 95.7 ± 5.25%.

6.4.4. Release Characteristics in Buffers

The SEC and reversed-phase HPLC assays described above were used to investigate the stability of 3TCSD and formation of 3TC and 3TCS at 37 °C in buffers at pH 4.4 (Figure 6.3) and blood at pH 7.4 (Figure 6.4). The conjugate was very stable at pH 4.4 as demonstrated by both SEC (Figure 6.3, top) and reversed-phase (Figure 6.3, bottom) assays. The concentrations of 3TCSD did not significantly change over 24 h of incubation at 37 °C at pH 4.4 (Figure 6.3, top). Additionally, reversed-phase analysis showed minor concentrations (< 1% of the initial concentration of 3TCSD) of 3TC and 3TCS released over the incubation time of 24 h (Figure 6.3, bottom). On the other hand, measurable hydrolysis of 3TCSD occurred at pH 7.4 (Figure 6.4). In the

SEC method, the concentrations of 3TCSD declined ~ 16% during 24 h of incubation at pH 7.4 and 37 °C, with an apparent first-order half life of 108 h (Figure 6.4, top). The decline in the concentration of 3TCSD (Figure 6.4, top) was associated with an almost identical increase in the concentrations of free 3TC and 3TCS in the sample analyzed by the reversed-phase method (Figure 6.4, bottom).

6.4.5. Release Characteristics in Rat Blood

Figure 6.5 shows the decline in the 3TCSD concentration (top) and associated increases in the concentrations of 3TC and 3TCS (bottom), after incubation of the conjugate in rat blood at 37 °C. The total 3TC (3TC plus 3TC succinate) released during 12 h of incubation in blood was 8.45 ± 0.04% (Figure 6.5, bottom) in agreement with an equivalent decline (7.75 ± 0.80%) in the concentration of the prodrug in the SEC assay (Figure 6.5, top). The first-order half life of the decline in the 3TCSD concentration in plasma was 110 h.

A comparison of 24-h degradation data at pH 7.4 (Figure 6.4) with 12-h degradation data in blood (Figure 6.5) suggests that the degradation of 3TCSD in blood is only due to a slow chemical hydrolysis of the conjugate. This is because the degradation half lives of 3TCSD in buffer at pH 7.4 and in blood are almost identical (108 and 110 h, respectively), indicating lack of enzymatic hydrolysis of the conjugate in blood. This data is consistent with our previous report on a dextran conjugate of methylprednisolone succinate, which similarly showed little, if any, enzymatic hydrolysis in blood (Mehvar et al., 2000). Nevertheless, the relatively long half life of

3TCSD in blood in vitro (110 h) indicates that the conjugate is stable in blood long enough for the uptake by the liver.

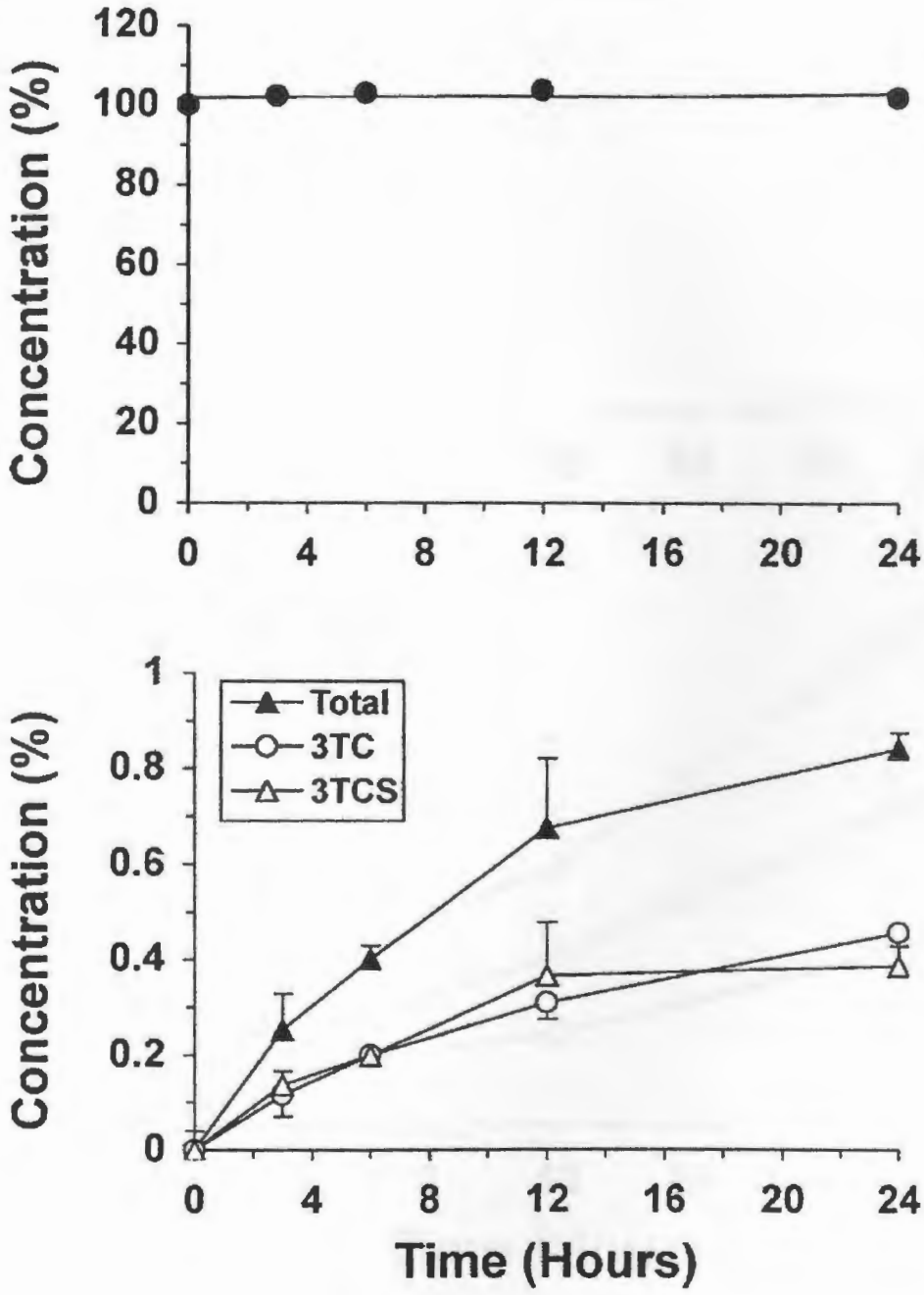

Figure 6.3. Average concentration–time courses of the intact 3TCSD (top) and released 3TC, 3TCS, and total 3TC (3TC plus 3TCS) (bottom) after incubation of the conjugate at pH 4.4 (37 °C). Error bars represent SD values (n = 3). Error bars for 3TCSD are too small to be observable.

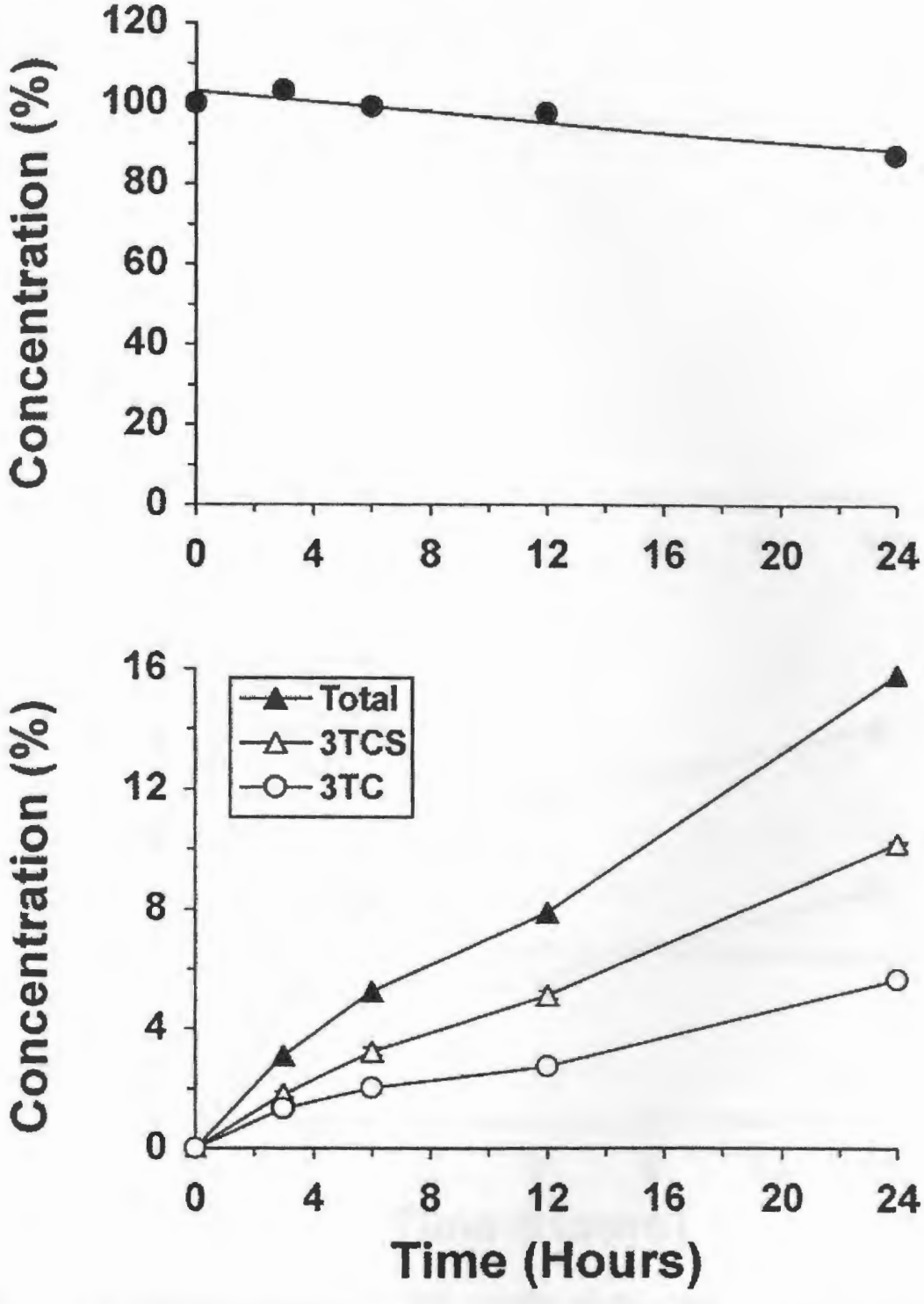

Figure 6.4. Average concentration–time courses of the intact 3TCSD (top) and released 3TC, 3TCS, and total 3TC (3TC plus 3TCS) (bottom) after incubation of the conjugate at pH 7.4 (37 °C). Error bars represent SD values (n = 3). In most cases, error bars are too small to be observable.

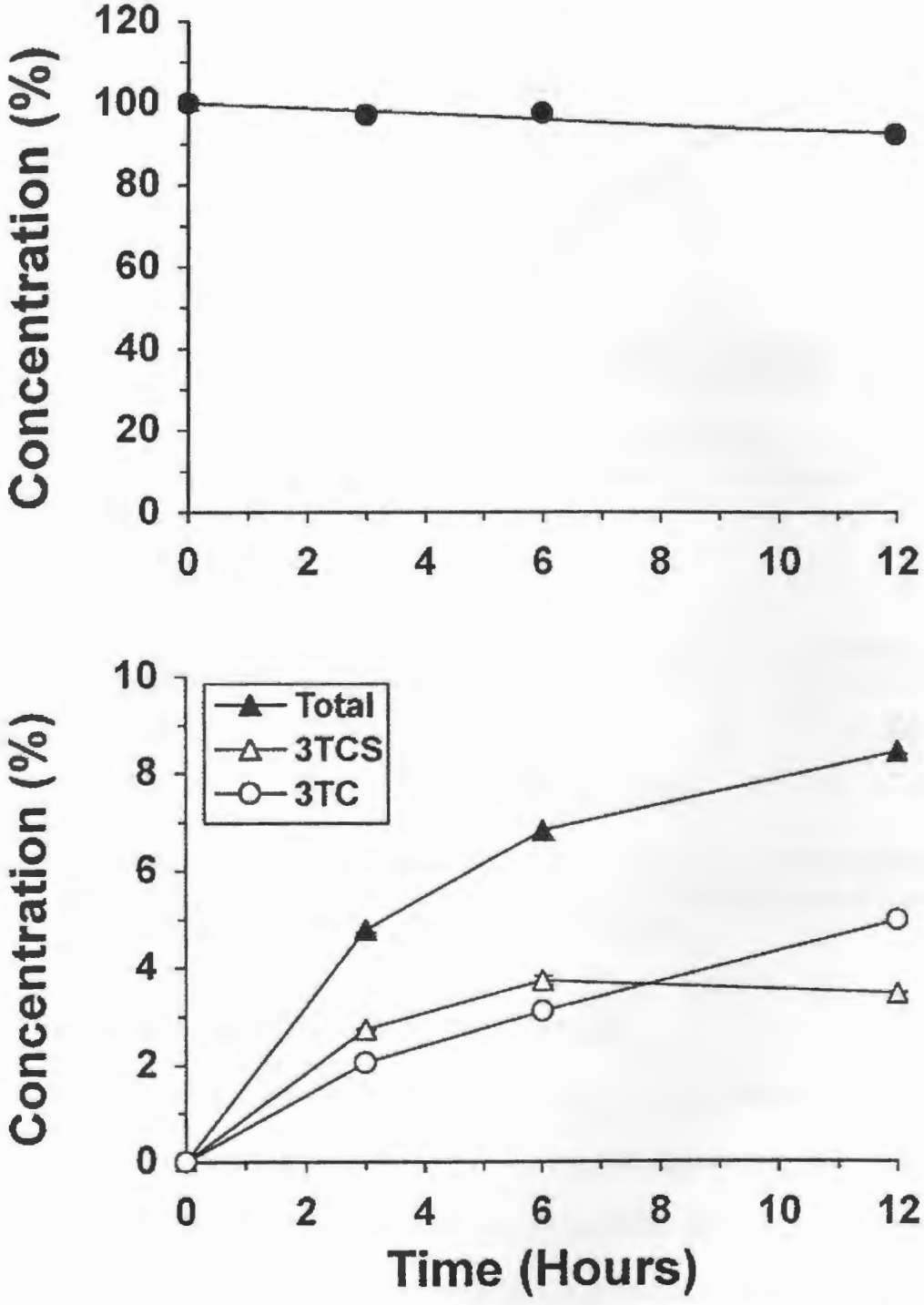

Figure 6.5. Average concentration–time courses of the intact 3TCSD (top) and released 3TC, 3TCS, and total 3TC (3TC plus 3TCS) (bottom) after incubation of the conjugate in rat blood (37 °C). Error bars represent SD values (n = 3). In most cases, error bars are too small to be observable.

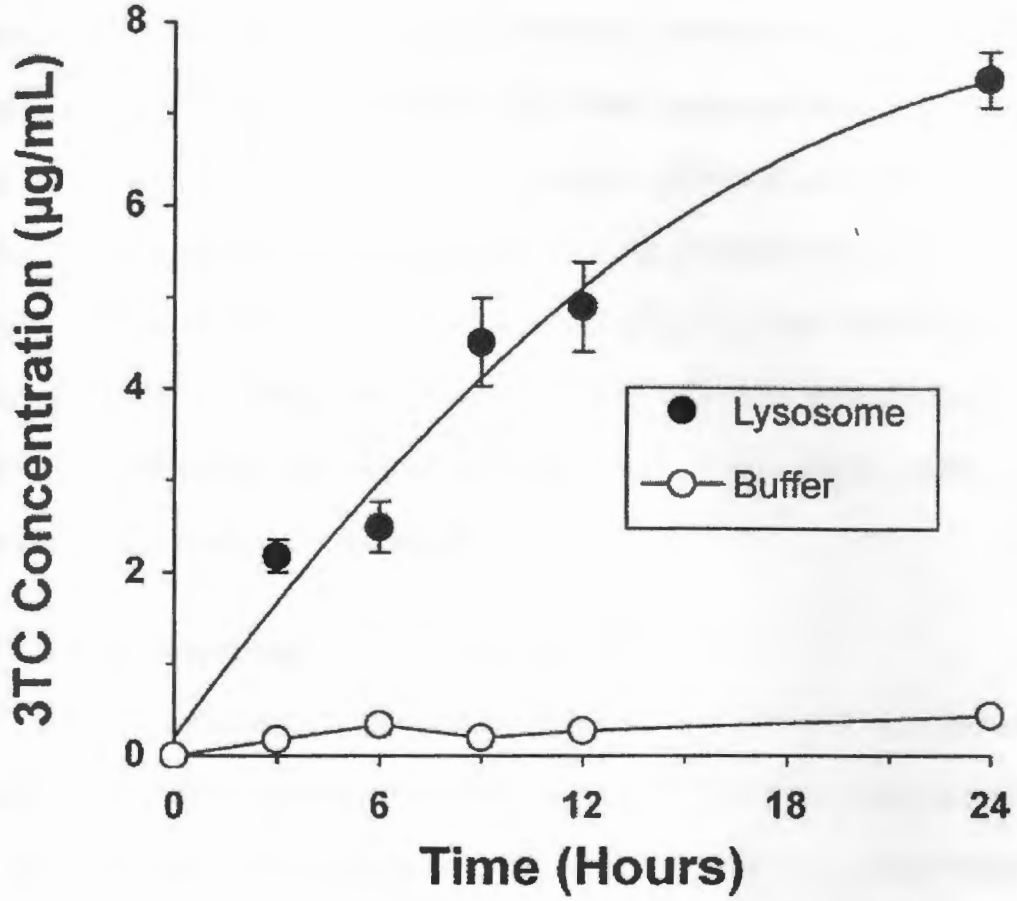

Figure 6.6. Average concentration–time courses of released 3TC after incubation of the conjugate in rat liver lysosomes or buffer (37 °C). Error bars represent SD values ($n = 3$). In most cases, error bars are too small to be observable.

6.4.6. Release Characteristics in Rat Liver Lysosomes

Previous works (Larsen et al., 1989, Zhang et al., 2001) on other ester conjugates of dextrans have proposed that the intact conjugates are resistant to the effects of esterases because of steric hindrance of dextrans. However, after exposure of the conjugate to dextranases, which depolymerize dextrans, esterases can hydrolyze the ester bonds in the conjugate. It has been reported (Larsen, 1989) that dextranases are present in lysosomes, predominantly in the liver. Additionally, dextrans enter cells via endocytosis, which results in their accumulation in the lysosomal compartments

(Lake et al., 1985, Stock et al., 1989). Therefore, lysosomal exposure of dextran conjugates to dextranases may facilitate their further enzymatic hydrolysis. *In vitro* data showed significant amounts of 3TC released at pH 4 only in the presence of rat liver lysosomes (Figure 6.6). It was found that the presence of lysosomes in the medium induced a slow release of 3TC (7.36 ± 0.30 μg/mL after 24 h) without any detectable 3TCS. In contrast, the release of 3TC or 3TCS in the same medium in the absence of lysosomes was negligible (Figure 6.6). These results confirms our hypothesis of 3TC release in lysosomes

6.4.7. In Vivo Disposition

Plasma concentration-time courses of 3TCSD and 3TC after the injection of single 5-mg/kg (3TC equivalent) doses of the prodrug or the parent drug are depicted in Figure 6.7. After the injection of unconjugated 3TC, the drug was eliminated relatively rapidly and could not be detected at the last sampling time of 3 h (Figure 6.7). In contrast, the concentrations of 3TCSD were several folds higher than those of 3TC and remained high even at the last sampling time after the injection of the conjugate. The plasma concentrations of both 3TC and 3TCSD declined multi-exponentially (Figure 6.7). Additionally, no quantifiable concentrations of 3TC or 3TCS were detected in plasma of 3TCSD-injected rats.

The plasma pharmacokinetic parameters of 3TC and 3TCSD after the injection of the parent drug or the prodrug are listed in Table 6.3. Conjugation of 3TC to dextran resulted in an almost forty-fold decrease in the total CL of the drug and a similar degree of increase in its plasma AUC. The decrease in total CL was associated with an eighty-fold decrease in the CL_R of the drug when conjugated to dextran.

Consequently, the fraction of the drug excreted unchanged into urine decreased from 65% for the parent drug to 31% for the conjugate (Table 6.3). Additionally, dextran conjugation decreased the extent of distribution of the drug as reflected in V_{ss} and V_z values (Table 6.3), although to a lesser degree than that seen with the CL values (7-12 fold versus 40-80 fold, respectively). The declines in both the clearance and volume of distribution upon conjugation resulted in longer terminal half life and MRT values for the conjugate, compared with the parent drug (Table 6.3).

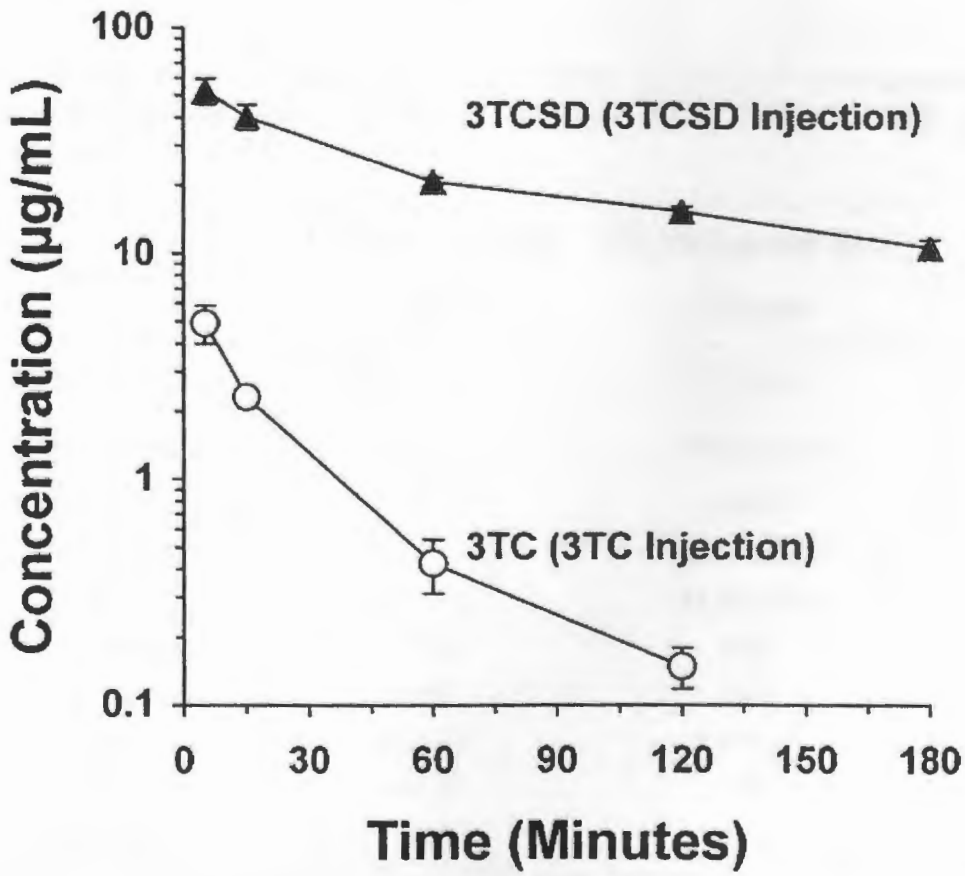

Figure 6.7. Plasma concentration–time courses of the conjugated (3TCSD) and unconjugated (3TC) lamivudine after iv administration of single 5-mg/kg doses (3TC equivalent) of 3TC or 3TCSD to rats. Standard deviation values are shown as error bars ($n = 3$ rats for each point).

The literature information about the pharmacokinetics of 3TC in rats is limited. We are aware of only one study reporting the plasma concentration-time course and AUC of the drug after a 230 mg/kg iv dose (Reddy et al., 2005). However, no other pharmacokinetic parameters were reported in that study. We estimated a CL value of 27.1 mL/min/kg from the AUC and dose values reported in that study. This value is very close to our value of 32.6 mL/min/kg after a much smaller dose of 5 mg/kg (Table 3), suggesting linear pharmacokinetics of 3TC in the dosage range of 5-230 mg/kg.

Table 6.3. Plasma Pharmacokinetic Parameters (Mean ± S.D.) of Unconjugated (3TC) and Dextran-Conjugated (3TCSD) Lamivudine after a Single iv Dose (5 mg/kg, 3TC Equivalent) of 3TC or 3TCSD

Parameter	3TC-Injected Rats	3TCSD-Injected Rats[a]
	3TC	3TCSD
C_{max}, μg/mL	4.94 ± 0.93[†]	52.5 ± 6.5
AUC, μg min/mL	153 ± 7[†]	5930 ± 153
CL, mL/min per kg	32.6[b]	0.844[b]
CL_R, mL/min per kg	21.3 ± 2.1[†]	0.263 ± 0.089
f_e, %	65.3 ± 6.5[†]	31.2 ± 10.6
V_z, mL/kg	1786[b]	152[b]
V_{ss}, mL/kg	930[b]	135[b]
λ_z, min^{-1}	0.0183[b]	0.00554[b]
$t_{1/2(\lambda_z)}$, min	37.9[b]	125[b]
MRT, min	28.5[b]	160[b]

[a] No quantifiable concentrations of 3TC or 3TCS were detected in plasma after 3TCSD injection.
[b] Standard deviations could not be determined because of destructive sampling method.
[†] Significantly different (P<0.05) from the corresponding value for the 3TCSD-injected rats.

The hepatic concentration-time courses (top) and AUC values (bottom) of the conjugate and regenerated 3TC after the administration of the conjugate and those of 3TC after the injection of the parent drug itself are depicted in Figure 6.8. After the injection of 3TC, the hepatic concentrations of the drug were measurable only in the first two samples; no detectable 3TC levels were found in the liver beyond 15 min following the administration of the parent drug (Figure 6.8, top). However, relatively high concentrations of 3TCSD were detected until the last sampling point. This resulted in > fifty-fold higher (P<0.0001) AUCs for the conjugated 3TC, compared with the parent drug (Figure 6.8, bottom). Additionally, the conjugated 3TC slowly released 3TC in the liver (Figure 6.8, top) with an AUC that was approximately 2.5-fold larger (P<0.0001) than that of the parent drug during the sampling time (Figure 6.8, bottom). No measurable concentrations of 3TCS were found in the liver.

Conjugation of 3TC to dextran substantially decreased both the CL and volume of distribution of 3TC (Table 6.3), while at the same time increasing the accumulation of the drug in the liver (Figure 8). A similar disposition pattern was also observed for a dextran prodrug of methylprednisolone with a succinate linker (Zhang et al., 2001). The simultaneous decrease in volume of distribution and increase in liver accumulation upon dextran conjugation is due to the relatively large pore sizes of the liver sinusoids in comparison with those in the vascular beds of most other organs, allowing unrestricted access of the conjugate to the space of Disse and internalization of the conjugate (Mehvar et al., 1994).

Because of limited number of liver samples with quantifiable 3TC concentrations after 3TC injection and slow apparent declines in the liver concentrations of the conjugate and regenerated 3TC after conjugate injection (Figure 6.8, top), terminal half lives were not estimated for the liver. Consequently, liver AUC values depicted in Figure 6.8 (bottom panel) are related to the sampling period without extrapolation to infinity. However, the significant differences between the liver AUCs after 3TC and 3TCSD injections would be expected to be even larger if extrapolated AUCs were used. This is because the apparent decline in the 3TCSD or regenerated 3TC concentrations was substantially slower than that in the liver concentrations of the parent drug (Figure 6.8, top).

The slow decline in the 3TCSD concentrations in the liver (Figure 6.8, top) is in agreement with previous ex vivo studies using isolated perfused rat livers (Mehvar 1997) showing that, once in the liver, the rate of exocytosis of dextrans from the liver cells is negligible. Therefore, the main reason for the decline in the liver concentrations of the conjugate is its elimination by the liver, which is relatively slow based on the in vitro studies in lysosomes (Figure 6.6). Nevertheless, in contrast to undetectable concentrations of 3TC in the liver beyond 15 min after the parent drug injection, high concentrations of the conjugate in the liver were associated with a gradual and sustained generation of the parent drug in this tissue (Figure 6.8).

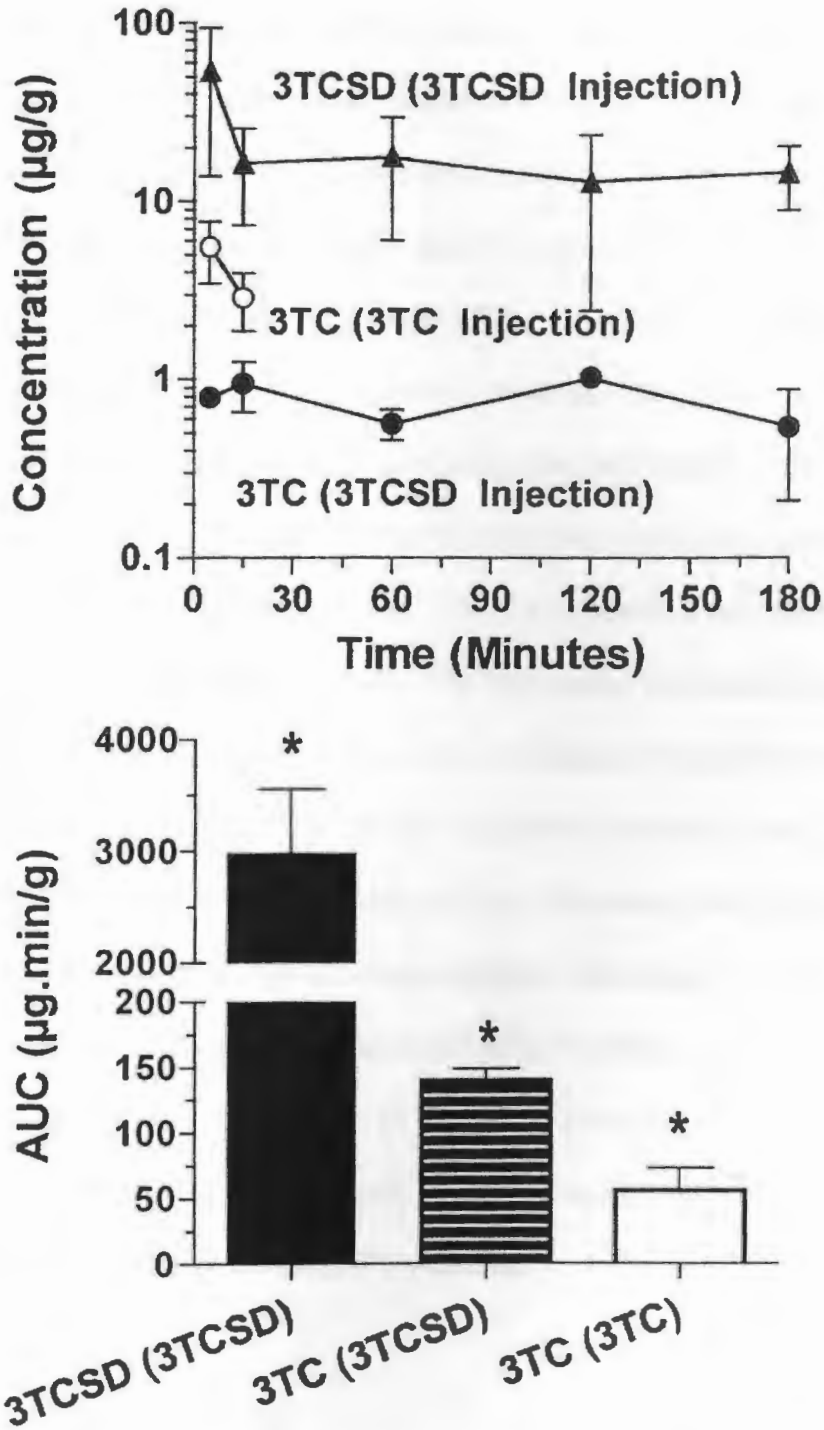

Figure 6.8. Liver concentration–time courses (top) and AUC values (bottom) of parent (3TC) and/or conjugated (3TCSD) lamivudine after iv administration of single 5 mg/kg doses (3TC equivalent) of 3TC or 3TCSD to rats. Standard deviation values are shown as error bars (n = 3 rats for each time point). Asterisks indicate significant differences from the other two groups.

The kidney concentration-time courses (top) and AUC values (bottom) of the conjugate and regenerated 3TC after the administration of the conjugate and those of 3TC after the injection of the parent drug itself are depicted in Figure 6.9 and Table 4. In addition to the liver (Figure 6.8), kidney was the only other organ where high concentrations of the conjugated and regenerated 3TC were found (Figure 6.9). In contrast to the liver (Figure 6.8), however, relatively high and persistent concentrations of 3TC were found in the kidney even after the injection of the parent drug (Figure 6.9). Therefore, conjugation of 3TC with dextran did not increase the availability of free 3TC in the kidneys, as the AUCs of regenerated and parent 3TC were not significantly different (Figure 6.9). The substantial accumulation of the conjugate in the kidneys is consistent with the M_w dependency of the renal excretion of the carrier dextrans in rats (*22*). Whereas a significant portion of the dose of dextrans with M_w's of 4 kDa and 20 kDa was excreted into urine, renal excretion of dextrans with M_w's of 70 kDa and 150 kDa was negligible. Interestingly, kidneys have been suggested as an extrahepatic site for virus replication in different models of HBV infection (Di Bisceglie et al., 1990, Ogston et al., 1989). Therefore, accumulation of the conjugate and release of 3TC in this organ, in addition to that in the liver, may be of potential therapeutic benefit in chronic HBV infection.

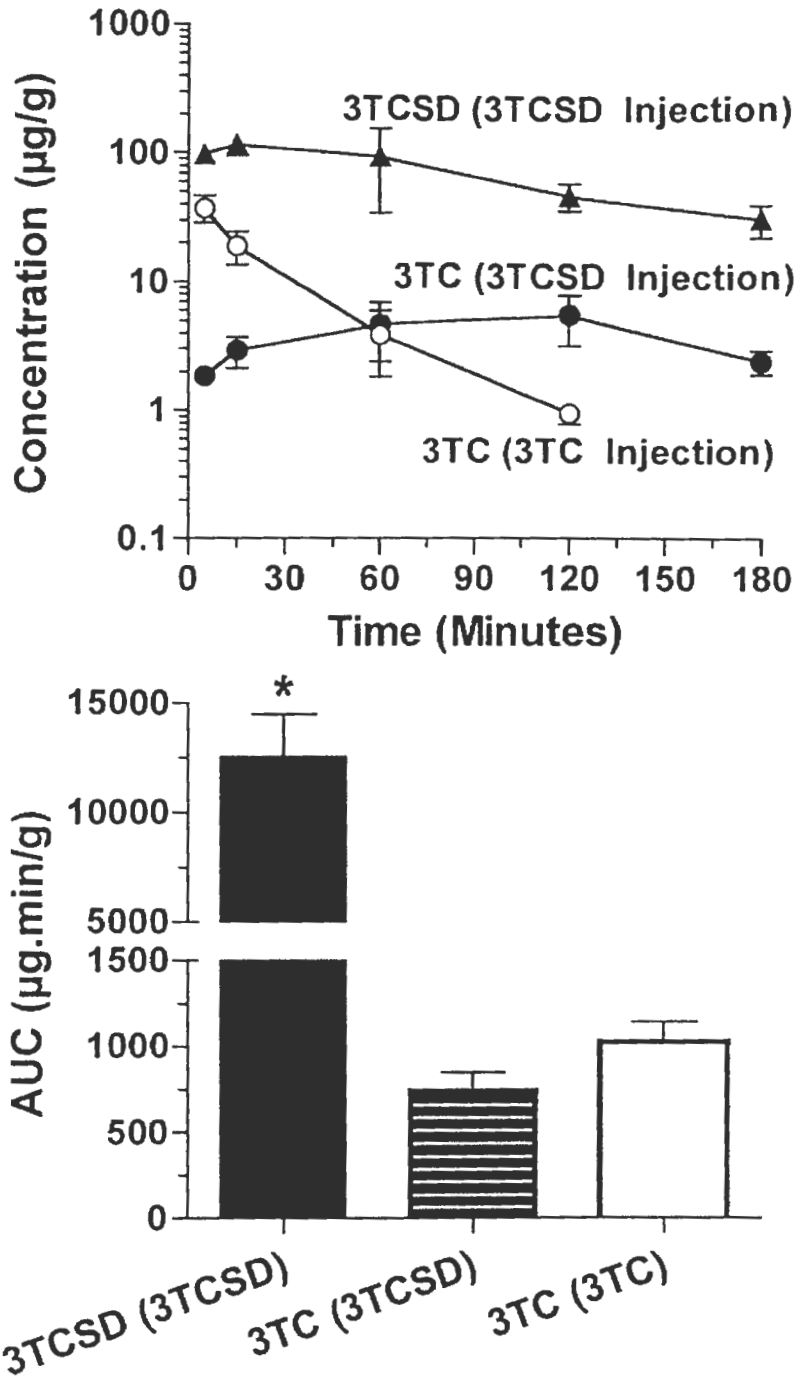

Figure 6.9. Kidney concentration–time courses (top) and AUC values (bottom) of parent (3TC) and/or conjugated (3TCSD) lamivudine after iv administration of single 5 mg/kg doses (3TC equivalent) of 3TC or 3TCSD to rats. Standard deviation values are shown as error bars (n = 3 rats for each time point). Asterisk indicates significant differences from the other two groups.

www.ma

In contrast to the liver (Figure 6.8) and kidneys (Figure 6.9), the concentrations of the conjugate and/or regenerated 3TC were very low or undetectable in the lungs, spleen, and heart (brain) after 3TCSD injection (data not shown). Additionally, no released 3TC could be detected in these tissues. The concentrations of 3TC after 3TC injection in organs other than kidney were also low or below the limit of detection in most of the samples.

Although our conjugate released both 3TC and 3TCS in vitro in buffers (Figures 6.3 and 6.4) and rat blood (Figure 6.5), only 3TC was observed in biological samples after in vivo administration of the conjugate (Figures 6.8 and 6.9). This suggests rapid conversion of any released 3TCS to 3TC in vivo. Our previous work on a methylprednisolone-succinate-dextran conjugate (Zhang et al., 2001) also showed similar results, in that no measurable concentrations of methylprednisolone succinate were found in biological samples after the administration of the conjugate to rats. The rapid conversion of 3TCS to 3TC in vivo is advantageous because 3TCS is not expected to have any biological effects by itself. This is due to the fact that to be effective, 3TC should undergo stepwise phosphorylation at the 5'-position to monophosphate, diphosphate, and triphosphate form before 5'-triphosphate 3TC is incorporated into the viral DNA (Johnson et al., 1999). Therefore, 3TCS, which has a succinate moiety at the 5'-position (Schemes 6.1, and 6.2), cannot be converted to the active 5'-triphosphate 3TC without first being converted to 3TC.

The tissue exposure to 3TC after the administrations of the equivalent doses of the conjugate and the parent drug is the most relevant parameter in terms of targeting index. The ratios of 3TC AUCs after the conjugate and parent drug administration were 2.41 for the liver, 0.721 for the kidneys, and zero for the remaining studied tissues. These data clearly show that the conjugation of 3TC to dextran only increased the targeting of the drug to the liver. On the other hand, conjugation decreased accumulation of 3TC in all the other tissues except the kidneys, where conjugation did not have any significant effect. The significantly higher accumulation of 3TC in the liver is in conformity with the hypothesis of the study, i.e., conjugation of 3TC with dextran allows preferential accumulation of the drug in the liver.

6.5. Conclusions

In conclusion, a method is presented for the synthesis of a conjugate of native dextran with the antiviral drug 3TC using a succinate linker. Additionally, validated size-exclusion and reversed phase assays are developed for the determination of purity, in vitro release characteristics, and in vivo disposition of 3TCSD. Using these methods, the parent conjugate and its degradation products, 3TC and 3TCS, may be quantitated in non-biological and biological samples. In vitro studies indicate an evidence of lysosomal degradation and relative stability of the conjugate in buffers and blood. Additionally, in vivo studies after the administration of the conjugate or the parent drug to rats suggest that the conjugation increases the delivery of the drug to the liver, resulting in higher exposure of the liver to the regenerated antiviral drug.

6.6. References

Agarwal, H. K., Kumar, A., Mehvar, R., and Parang, K. *American Chemical Society National Meeting*, **2007**, Chicago, Illinois.

Alnouti, Y., White, C. A., and Bartlett, M. G. Determination of lamivudine in plasma, amniotic fluid, and rat tissues by liquid chromatography. *J. Chromatogr. B Analyt. Technol. Biomed. Life Sci.*, **2004**, 803, 279-284.

Bailer, A. J. Testing for the equality of area under the curves when using destructive measurement techniques. *J. Pharmacokinet. Biopharm.*, **1988**, 16, 303-309.

Balboni, P. G., Minia, A., Grossi, M. P., Barbanti-Brodano, G., Mattioli, A., and Fiume, L. (1976) Activity of albumin conjugates of 5-fluorodeoxyuridine and cytosine arabinoside on poxviruses as a lysosomotropic approach to antiviral chemotherapy. *Nature*, **1976**, 264, 181-183.

Bezy, V., Morin, P., Couerbe, P., Leleu, G., and Agrofoglio, L. Simultaneous analysis of several antiretroviral nucleosides in rat plasma by high-performance liquid chromatography with UV using acetic acid/hydroxylamine buffer. Test of this new volatile medium-pH for HPLC-ESI-MS/MS. *J. Chromatogr. B Analyt. Technol. Biomed. Life Sci.*, **2005**, 821, 132-143.

Bijsterbosch, M. K., van de Bilt, H., and van Berkel, T. J. Specific targeting of a lipophilic prodrug of iododeoxyuridine to parenchymal liver cells using lactosylated reconstituted high density lipoprotein particles. *Biochem. Pharmacol.*, **1996**, 52, 113-121.

Chimalakonda, A. P., Montgomery, D. L., Weidanz, J. A., Shaik, I. H., Nguyen, J. H., Lemasters, J. J., Kobayashi, E., and Mehvar, R. Attenuation of acute rejection in a rat liver transplantation model by a liver-targeted dextran prodrug of methylprednisolone. *Transplantation*, **2006**, 81, 678-685.

Chimalakonda, A. P., and Mehvar, R. Dextran-methylprednisolone succinate as a prodrug of methylprednisolone: local immunosuppressive effects in liver after systemic administration to rats. *Pharm. Res.*, **2003**, 20, 198-204.

De Vrueh, R. L., Rump, E. T., van De Bilt, E., van Veghel, R., Balzarini, J., Biessen, E. A., van Berkel, T. J., and Bijsterbosch, M. K. Carrier-mediated delivery of 9-(2-phosphonylmethoxyethyl)adenine to parenchymal liver cells: a novel therapeutic approach for hepatitis B. *Antimicrob. Agents Chemother.*, **2000**, 44, 477-483.

Di Bisceglie, A. M., and Hoofnagle, J. H. Hepatitis B virus replication within the human spleen. *J. Clin. Microbiol.*, **1990**, 28, 2850-2852.

Enriquez, P. M., Jung, C., Josephson, L., and Tennant, B. C. Conjugation of adenine arabinoside 5'-monophosphate to arabinogalactan: synthesis, characterization, and antiviral activity. *Bioconjug. Chem.*, **1995**, 6, 195-202.

Erion, M. D., van Poelje, P. D., Mackenna, D. A., Colby, T. J., Montag, A. C., Fujitaki, J. M., Linemeyer, D. L., and Bullough, D. A. Liver-targeted drug delivery using HepDirect prodrugs. *J. Pharmacol. Exp. Ther.*, **2005**, 312, 554-60.

Fiume, L., Di Stefano, G., Busi, C., Mattioli, A., Bonino, F., Torrani-Cerenzia, M., Verme, G., Rapicetta, M., Bertini, M., and Gervasi, G. B. Liver targeting of antiviral nucleoside analogues through the asialoglycoprotein receptor. *J. Viral Hepat.*, **1997**, 4, 363-70.

Fiume, L., Di Stefano, G., Busi, C., Mattioli, A., Battista Gervasi, G., Bertini, M., Bartoli, C., Catalani, R., Caccia, G., Farina, C., Fissi, A., Pieroni, O., Giuseppetti, R., D'Ugo, E., Bruni, R., and Rapicetta, M. Hepatotropic conjugate of adenine arabinoside monophosphate with lactosaminated poly-L-lysine. Synthesis of the carrier and pharmacological properties of the conjugate. *J. Hepatol.*, **1997**, 26, 253-259.

Fiume, L., Bassi, B., Busi, C., Mattioli, A., Spinosa, G., and Faulstich, H. Galactosylated poly(L-lysine) as a hepatotropic carrier of 9-beta-D-arabinofuranosyladenine 5'-monophosphate. *FEBS Lett.*, **1986**, 203, 203-206.

Harboe, E., Larsen, C., Johansen, M., and Olesen, H. P. Macromolecular prodrugs. XV. Colon-targeted delivery-bioavailability of naproxen ester prodrugs varying in molecular size in the pig. *Pharm. Res.*, **1989**, 6, 919-923.

Jarvis, B., Faulds, D. Lamivudine. A review of its therapeutic potential in chronic hepatitis B. *Drugs*, **1999**, 58, 101-41.

Johnson, M. A., Moore, K. H., Yuen, G. J., Bye, A., and Pakes, G. E. Clinical pharmacokinetics of lamivudine. *Clin. Pharmacokinet.*,**1999**, 36, 41-66.

Kano, E. K., dos Reis Serra, C. H., Koono, E. E., Andrade, S. S., Porta, V. Determination of lamivudine in human plasma by HPLC and its use in bioequivalence studies. *Int. J. Pharm.*, **2005**, 297, 73-79.

Kenney, K. B., Wring, S. A., Carr, R. M., Wells, G. N., and Dunn, J. A. Simultaneous determination of zidovudine and lamivudine in human serum using HPLC with tandem mass spectrometry. *J. Pharm. Biomed. Anal.*, **2000**, 22, 967-983.

Lake, J. R., Licko, V., Van Dyke, R. W., and Scharschmidt, B. F. Biliary secretion of fluid-phase markers by the isolated perfused rat liver. Role of transcellular vesicular transport. *J. Clin. Invest.*, **1985**, 76, 676-684.

المنارة للاستشارات

www.man

Larsen, C. Dextran prodrugs-structure and stability in relation to therapeutic activity. *Adv. Drug Deliv. Rev.*, **1989**, 3, 103-154.

Larsen, C., Harboe, E., Johansen, M., and Olesen, H. P. Macromolecular prodrugs. XVI. Colon-targeted delivery-comparison of the rate of release of naproxen from dextran ester prodrugs in homogenates of various segments of the pig gastrointestinal tract. *Pharm. Res.*, **1989**, 6, 995-999.

McLeod, A. D., Friend, D. R., and Tozer, T. N. Synthesis and chemical stability of glucocorticoid-dextran esters: potential prodrugs for colon-specific delivery. *Int. J. Pharmaceut.*, **1993**, 92, 105-114.

McLeod, A. D., Friend, D. R., and Tozer, T. N. Glucocorticoid-dextran conjugates as potential prodrugs for colon-specific delivery: hydrolysis in rat gastrointestinal tract content. *J. Pharm. Sci.*, **1994**, 83, 1284-1288.

Mehvar, R. Recent trends in the use of polysaccharides for improved delivery of therapeutic agents: pharmacokinetic and pharmacodynamic perspectives. *Curr. Pharm. Biotechnol.*, **2003**, 4, 283-302.

Mehvar, R. Dextrans for targeted and sustained delivery of therapeutic and imaging agents. *J. Control. Release*, **2000**, 69, 1-25.

Mehvar, R., Dann, R. O., and Hoganson, D. A. Kinetics of hydrolysis of dextran-methylprednisolone succinate, a macromolecular prodrug of methylprednisolone, in rat blood and liver lysosomes. *J. Control. Release*, **2000**, 68, 53-61.

Mehvar, R., and Hoganson, D. A. Dextran-methylprednisolone succinate as a prodrug of methylprednisolone: immunosuppressive effects after in vivo administration to rats. *Pharm. Res.*, **2000**, 17, 1402-1407.

Mehvar, R. Kinetics of hepatic accumulation of dextrans in isolated perfused rat livers. *Drug Metab. Dispos.*, **1997**, 25, 552-556.

Mehvar, R., Robinson, M. A., and Reynolds, J. M. Dose dependency of the kinetics of dextrans in rats: effects of molecular weight. *J. Pharm. Sci.*, **1995**, 84, 815-818.

Mehvar, R., Robinson, M. A., and Reynolds, J. M. Molecular weight dependent tissue accumulation of dextrans: *in vivo* studies in rats. *J. Pharm. Sci.*, **1994**, 83, 1495-1499.

Mehvar, R., and Shepard, T. L. Molecular weight-dependent pharmacokinetics of fluorescein-labeled dextrans in rats. *J. Pharm. Sci.*, **1992**, 81, 908-912.

Nakane, S., Matsumoto, S., Takakura, Y., Hashida, M., and Sezaki, H. The accumulation mechanism of cationic mitomycin c-dextran conjugates in the liver: in-

المنارة للاستشارات

www.ma

vivo cellular localization and in-vitro interaction with hepatocytes. *J. Pharm. Pharmacol.*, **1987**, 40, 1-6.

Nishikawa, M., Kamijo, A., Fujita, T., Takakura, Y., Sezaki, H., and Hashida, M. Synthesis and pharmacokinetics of a new liver-specific carrier, glycosylated carboxymethyl-dextran, and its application to drug targeting. *Pharm. Res.*, **1993**, 10, 1253-1261.

Nishikawa, M., Yamashita, F., Takakura, Y., Hashida, M., and Sezaki, H. Demonstration of the receptor-mediated hepatic uptake of dextran in mice. *J. Pharm. Pharmacol.*, **1992**, 44, 396-401.

Nishida, K., Tonegawa, C., Nakane, S., Takakura, Y., Hashida, M., and Sezaki, H. Effect of electric charge on the hepatic uptake of macromolecules in the rat liver. *Int. J. Pharmaceut.*, **1990**, 65, 7-17.

Ogston, C. W., Schechter, E. M., Humes, C. A., and Pranikoff, M. B. Extrahepatic replication of woodchuck hepatitis virus in chronic infection. *Virology*, **1989**, 169, 9-14.

Reddy, K. R., Colby, T. J., Fujitaki, J. M., van Poelje, P. D., and Erion, M. D. Liver targeting of hepatitis-B antiviral lamivudine using the HepDirect prodrug technology. *Nucleosides Nucleotides Nucleic Acids*, **2005**, 24, 375-81.

Rensen, P. C. N., Devrueh, R. L. A., and Vanberkel, T. J. C. Targeting hepatitis B therapy to the liver: Clinical pharmacokinetic considerations. *Clin. Pharmacokinet.*, **1996**, 31, 131-155.

Shah, V. P., Midha, K. K., Dighe, S., McGilveray, I. J., Skelly, J. P., Yacobi, A., Layoff, T., Viswanathan, C. T., Cook, C. E., McDowall, R. D., Pittman, K. A., and Spector, S. Analytical methods validation: bioavailability, bioequivalence, and pharmacokinetics. *J. Pharm. Sci.*, **1992**, 81, 309-312.

Shaw, T., Locarnini, S. A. Preclinical aspects of lamivudine and famciclovir against hepatitis B virus. *J. Viral Hepat.*, **1999**, 6, 89-106.

Stock, R. J., Cilento, E. V., and McCuskey, R. S. A quantitative study of fluorescein isothiocyanate-dextran transport in the microcirculation of the isolated perfused rat liver. *Hepatology*, **1989**, 9, 75-82.

Takahashi, H., Fujimoto, J., Hanada, S., and Isselbacher, K. J. Acute hepatitis in rats expressing human hepatitis B virus transgenes. *Proc. Natl. Acad. Sci. U. S. A.*, **1995**, *92*, 1470-1474.

Takakura, Y., and Hashida, M. Macromolecular drug carrier systems in cancer chemotherapy: macromolecular prodrugs. *Crit. Rev. Oncol. Hematol.*, **1995**, 18, 207-

231.

Thoren, L. The dextrans-clinical data. *Develop. Biol. Stand.*, **1981**, 48, 157-167.

Tu, J., Zhong, S., and Li, P. Studies on acyclovir-dextran conjugate: synthesis and pharmacokinetics. *Drug Dev. Ind. Pharm.*, **2004**, 30, 959-65.

Vansteenkiste, S., Schacht, E., Duncan, R., Seymour, L., Pawluczyk, I., and Baldwin, R. Fate of glycosylated dextrans after in vivo administration. *J. Control. Release*, **1991**, 16, 91-100.

Wu, C. H., Ouyang, E. C., Walton, C., Promrat, K., Forouhar, F., and Wu, G. Y. Hepatitis B virus infection of transplanted human hepatocytes causes a biochemical and histological hepatitis in immunocopetentent rats. *World J. Gastroenterol.*, **2003**, 9, 978-83.

Wu, C. H., Ouyang, E. C., Walton, C., and Wu, G. Y. Liver cell transplantation -- novel animal model for human hepatic viral infections. *Croat. Med. J.*, **2001**, 42, 446-450.

Yamaoka, T., Kuroda, M., Tabata, Y., and Ikada, Y. Body distribution of dextran derivatives with electric charges after intravenous administration. *Int. J. Pharmaceut.*, **1995**, 113, 149-157.

Younger, H. M., Bathgate, A. J., and Hayes, P. C. Review article: Nucleoside analogues for the treatment of chronic hepatitis B. *Aliment. Pharmacol. Ther.*, **2004**, *20*, 1211-30.

Yuan, J. Estimation of variance for AUC in animal studies. *J. Pharm. Sci.*, **1993**, 82, 761-763.

Zhang, X., and Mehvar, R. Dextran-methylprednisolone succinate as a prodrug of methylprednisolone: dose-dependent pharmacokinetics in rats. *Int. J. Pharm.*, **2001**, 229, 173-182.

Zhang, X., and Mehvar, R. Dextran-methylprednisolone succinate as a prodrug of methylprednisolone: plasma and tissue disposition. *J. Pharm. Sci.*, **2001**, 90, 2078-2087.

Zheng, J. J., Wu, S. T., and Emm, T. A. High-performance liquid chromatographic assay for the determination of 2'-deoxy-3'-thiacytidine (lamivudine) in human plasma. *J. Chromatogr. B Biomed. Sci. Appl.*, **2001**, 761, 195-201.

Zhou, X. J., and Sommadossi, J. P. Rapid quantitation of (-)-2'-deoxy-3'-thiacytidine in human serum by high-performance liquid chromatography with ultraviolet detection. *J. Chromatogr. B Biomed. Sci. Appl.*, **1997**, 691, 417-424.

المنارة للاستشارات

www.man

Chapter 7

Synthesis and Anti-HIV Activities of Nucleoside-Sodium Cellulose Sulfate Conjugates

Hitesh K. Agarwal,[a] Anil Kumar,[a] Gustavo F. Doncel,[b] Keykavous Parang[a]

[a]Department of Biomedical and Pharmaceutical Sciences, University of Rhode Island, Kingston, RI, USA, 02881;[b]CONRAD, Department of Obstetrics and Gynecology, Eastern Virginia Medical School, Norfolk, VA, USA 23507

7.1. Abstract

Sulfonate and sulfate polyanionic microbicides, such as sodium cellulose sulfate (CS, **7.1**), are inhibitors of HIV entry and sperm-function. CS was first reacted with 2-bromoacetic acid to yield CS-acetate (CSA, **7.2**), which was further reacted with AZT, FLT, and 3TC to give AZT-CSA (**7.3**, 1.78% loading), FLT-CSA (**7.4**, 1.43% loading), and 3TC-CSA (**7.5**, 1.07% loading), respectively. Furthermore, CS was conjugated to nucleoside analogs (AZT, FLT, and 3TC) through succinate linker to produce bifunctional nucleoside-CS conjugates. For the synthesis of the conjugates containing succinate linker, CS was reacted with AZT-succinate and FLT-succinate to give AZT-succinate-CS (**7.6**, 18.48% loading) and FLT-succinate-CS (**7.7**, 7.87% loading), respectively. These conjugates were designed to improve the anti-HIV profile of parent compounds. It was expected that extracellular hydrolysis of conjugates will release nucleosides and CS providing broad-spectrum activity, a higher barrier to drug resistance, microbicidal, and contraceptive activity. The anti-HIV activities of the conjugates were evaluated and were compared with the corresponding physical mixtures of nucleoside analogs and anionic polymers and with different classes of polyanionic polymers, such as dextran acetate, cellulose phosphate, and cellulose acetate. Cellulose acetate, cellulose phosphate, and dextran acetate were found to have no anti-HIV activities, suggesting the importance of the presence of sulfate on the cellulose for generating anti-HIV activities. The conjugates containing CS-acetate were found to be more potent than CS and other derivatives. AZT-CSA (**7.3**) and FLT-CSA conjugates (**7.4**) exhibited higher anti-HIV activities than CS (**7.1**) and AZT-succinate-CS and FLT-succinate-CS-conjugates (**7.6** and **7.7**). The presence

of both sulfate and the acetate groups on cellulose were critical for generating maximum anti-HIV activity, possibly by increasing the negative charge density that is essential for blocking HIV entry. However, the compounds were less potent than the corresponding physical mixtures of nucleoside analogs with CSA (**7.2**), due to incomplete hydrolysis.

7.2. Introduction

Sulfonate and sulfate polyanionic microbicides inhibit the HIV entry into the cell (Chan and Kim, 1998; Gao et al., 1999; Ketas et al., 2003; Vlieghe et al., 2002) and sperm-function (Anderson et al., 2000). Sodium cellulose sulfate (Ushercell, CS) is a polyanionic non-cytotoxic microbicide and its 6% gel has been studied as vaginal contraceptive and a broad spectrum antimicrobial agent (Mauck et al., 2001, Malonza et al., 2005).

Polyanionic sulfates are the polymers such as dextran, cellulose, styrene etc with sulfate groups in their structure (Bugatti et al., 2007, Moulard et al., 2000, Gao et al., 1999, Vlieghe et al., 2002). The negatively-charged sulfate group interacts with positively-charged viral protein (Shattock et al., 2002). Viral envelop protein gp120 is know to have positively charged residues in its V3 loop. Viral entry in the host cell depends on the interaction with the negatively-charged surface of the coreceptors CXCR4 and CCR5 (Kajumo et al., 2000). Polyanionic sulfates exhibit their inhibitory activity by blocking the interaction between negatively-charged coreceptors and

positively charged V3 loop of viral gp120 protein (D'Cruz et al., 2004, Baba et al., 1998, Turpin, 2002).

Different strains of HIV are known to have different V3 loops and therefore show different interactions with the host cell. X4-strains of HIV possess a higher positive charge density on their V3 loop than R5 strains of virus (Shattock et al., 2002, Meylan et al., 1994). This property of X4 makes them susceptible to polyanionic inhibitors. On the other hand, several polyanionic derivatives like dextran sulfate and heparin show insignificant activity against R5 strain of virus (Scordi-Bello et al., 2005, D'Cruz et al., 2004).

Similar to other polyanionic derivatives, sodium cellulose sulfate (CS, **7.1**), interacts with the positively-charged viral envelope proteins, and prevents the virus from interaction with coreceptors. Various studies show that CS possesses significant anti-HIV activity against both the strains of virus, but it is more active against X4 strain (IC_{50} = 0.65 μg/ml) than R5 strain (IC_{50} = 18.67 μg/ml) of virus (Scordi-Bello et al., 2005, Neurath et al., 2002). The ability of CS to inhibit both strains of virus efficiently suggests that some additional mechanism may be involved for viral inhibition (Scordi-Bello et al., 2005, Neruth et al., 2002).

Other than the anti-microbial activity, CS also shows contraceptive activity because of its ability to reversibly inhibit hyaluronidase (IC_{50} = 1.7 mg/ml), which is an important enzyme for the interaction of spermatozoa with the egg (Anderson et al., 2002). CS also inhibits sperm penetration of cervical mucus membrane (Anderson et al., 2002).

CS showed promising results in the preclinical studies, phase I and phase II clinical trials sponsored by CONRAD. In preclinical studies, CS prevented conception in rabbits when applied vaginally before insemination, and was also found to inhibit HIV, *Neisseria gonorrhoeae*, and *Chlamydia trachomatis* (Crucitti et al., 2007, Anderson et al., 2002). Results from phase I clinical trials showed that CS was very safe and non-irritating to penile and vaginal application (Mauck et al., 2001, Mauck et al., 2001). CS vaginal gel (6%) was well tolerated as vaginal microbicide in both healthy and HIV-infected women and produced similar results in comparison to K-Y jelly, a commercially available product for contraceptive (El-Sadr et al., 2006, Malonza et al., 2005, Schwartz et al., 2006).

Despite the initial success, CS failed the phase III clinical trial study in January 2007 (Wakabi, 2007). It was found that after women stopped using CS gel, they were more prone to the HIV infection than those who were using placebo. Therefore, the study of 6% CS gel as anti-HIV and contraceptive agent was terminated as it was suspected to increase a woman's susceptibility to HIV infection (Conrad.org).

Herein, we report the synthesis and biological evaluation of bifunctional cellulose sulfate conjugates with nucleoside reverse transcriptase (RT) inhibitors, 3′-azido-2′,3′-dideoxythymidine (Zidovudine, AZT), 3′-fluoro-2′,3′-dideoxythymidine (Alovudine, FLT,), and 2',3'-dideoxy-3'-thiacytidine (Lamivudine, 3TC). Two different linkers (acetate and succinate) were used to conjugate the nucleoside analogs with CS with different loading values. It was expected that the conjugates would be cleaved by hydrolytic activity of cellular esterase enzymes, resulting in two separate components as CS (HIV entry blocker) and nucleoside analogs (RTIs). CS inhibits viral entry inside the cell and is active against X4 strain and cell-associated virus. On the other hand, nucleoside analogs are equally active against R5 and X4 strains and inhibit the function of RT enzyme and HIV replication. In general, the conjugates were expected to provide synergistic and broad-spectrum anti-HIV activity against susceptible and multidrug-resistant strains of virus. Conjugates were also expected to exert contraceptive activity from the released CS.

7.3. Materials and Methods

7.3.1. Materials.

All reagents including CS and cellulose phosphate, ether, dialysis membrane (3000 MW cut off) and solvents were purchased from Fisher Scientific. Size exclusion chromatography was carried out on a Hitachi analytical HPLC system on a analytical gel chromatography column (PolySep-GFC 3000, 300 mm × 7.8 mm; Phenomenex, Torrance, CA) to determine the loading of the nucleoside-linker-CS conjugates The mobile phase was comprised of potassium phosphate monobasic buffer (0.1 M, pH =

www.mar

7.4):acetonitrile (75:25, v/v) and was pumped at a flow rate of 1.0 mL/min. Cellulose sulfate derivatives were extracted by solvent precipitation method and precipitates were centrifuged by using Legend™ RT Refrigerated Tabletop Centrifuge.

7.3.2. Chemistry

Cellulose Sulfate Acetate (CSA, 7.2), Cellulose Acetate (CA, 7.14) and Dextran Acetate (DA, 7.15) The polymers, cellulose sulfate, cellulose, and dextran were converted to 2-acetyl substituted derivatives according to the previously reported procedure (Thomas et al., 1995). The polymer (1 g) and 2-bromoacetic acid (6 g, 43.5 mmol) were dissolved in water (25 mL). Sodium hydroxide (40%, 7.5 ml) was added to the reaction mixture and the mixture was stirred for 18 h at room temperature. The reaction mixture was concentrated at reduced pressure and dialyzed using a membrane (3000 M.Wt. cut off). The solution was further concentrated and dried under reduced pressure to afford 2-acetyl substituted polymers **7.2**, **7.14**, and **7.15**.

AZT-Cellulose Sulfate Acetate (AZT-CSA, 7.3) and FLT-Cellulose Sulfate Acetate (FLT-CSA, 7.4). Compound **7.2** (100 mg), nucleoside (AZT or FLT) (0.25 mmol), and dimethylaminopyridine (DMAP, 30 mg, 0.25 mmol) were dissolved in dimethyl sulfoxide (DMSO) (3 mL). Diisopropylcarbodiimide (DIC, 30 µL, 0.2 mmol) was added to the solution. The reaction mixture was stirred at 40 °C for 24 h. The reaction mixture was cooled to room temperature. Cold diethyl ether:methanol (45 mL, 50:50 v/v) was added to the reaction mixture, and then the layer was washed twice first with cold methanol:diethyl ether ((50 mL, 50:50, v/v) and ether (50 mL),

www.manar

cold methanol:diethyl ether ((50 mL, 50:50, v/v) and ether (50 mL), respectively. The mixture was centrifuged and the precipitate was dried under vacuum to afford **7.3** (loading percentage = 1.78% ± 0.00) or **7.4** (loading percentage = 1.43% ± 0.06).

3TC-Cellulose Sulfate Acetate (3TC-CSA, 7.5). 3TC-cellulose sulfate acetate was synthesized using (-)-N_4-(4,4′-dimethoxytrityl)-2',3'-dideoxy-3'-thiacytidine (**2.12**) and CSA as starting materials. The synthesis of **2.12** was described above in Chapter 2. CSA (100 mg), **2.12** (130 mg, 0.25 mmol), and DMAP (30 mg, 0.25 mmol) were dissolved in DMSO (3 mL). DIC (30 µL, 0.2 mmol) was added to the solution. The reaction mixture was stirred at 40 °C for 24 h. Acetic acid (80%, 10 ml) was added to the reaction mixture and the mixture heated at 80 °C for 30 min. Acetic acid was evaporated under reduced pressure. To the residue was added cold diethyl ether:methanol (45 mL, 50:50 v/v). The mixture was washed twice with cold methanol:diethyl ether (50 mL, 50:50, v/v) and ether (50 mL), respectively, and centrifuged. The precipitate was dried under vacuum to give **7.5** (loading percentage 1.07% ± 0.00).

AZT-Succinate-Cellulose Sulfate (AZT-Succinate-CS, 7.6). AZT-succinate (**3.2**) was synthesized as described in Chapter 3 from the reaction of AZT with succinic anhydride. Compound **3.2** (200 mg, 0.55 mmol), triphenylphosphine (TPP, 300 mg, 1.15 mmol), and sodium cellulose sulfate (**7.1**, 100 mg) were dissolved in DMSO (3 mL). DIAD (100 µl, 0.5 mmol) was added to the reaction mixture. The mixture was stirred at 40 °C for 24 h. Cold diethyl ether: methanol (45 mL, 50:50 v/v) was added to

www.mana

the reaction mixture. The mixture was washed twice with cold methanol:diethyl ether (50 ml, 50:50, v/v) and ether (50 mL), respectively, and was centrifuged. The precipitate was dried under vacuum to give AZT-succinate-cellulose sulfate (**7.6**, loading percentage= 18.48% ± 0.23).

FLT-Succinate-Cellulose Sulfate (7.7). FLT-succinate (**3.1**) was synthesized as described in Chapter 3 from the reaction of FLT with succinic anhydride. Compound **3.1** (200 mg, 0.58 mmol), DMAP (60 mg, 0.25 mmol) and sodium cellulose sulfate (**7.1**, 100 mg) were dissolved in DMSO (3 mL). DIC (50 µl, 0.32 mmol) was added to the reaction mixture. The mixture was stirred at 40 °C for 24 h. Cold diethyl ether:methanol (45 mL, 50:50 v/v) was added to the reaction mixture. The mixture was washed twice with cold methanol:diethyl ether (50 mL, 50:50, v/v) and ether (50 mL), respectively, and was centrifuged. The precipitate was dried under vacuum to give FLT-succinate-cellulose sulfate (**7.7**, loading percentage = 7.87% ± 0.11).

7.3.3. Purity and Loading Percentage Determination of Conjugates of Nucleoside Analogs with Cellulose Sulfate and Cellulose Sulfate Acetate. The percentage of purity and degree of substitution of the nucleoside analogs were determined using size exclusion chromatography (SEC). Initially, a method was developed and validated for parent nucleosides analogs, AZT, FLT and 3TC, dissolved in potassium phosphate monobasic (KH_2PO_4) buffer (pH = 7.4) on a 30 cm × 7.8 mm gel chromatography column (PolySep-GFC 3000). Calibration curves of different concentrations (3, 6, 9, 12 and 15 µg/ml) versus area under the curve (AUC) were plotted for each analog.

www.manar

Similarly, the conjugates were passed through the column. The loading percentage was calculated from the calibration curve. The mobile phase consisted of buffer:acetonitrile (75:25, v/v) and was pumped at a flow rate of 1.0 mL/min.

7.3.4. Anti-HIV Assays. Anti-HIV activities of the compounds were evaluated according to the previously reported procedure (Krebs et al., 1999). In summary, HeLa (Human cervical carcinoma: ATCC CCL-2.1) cell line was used to measure inactivation of both cell-free virus preparations and virus-infected cell preparations. Cells were plated in culture plates 24 hrs prior to each experiment. Cell-free viral preparations of HIV-1 strains IIIB (lymphocytotropic strain) and BaL (monocytotropic strain) were used for cell-free assay. For cell-associated assay, SulT1 cells were infected with IIIB virus 5 days prior to the experiment. Cell-free virus and virus-infected cells were mixed with different compounds and diluted to make different concentrations. The mixture was further diluted with the buffer and added to the HeLa cells. The cells were incubated at 37°C for 48 hrs, stained for β-galctosidease expression and compared with β-galctosidease expression from the β-gal-positive cells in absence of any microbicidal compound to get IC_{50} values.

7.4. Results and discussion

7.4.1. Chemistry

The synthesis of cellulose sulfate acetate conjugates with AZT, FLT, and 3TC was accomplished using building block synthesis strategy. For the synthesis of nucleoside-CSA conjugates, cellulose sulfate (**7.1**) was reacted first with 2-

www.mana

bromoacetic acid in presence of sodium hydroxide to afford cellulose sulfate acetate (CSA, **7.2**). CSA was then reacted with AZT, FLT, or N_4-DMTr-3TC to yield cellulose sulfate acetate conjugates of AZT (**7.3**, AZT-CSA, 1.78% loading), FLT (**7.4**, FLT-CSA, 1.43% loading), or N_4-DMTr-3TC-CSA (7.5′), respectively. Deprotection of DMTr group in **7.5′** afforded 3TC-CSA (**7.5**, 1.07% loading) (Scheme 7.1).

For the synthesis of sodium cellulose sulfate conjugates linked to AZT or FLT through a succinate linker, AZT and FLT were first reacted with succinic anhydride to synthesize AZT succinate and FLT succinate, which were then reacted with cellulose sulfate to afford cellulose sulfate succinate conjugates of AZT (**7.6**, 18.48% loading) and FLT (**7.7**, 7.87% loading) (Scheme 7.2). The Purity and percentage of loading of the nucleosides in the conjugates were determined using the SEC method as described above.

www.mar

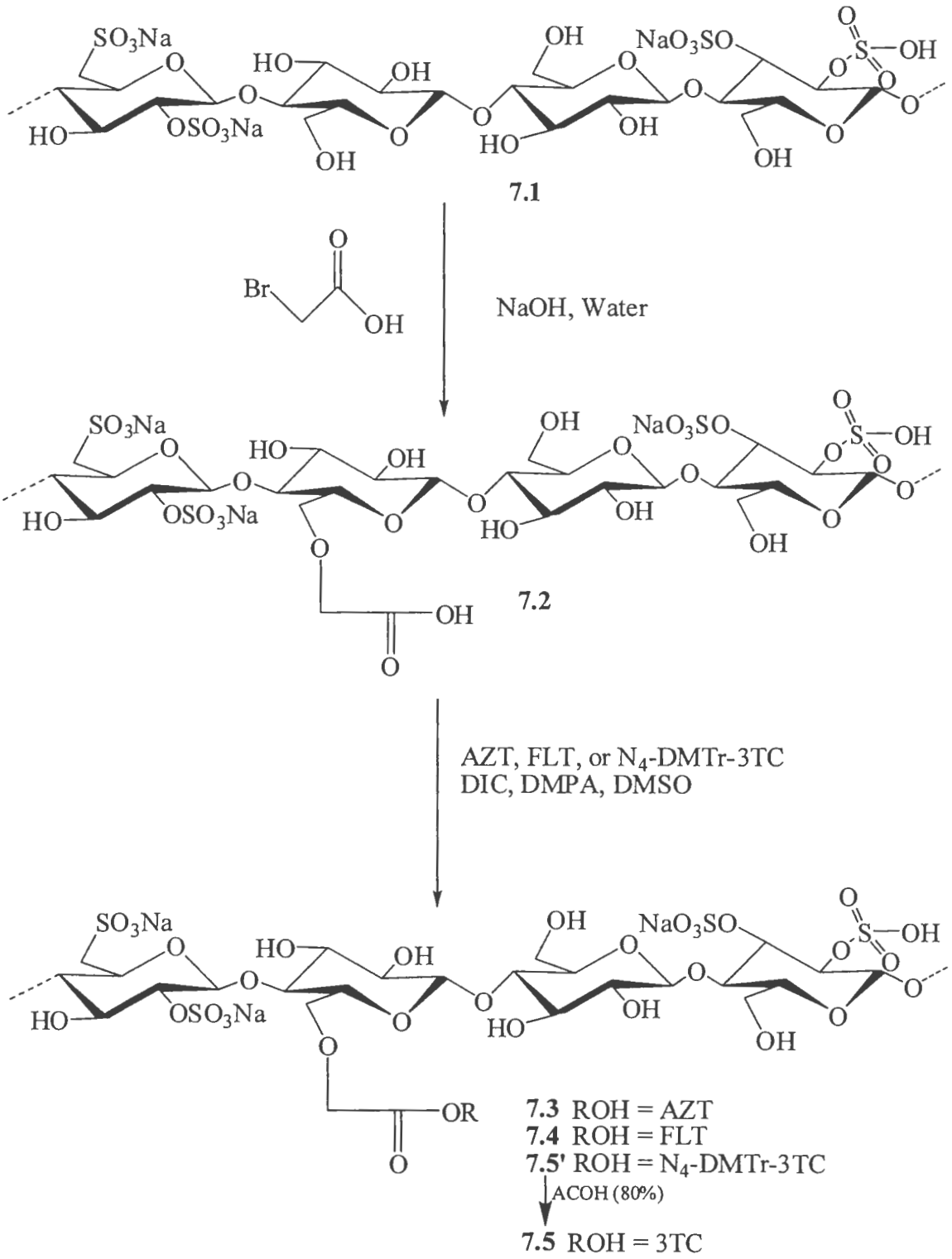

Scheme 7.1. Synthesis of cellulose sulfate acetate conjugates of AZT, FLT and 3TC.

www.mana

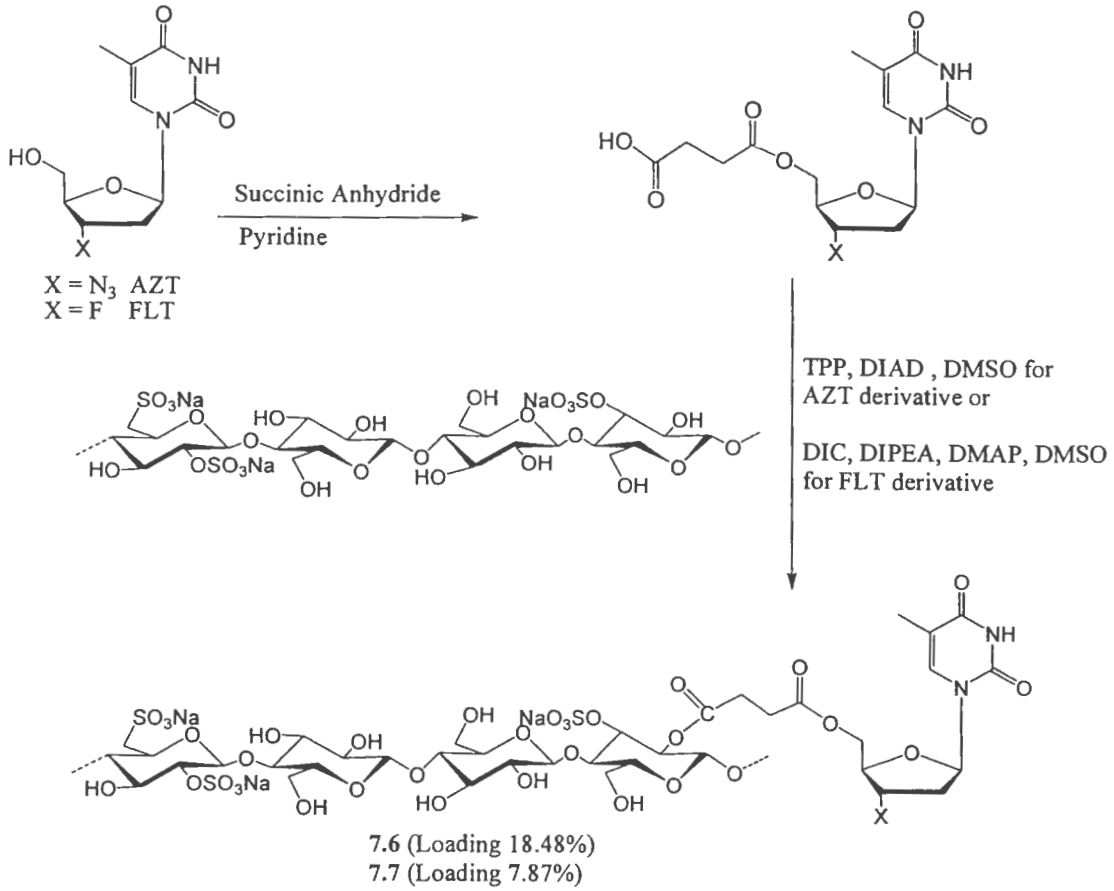

Scheme 7.2. Synthesis of AZT-succinate-CS (**7.6**) and FLT-succinate-CS (**7.7**) conjugates.

7.4.2. Biological Activities

7.4.2.1. Anti-HIV Activities Against Cell-Free and Cell-Associated Strains

Table 7.1 shows the antiviral activities of the cellulose sulfate-nucleoside conjugates with different loading percentages compared to those of CS, AZT, and FLT. CS exhibited approximately 10-fold higher activity against X4 virus (IIIB strain, EC_{50} = 5.9 μg/ml)) than R5 virus (BaL strain, EC_{50} = 62.5 μg/ml) (Table 7.1). The

www.mana

data is consistent with the reported data (Shattock et al., 2002, Meylan et al., 1994) that X4 strains possess higher number of positive charges on their V3 loop of gp120 protein surface compared to those of R5 strains. Higher number of positive charges on V3 loop of X4 strains makes them more susceptible to interaction with anionic polymer CS. On the other hand, conjugation of CS with nucleosides in all conjugates made R5 strains susceptible more susceptible sometimes even more than X4 strains.

Nucleoside-CSA conjugates (AZT-CSA, **7.3**, 1.78%; FLT-CSA, **7.4**, 1.43%) demonstrated higher anti-HIV activities than that of CS (**7.1**). Unlike AZT and FLT (EC_{50} > 100 μg/mL), the conjugates **7.3** and **7.4** were consistently active against cell-associated HIV (CTC assay) (EC_{50} = 5.6-5.8 μg/mL). The improved anti-HIV activities of **7.3** and **7.4** compared to CS is possibly due to the release of two anti-HIV agents with different mechanisms of action and the presence of additional negatively-charged acetate in the structure. Similarly, cellulose sulfate-acetate (**7.2**) exhibited significantly higher potency than CS (**7.1**) against cell-free virus.

The higher anti-HIV activity of **7.3** (EC_{50} = 8.1 μg/mL) and **7.4** (EC_{50} = 1.5 μg/mL) against R5 strains compared to that of CS (EC_{50} = 62.5 μg/ml) demonstrates the synergistic effect of CS conjugation with AZT or FLT. AZT and FLT are active against both R5 (BaL) and X4 (IIIB) strains of virus, but CS is more active against X4 (IIIB) and cell-associated virus.

www.manar

CSA (**7.2**) was tested for anti-HIV activity as a control, and surprisingly it showed slightly higher activity than **7.3** against cell-free virus and was almost equally active against X4 and R5 strains. The better activity of **7.2** and its conjugates, **7.3** and **7.4**, can also be attributed to the presence of free negatively-charged carboxylate group of the acetate groups substituted on CS that enhance the negative charge density along with sulfate. The presence of additional negative charges on the polymer may have improved the HIV entry blocking properties of CS by interacting with positive charges of the viral protein. Although the substitution of acetate group on cellulose sulfate increased the anti-HIV activity of CS, but cellulose acetate (**7.14**) was completely inactive (Table 7.2), suggesting that the presence of sulfate of cellulose is critical in maintaining the anti-HIV activity of the polymer.

3TC-CSA conjugate (**7.5**, 1.07% loading) showed significantly different anti-HIV profile compared with AZT-CSA and FLT-CSA conjugates. Conjugate **7.5** showed almost 37-fold less anti-HIV activity against X4 strain, and was not active against cell-associated virus. The poor anti-HIV activity of 3TC conjugate could be due to the interaction of free 4-amino group of 3TC with the negatively charged groups on CSA that reduces the available free negative charge of the conjugate for binding to V3 loops of the virus.

To determine the contribution of sulfate group in generating anti-HIV activity of CS, cellulose phosphate and dextran acetate were studied as controls. These compounds were found to be totally inactive in viral inhibition assay (Table 7.2),

المنارة للاستشارات
www.mana

suggesting that negatively charged acetate and phosphate alone are not sufficient for efficient interactions with V3 loops of the virus.

The anti-HIV activities of nucleoside-succinate-CS conjugates, AZT-succinate-CS (**7.6**, 18.48%) and FLT-succinate-CS (**7.7**, 7.87%) were also evaluated. Both conjugates demonstrated at least 6-fold higher anti-HIV activity against X4 strains than CS suggesting the contribution of nucleoside analog in anti-HIV activity (Table 7.1). However, **7.6** and **7.7** exhibited less anti-HIV activity against the cell associated virus (EC_{50} = 75-88 μg/mL) than that of CS (EC_{50} = 2.5 μg/mL). The conjugates also showed less anti-HIV activity against cell-free virus when compared with AZT and FLT.

Table 7.1. Anti-HIV activities of nucleoside-cellulose sulfate conjugates.

Compound Code	Chemical Name	CTS[a] EC(50)[b] (μg/ml)	VBI(IIIB)[c] EC(50) (μg/ml)	VBI(BaL)[d] EC(50) (μg/ml)	CTC[e] EC(50) (μg/ml)
7.1	Sodium Cellulose Sulfate (Mol. wt. 2,000,900 Da)	>100	5.9	62.5	2.5
7.2	Cellulose Sulfate Acetate (CSA)	>100	1.3	1.8	6.6
7.3	AZT-Cellulose Sulfate Acetate (AZT-CSA, 1.78% loading)	>100	2.5	8.1	5.6
7.4	FLT-Cellulose Sulfate Acetate (FLT-CSA, 1.43% loading)	>100	2.3	1.5	5.8
7.5	3TC-Cellulose Sulfate Acetate (3TC-CSA, 1.07% loading)	>100	92.4	75.1	>100
7.6	AZT-Succinate-Cellulose Sulfate (AZT-Suc-CS, 17.2% loading)	>100	2.2	9.9	74.8
7.7	FLT-Succinate-Cellulose Sulfate (FLT-Suc-CS, 7.87% loading)	>100	6.2	6.1	87.6
AZT	Zidovudine	>100	2.4	4.2	>100
FLT	Alovudine	>100	<0.1	<0.1	>100
3TC	Lamivudine	100	7.5	2.6	18.4

[a]Cytotoxicity assay; [b]50% Effective concentration; [c]Viral entry inhibition assay (lymphocytotropic strain); [d]Viral entry inhibition assay (monocytotropic strain); [e]Cell- to- cell transmission assay (IIIB).

www.mana

Although **7.6** and **7.7** had 10 and 6 times higher loading values than the corresponding conjugates substituted with acetate (**7.3** and **7.4**), respectively, the cellulose sulfate succinate conjugates were generally less active than cellulose sulfate acetate conjugates (Table 7.1). The less anti-HIV activity of conjugates containing succinate linker, despite of their higher nucleoside loading, compared to those containing acetate linker could be due to incomplete hydrolysis of **7.6** and **7.7** to parent nucleosides or the hydrolysis of the conjugate to generate inactive nucleoside-succinate derivatives instead of free nucleosides. Furthermore, upon hydrolysis of conjugates containing acetate linker, the acetate group will remain intact on the CS that contributes to overall negative charge of the anionic polymer.

Table 7.2 shows the anti-HIV activities (in μg/mL) of the nucleoside-CS conjugates compared with the corresponding physical mixtures. The physical mixture of AZT (1.78%) + CSA (**7.8**) showed slightly better anti-HIV activity against cell free virus than the corresponding AZT-CSA conjugate (**7.3**). In comparison to **7.3**, the anti-HIV activity of **7.8** was almost 1.5- and 3.5-fold higher against lymphocytotropic and monocytotropic strains of cell-free virus, respectively, but was 1.5-fold less active against cell associated virus.

When CSA was replaced with CS in the physical mixture with AZT in **7.11** (17.2%), the anti-HIV activity was reduced significantly (2-9 fold) against cell-free virus when compared with the corresponding CSA conjugate **7.8** containing even a lower loading of AZT (1.78%), suggesting the major contribution of CSA in overall

المنارة للاستشارات
www.mana

activity. The physical mixture of AZT with CS (**7.11**, 17.2%) that was in a similar ratio to the AZT-succinate-CS conjugate (**7.6**), showed 2-7-fold less anti-HIV activity against cell-free virus when compared with AZT-CSA conjugate **7.3** (1.78%) and AZT-succinate-CS conjugate **7.6** (17.2%).

Similar results were found in the case of FLT-CSA conjugate (**7.9**) and 3TC-CSA (**7.5**) when compared with the corresponding physical mixtures, **7.4** and **7.10**, respectively. Physical mixture of CSA and FLT (**7.9**, 1.43%) exhibited approximately 3-5 fold higher anti-HIV activity against VBI (cell-free virus) when compared with the corresponding FLT-CSA conjugate (**7.4**, 1.43%). In the case of **7.10**, the free amino group was not able to reduce the anionic interactions of sulfate group as described above in the conjugate **7.5**.

However, the overall anti-HIV activity of **7.9** was reduced by 8-22 times against cell-free virus when CSA in **7.9** (1.43%) was replaced with CS in **7.12** (1.43%), suggesting the importance of CSA in overall anti-HIV activity.

The anti-HIV activity in **7.12** was increased by 10-20 fold against cell-free virus when the FLT content was increased from 1.43% to 7.85% in **7.13**. The data indicates that higher concentration of FLT in the physical mixture improves activity.

The physical mixture of FLT with CS (7.13%) still exhibited 6-fold lower anti-HIV activity against cell-associated virus when compared with FLT-CSA conjugate

www.mana

(**7.9**, 1.43%). These data confirm that CSA is a more appropriate polymer for conjugation with nucleosides or making physical mixtures since all CSA derivatives exhibited better anti-HIV profile when compared with CS derivatives.

The physical mixture of AZT + cellulose acetate (**7.17**, 1.78%) showed significantly less activity against cell-free virus when compared with AZT-CSA conjugate (**7.3**, 1.78%) and AZT + CSA (**7.8**, 1.78%) and was inactive against cell-associated virus. Similarly, the physical mixture of FLT + cellulose acetate (**7.18**, 1.43%) showed 9-21 fold less activity against cell-free virus when compared with FLT + CSA (**7.9**, 1.43%) and was inactive against cell-associated virus. The result was not surprising since cellulose acetate is inactive polymer and the percentage of AZT or FLT were low in the physical mixture.

In general, the conjugation of nucleosides with CS provided better anti-HIV profile against both X4 and R5 strains of virus. The substitution of acetate group on CS improved the anti-HIV activity, possibly by creating new negative charges after hydrolysis or the presence of free acetate groups on the polymer. Succinate spacer was less optimal than the acetate group for linking of the nucleoside with CS.

www.mana

Table 7.2. Anti-HIV activities of cellulose acetate, dextran acetate, cellulose phosphate, and physical mixtures of nucleosides with CS, CSA, and cellulose.

Compound Code	Chemical Name	CTS[a] EC(50)[b] (μg/ml)	VBI(IIIB)[c] EC(50) (μg/ml)	VBI(BaL)[d] EC(50) (μg/ml)	CTC[e] EC(50) (μg/ml)
7.8	AZT (1.78 %) + CSA	>100	1.7	2.5	8.0
7.9	FLT (1.43 %) + CSA	>100	0.72	0.31	4.72
7.10	3TC (1.07%) + CSA	>100	0.65	1.73	5.79
7.11	AZT (17.2%) + CS	>100	16.2	15.3	7.6
7.12	FLT (1.43 %) + CS	>100	6.2	7.1	7.4
7.13	FLT (7.85 %) + CS	>100	0.7	0.3	26.4
7.14	Cellulose Acetate	>100	>100	>100	>100
7.15	Dextran Acetate	>100	>100	>100	>100
7.16	Cellulose Phosphate	>100	72.1	>100	>100
7.17	AZT (1.78%) + Cellulose Acetate	>100	75.5	8.5	>100
7.18	FLT (1.43%) + Cellulose Acetate	>100	6.8	6.5	>100
7.19	3TC (1.07%) + Cellulose Acetate	>100	73.9	22.4	>100

[e]CTS: Cytotoxicity assay; [f]EC(50) = 50% effective concentration; [g]VBI(IIIB): Viral entry inhibition assay (lymphocytotropic strain); [h]VBI(BaL): Viral entry inhibition assay (monocytotropic strain); [i]CTC: cell- to- cell transmission assay (IIIB).

7.4.2.2. Anti-HIV activities against Multi-Drug Resistant (MDR) Isolates

AZT-CSA (**7.3**) and FLT-CSA (**7.4**) conjugates were evaluated for their anti-HIV activities against MDR virus and the data were compared with the controls CS and dextran sulfate (Table 7.3). Both CS and dextran sulfate were active against MDR

www.mana

virus (IC_{50} = 1.61-3.12 μg/mL), but showed less activity against R5 strain of virus (IC_{50} > 15 μg/mL). the result was expected since R5 virus has less positively charged V3 loops in gp120 protein required for interactions with anionic polymers.

On the other hand, AZT-CSA (**7.3**) showed almost similar anti-HIV activity against both R5 and MDR strains than CS. AZT-CSA (**7.3**) was more effective than CS, against the R5 HIV-1 lab-adapted strain BaL. The higher activity against R5 strain is a result of AZT attachment. Furthermore, AZT is not active against MDR strain and hence its conjugate with CS in AZT-CSA (**7.3**), is 2-fold less active than CS against MDR strain. Similarly FLT-CSA (**7.4**) showed significantly higher activity against R5 strain versus CS (**7.1**) due to the presence of FLT in the conjugate. The anti-HIV activity of **7.4** against MDR is 5-fold higher than R5 strains, since released FLT has anti-HIV activity against AZT-MDR resistant.

Table 7.3. Anti-HIV activities of AZT-CSA and FLT-CSA conjugates against R5 and multidrug resistant HIV-1 clinical isolates.

Compound	Chemical Name	Type of Virus	IC_{50} (μg/mL)
7.3	AZT-Cellulose Sulfate Acetate	R5	3.52
		MDR	4.22
7.4	FLT-Cellulose Sulfate Acetate	R5	2.67
		MDR	0.50
7.1	Cellulose sulfate	R5	>20.0
		MDR	1.61
Dextran Sulfate	Dextran sulfate	R5	15.7
		MDR	3.12

Assay endpoint = p24 level (ELISA)
IC_{50} = The minimum drug concentration that inhibits HIV-induced cytopathic effect by 50%, calculated by using a regression analysis program for semilog curve fitting
HIV-1 clinical isolates: R5 = 92TH014; MDR = Multidrug resistant virus 7324-1

www.mana

7.4.2.3. Contraceptive activity

AZT-CSA conjugate (**7.3**) was selected for *in vivo* testing in rats for contraceptive activity. Application of CS and **7.3** in female rats prevented the pregnancy to 100% (Table 7.4). CS is known to have contraceptive properties and this result indicated that contraceptive property of the CS is retained after the AZT conjugation to the polymer.

Table 7.4. Contraceptive efficacy of AZT-CSA conjugate.

Group	Concentration (mg/ml)	No. of Pregnant females/total	Pregnancy rate (%)
TALP	Control	4/4	100
7.1	1	0/5	0
7.3	1	0/5	0

Female rabbits were inseminated with pooled rabbit semen containing 1 mg/mL of test compound or medium control (TALP)

7.5. Conclusions

HIV entry blocker cellulose sulfate was conjugated with RT inhibitor nucleosides, AZT, FLT, and 3TC, through different linkers to synthesize CS-nucleoside conjugates as bifunctional anti-HIV agents targeting different events in HIV life cycle. The conjugates were evaluated for their anti-HIV activity against cell-free, cell-associated and MDR virus.

The conjugation of AZT or FLT with CS provided higher anti-HIV activity against R5 strain of virus verses CS in all conjugates, suggesting the contribution of released nucleosides in generating broad-spectrum activities.

www.manar

CS conjugates of AZT and FLT with acetate linker (AZT-CSA and FLT-CSA) and the physical mixture of AZT or FLT with CSA exhibited higher anti-HIV activity in cell-free virus when compared to their corresponding conjugates with succinate linker (AZT-succinate-CS and FLT-succinate-CS), the physical mixtures of CS + AZT or FLT, and CS, possibly due to the creation of additional negative charges provided from carboxylic acid of acetate group on the polymer. Similarly, cellulose sulfate-acetate exhibited significantly higher potency than CS against cell-free virus. Higher negative charge density may have contributed in stronger interactions of CS with positive charges present in V3 Loops of gp120 and thereby blocking HIV entry.

Furthermore, AZT-CSA and FLT-CSA conjugates were more effective than CS against both X4 and R5 HIV-1 viruses. The above-described conjugates present the advantage of not displaying weaker activity against HIV R5 strains. Although in weight the AZT-CSA and AZT were similarly potent against cell-free virus, in moles (based on CS ~ 2×10^6 Daltons), the conjugate was 5 orders of magnitude more potent (from μM to subnanomolar). Furthermore, unlike AZT, the conjugate was consistently active against cell-associated HIV.

This study presents an alternative approach for designing more optimal anti-HIV agents that may have broad-spectrum anti-HIV activities against cell-free, cell-associated and MDR virus by targeting both HIV entry and reverse transcription in HIV life cycle.

المنارة للاستشارات

www.manar

7.6. References

Anderson, R. A., Chany, C., Feathergill, K., Diao, X., Cooper, M., Kirkpatrick, R., Spear, P., Waller, D. P., Doncel, G. F., Zaneveld L. J. D. Evaluation of the potential of poly(styrene-4-sulfonate) as an effective preventative agent against conception and sexually transmitted diseases. *J. Androl.*, **2000**, 21, 862-875.

Anderson, R. A., Feathergill, K. A., Diao, X. H., Cooper, M. D., Kirkpatrick, R., Herold, B. C., Doncel, G. F., Chany, C. J., Waller, D. P., Rencher, W. F., Zaneveld, L. J. Preclinical evaluation of sodium cellulose sulfate (Ushercell) as a contraceptive antimicrobial agent. *J. Androl.*, **2002**, *23*, 426-438.

Baba, M., Pauwels, R., Balazarini, J., Arnout, J. and Desmyter, J. Mechanism of inhibitory effect of dextran sulfate and heparin on replication of human immunodeficiency virus in vitro. *Proc. Natl. Acad. Sci. U. S. A.*, **1988**, 85, 6132-6136.

Bugatti, A., Urbinati, C., Ravelli, C., De Clercq, E., Liekens, S., Rusnati, M. Heparin-mimicking sulfonic acid polymers as multitarget inhibitors of human immunodeficiency virus type I tat and gp120 proteins, *Antimicroib. Agents Chmother.*, **2007**, 51, 2337-2345.

Chan, D. C., Kim, P. S. HIV entry and its inhibition. *Cell*, **1998**, 93, 681-684.

Crucitti, T., Jespers, V., Damme, L. V., Dyck, E. V., Buve, A. Vaginal microbicides can interfere with nucleic acid amplification tests used for the diagnosis of Chlamydia trachomatis and Nisseria gonorrhoeae infection. *Diagn. Micr. Infec. Dis.*, **2007**, 57, 97-99

D'Cruz, O. J. and Uckun, F. M. Clinical development of microbicides for the prevention of HIV infection. *Curr. Pharm. Design*, **2004**, 10, 315-336.

El-Sadr, W. M., Mayer, K. H., Maslankowski, L., Hoesley, C., Justman, J., Gai, F., Mauck, C., Absalon, J., Morrow, K., Masse, B., Soto-Torres, L. and Kwiecien, A. Safety and acceptability of cellulose sulfate as a vaginal microbicide in HIV-infected women. *AIDS*, **2006**, 20, 1109-1116.

Gao, Y., Katsuraya, K., Kaneko, Y., Mimura, T., Nakashima, H. and Uryu, T. Synthesis, enzymatic hydrolysis and anti-HIV activity of AZT-spacer-Curdlan sulfates. *Macromolecules*, **1999**, 32, 8319-8324.

Kajumo, F., Thompson, D. A. D., Guo, Y. and Dragic, T. Entry of R5X4 and X4 HIV-1 strains is mediated by negatively charged and tyrosine residues in the amino-terminal domain and the second extracellular loop of CXCR4. *Virology*, **2000**, 271, 240-247.

المنارة للاستشارات

www.manar

Ketas, T. J., Frank, I., Klasse, P. J., Sullivan, B. M., Gardner, J. P., Spenlehauer, C., Nesin, M., Olson, W. C., Moore, J. P., Pope, M. Human immunodeficiency virus type 1 attachment, coreceptor, and fusion inhibitors are active against both direct and trans infection of primary cells. *J. Virol.*, **2003**, 77, 2762-2767

Krebs, F. C., Miller, S. R., Malamud, D., Howett, M. K., Wigdahl, B. Inactivation of human immunodeficiency virus type 1 by nonoxynol-9, C21G, or an alkyl sulfate, sodium dodecyl sulfate. *Antiviral. Res.*, **1999**, 43, 147-163.

Malonza, I. M., Mirembe, F., Nakabiito, C., Odusoga, L. O., Osinupebi, O. A., Hazari, K., Chitlange, S., Ali, M. M., Callahan, M and Dmme, L. V. Expanded phase I safety and acceptability study of 6% cellulose sulfate vaginal gel. *AIDS*, **2005**, 19, 2157-2163.

Mauck, C., Frezieres, R., Walsh, R., Robergeau, K. and Callahan, M. Cellulose sulfate: tolerance and acceptability of penile application. *Contraception*, **2001**, 64, 377-381.

Mauck, C., Weiner, D. H., Ballagh, S., Creinin, ., Archer, D. F., Schwarts, J., Pymar, H., Lai, J. and Callahan, M. single and multiple exposure tolerance study of cellulose sulfate gel: a phase I safety and colposcopy study. *Contraception*, **2001**, 64, 383-391.

Meylan, P. R. A.,Kornbluth, R. S., Zbinden, I. And Dichman, D. D. Influence of host cell type and V3 loop of the surface glycoprotein on susceptibility of human immunodeficiency virus type 1 to polyanion compounds. *Antimicroib. Agents Chemother.*, **1994**, 38, 2910-2916.

Moulard, M., Lortat-Jacob, H., Mondor, I., Roca, G., Wyatt, R., Sodroski, J., Zhao, L, Olson, W., Kwong P. D., Attentau, Q. J. Selective interactions of polyanions with basic surfaces on human immunodeficiency virus type 1 gp120, *J. Virol.*, **2000**, 74, 1948-1960.

Neurath, A. R., Strick, N. and Li, Y. Anti-HIV-1 activity of anionic polymers: a comparative study of candidate microbicides. *BMS infectious diseases*, **2002**, 2, 1-11

Schwartz, J. L., Mauck, C., Lai, J., Creinin, M. D., Brache, V., Ballagh, S. A., Weiner, D, H., Hillier, S. L., Fichorova, R. N. and Callahan, M. Fourteen day safety and acceptability study of 6% cellulose sulfate gel a randomized double-blind phase I safety study. *Contraception*, **2006**, 131-140.

Scordi-Bello, I. A., Mosoian, A., He, C., Chen, Y., Cheng Y., Jarvis, G. A., Keller, M. J., Hogarty, K., Waller, D. P., Profy, A. T.,m Herold, B. C., Klotman, M. E. Candidate sulfonated and sulfated topical microbicides: Comparion of Anti-Human Immunodeficiency Virus activities and mechanisms of action. *Antimicroib. Agents Chemother.*, **2005**, 49, 3607-3615.

المنارة للاستشارات

www.mana

Shattock, R. J. and Doms, R. W. AIDS models: Microbicides could learn from vaccines. *Nat. Med.*, **2002**, 8, 425.

Turpin, J. A. Considerations and development of topical microbicides to inhibit the sexual transmission of HIV, *Expert Opin. Inv. Drugs*, **2002**, 11, 1077-1097.

Usher T., C., Patel, N. T., Chhagan W., Louis, I. Pharmaceutical preparation and a method for inhibiting the replication of various viruses. WO 1995/00177, PCT/CA94/00343, **1995**.

Vlieghe, P., Clerc, T., Pannecouque, C., Witvrouw, M., Clercq, E. D., Salles, J. P. and Kraus, J, L. Synthesis of new covalently bound κ-Carrageenan-AZT conjugates with improved anti-HIV activities. *J. Med. Chem.*, **2002**, *45*, 1275-1283.

Wakabi, W. HIV microbicide trials halted. *Can. Med. Assoc. J.*, **2007** 176: 1569-1570.

المنارة للاستشارات

www.mana

Bibliography

Acharya, K.R., Sturrock, E.D., Riodan, J.K., Ehlers, M.R. ACE revisited: A New Target for Structure-Based Dug Design. *Nat. Rev. Drug Discov.*, 2003, 2, 891-902

Agarwal, H. K., Doncel, G. F., Parang, K. Synthesis and anti-HIV activities of phosphate triester derivatives of 3'-fluoro-2',3'-dideoxythymidine and 3'-azido-2',3'-dideoxythymidine. *Tet. Lett.*, **2008**, 49, 4905-4907.

Agarwal, H. K., Kumar, A., Mehvar, R., and Parang, K. *American Chemical Society National Meeting*, **2007**, Chicago, Illinois.

Agarwal, H. K., Parang, K. Application of solid phase chemistry for the synthesis of 3'-fluoro-3'-deoxythymidine. *Nucleoside, Nucleotide Nucleic acid.*, **2007**, 26, 317-322.

Agarwal, S., Boddu, S.H.S., Jain, R., Samanta, S., Pal, D., Mitra, A. K. Peptide prodrugs: Improved oral absorption of lopinavir, anti- HIV protease inhibitor. *Intl. J. Pharm.*, **2008**, 359, 7–14.

Alkhatib, G., Combadiere, C., Broder, C. C., Feng, Y., Kennedy, P. E., Murphy, P. M., Berger, E. A. CC-CKR5: A RANTES, MIP-1α and MIP-1β receptor as a fusion cofactor for macrophage-tropic HIV-1. *Science*, **1996**, 272, 1955-1958.

Alnouti, Y., White, C. A., and Bartlett, M. G. Determination of lamivudine in plasma, amniotic fluid, and rat tissues by liquid chromatography. *J. Chromatogr. B Analyt. Technol. Biomed. Life Sci.*, **2004**, 803, 279-284.

Anderson, R. A., Chany, C., Feathergill, K., Diao, X., Cooper, M., Kirkpatrick, R., Spear, P., Waller, D. P., Doncel, G. F., Zaneveld L. J. D. Evaluation of the potential of poly(styrene-4-sulfonate) as an effective preventative agent against conception and sexually transmitted diseases. *J. Androl.*, **2000**, 21, 862-875.

Anderson, R. A., Feathergill, K. A., Diao, X. H., Cooper, M. D., Kirkpatrick, R., Herold, B. C., Doncel, G. F., Chany, C. J., Waller, D. P., Rencher, W. F., Zaneveld, L. J. Preclinical evaluation of sodium cellulose sulfate (Ushercell) as a contraceptive antimicrobial agent. *J. Androl.*, **2002**, *23*, 426-438.

Baba, M., Pauwels, R., Balazarini, J., Arnout, J. and Desmyter, J. Mechanism of inhibitory effect of dextran sulfate and heparin on replication of human immunodeficiency virus in vitro. *Proc. Natl. Acad. Sci. U. S. A.*, **1988**, 85, 6132-6136.

Bailer, A. J. Testing for the equality of area under the curves when using destructive measurement techniques. *J. Pharmacokinet. Biopharm.*, **1988**, 16, 303-309.

Balboni, P. G., Minia, A., Grossi, M. P., Barbanti-Brodano, G., Mattioli, A., and Fiume, L. (1976) Activity of albumin conjugates of 5-fluorodeoxyuridine and cytosine

www.mana

arabinoside on poxviruses as a lysosomotropic approach to antiviral chemotherapy. *Nature*, **1976**, 264, 181-183.

Bezy, V., Morin, P., Couerbe, P., Leleu, G., and Agrofoglio, L. Simultaneous analysis of several antiretroviral nucleosides in rat plasma by high-performance liquid chromatography with UV using acetic acid/hydroxylamine buffer. Test of this new volatile medium-pH for HPLC-ESI-MS/MS. *J. Chromatogr. B Analyt. Technol. Biomed. Life Sci.*, **2005**, 821, 132-143.

Bijsterbosch, M. K., van de Bilt, H., and van Berkel, T. J. Specific targeting of a lipophilic prodrug of iododeoxyuridine to parenchymal liver cells using lactosylated reconstituted high density lipoprotein particles. *Biochem. Pharmacol.*, **1996**, 52, 113-121.

Boudinot, F. D., Smith, S. G., Funderburg, E. D., and Schinazi R. F. Pharmacokinetics of 3'-fluoro-3'-deoxythymidine and 3'-deoxy-2',3'-didehydrothymidine in rats. *Antimicrob. Agents Chemther.*, **1991**, 35, 747-749.

Bourre, L., Giuntini, F., Eggleston, I. M., Wilson, M. W., MacRobert, A. J. 5-Aminolaevulinic acid peptide prodrugs enhance photosensitization for photodynamic therapy. *Mol. Cancer Ther.*, **2008**, 7, 1720-1729.

Bryant, M. L., McWherter, C. A., Kishore, N. S., Gokel, G. W., and Gordon, J. I. MyristoylCoA: Protein *N*-myristoyltransferase as a therapeutic target for inhibiting replication of human immunodeficiency virus-1. *Perspect. Drug Dis. Des.*, **1993**, 1, 193-209.

Bugatti, A., Urbinati, C., Ravelli, C., De Clercq, E., Liekens, S., Rusnati, M. Heparin-mimicking sulfonic acid polymers as multitarget inhibitors of human immunodeficiency virus type I tat and gp120 proteins, *Antimicrob. Agents Chmother.*, **2007**, 51, 2337-2345.

Calvez, V., Tubiana, R., Ghosn, J., Wirden, M., Marcelin, A. G., Westling, C., Shoen, H., Harmenberg, J., Mardh, G., Oberg, B., Katlama, C. MIV-310 reduces markedly viral load in patients with virological failure despite multiple-drug therapy: Results from a 4-week phase II study. *Antivir. Ther.*, **2002**, 7, Abs S4.

Chan, D. C. and Kim, P. S. HIV entry and its inhibition. *Cell*, **1998**, 93, 681-684.

Chau, Y., Dang, N. M., Tan, F. E., Langer, R. Investigation of Targeting Mechanism of New Dextran-Peptide-Methotrexate Conjugates Using Biodistribution Study in Matrix-Metalloproteinase-Overexpressing Tumor Xenograft Model. *J. Pharm. Sci.*, **2006**, 95, 542-551.

المنارة للاستشارات

www.manar

Chau, Y., Padera, R. F., Dang1, N. M., Langer, R. Antitumor efficacy of a novel polymer–peptide–drug conjugate in human tumor xenograft models. *Int. J. Cancer*, **2006**, 118, 1519–1526.

Chau, Y., Tan, F. E., Langer, R. Synthesis and Characterization of Dextran-Peptide-Methotrexate Conjugates for Tumor Targeting via Mediation by Matrix Metalloproteinase II and Matrix Metalloproteinase IX. *Bioconjug. Chem.*, **2004**, 15, 931-941.

Cheng, Y.C.; Dutschman, G.E.; Baston, K.F.; Sarngadharan, M.G.; Ting R.Y.C. Human immunodeficiency virus reverse transcriptase: general properties and its interactions with nucleotide triphosphate analogs. *J. Biol. Chem.* **1987**, 262, 2187–2189.

Cheng-Mayer, C., Liu, R., Landau, N. R., Stamatatos, L. Macrophage Tropism of human immunodeficiency virus type 1 and utilization of the CC-CKR5 coreceptor. *J. Virol.*, **1997**, 71, 1657-1661.

Chimalakonda, K. C., Agarwal, H. K., Kumar, A., Parang, K., Mehvar, R. Synthesis, analysis, in vitro characterization and in vivo disposition of a lamivudine-dextran conjugate for selective antiviral delivery to the liver. *Bioconjug. Chem.*, **2007**, 18, 2097-2108.

Chimalakonda, A. P., Montgomery, D. L., Weidanz, J. A., Shaik, I. H., Nguyen, J. H., Lemasters, J. J., Kobayashi, E., and Mehvar, R. Attenuation of acute rejection in a rat liver transplantation model by a liver-targeted dextran prodrug of methylprednisolone. *Transplantation*, **2006**, 81, 678-685.

Chimalakonda, A. P., and Mehvar, R. Dextran-methylprednisolone succinate as a prodrug of methylprednisolone: local immunosuppressive effects in liver after systemic administration to rats. *Pharm. Res.*, **2003**, 20, 198-204.

Cohen, M. S., Hellmann, N., Levy, J. A., DeCock, K. and Lange J. The spread, treatment, and prevention of HIV-1: evolution of a global pandemic. *J. Clin. Invest.*, **2008**, 118, 1244-1254.

Costin, J. M. Cytopathic Mechanisms of HIV-1. *Virol. J.*, **2007**, 4, 100-122.

Crucitti, T., Jespers, V., Damme, L. V., Dyck, E. V., Buve, A. Vaginal microbicides can interfere with nucleic acid amplification tests used for the diagnosis of Chlamydia trachomatis and Nisseria gonorrhoeae infection. *Diagn. Micr. Infec. Dis.*, **2007**, 57, 97-99

Cvetkovic, R.S., Goa, K.L. Lopinavir/ritonavir: a review of its use in the management of HIV infection. *Drugs*, **2003**, 63, 769-802.

المنارة للاستشارات

www.mar

D'Cruz, O. J. and Uckun, F. M. Clinical development of microbicides for the prevention of HIV infection. *Curr. Pharm. Design*, **2004**, 10, 315-336.

Das, K., Xiong, X., Yang, H., Westland, C. E., Gibbs, C. S., Sarafianos, S. G., Arnold, E. Molecular modeling and biochemical characterization reveal the mechanism of hepatitis b virus polymerase resistance to lamivudine (3TC) and emtricitabine (FTC). *J. Virol.*, **2001**, 75, 4771-4779.

De Vrueh, R. L., Rump, E. T., van De Bilt, E., van Veghel, R., Balzarini, J., Biessen, E. A., van Berkel, T. J., and Bijsterbosch, M. K. Carrier-mediated delivery of 9-(2-phosphonylmethoxyethyl)adenine to parenchymal liver cells: a novel therapeutic approach for hepatitis B. *Antimicrob. Agents Chemother.*, **2000**, 44, 477-483.

Deng, H., Liu, R., Ellmeier, W., Choe, S., Unutmaz, D., Burkhart, M., Marzio, P. D., Marmon, S., Sutton, R. E., Hill, C. M., Davis, C. B., Peiper, S. C., Schall, T. J., Littman, D. R., Landau, N. R. Identification of a major co-receptor for primary isolates of HIV-1. *Nature*, **1996**, 381, 661-666.

Di Bisceglie, A. M., and Hoofnagle, J. H. Hepatitis B virus replication within the human spleen. *J. Clin. Microbiol.*, **1990**, 28, 2850-2852.
Enriquez, P. M., Jung, C., Josephson, L., and Tennant, B. C. Conjugation of adenine arabinoside 5'-monophosphate to arabinogalactan: synthesis, characterization, and antiviral activity. *Bioconjug. Chem.*, **1995**, 6, 195-202.

Diallo, K., Götte, M., Wainberg1, M. A. Molecular Impact of the M184V Mutation in Human Immunodeficiency Virus Type 1 Reverse Transcriptase. *Antimicrob. Agents Chemother.*, **2003**, 47, 3377-3383.

Dimitrov, A. S., Louis, J. M., Bewley, C. A., Clore, M. G., Blumenthal, R. Conformational changes in HIV-1 gp41 in the course of HIV-1 envelope glycoprotein-mediated fusion and inactivation. *Biochemistry*, **2005**, 44, 12471-12479.

El-Sadr, W. M., Mayer, K. H., Maslankowski, L., Hoesley, C., Justman, J., Gai, F., Mauck, C., Absalon, J., Morrow, K., Masse, B., Soto-Torres, L. and Kwiecien, A. Safety and acceptability of cellulose sulfate as a vaginal microbicide in HIV-infected women. *AIDS*, **2006**, 20, 1109-1116.

Erion, M. D., van Poelje, P. D., Mackenna, D. A., Colby, T. J., Montag, A. C., Fujitaki, J. M., Linemeyer, D. L., and Bullough, D. A. Liver-targeted drug delivery using HepDirect prodrugs. *J. Pharmacol. Exp. Ther.*, **2005**, 312, 554-60.

Fais, S., Lapenta, C., Santini, S. M., Spada, M., Parlato, S., Logozzi, M., Rizza, P., Belardelli, R. Human immunodeficiency virus type 1 strains R5 and X4 induce different pathogenic effects in hu-PBL-SCID mice, depending on the state of activation/differentiation of human target cells at the time of primary infection. *J. Virol.*, **1999**, 73, 6453-6459.

المنارة للاستشارات

www.manar

Farazi, T. A., Waksman, and G., Gordon, J. I. The Biology and Enzymology of Protein *N*-Myristoylation. *J. Biol. Chem.*, **2001**, 276, 39501–39504.

Farquhar, D., Khan, S., Srivastva, D. N., Saunders, P. P. Synthesis and Antitumor Evaluation of Bis[(pivaloyloxy)methyl] 2'-Deoxy-5-fluorouridine 5'-Monophosphate (FdUMP): A Strategy To Introduce Nucleotides into Cells. *J. Med. Chem.*, **1994**, 37, 3902–3909.

Fiume, L., Di Stefano, G., Busi, C., Mattioli, A., Bonino, F., Torrani-Cerenzia, M., Verme, G., Rapicetta, M., Bertini, M., and Gervasi, G. B. Liver targeting of antiviral nucleoside analogues through the asialoglycoprotein receptor. *J. Viral Hepat.*, **1997**, 4, 363-70.

Fiume, L., Di Stefano, G., Busi, C., Mattioli, A., Battista Gervasi, G., Bertini, M., Bartoli, C., Catalani, R., Caccia, G., Farina, C., Fissi, A., Pieroni, O., Giuseppetti, R., D'Ugo, E., Bruni, R., and Rapicetta, M. Hepatotropic conjugate of adenine arabinoside monophosphate with lactosaminated poly-L-lysine. Synthesis of the carrier and pharmacological properties of the conjugate. *J. Hepatol.*, **1997**, 26, 253-259.

Fiume, L., Bassi, B., Busi, C., Mattioli, A., Spinosa, G., and Faulstich, H. Galactosylated poly(L-lysine) as a hepatotropic carrier of 9-beta-D-arabinofuranosyladenine 5'-monophosphate. *FEBS Lett.*, **1986**, 203, 203-206.

Furuishi, K., Matsuoko, H., Takama, M., Takahashi, I., Misumi, S., and Shoji, S. Blockage of N-myristoylation of HIV-1 Gag induces the production of impotent progeny virus. *Biochem. Biophys. Res. Commun.*, **1997**, 237, 504-511.

Gallant, J. E., DeJesus, E., Arras, J. R., et al. Tenofovir DF, Emtricitabine, and Efavirenz vs Zidovudine, and Efavirenz for HIV. *N. Engl. J. Med.*, **2006**, 354, 251-260.

Gao, Y., Katsuraya, K., Kaneko, Y., Mimura, T., Nakashima, H. and Uryu, T. Synthesis, enzymatic hydrolysis and anti-HIV activity of AZT-spacer-Curdlan sulfates. *Macromolecules*, **1999**, 32, 8319-8324.

García-Lerma, J. G., MacInnes, H., Bennett, D., Reid, P., Nidtha, S., Weinstock, H., Kaplan, J. E., Heneine, W. A novel genetic pathway of human immunodeficiency virus type 1 resistance to stavudine mediated by the K65R mutation. *J. Virol.*, **2003**, 77, 5685–5693.

Ghosn, J., Quinson, A-M., Sabo, N. D., Cotte, L., Piketty, C., Dorléacq, N., Bravo, M-L., Mayers, D., Harmenberg, J., Mårdh, G., Valdez, H., and Katlama, C. Antiviral activity of low-dose alovudine in antiretroviral experienced patients: results from a 4-week randomized, double-blind, placebo-controlled dose-ranging trial. *HIV Med.*, **2007**, 8, 142-147

المنارة للاستشارات

www.ma

Hager, M. W.; Liotta, D. C. An efficient synthesis of 3'-fluoro-3'-deoxythymidine (FLT). *Tet. Lett.*, **1992**, 33, 7083–7086.

Harboe, E., Larsen, C., Johansen, M., and Olesen, H. P. Macromolecular prodrugs. XV. Colon-targeted delivery-bioavailability of naproxen ester prodrugs varying in molecular size in the pig. *Pharm. Res.*, **1989**, 6, 919-923.

Herdewijn, P.; Balzarini, J.; De Clercq, E.; Pauwels, R.; Baba, M.; Broder, S.; Vanderhaeghe, H. 3'-Substituted 2',3'-dideoxynucleoside analogues as potential anti-HIV (HTLV-III/LAV) agents. *J. Med. Chem.*, **1987**, 30, 1270–1278.

Hoshi, A.; Castaner, J. Alovudine. *Drugs Future*, **1994**, 19, 221–224.

Hurst, M and Noble, S. Stavudine, an update of its use in the treatment of HIV infection. *Drugs*, **1999**, 58, 919-949.

Jarvis, B., Faulds, D. Lamivudine. A review of its therapeutic potential in chronic hepatitis B. *Drugs*, **1999**, 58, 101-41.

Jochum, A., Schlienger, N., Egron, D., Peyrottes, S., Périgaud, C. Biolabile constructs for pronucleotide design. *J. Organometallic Chem.*, **2005**, 690, 2614–2625.

Johnson, M. A., Moore, K. H., Yuen, G. J., Bye, A., and Pakes, G. E. Clinical pharmacokinetics of lamivudine. *Clin. Pharmacokinet.*,**1999**, 36, 41-66.

Kajumo, F., Thompson, D. A. D., Guo, Y. and Dragic, T. Entry of R5X4 and X4 HIV-1 strains is mediated by negatively charged and tyrosine residues in the amino-terminal domain and the second extracellular loop of CXCR4. *Virology*, **2000**, 271, 240-247.

Kano, E. K., dos Reis Serra, C. H., Koono, E. E., Andrade, S. S., Porta, V. Determination of lamivudine in human plasma by HPLC and its use in bioequivalence studies. *Int. J. Pharm.*, **2005**, 297, 73-79.

Kenney, K. B., Wring, S. A., Carr, R. M., Wells, G. N., and Dunn, J. A. Simultaneous determination of zidovudine and lamivudine in human serum using HPLC with tandem mass spectrometry. *J. Pharm. Biomed. Anal.*, **2000**, 22, 967-983.

Ketas, T. J., Frank, I., Klasse, P. J., Sullivan, B. M., Gardner, J. P., Spenlehauer, C., Nesin, M., Olson, W. C., Moore, J. P., Pope, M. Human immunodeficiency virus type 1 attachment, coreceptor, and fusion inhibitors are active against both direct and trans infection of primary cells. *J. Virol.*, **2003**, 77, 2762-2767.

المنارة للاستشارات

www.mana

Kim, E.Y.; Vrang, L.; Oberg, B.; Merigan, T.C. Anti-HIV type 1 activity of 3′-fluoro-3′-deoxythymidine for several different multi-drug-resistant mutants. *AIDS Res. Hum. Retroviruses.*, **2001**, 17, 401–407.

Krebs, F. C., Miller, S. R., Malamud, D., Howett, M. K., Wigdahl, B. Inactivation of human immunodeficiency virus type 1 by nonoxynol-9, C21G, or an alkyl sulfate, sodium dodecyl sulfate. *Antiviral. Res.*, **1999**, 43, 147-163.

Kumar, P.; Ohkura, K.; Balzarini, J.; De Clercq, E.; Seki, K.; Wiebe, L. I. Synthesis and antiviral activity of novel fluorinated 2',3'-dideoxynucleosides. *Nucleosides Nucleotides Nucleic Acids,* **2004**, 23, 7–29.

Knox, K. S., Day, R. B., Wood, K. L., Kohli, L. L., Hage, C. A., Foresman, B. H., Schnizlein-Bick, C. T., Twigg, H. L. Macrophages exposed to lymphotropic and monocytotropic HIV induce similar CTL responses despite differences in productive infection. *Cell. Immunol.*, **2004,** 229, 130-138.

Kong, X. B., Zhu, Q. Y., Vidal, P. M., Watanabe, K. A., Polsky, B., Armstrong, D., Ostrander, M., Stanley A. Lang, S. A., Muchmore, E. And Chou T. C. Comparisons of anti-human immunodeficiency virus activities, cellular transport, and plasma and intracellular pharmacokinetics of 3'-fluoro-3'-deoxythymidine and 3'-azido-3'-deoxythymidine. *Antimicrob. Agents Chemother.*, **1992**, 36, 808-818.

Krebs, F. C., Miller, S. R., Malamud, D., Howett, M. K., Wigdahl, B. Inactivation of human immunodeficiency virus type 1 by nonoxynol-9, C21G, or an alkyl sulfate, sodium dodecyl sulfate. *Antiviral Res.* **1999**, 43, 147-163.

Lake, J. R., Licko, V., Van Dyke, R. W., and Scharschmidt, B. F. Biliary secretion of fluid-phase markers by the isolated perfused rat liver. Role of transcellular vesicular transport. *J. Clin. Invest.*, **1985**, 76, 676-684.

Larsen, C. Dextran prodrugs-structure and stability in relation to therapeutic activity. *Adv. Drug Deliv. Rev.*, **1989**, 3, 103-154.

Larsen, C., Harboe, E., Johansen, M., and Olesen, H. P. Macromolecular prodrugs. XVI. Colon-targeted delivery-comparison of the rate of release of naproxen from dextran ester prodrugs in homogenates of various segments of the pig gastrointestinal tract. *Pharm. Res.*, **1989**, 6, 995-999.

Lazzarin, A. Enfuvirtide: The first HIV fusion Inhibitor. *Expert Opin. Pharmacother.*, **2005**, 6, 453-464.

Lee, K., Chu, C. K. Molecular modeling approach to understanding the mode of action of L-nucleosides as antiviral agents. *Antimicrob. Agents Chemother.*, **2001**, 45, 138–144.

www.manar

Lewisa, W., Kohlera, J. J., Hosseinia, S. H., Haasea, C. P., Copelandb, W. C., Bienstockb, R. J., Ludawaya, T., McNaughta, J., Russa, R., Stuarta, T., Santoiannia, R. Antiretroviral nucleosides, deoxynucleotide carrier and mitochondrial DNA: evidence supporting the DNA pol γ hypothesis. *AIDS*, **2006**, 20, 675–684.

Lund, K. C., Peterson, L. L., and Wallace, K. B. Absence of a Universal Mechanism of Mitochondrial Toxicity by Nucleoside Analogs. *Antimicrob. Agents Chemother.*, **2007**, 51, 2531–2539.

Lundgren, B.; Bottiger, D.; Ljungdahl-Stahle, E.; Norrby, E.; Stahle, L.; Wahren, B.; Orberg, B. Antiviral effects of 3′-fluorothymidine and 3′-azidothymidine in cynomolgus monkeys infected with simian immunodeficiency virus. *J. Acquir. Immune Defic. Syndr.*, **1991**, 4, 489–498.

Malonza, I. M., Mirembe, F., Nakabiito, C., Odusoga, L. O., Osinupebi, O. A., Hazari, K., Chitlange, S., Ali, M. M., Callahan, M and Dmme, L. V. Expanded phase I safety and acceptability study of 6% cellulose sulfate vaginal gel. *AIDS*, **2005**, 19, 2157-2163.

Mansuri, M. M., Hitchcock, M. J. M., Buroker, R. A., Bregman, C. L., Ghazzouli, I., Desiderio, J. V., Starrett, J. E., Sterzycki, R. Z. and Martin, J. C. Comparison of in vitro biological properties and mouse toxicities of three thymidine analogs active against human immunodeficiency virus. *Antimicrob. Agents Chemother.*, **1990**, 34, 637-641.

Masho, S. W., Wang, C. L., Nixon, D. E. Review of tenofovir-emtricitabine. *Ther.Clin. Risk Manag.*, **2007**, 3, 1097-1104.

Matthes, E.; Lehmann, C.H.; Scholz, D.; Von Janta-Lipinski, M.; Gaerther, K.; Rosenthal, H.A.; Langen, P. Inhibition of HIV-associated reverse transcriptase by sugar-modified derivatives of thymidine 5'-triphosphate in comparison to cellular DNA polymerases A and B. *Biochem. Biophys. Res. Commun.*, **1987**, 148, 78–85.

Mauck, C., Frezieres, R., Walsh, R., Robergeau, K. and Callahan, M. Cellulose sulfate: tolerance and acceptability of penile application. *Contraception*, **2001**, 64, 377-381.

McGuigan, C., Nicholls, S. R., O'Connor, T. J., Kinchington, D. Synthesis and anti-HIV activity of some novel substituted dialkyl phosphate derivatives of AZT and ddCyd. *Antiviral Chem. Chemother.*, **1990**, 1, 25–33.

McGuigan, C., Pathirana, R. N., Davis, M. P. H., Balzarini, J., De Clercq, E. Diaryl phosphate derivatives act as pro-drugs of AZT with reduced cytotoxicity compared to the parent nucleoside. *Bioorg. Med. Chem. Lett.*, **1994**, 4, 427–430.

المنارة للاستشارات

www.manar

McLeod, A. D., Friend, D. R., and Tozer, T. N. Synthesis and chemical stability of glucocorticoid-dextran esters: potential prodrugs for colon-specific delivery. *Int. J. Pharmaceut.*, **1993**, 92, 105-114.

McLeod, A. D., Friend, D. R., and Tozer, T. N. Glucocorticoid-dextran conjugates as potential prodrugs for colon-specific delivery: hydrolysis in rat gastrointestinal tract content. *J. Pharm. Sci.*, **1994**, 83, 1284-1288.

Mehvar, R. Recent trends in the use of polysaccharides for improved delivery of therapeutic agents: pharmacokinetic and pharmacodynamic perspèctives. *Curr. Pharm. Biotechnol.*, **2003**, 4, 283-302.

Mehvar, R. Dextrans for targeted and sustained delivery of therapeutic and imaging agents. *J. Control. Release*, **2000**, 69, 1-25.

Mehvar, R., Dann, R. O., and Hoganson, D. A. Kinetics of hydrolysis of dextran-methylprednisolone succinate, a macromolecular prodrug of methylprednisolone, in rat blood and liver lysosomes. *J. Control. Release*, **2000**, 68, 53-61.

Mehvar, R., and Hoganson, D. A. Dextran-methylprednisolone succinate as a prodrug of methylprednisolone: immunosuppressive effects after in vivo administration to rats. *Pharm. Res.*, **2000**, 17, 1402-1407.

Mehvar, R. Kinetics of hepatic accumulation of dextrans in isolated perfused rat livers. *Drug Metab. Dispos.*, **1997**, 25, 552-556.

Mehvar, R., Robinson, M. A., and Reynolds, J. M. Dose dependency of the kinetics of dextrans in rats: effects of molecular weight. *J. Pharm. Sci.*, **1995**, 84, 815-818.

Mehvar, R., Robinson, M. A., and Reynolds, J. M. Molecular weight dependent tissue accumulation of dextrans: *in vivo* studies in rats. *J. Pharm. Sci.*, **1994**, 83, 1495-1499.

Mehvar, R., and Shepard, T. L. Molecular weight-dependent pharmacokinetics of fluorescein-labeled dextrans in rats. *J. Pharm. Sci.*, **1992**, 81, 908-912.

Meier, C. CycloSal-Pronucleotides – Design of Chemical Trojan Horses *Mini-Rev. Med. Chem.*, **2002,** 2, 219–234.

Meier, C., Ruppel, M. F., Vukadinovic, D., Balzarini, J. "Lock-in"-cycloSal-Pronucleotides - A New Generation of Chemical Trojan Horses? *Mini-rev. Med. Chem.*, **2004**, 4, 383–394.

Meier, C., Balzarini, J. Application of the *cyclo*Sal-prodrug approach for improving the biological potential of phosphorylated biomolecules. *Antiviral Res.*, **2006**, 71, 282–292.

المنارة للاستشارات

www.manar

Meylan, P. R. A., Kornbluth, R. S., Zbinden, I., Dichman, D. D. Influence of host cell type and V3 loop of the surface glycoprotein on susceptibility of human immunodeficiency virus type 1 to polyanion compounds. *Antimicrob. Agents Chemother.*, **1994**, 38, 2910-2916.

Moulard, M., Lortat-Jacob, H., Mondor, I., Roca, G., Wyatt, R., Sodroski, J., Zhao, L, Olson, W., Kwong P. D., Attentau, Q. J. Selective interactions of polyanions with basic surfaces on human immunodeficiency virus type 1 gp120, *J. Virol.*, **2000**, 74, 1948-1960.

Mulder, L. C. F., Harari, A., Simon, V. Cytidine deamination induced HIV-1 drug resistance. *Proc. Natl. Acad. Sci. U. S. A.* **2008**, 105, 5501–5506.

Nakane, S., Matsumoto, S., Takakura, Y., Hashida, M., and Sezaki, H. The accumulation mechanism of cationic mitomycin c-dextran conjugates in the liver: in-vivo cellular localization and in-vitro interaction with hepatocytes. *J. Pharm. Pharmacol.*, **1987**, 40, 1-6.

Neurath, A. R., Strick, N. and Li, Y. Anti-HIV-1 activity of anionic polymers: a comparative study of candidate microbicides. *BMS infectious diseases*, **2002**, 2, 1-11

Nikolenko, G. N., Palmer, S., Maldarelli, M., Mellors, j. W., Coffin, J. M., Pathak, V. K. Mechanism for nucleoside analog-mediated abrogation of HIV-1 replication: Balance between RNase H activity and nucleotide excision. *Proc. Natl. Acad. Sci. U. S. A.* **2005**, 102, 2093–2098.

Nishikawa, M., Kamijo, A., Fujita, T., Takakura, Y., Sezaki, H., and Hashida, M. Synthesis and pharmacokinetics of a new liver-specific carrier, glycosylated carboxymethyl-dextran, and its application to drug targeting. *Pharm. Res.*, **1993**, 10, 1253-1261.

Nishikawa, M., Yamashita, F., Takakura, Y., Hashida, M., and Sezaki, H. Demonstration of the receptor-mediated hepatic uptake of dextran in mice. *J. Pharm. Pharmacol.*, **1992**, 44, 396-401.

Nishida, K., Tonegawa, C., Nakane, S., Takakura, Y., Hashida, M., and Sezaki, H. Effect of electric charge on the hepatic uptake of macromolecules in the rat liver. *Int. J. Pharmaceut.*, **1990**, 65, 7-17.

Ogston, C. W., Schechter, E. M., Humes, C. A., and Pranikoff, M. B. Extrahepatic replication of woodchuck hepatitis virus in chronic infection. *Virology*, **1989**, 169, 9-14.

Pan, X.-Z.; Qui, Z.-D.; Baron, P.A.; Gold, J.W. M.; Polsky, B.; Chou, T.-C.; Armstrong, D. Three-drug synergistic inhibition of HIV-1 replication in vitro by 3′-

www.manara

fluoro-3′-deoxythymidine, recombinant soluble CD4 and recombinant interferon-alpha. *AIDS Res. Hum. Retroviruses*, **1992**, 8, 589–595.

Parang, K., Wiebe, L. I., Knaus, E. E. Syntheses and biological evaluation of 5'-*O*-myristoyl derivatives of thymidine against human immunodeficiency virus (HIV-1). *Antiviral. Chem. Chemother.*, **1997**, 8, 417-427.

Parang, K., Wiebe, L. I., Knaus, E. E., Huang, J. S., Tyrrell, D. L., Csizmadia, F. In vitro antiviral activities of myristic acid analogs against human immunodeficiency and hepatitis B viruses. *Antiviral Res.*, **1997**, 34, 75–90.

Parang, K., Knaus, E. E., Wiebe, L. I. Synthesis, *in vitro* anti-HIV structure-activity relationships and stability of 5'-*O*-myristoyl analogue derivatives of 3'-azido-2',3'-dideoxythymidine as potential prodrugs of 3'-azido-2',3'-dideoxythymidine (AZT). *Antiviral. Chem. Chemother.*, **1998**, 9, 311-323.

Parang, K., Wiebe, L. I., Knaus, E. E. *In vivo* pharmacokinetic parameters, liver and brain uptake of (±)-3'-azido-2',3'-dideoxy-5'-*O*-(2-bromomyristoyl)thymidine as potential prodrug of 3'-azido-3'-deoxythymidine. *J. Pharm. Pharmacol.* **1998**, 50, 989-996.

Parang, K., Knaus, E. E., Wiebe, L. I. Synthesis, *in vitro* anti-HIV activity, and biological stability of 5'-*O*-myristoyl analogue derivatives of 3'-fluoro-2',3'-dideoxythymidine (FLT) as potential prodrugs of FLT. *Nucleosides & Nucleotides*, **1998**, 17, 987-1008.

Parang, K., Wiebe, L. I., Knaus, E. E., Huang, J. S., Tyrrell, D. L. In Vitro Anti-Hepatitis B Virus Activities of 5'-O-Myristoyl Analogue Derivatives of 3'-Fluoro-2',3'-dideoxythymidine (FLT) and 3'-Azido-2',3'-dideoxythymidine (AZT). *J. Pharm. Pharmaceut. Sci.*, **1998**, 1, 107–113.

Parang, K., Knaus, E. E., Wiebe, L. I., Sardari, S., Daneshtalab, M., Csizmadia, F. Synthesis and antifungal activities of myristic acid analogs. *Arch. Pharm.-Pharm. Med. Chem.* **1996**, 329, 475-482.

Parang, K., Wiebe, L. I., Knaus, E. E. Novel approaches in designing prodrugs of AZT. *Curr. Med. Chem.*, **2000**, 7, 995-1039.

Parang, K., Wiebe, L. I., Knaus, E. E., Huang, J.-S., Tyrrell, D. L., Csizmadia, F. *In vitro* antiviral activities of myristic acid analogs against human immunodeficiency and hepatitis B viruses. *Antiviral Res.* **1997**, 34, 75-90.

Penugonda, S., Kumar, A., Agarwal, H. K., Parang, K., Mehvar, R. Synthesis and in vitro characterization of novel dextran-methylprednisolone conjugates with peptide linkers: Effects of linker length on hydrolytic and enzymatic release of

www.mana

methylprednisolone and its peptidyl intermediates. *J. Pharm. Sci.*, **2008**, 97, 2649–2664.

Pollakis, G., Abebe, A., Kliphuis, A., Chalaby, M. I. M., Bakker, M., Mengistu, Y., Brouwer, M., Goudsmit, J., Schuitemaker, H.. Paxton W. A. Phenotypic and genotypic comparisons of CCR5- and CXCR4-tropic human immunodeficiency virus type 1 biological clones isolated from subtype C-infected individuals. *J. Virol.*, **2004**, 78, 2841-2852.

Pozniak, A. L., Gallant, J. E., DeJesus, E., Arribas, J. R., Gazzard, B., Campo, R. E., Chen, S. S., McColl, D., Enejosa, J., Toole, J. J, Cheng, A. K. Tenofovir disoproxil fumarate, emtricitabine, and efavirenz versus fixed-dose zidovudine/lamivudine and efavirenz in antiretroviral-naive patients: virologic, immunologic, and morphologic changes – a 96-week analysis. *J. Acquir. Immune. Defic. Syndr.*, **2006**, 43, 535-540.

Reddy, K. R., Colby, T. J., Fujitaki, J. M., van Poelje, P. D., and Erion, M. D. Liver targeting of hepatitis-B antiviral lamivudine using the HepDirect prodrug technology. *Nucleosides Nucleotides Nucleic Acids*, **2005**, 24, 375-81.

Rensen, P. C. N., Devrueh, R. L. A., and Vanberkel, T. J. C. Targeting hepatitis B therapy to the liver: Clinical pharmacokinetic considerations. *Clin. Pharmacokinet.*, **1996**, 31, 131-155.

Rose, J. D., Parker, W. B., Secrist III, J. A. bis(*t*BuSATE) Phosphotriester Prodrugs of 8-Azaguanosine and 6-Methylpurine Riboside; bis(POM) Phosphotriester Prodrugs of 2'-Deoxy-4'-Thioadenosine and Its Corresponding 9α Anomer. *Nucleoside Nucleotides Nucleic Acids*, **2005**, 24, 809–813.

Rusconi, S. Alovudine Medivir. *Curr. Opin. Invest. Drugs*, **2003**, 4, 219–223.

Rusconi, S., Moonis, M., Merrill, D. P., Pallai, P. V., Neidhardt, E. A., Singh, S. K., Willis, K. J., Osburne, M. S., Profy, A. T., Jenson, J. C., Hirsch, M. S. Naphthalene sulfonate polymers with CD4-blocking and anti-human immunodeficiency virus type 1 activities. *Antimicrob. Agents Chemother.*, **1996**, 40, 234-236.

Sarafianos, S. G., Das, K., Clark, Jr., A. D., Ding, J., Boyer, P. L., Hughes, S. H., Arnold, E. Lamivudine (3TC) resistance in HIV-1 reverse transcriptase involves steric hindrance with b-branched amino acids. *Proc. Natl. Acad. Sci. U. S. A.*, **1999**, 96, 10027-10032.

Schwartz, J. L., Mauck, C., Lai, J., Creinin, M. D., Brache, V., Ballagh, S. A., Weiner, D, H., Hillier, S. L., Fichorova, R. N. and Callahan, M. Fourteen day safety and acceptability study of 6% cellulose sulfate gel a randomized double-blind phase I safety study. *Contraception*, **2006**, 131-140.

المنارة للاستشارات

www.manara

Scordi-Bello, I. A., Mosoian, A., He, C., Chen, Y., Cheng Y., Jarvis, G. A., Keller, M. J., Hogarty, K., Waller, D. P., Profy, A. T.,m Herold, B. C., Klotman, M. E. Candidate sulfonated and sulfated topical microbicides: Comparion of Anti-Human Immunodeficiency Virus activities and mechanisms of action. *Antimicroib. Agents Chemother.*, **2005**, 49, 3607-3615.

Shah, V. P., Midha, K. K., Dighe, S., McGilveray, I. J., Skelly, J. P., Yacobi, A., Layoff, T., Viswanathan, C. T., Cook, C. E., McDowall, R. D., Pittman, K. A., and Spector, S. Analytical methods validation: bioavailability, bioequivalence, and pharmacokinetics. *J. Pharm. Sci.*, **1992**, 81, 309-312.

Sahlberg, C. Synthesis of 3'-ethynylthymidine, 3'-vinylthymidine and 3'-bromovinylthymidine as potential antiviral agents. *Tet. Lett.*, **1992**, 33, 679–682.

Seitz, U.; Wagner, M.; Neumaier, B.; Wawra, E.; Glatting, G.; Leder, G.; Schmid, R. M.; Reske, S. N. Evaluation of pyrimidine metabolising enzymes and in vitro uptake of 3'-[(18)F]fluoro-3'-deoxythymidine ([(18)F]FLT) in pancreatic cancer cell lines. *Eur. J. Nucl. Med. Mol. Imaging*, **2002**, 29, 1174–1181.

Shattock, R. J. and Doms, R. W. AIDS models: Microbicides could learn from vaccines. *Nat. Med.*, **2002**, 8, 425.

Shaw, T., Locarnini, S. A. Preclinical aspects of lamivudine and famciclovir against hepatitis B virus. *J. Viral Hepat.*, **1999**, 6, 89-106.

Shields, A. F.; Grierson, J. R.; Dohmen, B. M.; Machulla, H. J.; Stayanoff, J. C.; Lawhorn-Crews, J. M.; Obradovich, J. E.; Muzik, O.; Mangner, T. J. Imaging proliferation in vivo with [F-18]FLT and positron emission tomography. *Nature Med.*, **1998**, 4, 1334–1336.

Skalaski, V., Chang, C. N., Dutachman, G., Cheng, Y. C. The biochemical basis for the differential anti-human immunodeficiency virus activity of two cis enantiomers of 2',3'-dideoxy-3'-thiacytidine. *J. Biol. Chem.*, **1993**, 268, 23234-23238.

Soyez, H., Schacht, E., Vanderkerken, S. The crucial role of spacer groups in macromolecular prodrug design. *Adv. Drug Deliv. Rev.*, **1996**, 21, 81–106.

Stock, R. J., Cilento, E. V., and McCuskey, R. S. A quantitative study of fluorescein isothiocyanate-dextran transport in the microcirculation of the isolated perfused rat liver. *Hepatology*, **1989**, 9, 75-82.

Subr, V., Strohalm, J., Ulbrich, K., Duncan, R., Hume, I. C. Polymers containing enzymatically degradable bonds, XII. Effect of spacer structure on the rate of release of daunomycin and adriamaycin from poly [N-(2-hydroxypropyl)-methylacrylamide] copolymer drug carriers in vitro and antitumor activity measured in vivo. *J. Control Release*, **1992**, 18, 123–132.

المنارة للاستشارات

www.manara

Sundseth, R., Joyner, S. S., Moore, J. T. Dornsife, R. E., Dev, I. K. The anti-human immunodeficiency virus agent 3'-fluorothymidine induces DNA damage and apoptosis in human lymphoblastoid cells. *Antimicrob. Agents Chemother.*, **1996**, 40, 331–335.

Takahashi, H., Fujimoto, J., Hanada, S., and Isselbacher, K. J. Acute hepatitis in rats expressing human hepatitis B virus transgenes. *Proc. Natl. Acad. Sci. U. S. A.*, **1995**, *92*, 1470-1474.

Takakura, Y., and Hashida, M. Macromolecular drug carrier systems in cancer chemotherapy: macromolecular prodrugs. *Crit. Rev. Oncol. Hematol.*, **1995**, 18, 207-231.

Takamune, N., Hamada, H. Misumi, S. And Shoji, S. Novel strategy for anti-HIV-1 action: selective cytotoxic effect of *N*-myristoyltransferase inhibitor on HIV-1 infected cells. *FEBS letters*, **2002**, 527, 138-142.

Thoren, L. The dextrans-clinical data. *Develop. Biol. Stand.*, **1981**, 48, 157-167.

Thumann-Schweitzer, C., Gosselin, G., Périgaud, C., Benzaria, S., Girardet, J. L., Lefebvre, I., Imbach, J. L., Kirn, A., Aubertin, A. M. Anti-human immunodeficiency virus type 1 activities of dideoxynucleoside phosphotriester derivatives in primary monocytes/macrophages. *Res Virol.*, **1996**, 147,155–163.

Tu, J., Zhong, S., and Li, P. Studies on acyclovir-dextran conjugate: synthesis and pharmacokinetics. *Drug Dev. Ind. Pharm.*, **2004**, 30, 959-65.

Turpin, J. A. Considerations and development of topical microbicides to inhibit the sexual transmission of HIV, *Expert Opin. Inv. Drugs*, **2002**, 11, 1077-1097.

Usher T., C., Patel, N. T., Chhagan W., Louis, I. Pharmaceutical preparation and a method for inhibiting the replication of various viruses. WO 1995/00177, PCT/CA94/00343, **1995**.

Van Roey, J. P., Taylor, E. W., Chu, C. K., Shinazi, R. F. Correlation of molecular conformation and activity of reverse transcriptase inhibitors. *Ann. N. Y. Acad. Sci.*, **1990**, 616, 29–40.

Vansteenkiste, S., Schacht, E., Duncan, R., Seymour, L., Pawluczyk, I., and Baldwin, R. Fate of glycosylated dextrans after in vivo administration. *J. Control. Release*, **1991**, 16, 91-100.

Van Roey, J. P., Taylor, E. W., Chu, C. K., Shinazi, R. F. Correlation of molecular conformation and activity of reverse transcriptase inhibitors. *Ann. N. Y. Acad. Sci.*, **1990**, 616, 29–40.

المنارة للاستشارات

www.mana

Vlieghe, P., Clerc, T., Pannecouque, C., Witvrouw, M., Clercq, E. D., Salles, J. P. and Kraus, J, L. Synthesis of new covalently bound κ-Carrageenan-AZT conjugates with improved anti-HIV activities. *J. Med. Chem.*, **2002**, *45*, 1275-1283.

Wagner, M.; Seitz, U.; Buck, A.; Neumaier, B.; Schultheiss, S.; Bangerter, M.; Bommer, M.; Leithauser, F.; Wawra, E.; Munzert, G.; Reske, S. N. 3'-[^{18}F]fluoro-3'-deoxythymidine ([^{18}F]-FLT) as positron emission tomography tracer for imaging proliferation in a murine B-Cell lymphoma model and in the human disease. *Cancer Res.*, **2003**, 63, 2681–2687.

Wakabi, W. HIV microbicide trials halted. *Can. Med. Assoc. J.*, **2007** 176: 1569-1570.

Weissenhorn, W., Dessen, A., Harrison, S. C., Skehel, J. J., Wiley, D. C. Atomic structure of the ectodomain from HIV-1 gp41. *Nature*, **1997**, 387, 426-430.

Wodarski, C.; Eisenbarth, J.; Weber, K.; Henze, M.; Haberkorn, U.; Eisenhut, M. Synthesis of 3′-deoxy-3′-[^{18}F]fluoro-thymidine with 2,3′-*O*-anhydro-5′-*O*-(4,4′-dimethoxy-trityl)thymidine. *J. Lab. Compds. Radiopharm.*, **2000**, 43, 1211–1218.

Wu, C. H., Ouyang, E. C., Walton, C., Promrat, K., Forouhar, F., and Wu, G. Y. Hepatitis B virus infection of transplanted human hepatocytes causes a biochemical and histological hepatitis in immunocopetentent rats. *World J. Gastroenterol.*, **2003**, 9, 978-83.

Wu, C. H., Ouyang, E. C., Walton, C., and Wu, G. Y. Liver cell transplantation -- novel animal model for human hepatic viral infections. *Croat. Med. J.*, **2001**, 42, 446-450.

Wu, Z., Alexandratos, J., Ericksen, B., Lubkowshi, J., Gallo, R. C., Lu, W. Total chemical synthesis of N-myristoylated HIV-1 matrix protein p17: Structural and mechanistic implications of p17 myristoylation. *Proc. Natl. Acad. Sci. U. S. A.*, **2004**, 101, 11587-11592.

Yamaoka, T., Kuroda, M., Tabata, Y., and Ikada, Y. Body distribution of dextran derivatives with electric charges after intravenous administration. *Int. J. Pharmaceut.*, **1995**, 113, 149-157.

Yi, Y., Isaacs, S. N., Williams, D. A., Frank, I., Schols, D., Clerco, E. D., Kolson, D. L., Collman, R. G. Role of CXCR4 in cell-cell fusion and infection of monocyte-derived macrophages by primary human immunodeficiency virus type 1 (HIV-1) strains: Two distinct mechanisms of HIV-1 dual tropism. *J. Virol.*, **1999**, 73, 7117-7125.

Younger, H. M., Bathgate, A. J., and Hayes, P. C. Review article: Nucleoside analogues for the treatment of chronic hepatitis B. *Aliment. Pharmacol. Ther.*, **2004**, *20*, 1211-30.

المنارة للاستشارات

www.manara

Yuan, J. Estimation of variance for AUC in animal studies. *J. Pharm. Sci.*, **1993**, 82, 761-763.

Yun, M.; Oh, S. J.; Ha, H.-J.; Ryu, J. S., Moon, D. H. High radiochemical yield synthesis of 3′-deoxy-3′-[^{18}F]fluorothymidine using (5′-*O*-dimethoxytrityl-2′-deoxy-3′-*O*-nosyl-β-D-*threo* pentofuranosyl)thymine and its 3-*N*-BOC-protected analogue as a labeling precursor. *Nucl. Med. Biol.*, **2003**, 30, 151–157.

Zdanowicz, M. M. The pharmacology of HIV drug resistance. *Am. J. Pharm. Educ.*, **2006**, 70, 100-122.

Zhang, X., and Mehvar, R. Dextran-methylprednisolone succinate as a prodrug of methylprednisolone: dose-dependent pharmacokinetics in rats. *Int. J. Pharm.*, **2001**, 229, 173-182.

Zhang, X., and Mehvar, R. Dextran-methylprednisolone succinate as a prodrug of methylprednisolone: plasma and tissue disposition. *J. Pharm. Sci.*, **2001**, 90, 2078-2087.

Zheng, J. J., Wu, S. T., and Emm, T. A. High-performance liquid chromatographic assay for the determination of 2'-deoxy-3'-thiacytidine (lamivudine) in human plasma. *J. Chromatogr. B Biomed. Sci. Appl.*, **2001**, 761, 195-201.

Zhou, X. J., and Sommadossi, J. P. Rapid quantitation of (-)-2'-deoxy-3'-thiacytidine in human serum by high-performance liquid chromatography with ultraviolet detection. *J. Chromatogr. B Biomed. Sci. Appl.*, **1997**, 691, 417-424.

المنارة للاستشارات
www.manar